Caenorhabditis elegans Dosage Compensation Directs Chromatin and Transcriptional Regulation on Hermaphrodite X Chromosomes

by

Michael B. Wells

A dissertation submitted in partial fulfillment
of the requirements for the degree of
Doctor of Philosophy
(Molecular, Cellular, and Developmental Biology)
in The University of Michigan
2012

Doctoral Committee:

Assistant Professor Györgyi Csankovszki, Chair
Professor Kenneth M. Cadigan
Associate Professor Anuj Kumar
Assistant Professor Yali Dou
Assistant Professor Andrzej Wierzbicki

This work is dedicated
to my lovely wife, Kim,
my family and friends, past and present,
my scientific mentors and role models,
golf, my influx of serenity
and finally, to DPY-21, the inspiring enigma

Acknowledgements

First and foremost, thank you to my lovely wife, Kimberly Miller. It is your unwaivering confidence in me that has been such a comfort through the past five years and before. I want to also thank you for choosing to journey through life with me as a team, including the adventures of living half way across the country from the area in which we both grew up, Boise, ID. Further, you are such an incredibly good influence on me. From getting me to try new things, such as Indian cuisine, to opening my eyes to countless new ways to see the world, I'm forever grateful, and I so look forward to continuing on our journey through life together. We've raised a wonderful dog, Willow, and she adds so much happiness and excitement to our home. I'm so glad that you and I have each other. You make each day a memorable joy. You are the most important part of my life, and you are my inspiration.

Second, I wish to express my sincerest gratitude to my doctoral mentor, Dr. Györgyi Csankovszki. You gave me the opportunity to work on a project that had produced only negative results in the past and have given me the training and support to turn this work into a real contribution to the field. I have no doubt that the abilities I've learned from you and others in the lab will be a firm foundation for the next stage of my career in science. You have shown me so much about what I will continue to strive to become as a professional, a researcher, a professor, and as a mentor. Thank you for everything. Thanks also to my thesis committee members, whose insights elevated the quality of this work and broadened my horizons as a scientist.

I also have to thank my family, for all of their kind support and love. Chief among these, I have to acknowledge my parents, David and Joyce Wells, for providing me with the tools and opportunities to make whatever I wanted of myself. I am deeply appreciative of all they have done for me, and they mean the world to me. Also, I want to recognize what a great influence my Grandmother, LaVonne Rasmussen, has been in shaping my life. From teaching me to tie my shoes, to going on weekend adventures, and allowing me the opportunity to teach her and Grandpa Wayne how to play the sport I love, golf, she has always supported and encouraged me. I also want to thank my Grandma Marcheta Mason, for all these years of love and support, as well as the chance she helped give me to go to a College where I received the preparation and knowledge essential for undertaking a doctoral degree. Thank you as well to every other member of my family: Grandma and Grandpa Vern and Ruthie, Steve Wells and family, Carla and Gordon, Sara and Steve and family, and everyone else. Thank you also to the Simpsons, Larry, Dale, Linda, and Dawn. Your friendship means so much to me, and among many other things, thank you for introducing me to the joy that having a dog in your life can bring. You are all incredible people, and I'm so proud to say that you're like a second family to me. It is in large part because of the influence of all of these people in my life that I have the courage and strength to reach for my dreams.

This experience would also not have been possible without the guidance that I received as an undergraduate at the College of Idaho from my first mentor, Dr. Sara Heggland. She taught me how to think about science in a logical, yet creative, way and to remember that doing research is an unending thirst: there is always another question to address and another interesting paper to read. The time I spent doing research in her lab was full of surprises and always interesting. The freedom to explore a daring project with a model system not previously used on campus, zebrafish scales, to complete award-winning research on cadmium toxicity and amelioration by estrogen helped to establish broad horizons in my mind as to what is possible in science. Further, the one on one attention that I received from her fueled my passion for

science and inspired me to pursue a similar academic career, in the hopes of teaching and training a new crop of students to think critically and appreciate science - perhaps even inspire some to become scientists themselves. In time, we'll see if this dream becomes a reality.

Thank you as well to the friends I've made at work in the lab, both as an undergraduate and as a graduate student. Your encouragement, feedback, and insight makes doing research so much more fulfilling. It is interacting with others in the lab, such as Martha Snyder, Laura Custer, Margarita Sifuentes, and the undergraduates I've had the good fortune to work with (Anna Cacciaglia, Michael Totten, and Emily Laughlin) that made this time and the science so meaningful to me. It was a privilege working with you.

Table of Contents

List of Figures

List of Tables

CHAPTER 1

Introduction

Some elements and ideas described in this chapter were published as Wells et al. (2012) in *Genetics Research International* as "Finding a Balance: How Diverse Dosage Compensation Strategies Modify Histone H4 to Regulate Transcription." Volume 2012, Article ID 795069. Laura Custer and I equally split the writing of this article. For that publication, I created the diagrams in Figures 2 and 3, and completed the imaging shown in Figure 4. Laura constructed Figure 1. Figure 1.9 in this introduction was taken from that article (Figure 2).

Complex genetic programs govern the viability, development, and fitness of an organism

Living organisms are the result of complex genetic programs which govern numerous important processes. From development, to metabolism, to reproduction and beyond, there are many occurrences of signaling pathway usage that determine how well an organism can cope with stress. Molecular signaling is an extension of the foundational principle of the Central Dogma [1-6], the notion of a linear pathway from DNA to mRNA to protein effectors.

Signaling pathways often require finely-tuned responses that involve diffusible molecules (chemical compounds, peptides, and proteins) in order to achieve the proper cellular response to a stimulus [1,3,7]. A stimulus could be a developmental cue, an environmental stress, a mating display, or any number of other signals. However, recent studies have highlighted the stochastic nature of gene expression and single molecule studies have demonstrated the tenuous nature of regulating such a complex set of interactions [1,3]. Gene expression can only truly be measured on a single molecule basis, and the individual number of copies of any given mRNA varies from cell to cell [1]. Coordinating multiple signaling pathways to achieve a common goal, e.g. completing the proper developmental program, is a truly complex affair. Numerous additional complexities in molecular biology have been identified over the past 40+ years that expand the ideas of the Central Dogma, including: DNA repair, regulatory RNAs, RNA editing, and epigenetics/chromatin regulation [2,8,9]. Further, proteins can also affect DNA structure and subsequent transcription, as illustrated by the following example of the immune system. Research such as this highlights the need to consider and incorporate the true complexity of molecular biology into the Central Dogma.

One particularly poignant example of the complexity of molecular biology beyond the Central Dogma is antibody production. Antibody production is the creation of a new gene product to specifically interact with an antigen. This process requires a clear distinction between native and foreign molecules. This distinction mechanism is achieved by protein-directed nucleic acid processing [10-12] and selection from a variety of candidate molecules. The immature lymphocytes contain several hundred short immunogenic genes [12]. These genes, which encode the variable domains of the two heavy or two light chains of immunoglobulins, are rearranged in lymphocytes, being highly susceptible to recombination and mutation [13]. These genes are represented on the lymphocyte cell surface as mobile and variable receptor proteins [14]. The native arrangements of these variable domain genes are fully compatible with the molecules that invade the lymphocyte's environment [13,14].

In summary, when an antigen arrives, it will cause rearrangement of the domains of the lymphocyte receptors, which in turn will rearrange the domains of the variable and constant genes to tailor the immune response to specific foreign antigens [15,16]. Interestingly, several studies have identified roles for cohesin and condensin in proper T cell differentiation in response to antigens [17-20]. Cohesin and condensin participate in chromosome condensation and sister chromosome cohesion during mitosis and meiosis [21-23], so it is not obvious why they would also play such an important role in immunity. These studies have shown that proper differentiation of naïve T cells involves regional chromosomal condensation and long-range enhancer-promoter interactions to promote proper gene expression [17-20]. This paradigm turns out to be directly relevant when considering the role of condensin in *C. elegans* dosage compensation, the process central to my thesis work, as discussed later in this chapter and beyond.

Proper gene expression is critical for the success of complex genetic circuits. Because of this, gene expression is controlled at many critical points by multiple sets of both positive and negative regulators. Their coordinated action promotes optimal levels of gene expression locally and globally and increased fitness for the organism [24,25]. Mutations in DNA may affect the activity of the expressed gene product or the efficiency of the process of transcription in *cis* [26,27], or transcription/translation efficiency through effects in *trans*, further complicating the overall picture of gene regulation within each individual of a species.

Chromosome copy number and regulation of gene expression are two critical molecular determinants of gene dose [28-30]. Most differences in chromosome number, or aneuploidies, cannot be tolerated, and result in inviability [31-33]. Few changes in the copy number of chromosomes or large portions of chromosomes are viable, but these result in harmful and lasting effects on development and fitness. One example of this scenario in humans is trisomy 21, or possessing three copies of chromosome 21; this causes aberrant expression of chromosome 21 gene products contributing to the Down syndrome phenotype [31,34-37]. Down syndrome is characterized, in part, by decreased cognitive and reproductive function [31,35].

The implications of a chromosome-based method of sex determination

Organisms employ a variety of sex determination mechanisms. Several reptiles, such as turtles and crocodiles, use a temperature-based sex determination system [38,39]. In birds, sex determination is executed by the dosage of a DNA methyltransferase (*DMRT1*) and an unidentified cell autonomous factor [39]. Some species' gender can be affected both by genetic and environmental signals [39,40]. Certain species of reef fish display a highly flexible sex determination system that can act either in juvenile stages or adulthood; the driving force behind gender in these fish species are social interactions that affect hormone production [41].

For many species, there is a difference in chromosome copy number which must be tolerated. Species that utilize a chromosome-based method of sex determination require a difference in sex chromosome number as the underpinnings of female versus male development. There are two ways sex chromosomes can be used to determine sex: either chromosomes are counted, or there is a sex determining gene on the sex chromosome which exists in only one gender. Under these systems, there is a homogametic (XX or ZZ) and a heterogametic (XY or ZW) gender [40,42]. In XY systems, males are heterogametic, while in ZW systems, females are heterogametic [42]. Mammals, medaka fish, insects, worms, some reptiles, and some amphibians use an XY or XY-like system [38,39,43-48], while other reptiles, other amphibians, and birds use a ZW system [38,39,49,50]. Other species have highly unique and odd chromosome-based methods of sex determination [38,40,51,52]. Within an individual, there are chromosome counting methods that sense copy number based on one or more sex chromosome signal elements [39,53-55]. Furthermore, some species use the ratio of X chromosomes to autosomes based on signal element counting to determine sex [53-55]. In mammals, it is the presence or absence of a Y chromosome, specifically *sry* expression, that commits an individual to the male determination pathway [56-59].

It was noticed very early on in chromosome research that sex chromosome gene expression must not only be equalized between genders, but also to the autosomal expression within an individual (Fig. 1.1); this is Ohno's hypothesis [28,60]. It was proposed that upregulation of X in the heteromorphic sex corrects the apparent monosomy [28]. However, this would lead to X-linked hyperexpression in the homomorphic sex if the mechanism of upregulation was not gender-specific. Thus, a second active mechanism is thought to be required to ensure that both sexes remain viable and fit. This mechanism is known as dosage compensation (DC) [61-65]. By definition, dosage compensation is the process by which X-linked (or Z-linked) gene expression is equalized between the sexes [61-65]. These chromosome dosage effects, the combination of homomorphic and/or heteromorphic X upregulation and homomorphic downregulation, are equilibrated using a variety of strategies across different organisms (Fig. 1.2) in response to selective pressures against X-linked gene loss in the heterogametic sex over evolutionary time.

In flies, dosage compensation occurs in the heteromorphic male sex as a two-fold upregulation of expression from the single X chromosome (Fig. 1.2b) [65-89]. This accomplishes both goals of chromosome dosage equalization: X chromosome dose is "two" in both males and females, and X and autosome dose are both "two" within males and females. In mammals and worms, X upregulation is thought to occur in both sexes early in development, balancing X:A expression in males, but leading to hyperexpression of X in females/hermaphrodites (Fig. 1.2a, c) [60,75,90]. Then, in a second step, dosage compensation acts in the female/hermaphrodite to halve overall X-linked expression, fulfilling both levels of chromosome dosage equalization (Fig. 1.2a, c)[64]. It is not known whether X upregulation and dosage compensation happen simultaneously or sequentially in mammals and worms.

Some organisms, such as the chicken, the platypus, and marsupials, do not require chromosome-wide dosage compensation [91-96]. Balance in these cases is thought to be achieved at a local level for particularly important genes. For example, the platypus has either ten copies of the X chromosome or five copies of X and five copies of Y (Fig. 1.2e) [91,93]. These chromosomes chain together, and recent work has shown that gene expression from X is controlled locally, and loci are either stochastically monoallelic or biallelic and not compensated [91].

Recent publications have debated the existence of X upregulation and dosage compensation in mammals and worms through ChIP-chip and RNA-seq studies [60,75,97]. Data analysis has proven critical in this instance, as different sources of error have required clarification in order to resolve these disputes. The prevailing view in the field favors the existence of dosage compensation and X upregulation in both mammals and worms [60]. Because there is no biological necessity to fine-tune expression levels of non-expressed genes, I also favor this view. It is imperative to filter out the non-expressed genes to uncover chromosome dosage equalization, and in worms it is also necessary to consider the contribution of the non-dosage compensated germline tissue to sample preparations in expression analyses [60].

Mechanisms of dosage compensation vary across species

To enact the diverse strategies of dosage compensation present across species, organisms have also developed, or sometimes co-opted, distinctive dosage compensation machineries. In mammals, dosage compensation is achieved by the long non-coding RNA *Xist*, which binds one of the two X chromosomes in female nuclei and silences it (X inactivation; Fig. 1.2a), with the help of downstream effector proteins recruited by *Xist* [90,98-109]. *Xist* is initially expressed from the Xic region (X inactivation center that includes Xist and its nearby regulatory elements) of both X chromosomes [94,95,102,110-113]. In mice, *Tsix* is a non-coding RNA that is anti-sense to, and encompasses, *Xist* that is known to help establish X inactivation by limiting *Xist* expression to only one X [95,98,111,112,114-119]. Evidence suggests that human *Tsix* lacks functional elements required for it to act in the same manner as its mouse homolog [95,111].

X inactivation in mammals is thought to occur differently through two stages in development. In mice, imprinting leads to the silencing of the paternal X in extraembryonic tissue and stochastic silencing of either allele occurs within embryonic cells. Inactivation is thought to happen randomly between either copy of X in humans [95]. Loading of *Xist* and its effectors culminates in a series of structural changes to the chromatin, DNA and associated proteins important for packaging into higher order conformations, of the inactivated X [98,99]. RNA Pol II is excluded from the inactive X, and Polycomb group and other chromatin modifiers (including the DNA methyltransferase Dnmt1) are recruited to the inactive X for stable repression [90,95,98,99,120-124]. The chromatin regulation associated with X inactivation is maintained throughout the remainder of an individual's lifespan. Once established, the inactive state on X can be maintained in the absence of the *Xist* RNA, suggesting that X inactivation is an epigenetic process [125]. The DNA methyltransferase Dnmt1, as well as *Xist* and histone deacetylation, play a vital role in the maintenance of this inactive X state [108].

There is quite a range of mechanistic differences among X inactivation strategies, elements, and timing across mammals (Fig. 1.3a) [93-95,102,120]. *Xist* is conserved among placental mammals [94,120]. However, *Xist* structure, *Xist* functional onset, and X chromosome structure have diverged among placental mammals [94,102,111]. Similar to *Xist*, DNA methylation is not seen in monotremes or marsupials [120]. Chromatin modifications indicative of constitutive heterochromatin are co-enriched with Polycomb silencing in marsupials, whereas they show a mutually exclusive pattern in human cells [120,126]. A model [120] summarizing the features of X inactivation is shown in Fig. 1.3a.

Fly dosage compensation is achieved by the *male-specific lethal* (MSL) complex (Fig. 1.4) [127], which binds the single male X chromosome and upregulates X-linked transcription two-fold [65-88]. This increased activation is mediated by the chromatin modifier and activator *males absent on the first*, or MOF [68,128-131]. MSL complex assembly is thought to occur in two stages. First, MSL-1 and MSL-2 bind to so-called high-affinity, or chromatin entry, sites dictated by a DNA sequence element (GAGAGAGA) and enrichment of a particular histone modification, H3K36me3 [69,72,74,84,132-136]. Once bound, these two proteins are capable of recruiting the remainder of the MSL complex: MSL-3, MOF, MLE (*maleless*), and one of two non-coding *roX* RNAs [127]. MOF acetylation of MSL-3 then acts to ratchet the complex along nucleosomes to accomplish spreading of the complex to many more sites along X [137]. Further data suggests that MSL-3 contributes to MSL complex localization by binding H4K20me1 [133,134]. Known biochemical functions and distinguishing properties of the MSL complex members are listed in [127].

Lively debate over the true function of the MSL proteins in regulation of MOF is ongoing. While it is clear that MOF activity leads to transcriptional hyper-activation of the single male X chromosome [66,138], whether the other MSL components aid or restrict MOF function remains a topic of debate [65,82,128]. Results from the Becker lab show that when MOF is tethered to a reporter in females, transgene expression is high, but activation is restricted to 2-fold in males, where MOF and the rest of the MSL complex are recruited [128]. Adding further complexity to MOF action is the finding that MOF acts in another transcriptional activator complex called *nonspecific lethal* (or NSL) complex with relaxed lysine acetylation specificity and genome-wide binding distinct from the MSL complex [76,139,140]. The Birchler group has put forth the idea that in flies, similar to the X upregulation proposed for mammals and worms, there is an inverse dosage effect that modulates gene expression from X or autosomes proportionally to copy number [65].

Interestingly, the MSL complex is thought to be active in both sexes early in development, around the blastoderm stage or perhaps earlier [141-144]. In females, this action may promote expression of *sex-lethal*, the transcriptional regulator responsible for preventing further transcription of MSL-2 [45,143,145-155], the component of the MSL complex that is not zygotically transcribed in females, preventing future MSL complex formation in females for the remainder of their lifespan in order to maintain proper X chromosome dose [141].

The mechanism of *Caenorhabditis elegans* (worm) dosage compensation involves two-fold downregulation of both hermaphrodite X chromosomes (Fig. 1.2c) by the dosage compensation complex, or DCC [53,156]. The DCC (Fig. 1.5a) is composed of a five-subunit condensin-like complex (Condensin I^{DC}), a recruitment complex composed of three SDC (sex determination and dosage compensation) proteins, and two associated proteins: DPY-21 and DPY-30 [53,156-165]. Across all organisms, condensin is composed of two SMC proteins and three CAP proteins. Most organisms have two condensins which act during meiosis and mitosis, while *C. elegans* has an additional condensin, Condensin I^{DC}, which acts on X during interphase [157,166]. The SMC (structural maintenance of chromosomes)-4 homolog DPY-27 is specific to the DCC, and the SMC-2 homolog in the DCC is MIX-1 [162,167]; the CAP (chromosome-associated polypeptide) subunits are CAPG-1, DPY-26, and DPY-28 [157,160,165]. The members of condensin I^{DC} were identified through a combination of forward genetic screens and biochemical approaches [162,165,167,168].

DCC loading and spreading is thought to be achieved via a two-step model. *sdc-2* is the only member of the DCC not maternally loaded into the oocyte [169,170]. Around the 30-cell stage, hermaphrodite-specific *sdc-2* transcription initiates assembly of the DCC at a set of ~75 primary binding sites (or *rex*, recruitment element on X, sites), partially defined by a DNA sequence element known as *mex* (Fig. 1.5b), or motif enriched on X, and able to recruit the DCC as multi-copy transgenic arrays outside of the context of the X chromosomes [171,172]. Subsequently, the DCC spreads to many more *dox* (dependent on X) sites, which are unable to recruit the DCC outside their native chromosomal context, across the X chromosomes in a transcription-dependent manner [171,172]. It is possible that at least a subset of DCC binding targets are thought to change during the course of development (data not shown), and DCC binding is not indicative of dosage compensation status (Fig. 2.4) [171,173,174]. Data from the Csankovszki lab further suggests that not all *rex* sites are equal. Some sites are able to recruit the DCC to an extra locus present as a small or large X chromosome region duplication, while others (termed waystations) are not [175].

Through the use of two temperature sensitive alleles, *dpy-27(y57)* and *dpy-28(y1)*, it has been demonstrated that the DCC is required for viability between five and nine hours post fertilization, during mid-embryogenesis [165]. Nothing is known about the necessity of the DCC outside of this time window. However, the DCC is visibly localized to the X chromosomes in hermaphrodite somatic tissues from around the 30-50-cell stage on, through the entire life of the animal [176]. Because of the homology of Condensin I^{DC} to condensin, the mitotic and meiotic regulator of chromosome structure, it is thought that *C. elegans* dosage compensation involves changes in X chromosome structure [53,158,167,177]. The molecular mechanism of worm dosage compensation, however, has remained largely a mystery. Recent work has suggested that dosage compensation modulates and spreads with RNA polymerase II on X, arguing in favor of a role in transcriptional regulation, but no further details were uncovered [172,173].

Condensin function and the actions of other DCC subunits

C. elegans is special in that it contains three condensin complexes, whereas other organisms studied have only one or two, which are involved in meiosis and mitosis [21-23,178-182]. The biochemical function of purified condensin complexes has been well studied in yeast [183], *Xenopus* [166,184,185], *C. elegans* [186], and humans [187]. Condensin can positively supercoil naked DNA in an ATP-dependent manner *in vitro* and can compact single DNA molecules [188]. Other data suggests that condensin action requires looping around chromatin as well as electrostatic bonds formed with the DNA it surrounds [189]. How this activity contributes to meiosis and mitosis, or *C. elegans* dosage compensation, is not understood. Depletion of condensin subunits leads to chromosome condensation defects in some systems [183,190-192]. DCC function in dosage compensation is known to be ATP-dependent. The ATP-binding domains of DPY-27 and SDC-3 are necessary for *her-1* repression [193,194]. Also, mutation of either the DPY-27 or MIX-1 ATP-binding domain results in loss of dosage compensation function [162,167]. It is not known whether condensin I^{DC} is capable of the same structural modifications to DNA as condensin.

Within the recruitment complex, the hermaphrodite- and DCC-specific SDC-2 is very large (344 kDa), and the only known features are a predicted phosphorylation site and several N-coil domains [170]. Because SDC -2 is capable of binding to X in the absence of other complex members and is required for optimal binding of the complete complex, it is thought that SDC-2 is one anchor for the DCC to chromatin [170]. SDC-3 may also interact directly with DNA, through its zinc finger domains, and SDC-3 contributes to subsequent recruitment of the other DCC components [172,193]. *sdc -2* and *sdc-3* mutations result in failure of DCC localization; all nuclear DCC signal is then lost as development proceeds [169,170,172,193,195]. SDC-1 is also required for dosage compensation, but it is not required for X chromosome binding of the DCC

[173]. SDC-1 contains two N-terminal C2H2 zinc fingers, suggesting a function in DNA binding [196].

Two other proteins are considered members of the DCC: DPY-21 and DPY-30. DPY-30 is expressed in both males and hermaphrodites, and its localization appears to be diffuse nuclear, not strictly X-specific, suggesting a genome-wide regulatory role [177,197]. Unlike in *sdc-2* and *sdc-3* mutants, mislocalized DCC signal persists into adulthood in *dpy-30* mutants [198]. DPY-30 has been shown to interact with SDC-2 and SDC-3 [172], but its stable expression is not dependent on other members of the DCC [199]. DPY-30 proteins have a conserved functional role in H3K4 methyltransferase complexes [172,198,200-203]. However, participation of DPY-30 in COMPASS complex action has not been linked to dosage compensation [172,198]. DPY-21, like DPY-30, is expressed in both males and hermaphrodites [159,197,199,204,205], and it has been shown to be important for sensing X chromosome dosage and executing the proper sex determination pathway [159,204,205]. DPY-21 is only loosely associated with other members of the DCC, and loss of DPY-21 does not perturb localization of the rest of the DCC [159]. DPY-21 has a proline rich N-terminus, which has been postulated to serve as a docking site for other proteins [159].

Worm DC is linked at multiple points to sex determination

In mammals, the master regulator of sex determination is the presence or absence of SRY, which is located on the male Y chromosome [57-59,206,207]. Flies and worms use a different mechanism of sex determination. The decision of gender and associated signaling is set into motion by the X:A ratio, as determined by the expression of X and autosomal signal elements, or XSEs and ASEs [146,208-210]. In worms and flies, the processes of dosage compensation and sex determination are linked (Fig. 1.6)[208].

In flies (Fig. 1.6a), the X:A signal, determined by expression of signal element genes, controls expression of the *Sxl* gene through an elaborate RNA splicing mechanism [145,147,148,154,155,211-213]. Autoregulation of *Sxl* is established in XX female, but not XY male embryos [147]. The *Sxl* autoregulatory feedback loop limits protein levels throughout the rest of the fly lifespan. Sxl limits expression of the female-required *Tra* genes and allows for *Msl-2* transcription in males. Vice versa, *Sxl* allows for TRA protein production and limits MSL-2 in females [147,213]. The TRA proteins regulate somatic sex determination, while *Msl-2* triggers dosage compensation [147,213].

Sex determination in *C. elegans* follows a similar scheme (Fig. 1.6b). Several XSEs and ASEs are known in *C. elegans*, including: sex-1, fox-1, ceh-39, and fox-2 on X, and sea-1 and sea-2 on autosomes [47,53,210]. In XX worms, the X:A ratio is high. This induces both dosage compensation and sex determination through SDC protein activation, and perhaps an XSE-independent function of SEX-1, by blocking the expression of the master regulator *her-1*, which encodes a secreted protein [47,53,170,214]. HER-1 deficiency in XX animals results in activation of TRA-2, the Patched-like transmembrane protein [214-219], which antagonizes the proteins FEM-1 (novel), FEM-2 (protein phosphatase), and FEM-3 (ankryin repeat-containing protein) [220-222]. Low FEM activity results in the activation of TRA-1 (zinc finger protein) [217,220,223,224]. High TRA-1 activity promotes hermaphrodite somatic development. In XO animals, the X:A ratio is low, which blocks dosage compensation and induces *her-1* expression. HER-1 inhibits TRA-2 activity, allowing high FEM activity, resulting in low TRA-1 activity. Low TRA-1 activity is insufficient to promote hermaphrodite development, so XO animals develop into males [220]. TRA-1 activity then feeds back onto XOL-1 to reinforce repression [223]. Further work has demonstrated that TRA-4 (zinc finger protein) acts in a pathway parallel to TRA-1 to repress male development through chromatin regulation [220], and other chromatin regulators are also important for effecting sex determination. Loss of these chromatin regulators, also known as synMuv (synthetic Multivulva) mutants, play a well-studied role in larval hermaphrodite reproductive development [220,225,226].

Germline silencing of X in *C. elegans* is independent of dosage compensation

Because there is no homolog for the single male X to pair with during meiosis, it is protected by adopting a particularly compact chromatin conformation, similar to heterochromatin [227,228]. This mechanism is needed to prevent loss of male X chromosome DNA from recombination without a repair template [228]. The result is loss of most X-linked transcription during these portions of meiosis, leading to an explanation for the relative scarcity of genes important for early development on X [229]. This process involves enrichment of repressive histone modifications, particularly H3K9me2/3 and H3K27me3, as well as loss of activating marks, including H4K16ac, during late stages of meiosis in the germline(s) of both sexes [228]. Even though this mechanism should only be essential for X preservation during male meiosis, the hermaphrodite germline X chromosomes also undergo this process [228].

Germline silencing is mediated by the *maternal effect sterile* (MES) proteins [230-233]. MES-2, MES-3, and MES-6 form a complex homologous to Polycomb, specifically PRC2, found in other organisms [231], which enriches H3K27me3 on the germline X. The MES complex exists in balance with an activator, MES-4, which localizes to autosomes and is important for germline transcriptional memory transmission [230,234]. MES-4 is an H3K36 histone methyltransferase (HMT), a modification linked to transcriptional elongation through repression of aberrant transcription [235], prominently active in the germline and early embryo until ~40 cell-stage [230]. MRG-1 functions similarly to, but independently of, MES-4 to silence X-linked genes and protect germline immortality. MRG-1 may also be associated with H4K16ac through TIP60 complex recruitment or function [236]. MRG-1 (a *Drosophila* DCC subunit MSL-3 homolog) contains a chromodomain that binds H3K36me3 [236]. The interdependent relationship among MES effects is quite complex. MES-4 action does not require transcription [230,237], and some evidence suggests that MES-4 has both activating and repressive effects [230]. Further, MES-2, -3, -6 may function to focus repression by MES-4 and the chromatin remodeler NuRD to preserve proper gene expression in the germline and prevent germline gene expression in the soma [230,236]. Loss of MES-4 causes aberrant RNA Pol II activation and degeneration of the primordial germ cells [237], suggesting a role in transmission of the germ cell program to the offspring [234]. At high temperatures, the soma of synMuv B mutants gains a germline-like gene expression pattern, dependent on global chromatin modifiers such as NuRD, the MES proteins, and ISWI, through a failure to antagonize an inherited chromatin state, leading to early larval arrest [238].

Transcriptional regulation begins with chromatin regulation at the level of the nucleosome

One way that gene expression can be regulated is at the level of transcription. It has been shown that transcriptional regulation plays key roles in mammalian, fly, and in lesser detail in worm, dosage compensation [66,98,121,172]. It has been further demonstrated in flies and mammals that the regulation of transcription by dosage compensation is executed by changes in chromatin [71,90,93,98,120,132,133,136,138], which is the DNA and the histone proteins with which DNA is packaged. The fundamental unit of chromatin is the nucleosome (Fig. 1.7), which is composed of 147bp (1.6 turns) of DNA wrapped around an octamer of histone proteins [239-241]. Each nucleosome contains two copies of histones H2A, H2B, H3, and H4. However, each histone may be encoded by multiple genes, and each histone protein may be substituted out for a histone variant protein [241,242].

The strength of the interaction between DNA and the histones is greatly influenced by the complement of post-translational modifications present on their N- and/or C-terminal tail domains (summarized in Fig. 1.8) [243-246]. As of November 2011, 160+ histone modifications have been identified [247], but new modifications continue to be identified. Principally, there are 9 functional groups known to be used to modify histone protein tails: acetylation, ADP-ribosylation, citrullination, crotonylation, methylation, O-GlcNAcylation, phosphorylation, sumoylation, and ubiquitination [241,244,245,247,248]. Together, these modifications and histone variants represent the "letters" in what is thought of as the "histone language" [249-252]. Rather than a simple, input-predicts-output-style, a 1:1 relation between these modifications and effects on transcription, or other processes, as would be expected of a "histone code," it is believed that chromatin modifications represent a complex, multivariate, combinatorial determinant of chromatin meaning [249,251,252].

Although there is no steadfast rule, certain chromatin modifications (e.g. H4K16ac) are thought to be activating, while others (e.g. H3K9me3) are associated with repression [241,244-246]. Chromatin in an active, open conformation is known as euchromatin, while repressive, closed chromatin is heterochromatin [241]. Heterochromatin can either be facultative (switchable to an active state) or constitutive (maintained as highly repressive) [253]. Further, there is considerable evidence that at least certain modifications, perhaps the majority, achieve different outcomes depending upon the absence or presence of other nearby modifications. One example of this is the recruitment of chromatin modifiers, the "readers" and "writers" of the "histone language" [249,251], to sites of action. The majority of reader interactions with chromatin are achieved through several known domains, including: 14-3-3 (H3S10ph, H3S28ph), chromo (H3K9me2/3, H3K27me2/3), bromo (lysine acetylation), MBT (lysine mono- or dimethylation), PHD finger (H3K4me0, H3K4me3, H3K9me3, H3K36me3), and tudor (arginine dimethylation) [254,255]. Recent work has demonstrated additional complexity in recognition through combinatorial modification substrate recognition by chromatin enzymes [245,254,256,257].

A series of techniques based on chromatin conformation capture, 3C [258], have been used to interrogate the higher order structure and organization of the genomes [259,260] of several organisms [110,261-263]. Application of allele-specific 4C, analyzing the interactions of one locus with the rest of the genome either using microarrays or next generation sequencing, to mammalian X inactivation demonstrated that active X genes in mouse tend to interact even over long physical distances, whereas inactive genes do not [110]. Inactive genes are located randomly within the inactive X territory, and escapers of X inactivation tend to cluster to the periphery of the *Xist* domain and, similar to active X genes, show more interactions with regions of other chromosomes [110]. Similar observations were made in *Drosophila* [262]. Inactive domains occupy condensed, restricted territories, while active domains are far-reaching and participate in many more long-range interchromosomal associations [262].

In summary, chromatin modifications contribute to the long-range interactions between regions of DNA both within and across chromosomes, directly and indirectly (through recruitment of chromatin modifying enzymes and transcription factors), as well as the definition of territories of active and repressed gene expression. Chromatin and transcription adaptively regulate nuclear architecture to suit the genetic program of a cell throughout the development and lifespan of an organism.

H4K16ac regulates chromatin structure

Histone H4 modifications are important for transcription and the dosage compensation strategies in many organisms, so we decided to focus our studies in worms on these sites. Histone H4 can be acetylated on lysines 5, 8, 12, and 16 in animals, and additionally on lysine 20 in plants [264,265]. Studies employing site-specific antibodies have indicated that H4K16ac is most prevalent as the singly acetylated form of the H4 tail [266,267]. In newly produced histone tails, H4K5 and K12 are acetylated first [268]. In contrast, the order of acetylation of lysines following K16 on pre-existing H4 tails occurs in a C- to N-terminal fashion: from K12 toward K5 [269]. This acetylation pattern on the H4 tail is conserved among humans, mice, yeast, and *Tetrahymena*, highlighting the fundamental importance and conservation of the H4 acetylation mechanism [270].

Regulation of K16 acetylation is unique among H4 lysines [264], due to the mechanistic importance of this modification. Regulation of H4K16ac is achieved by the balance between MYST domain histone acetyltransferase (HAT) and class I and III histone deacetylase (RPD3 and Sir2 family HDAc) activities [271]. However, recent evidence suggests that this acetylation/deacetylation balance is quite complex. In humans, SIRT1 (a Sir2 homolog) activity is needed to limit hMOF (MYST HAT) auto-acetylation to promote hMOF binding to DNA [272]. This work also suggested that direct regulation of MYST HAT activity by HDAC proteins is conserved across species, including additional mammalian systems, *C. elegans* , and *D. melanogaster* [272]. This mechanism indicates that both direct and indirect methods are used by the deacetylase SIRT1 to regulate histone acetylation.

H4K16ac plays a unique and critical role in modulating chromatin structure (Fig. 1.9a). This modification directly affects the structure of the chromatin fiber. H4K16ac negates the positive charge of the histone H4 tail, destabilizes its native α-helical conformation, and disrupts the interaction of the H4 tail with the H2A/H2B dimer surface acidic patch [239,273]. H4K16ac thus triggers chromatin unfolding by disrupting the interactions between nearby nucleosomes. Sedimentation assays, which evaluate the degree of nucleosome array folding as a proxy for the 30nm fiber, have demonstrated that H4K16ac inhibits intra-association of nucleosomes [274,275]. Tetra-acetylated H4 does inhibit intra-array folding more than H4K16ac alone, suggesting that additional acetylation of the H4 tail further disrupts nucleosome folding [274,275]. Acetylation of K16 also perturbs the self-aggregation of nucleosome arrays, indicative of higher-order folding [274,275]. Mutation of K16 to glutamine, an acetyl-lysine mimic, does not lead to nucleosome array decompaction, indicating that the lysine at position 16 is critical for decompaction [276]. Array self-aggregation is further prevented using histone H4 tail forms carrying multiple acetylations [274].

H4K20me1 antagonizes H4K16ac and is an intermediary in heterochromatin formation

Histone H4 lysine 20 can be mono-, di-, or trimethylated [277]. H4K20me1 is catalyzed by PR-SET7/Set8 [278,279], and Ash1 in Drosophila [280], while H4K20me2/3 are the action of SUV4-20 [281,282]. Evidence suggests that Suv4-20h can di- and tri-methylate H4K20 in the absence of PR-SET7 action, at least in the context of heterochromatin [281,283]. However, the relationship between these two marks is complex. H4K20 methylation antagonizes H4K16ac *in vitro* and *in vivo* [279,284]. Thus, H4K20 methylation is regarded an important regulator of gene expression [279,284-286]. Other work suggests that H4K20me1 and H4K16ac significantly overlap at the β-globin locus, indicating that these marks coexist in certain contexts [287].

The effect of H4K20me1 on chromatin also varies with context. H4K20me1 is associated with active genes in some cases [288-291] and with transcriptional repression in other instances [292-295]. H4K20me1 is known to induce chromatin compaction through recruitment of MBT domain proteins (Fig. 1.9b) [296,297]. This modification is found in the same domain as other repressive marks in many systems, and H4K20me1 is thought to regulate facultative heterochromatin packaging and promote a transition to H4K20me3 enrichment typical of constitutive heterochromatin [244,292,293,298-301]. In some contexts, however, H4K20me3 and heterochromatin are thought to form in an H3K9me3-, HP1-depedent, H4K20me1-independent manner, and no increase in H4K20me1 was seen with knockdown of the H4K20 di-and trimethylase Suv4-20h [281]. From these results, H4K20me1 dependence or independence could be indicative of varying degrees of heterochromatinization or the potential for reversion to a more euchromatic state. Depletion of PR-Set7 results in decondensed chromosomes, consistent with a role for this protein in chromatin compaction [302]. H4K20me1 is required for binding of malignant brain tumor (MBT) domain-containing proteins implicated in chromatin compaction. This mechanism is not fully understood, but it may involve MBT protein binding to multiple nucleosomes, DNA bending, or bridging of neighboring nucleosomes through MBT domain dimerization [297,303,304].

Dosage compensation regulates chromatin modifications across organisms

In mammals, Xist action recruits chromatin modifying enzymes to the inactive X, and their action enriches repressive chromatin modifications (including H3K27me3) and depletes activating modifications (such as H4 acetylation) on that chromosome. A full list of the chromatin modification differences between mammalian female X chromosomes is located in Fig. 1.3b [95,98,105]. See Suganuma and Workman, 2011 for a full account of known modifications, their functions, modifying enzymes, and domain associations to many known chromatin modifications [255]. Subtle differences in level or onset of chromatin changes across all mammals have been noted for certain species [102,120,305].

Recent studies have focused on uncovering the characteristics and importance of genes found to escape X inactivation [94,306-313]. These genes have a chromatin profile similar to genes on the active X [312], suggesting bi-allelic expression of these genes is either critical or not harmful to the organism. Interestingly, X inactivation escapees also loop out, away from the *Xist* domain, perhaps making them more accessible to the transcription machinery [312].

In flies, MSL complex association with chromatin depends in large part on specific histone modifications. The chromodomain of MSL-3 interacts with H3K36me3 and H4K20me1, and these interactions, along with direct DNA binding, stabilize MSL complex association to the X chromosomes [72,74,132-134]. It is interesting to note that H4K20me1 is important for localization of the MSL complex, given that this mark antagonizes H4K16ac, the modification enriched on X by MOF action. This link likely contributes to the model of ratcheted MSL complex spreading proposed by Akhtar and others [133,134,314]. In this model: 1) the MSL complex binds H3K36me3, DNA [314], and H4K20me1 [133,134]; 2) MOF acetylates H4K16 and MSL-3 [314]; 3) MSL-3 is deacetylated to facilitate binding to a nearby site for the process to repeat [314].

Chromatin modification by the MSL complex is also essential to its action. H4K16ac is enriched on the X chromosomes by MOF and the rest of the MSL complex. H4K16ac is known to both open chromatin and, along with H3S10ph, increase transcriptional elongation and overcome RNA polymerase II stalling [129,138,315-317].

Dosage compensation in birds is mechanistically similar to that of flies [92]. H4K16ac is increased at an important locus that must only be transcribed in females, male hypermethylated (MHM), which is thought to produce a gene product that deactivates a DNA methylase important for execution of additional dosage compensation between the sexes in males [92,318]. This compensatory effect appears to occur on a gene-by-gene basis, not on a Z chromosome-wide level.

Work from our lab and another has highlighted the role of the H2A variant, H2A.Z/HTZ-1 in DCC regulation in *C. elegans* [319,320]. HTZ-1 demonstrates a bias toward the 5' end of genes across species, but it is associated with both activation and repression in a context-dependent manner [289,320-326]. HTZ-1 is depleted on X in hermaphrodite soma and germline [319]. DPY-30 functions in the COMPASS complex, which travels with RNA polymerase II to reinforce active transcription by placing the chromatin modification H3K4me3 [327-332], a role thought to be distinct from participation of DPY-30 in dosage compensation [198].

Recent work published by the modENCODE consortium surveyed many histone modifications by ChIP-chip and ChIP-seq methodologies [333,334]. In this work, numerous differences between the X chromosomes and autosomes at two developmental time points (early-biased embryonic and larval stage 3 samples) were documented [333,334] , but not investigated in further detail. These authors, and my work, found that levels of H4K20me1 are highly enriched on X at both time points and that many modifications, including H4K16ac and others associated with activation, are present at reduced levels on X compared to autosomes [64,333,334]. Chapter 2 of this thesis focuses on our work describing the role the DCC plays in regulating the balance between H4K16ac and H4K20me1 on the X chromosomes, facilitating a more repressive chromatin environment [335]. Further, in Chapter 3, I will present our work elaborating on these studies to examine levels of histone modifications and other features at dosage compensated and non-dosage compensated genes.

The RNA polymerase II transcription cycle

The sequence of events leading to transcription by RNA polymerase II (Fig. 1.10) has been well characterized [336-341]. Environmental or developmental cues stimulate general transcription factor and chromatin remodeler binding to target loci [337]. The histone acetyltransferase CBP-1 is known to play a vital role in opening the chromatin for general transcription factor binding at target loci through Polycomb antagonism by acetylation of H3K27 [342]. General transcription factor binding leads to recruitment of additional activators and the chromatin remodeler SWI/SNF [343] that prepares the promoter for Pol II recruitment. General transcription factors (GTFs) and Mediator work together to recruit RNA polymerase II (RNA Pol II) to the DNA, completing formation of the preinitiation complex, or PIC [344,345]. RNA Pol II is phosphorylated by CDK7, the catalytic subunit of TFIIH, at the serine 5 residues of the c-terminal domain (CTD) heptad repeat (PSer5) [346-349]. This signals the first stage of polymerase initiation, allowing it to release from the PIC [336,337,350]. However, TFIIH action is not required for transcription in *Saccharomyces cerevisiae* [347]. Some of the GTFs remain with RNA Pol II as it transcribes, while others remain at the promoter [336,337].

The RNA Pol II CTD is composed of a number of heptad amino acid repeats (YSPTSPS), which varies in length across species from 26 in yeast, to 45 in Drosophila, and 52 in mammals [351]. The *C. elegans* RNA Pol II (AMA-1) CTD contains 42 heptad repeats [352]. The gene name, AMA-1, refers to the α-amanatin drug sensitivity, which stops transcription by acting on RNA Pol II itself [353].

In most systems, the upstream portion of the CTD conforms well to the consensus repeat sequence (YSPTSPS), while the downstream portion includes minimal to moderate degeneracy (Fig. 1.11a) [354]. In more removed phyla, there is a tendency away from the consensus CTD repeat structure, but the length of 7 amino acids per repeat remains consistent (Fig. 1.11a) [354]. In *C. elegans*, this is not exactly the case. Instead, there is degeneracy, especially at the 4 and 7 positions throughout the CTD (Fig. 1.11b - Figure 11 from Bird and Riddle 1989), such that these two residues deviate from consensus approximately half of the time (Fig. 1.11c - Figure 11 from Bird and Riddle 1989) [352]. Selective mutational analyses of the AMA-1 CTD identified residues critical for susceptibility to transcription inhibitor drug treatment [352,355-357]. It is possible, but not established, that the greater deviation from a consensus CTD confers specific benefits to *C. elegans* RNA Pol II or affects transcription. One possibility is that these deviations somehow impede the fidelity of transcriptional elongation in such a way that compensates for the loss of the stalling factor NELF, which has not been identified in *Caenorhabditis* species [358].

RNA polymerase II initiation proceeds in three steps. First, the partially initiated polymerase scans the promoter for the transcription start site. Abortive initiation, or promoter proofreading, occurs if less than 5 nucleotides can be transcribed, which depends on the strength of contacts between Pol II and DNA as well as transcription factor occupancy [359]. In further steps, the length of the nascent transcript increases to 10 nucleotides, which disrupts connections to TFIIB, favors promoter escape, and greatly increases likelihood of elongation; then, nascent transcripts that reach 25 nucleotides reach a third state, the stable elongation complex [359]. Initiated RNA Pol II recruits, via CTD serine 5 phosphorylation, the stalling and elongation factor *DRB-induced sensitivity factor* (DSIF), so named because treatment with DRB (5,6 dichloro-beta-D-ribofuranosylbenzimidazole) causes inhibition of transcription elongation by blocking TFIIH action in a manner dependent upon this protein complex [360-362] . DSIF is a heterogeneous protein complex composed of SPT-4 (a small regulator subunit) and SPT-5 (the large catalytic subunit) [358,360,363]. At some proportion of genes, RNA Pol II stalls, meaning that transcription elongation ceases, either in a reversible or an irreversible manner [364], around 70bp downstream of the transcription start site [336,337]. It is thought that stalling is a rate-limiting step in transcription for ~20% of genes in mammals and as much as 50% of genes in flies [365-372]. However, mounting evidence suggests that the process of stalling is a general feature of transcription, perhaps occurring at all loci, but happening in a transient manner at the remainder of genes [336,365,366,370,371]. Reversible stalling of RNA Pol II is also referred to as pausing [364,372]. Pausing occurs in a DSIF and NELF (negative elongation factor)-dependent manner and is overcome by sufficient recruitment of the positive elongation factor-b complex, P-TEFb [336,337,358,373-380]. Recent evidence has shown that cohesin is selectively recruited to paused genes, and that cohesin function is critical for pausing [381].

Irreversible stalling of RNA Pol II is also referred to as arrest [364,382-388]. Arrest can be triggered by the base pair sequence in the DNA, variation in RNA-DNA hybrid length, nucleosome positioning, and local chromatin composition [389-398]. Arrest occurs when the RNA Pol II molecule encounters a physical barrier, causing loss of alignment of the nascent transcript to the polymerase holoenzyme, and resulting in unproductive elongation and transient backtracking along a short region of DNA [389-398]. If the barrier to elongation is a nucleosome, a collision from a second polymerase molecule can push the first RNA Pol II through the barrier [399]. In many cases, however, realignment of the nascent transcript to the RNA Pol II active site is necessary. This is accomplished through nascent transcript cleavage by TFIIS [383,390,400]. TFIIS is necessary for viability in some, but not all organisms, and some work has suggested that 18 nucleotide transcripts cleaved by TFIIS participate in transcriptional activation [401-404]. Serine 5 phosphorylation and DSIF recruitment are required for recruitment of the 5' capping enzyme and capping, which are necessary for mRNA stability [405-409].

After arrest or to overcome pausing, DSIF and the local chromatin recruit PTEF-b away from a 7SK RNA-containing sequestration complex in an elaborate mechanism that involves activators including BRD4 or c-myc [315,365,376,410]. P-TEFb then phosphorylates both DSIF (on the SPT-5 subunit) and the serine 2 residues of the RNA Pol II CTD, signaling the transition to productive transcriptional elongation [336,337,373-375,379]. In systems other than *C. elegans*, phosphorylation by P-TEFb also causes NELF dissociation from DSIF and RNA Pol II [361,380,411]. Once productive, RNA Pol II elongates through the gene body with less resistance due to chromatin modifications made cotranscriptionally by a suite of modifiers recruited by the productive complex, including FACT, COMPASS, SPT-6, and TIP60 [361,412-418], which reinforce features of active chromatin to promote subsequent rounds of transcription [418,419].

Mediator is an essential regulator of eukaryotic gene expression across species [420,421]. The complex is composed of up to 30 subunits that cluster into head, middle, and tail groups (Fig. 1.12a) [420], and 28 subunits are conserved in *C. elegans* (Fig. 1.12b) [420,421]. Mediator is critical for bridging interactions between RNA Pol II and transcription factors bound to regulatory DNA regions (Fig. 1.12c) [420,421]. RNA Pol II CTD phosphorylation promotes dissociation of Mediator binding during transcriptional elongation (Fig. 1.12c) [421-423]. Functional interplay between Mediator and DSIF has also been noted [424]. In *C. elegans*, Mediator is required for embryonic asymmetric cell divisions [425]. Interestingly, the DCC component-encoding *dpy-21* interacts with *dpy-22*, a mediator component, in a genetic assay for dosage compensation effects [204], and DPY-21 is thought to be a critical sensor of transcription for both sex determination and dosage compensation [205].

Dot1 is a histone methyltransferase with catalytic activity toward histone H3 lysine 79 [426,427]. Work from the Gerstein lab identified the histone modifications most closely associated with gene expression [428]. H3K79me2 and H3K79me3 (along with H3K4me2, comprised the top three [428], making these modifications good readouts for dosage compensation status. This enzyme, and its known homologs, are able to place one, two, or three methyl groups at this residue in any (not just a sequential) order [426,427]. Multiple Dot1 paralogs have been identified in *C. elegans*, and Y39G10AR.18 is the closest homolog [426,429,430]. Dot1 is thought to be recruited through ubiquitination of histone H2B at lysine 123, and it has been proposed that the COMPASS complex bridges this interaction [426,427]. Work using recent ChIP-chip datasets created by the modENCODE consortium has concluded that three histone modifications show a higher correlation with gene expression than RNA Pol II occupancy: H3K4me2, as well as H3K79me2, and H3K79me3 (Fig. 1.13) [428]. Surprisingly, H3K36me3, which has previously been well correlated with transcriptional elongation [431-433], but has recently been linked to heterochromatin and repression [434], does not show a similarly strong trend (Fig. 1.13) [428]. Dot1 action contributes to yeast telomeric silencing, but across organisms, this modification correlates best with active transcription [426,427]. Dot1 is not found in the superelongation complex nor AEP, but it is found in two other large complexes associated with transcriptional elongation, EAP and DotCom [427]. Dot1 occupancy and action has been characterized by ChIP-chip in *C. elegans* [333,334], and its relationship to dosage compensation will be examined further in Chapter 3.

The events of the transcription cycle occur countless times through the course of the life of any given organism and are critical to viability and fitness. Detailed experiments have shown that single molecule transcription occurs in a uniform kinetic manner on the order of 10-15nt/s of elongation, about 13 seconds between pauses, and pauses which last 1-5 seconds *in vitro* using *E. coli* transcription components [341,435,436].

Studying heat shock gene expression regulation offers a unique opportunity to dissect the mechanisms regulating inducible genes and the proteins that interact with RNA Pol II [437,438]. Heat shock factor is recruited to target genes to facilitate rapid changes in transcription in part through a sequence motif and an active chromatin state [439]. Heat shock factor facilitates nucleosome loss by redirecting poly(ADP-ribose) polymerase, or PARP, action from promoter restriction to a wave through target gene bodies [440,441]. PARP is known to interact with Condensin I at sites of DNA damage [442], and heat shock factor 2 facilitates condensin dephosphorylation by protein phosphatase 2A (PP2A) to ensure an open chromatin structure over hsp70i during mitosis [443]. Together, these data suggest a possible mechanism whereby heat shock factor antagonizes condensin action in mitosis to ensure heat shock gene inducibility, using the same machinery that functions in heat shock gene induction (PARP).

Enhancer function and regulation alter chromatin conformation and modulate gene expression

Enhancer elements (Figure 1.14A) are DNA sequences across the genome which can be bound by activator proteins, such as histone acetyltransferases. Upon activator binding and Mediator complex recruitment, these regions are capable of interacting with formed pre-initiation complexes (PICs) to form chromatin loops [444]. These loops are stabilized by cohesin action and may represent adjacent or physically distant DNA interactions [444]. Loops are broken apart to accommodate mitosis, but are reestablished in the next interphase [445] (Figure 1.14B). Enhancer loops play a critical role in transcription initiation, through Mediator recruitment, and downstream processes such as reformation of the PIC (Figure 1.14A). Enhancer activity state is often categorized by the complement of histone modifications and variants present at enhancer sites [446] (Figure 1.14C). While enhancers in general contain H3K4me1, active enhancers also possess H3K27ac, other active modifications, and marks associated with transcriptional elongation (Figure 1.14C). Conversely, off enhancers (for the purpose of this thesis) will be defined as those which lack these additional active modifications. Finally, poised enhancers, those which are ready for activation at a future time, tend to lack H3K27me3 at the gene promoter, but possess marks of activity at the enhancer site (Figure 1.14C). In sum, enhancers represent a crucial regulatory point for RNA Pol II recruitment and transcription initiation. In Chapter 3, I explore the possibility of enhancer regulation by *C. elegans* dosage compensation.

Regulation of transcription by chromatin modifiers

Yeast Set Complexes - H3K4 and H3K36 methylation are used to create an elaborate system of regulation of transcriptional elongation, which has been well described in yeast (Fig. 1.15) [447]. At promoter-proximal nucleosomes, H3K4me3 by the COMPASS complex (Set1) and interactions with transcriptional activators target NuA3 and NuA4 (TIP60) HAT complexes [448-450]. H3K4me3 can also interact with the Rpd3L HDAc complex to modulate acetylation levels near transcription start sites [451]. Just downstream, H3K4me2 targets the dual deacetylation activities (one Sir2-like and one Rpd3-like) of Set3C to the 5′ half of transcribed regions [452]. In the 3′ half of transcribed regions, H3K36 di- and trimethylation are necessary to target Rpd3S HDAc complex activity [453]. The combined outcome is greater promoter region accessibility due to acetylated nucleosomes that undergo rapid remodeling. In contrast, histones at downstream transcribed regions are more stably associated with the DNA due to higher methylation and lower acetylation levels [454]. Other work has shown that DSIF action is a chief antagonist of the slower transcription through the gene body induced by high methylation and low acteylation [455]. It remains unclear to what degree this signaling is conserved across species.

ISWI - H4K16ac disturbs the interactions of particular chromatin-associated proteins with the nucleosome, including the nuclear remodeler ISWI. ISWI is a member of the family of chromatin remodeling ATPases that promotes regularity of nucleosome spacing and chromatin folding [456-458]. The founding member of this family was the nucleosome remodeling factor NURF [458]. ISWI complexes bind the histone H4 N-terminal tail at amino acids 17–19, stimulating ISWI activity [459-461]. Acetylation of the nearby H4 lysines 12 and 16 impairs the ability of ISWI to recognize its target binding site, compact chromatin, and slide nucleosomes along DNA [275,459,461]. ISWI has been shown to function in Polycomb eviction [462] and is associated with HDAc activity [456]. The nucleosome remodeler SPT-6, which is recruited by the RNA Pol II stalling and elongation factor DSIF, cooperates with ISWI and TFIIS during transcription [463]. Paradoxically, ISWI action antagonizes action of the DSIF component SPT-4 [464].

SWI/SNF - SWI/SNF is a protein complex with nucleosome remodeling activity that promotes irregular nuclear spacing and assists in transcriptional activation [465-471]. Although, in some contexts, SWI/SNF is both an activator and a repressor of transcription [466,472,473]. SWI/SNF is just one of many similar remodeling complexes, such as NuRD [474]. SWI/SNF antagonizes ISWI function [475], and it is important for the heat shock response and RNA Pol II stalling [465,467,476]. SWI/SNF also contributes to incorporation of the histone H2A variant, H2A.Z [477-479].

RPD-3 - RPD-3 is an integral part of the numerous NURD (nucleosome remodeling and deacetylation) complexes [474]. Some RPD-3 complexes repress expression of germline genes in the soma [480]. Further, these complexes are recruited by Pol II P-CTD and DSIF [481] or H3K36-Me2 [482] and oppose aberrant transcription [455] by enforcing promoter and gene body transcriptional directionality [235,481,483]. Similarly, the FACT complex facilitates nucleosome remodeling that represses cryptic transcription [415,484-487]. RPD-3 also functions as a downstream PcG silencing effector complex [488], and shows an antagonistic genetic interaction with the Polycomb antagonist CBP-1 [489]. RPD-3 complexes are required for yeast heat-shock response [490]. Further, they inhibit recruitment of several RNA Pol II transcription activators and/or initiators [491] and cooperate with Sir2 in control of lifespan [492] and regulation of condensed, non-constitutive heterochromatin gene expression [493]. Interestingly, MuD-PIT experiments conducted in our lab identified several possible interactions between RPD-3 complex components and *C. elegans* DCC member proteins (Karishma Collette & Gyorgyi Csankovszki, unpublished data).

SIR-2.1 - Sirtuins are a conserved family of protein deacetylases [494]. Sir2/SirT1/Sir-2.1 is important for insulin signaling and the aging response [495]. Sir2 activity is directed toward histone H4 lysine 16, while other sirtuins are thought primarily to deacetylate non-histone proteins [496]. Sir2 is known to regulate transcription from the yeast mating type loci at a stage after Pol II recruitment [497]. Condensin has been previously shown to regulate Sir2 localization and Sir2-mediated rDNA silencing in budding yeast [498].

Transcriptional regulation by dosage compensation across species

RNA Pol II exclusion from the majority of genes on the inactive X chromosomes occurs relatively early in the X inactivation process [121]. Interestingly, this is before transcription from the inactive X has entirely stopped [121]. Genes that continue to be transcribed as escapers from dosage compensation are always found on the X periphery, associated with the transcription machinery, and away from *Xist* coverage [95,121].

In fly dosage compensation, the molecular mechanism of upregulation of the single male X chromosome is well understood. H4K16ac is enriched on X by MOF, a component of the MSL complex [129,499]. H3S10ph and H4K16ac cooperate to help RNA Pol II overcome transcriptional stalling [315,316]. GRO-seq analysis has shown that MSL complex action (H4K16ac) correlates well with an increase in transcriptional elongation on X [66].

In *C. elegans*, evidence suggests that dosage compensation acts primarily at the transcriptional level [172,173]. DPY-21 is thought to be both a dosage sensor and a regulator of transcription [204,205]. *dpy-21* is also known to interact with the Mediator component *dpy-22* [204]. More recent work has suggested that the DCC spreading involves transcription [173] and that the DCC regulates RNA Pol II occupancy [172], but further details are lacking. One interesting possibility to consider is that the function of DPY-30 in dosage compensation is linked to an evolutionarily conserved role in H3K4 methylation, but so far evidence contradicts this idea [172,198]. My work seeks, in part (see Chapter 4 and Further Directions), to address the mechanism of DCC-dependent gene regulation in greater detail.

Condensin regulates chromatin and transcriptional repression by an unknown mechanism

Condensin was first identified as a critical component of chromosome structure, with strong binding to DNA, in *Xenopus* [166,179,182,187]. The role of condensin in chromatin supercoiling has been thoroughly investigated [166]; however, multiple studies have indicated a role for condensin in the regulation of gene expression [17,18,53,156,498]; chief among them are studies of *C. elegans* dosage compensation [53,156]. Several clues have suggested a role for condensin in transcriptional control [172,173,381], but details as to its molecular contribution to gene expression are lacking.

My work seeks to address this question within the context of *C. elegans* dosage compensation at three levels: 1) How does the DCC contribute to repression on X through chromatin regulation? 2) How does DCC action affect RNA Pol II on the hermaphrodite X chromosomes? 3) What effects do chromatin and RNA Pol II regulators have on the DCC and its function? Chapter 2 focuses on the role of dosage compensation in controlling chromatin activity through regulation of the balance between H4K16ac and H4K20me1 and their regulator proteins. Chapter 3 details our studies of high-resolution chromatin datasets looking for the distinguishing features of dosage compensated and non-dosage compensated genes across development; also, I assess the contributions of HAT and HDAc protein-containing complexes to DCC localization and function. Chapter 4 explores the role of the DCC in control of RNA Pol II transcriptional elongation on X. Chapter 5 expands my research by putting forth our unresolved questions drawn from our overall conclusions and preliminary data for further interpretation and possible lines of further investigation. Finally, additional methods and experiments are listed in Appendix A. Within the Appendix, I discuss, among other topics, the molecular function of the poorly characterized DCC protein DPY-21. Collectively, this work uncovers novel molecular insights into the process by which the *C. elegans* dosage compensation machinery regulates chromatin and transcription to affect changes in gene expression.

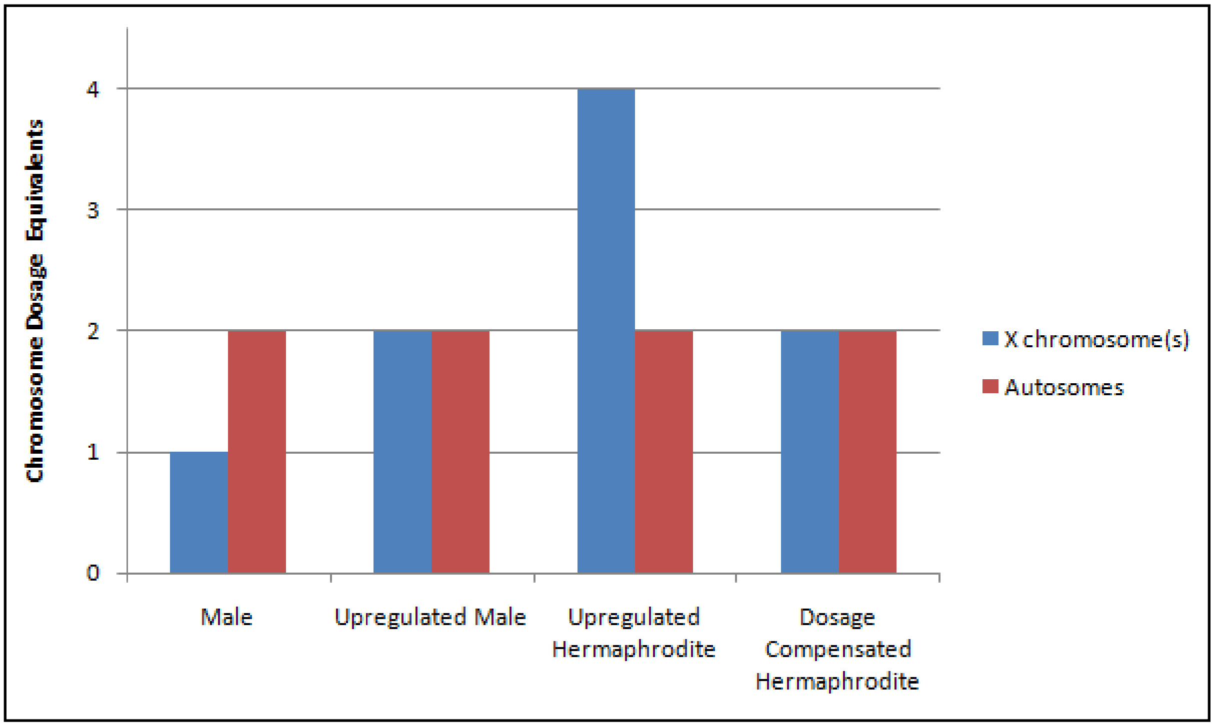

Figure 1.1. Chromosome dosage equalization theory. Male flies upregulate X-linked gene expression two-fold, leading to both X:XX equalization between the sexes and X:A equalization within each individual. In mammals and worms, however, the case is different. Shown here, it has been hypothesized by Ohno and others that X upregulation is non-sex specific in mammals (and others have suggested this may also be the case in worms). This leads to equalization of X:A within males, but causes X overexpression in females/hermaphrodites. Then, what we regard as dosage compensation restricts X-linked gene expression in the female/hermaphrodite, resulting in X:XX equalization between the sexes.

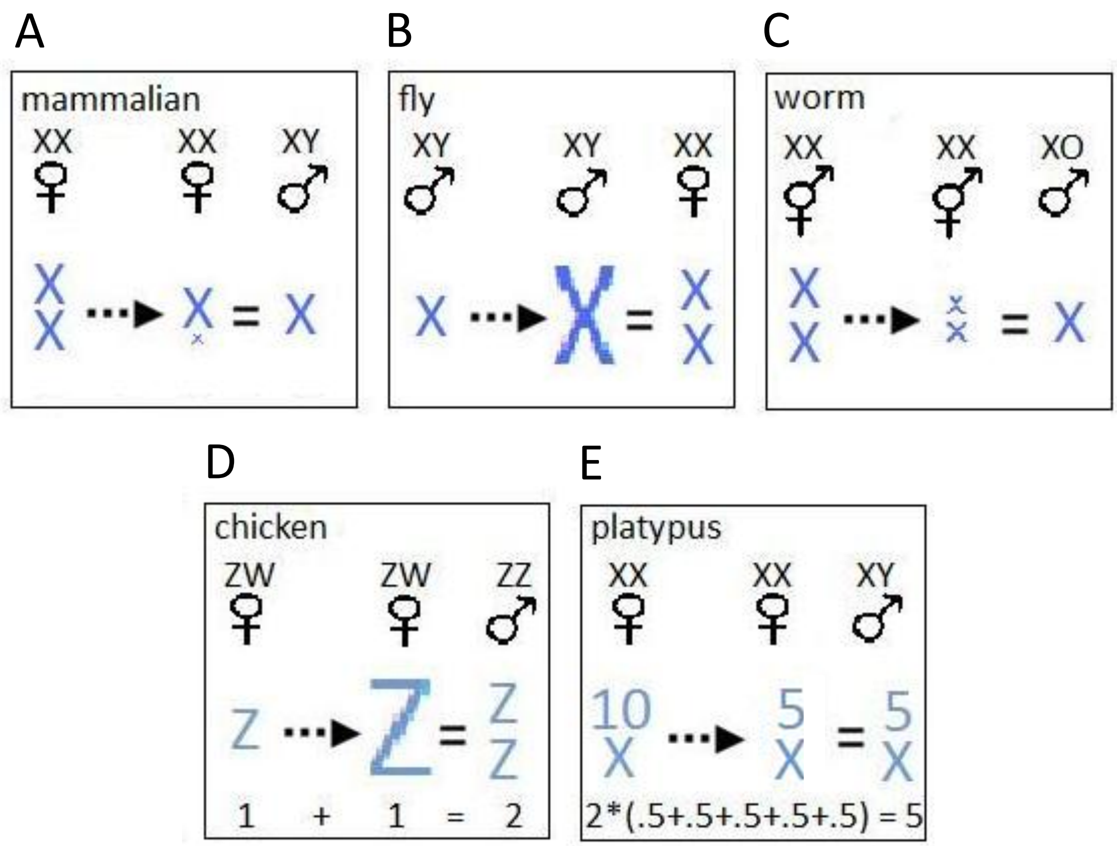

Figure 1.2. Known methods of dosage compensation. Shown are summary diagrams illustrating the major known methods of X-linked expression equalization by dosage compensation among species. A) In mammals, one X chromosome in females is transcriptionally inactivated (X inactivation). B) In flies, the single male X chromosome is transcriptionally upregulated two-fold. C) In worms such as *Caenorhabditis elegans*, expression from both hermaphrodite X chromosomes is halved. D) In chickens, important female loci are upregulated two-fold. Dosage compensation is not chromosome-wide, and females are the heterogametic sex. E) In platypuses, important genes are stochastically non-expressed, or expressed mono- or biallelically. Again, there is no chromosome-wide mechanism of dosage compensation in this species.

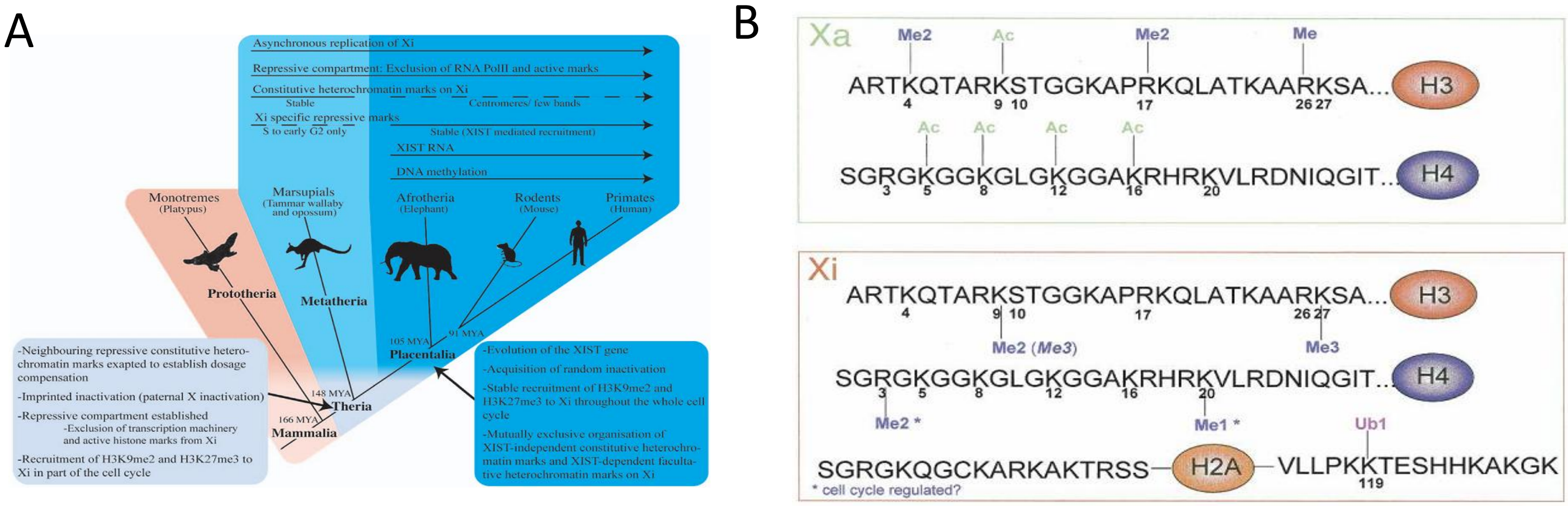

Figure 1.3. The evolution of and molecular mechanism of mammalian X inactivation. Diagrams were taken from: Chaumeil et al., 2011, PubMed ID: 21541345 (A); Heard and Disteche, 2006, PubMed ID: 16847345 (B). (A) illustrates the evolution of X inactivation. In (B), Xa is the active X and Xi is the inactive X. Shown are modifications enriched on either Xa or Xi compared to the other X chromosome.

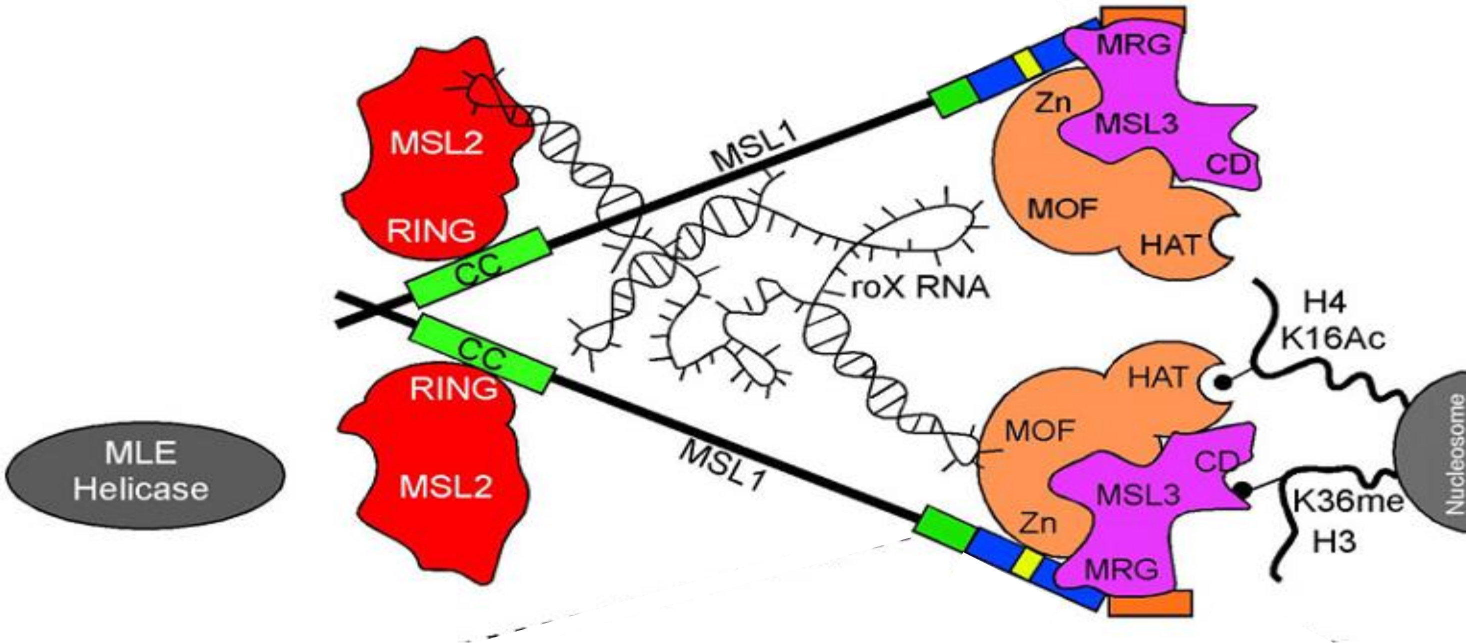

Figure 1.4. Known interactions between MSL complex members. Diagram taken from: Prabhakaran and Kelley, 2010, PubMed ID: 20537125. Notice the striking similarities between MSL complex and condensin structure (compare 1.4 and 1.5A). One interesting possibility is that this structure assists the MSL complex in promoting an open chromatin state, whereas worm DCC function leads to a more repressive chromatin state. This complex structure may be uniquely suited to the needs of chromatin modifying complexes that affect changes in transcriptional output.

A

B

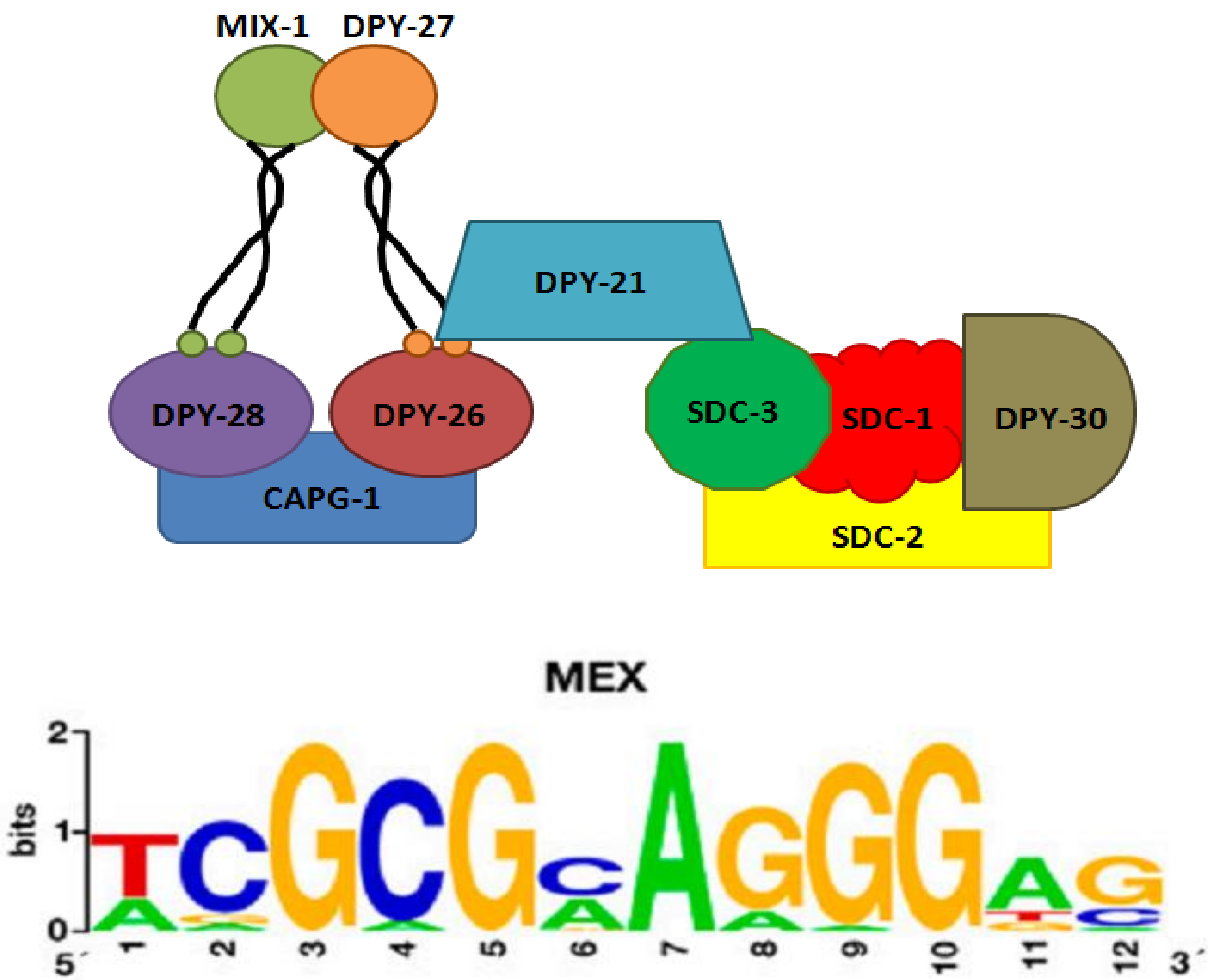

Figure 1.5. Worm Dosage Compensation Complex (DCC) composition and the identified sequence which contributes to DCC binding. Shown are: (A) a schematic diagram depicting the 10 protein DCC, which is composed of Condensin I^{DC} (CAPG-1, DPY-26, DPY-27, DPY-28, and MIX-1), a recruitment complex (SDC-1, SDC-2, and SDC-3), and two associated proteins with less well-characterized contributions to DCC function, DPY-21 and DPY-30; (B) The MEX motif [171] is mildly enriched on the X chromosomes and correlates well with DCC binding peaks.

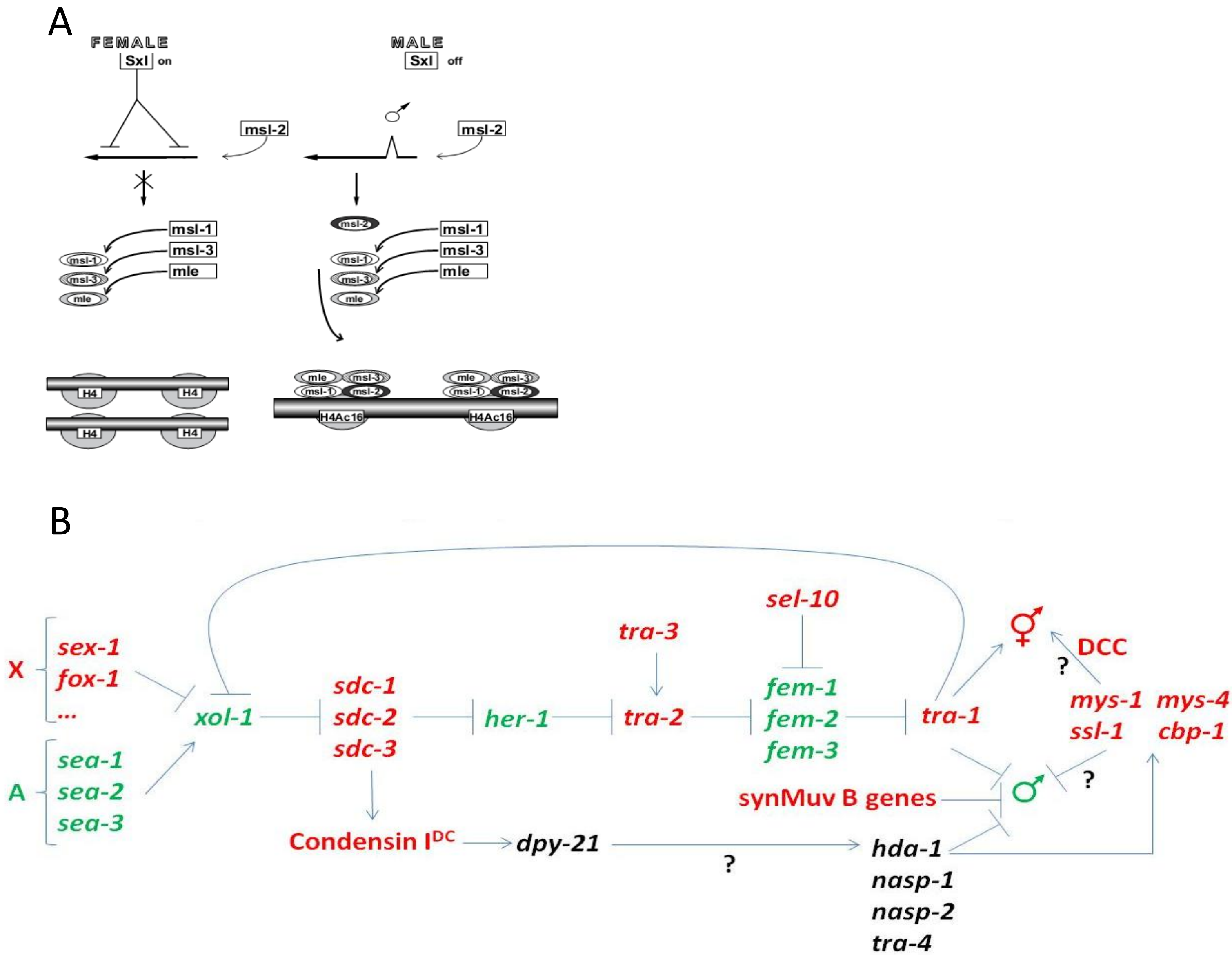

Figure 1.6. Molecular linkages between sex determination and dosage compensation in flies and worms. Shown are diagrams of sex determination and dosage compensation in flies and worms. These processes must be coupled in these species due to the chromosome counting methods of sex determination that each employs. The fly diagram (A) is taken from Bashaw and Baker, 1995, PubMed ID: 7588059, and the worm diagram (B) is a composite of information gathered from: Grote and Conradt, 2006, PubMed ID: 17011494, Gladden et al., 2007, PubMed ID: 17947428, and MW unpublished observations. All interactions are published, except for the following: the placement of *dpy-21*, *dpy-21* interactions with a TRA-4-containing complex, and placement and interactions of *mys-4* and *cbp-1*, as well as the function of *mys-1*, *ssl-1*, *mys-4*, and *chp-1* in hermaphrodites via dosage compensation.

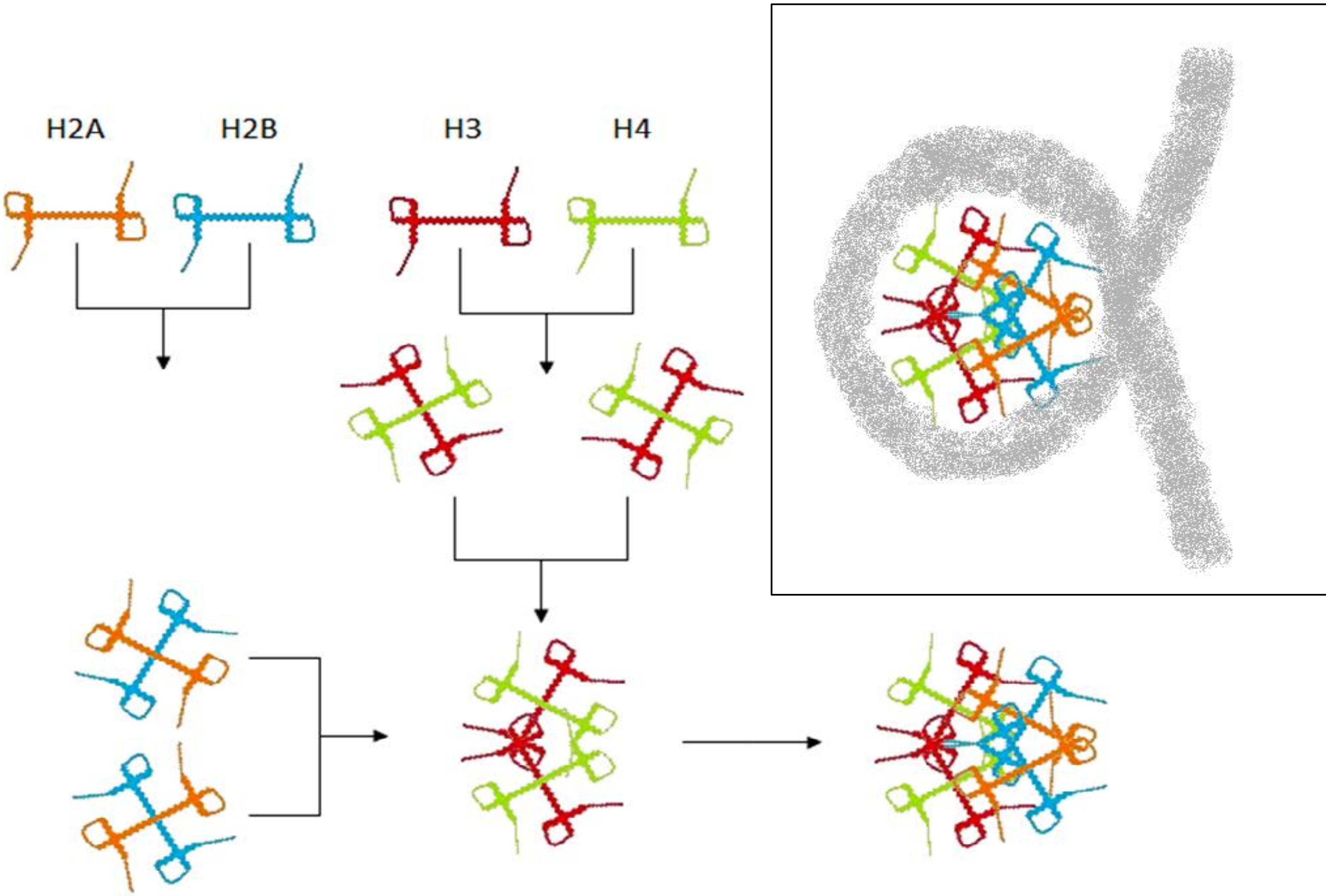

Figure 1.7. Nucleosome composition. Shown is a schematic diagram of nucleosome composition. Each nucleosome is made up of DNA interacting with 8 histone proteins, two copies each of histones H2A, H2B, H3, and H4 (or their respective variants). The H3-H4 tetramer is thought to form first, followed by H2A-H2B dimer interaction. Inset: Approximately 147bp of DNA (grey track) wraps twice around each histone octamer to form a nucleosome.

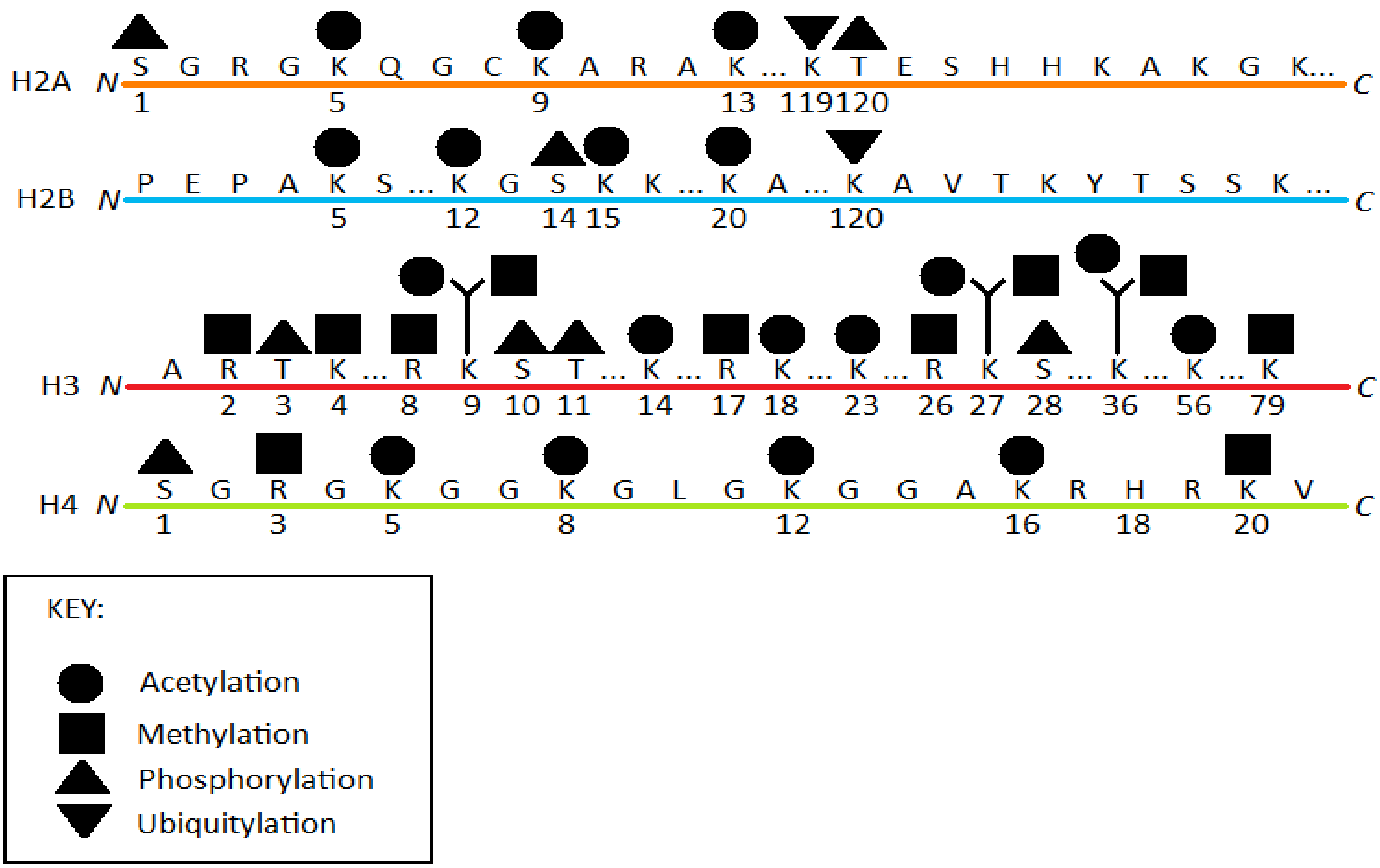

Figure 1.8. A selection of post-translational histone modifications. Shown is a schematic diagram of the N-terminal tail domains of each of the four major histones depicting sites and common types of known chemical modifications. This is not an exhaustive list.

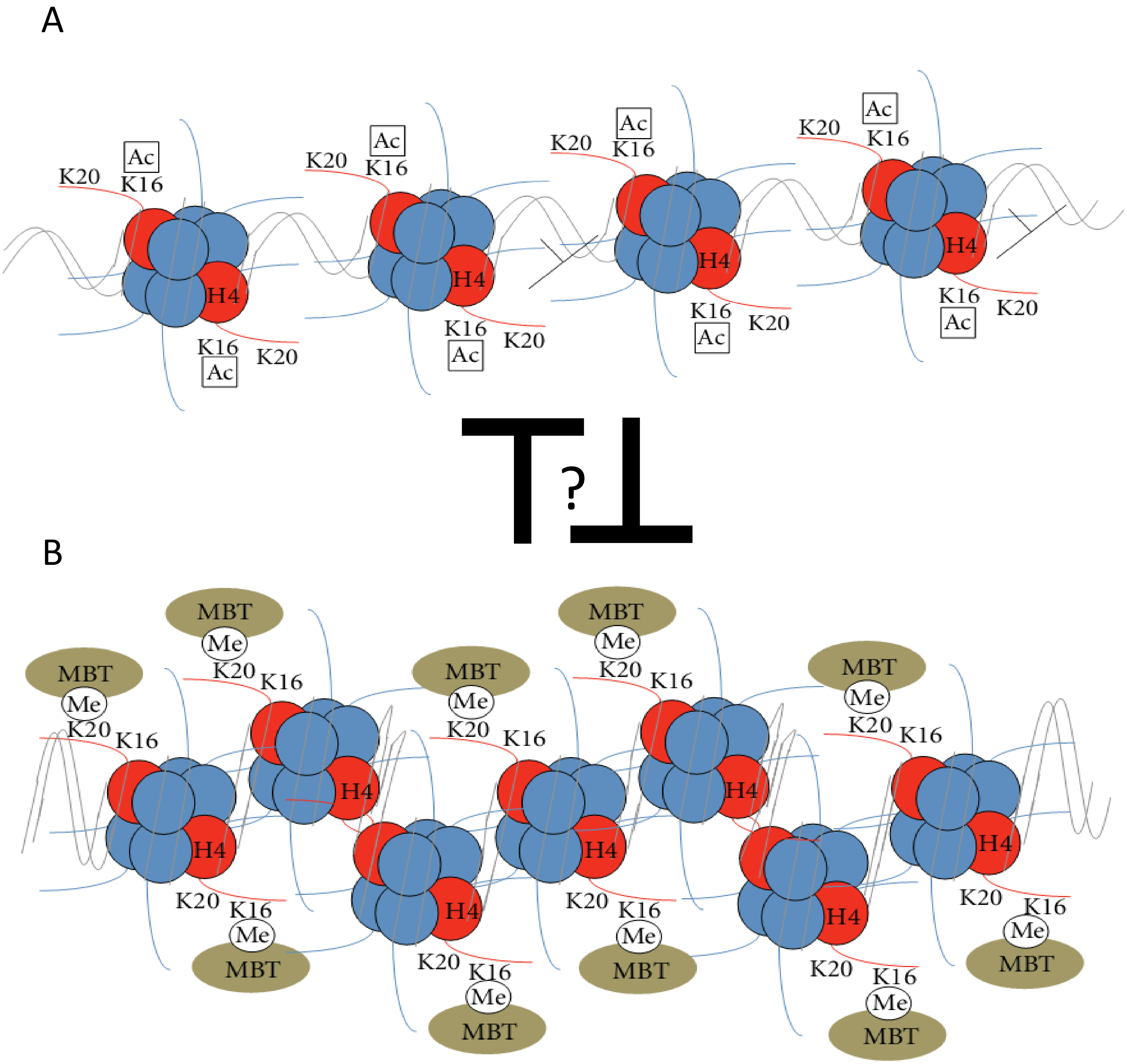

Figure 1.9. Effect of Histone H4 modification on chromatin state. Shown are schematic diagrams showing open H4K16ac-associated chromatin and closed H4K20me1-associated chromatin from Wells et al., 2012, PubMed ID: 22567401.

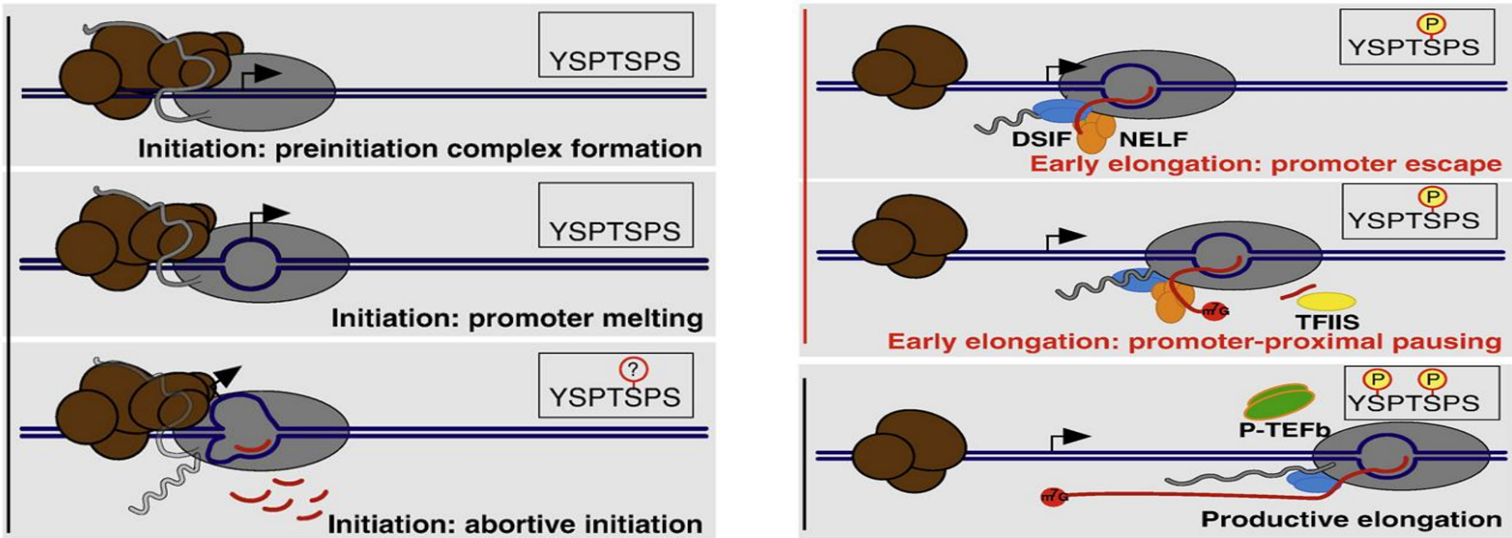

Figure 1.10. Steps in the RNA polymerase II transcription cycle. Shown are schematic diagrams depicting the stages in eukaryotic RNA Pol II transcription from Nechaev and Adelman, 2011, PubMed ID: 21081187.

A

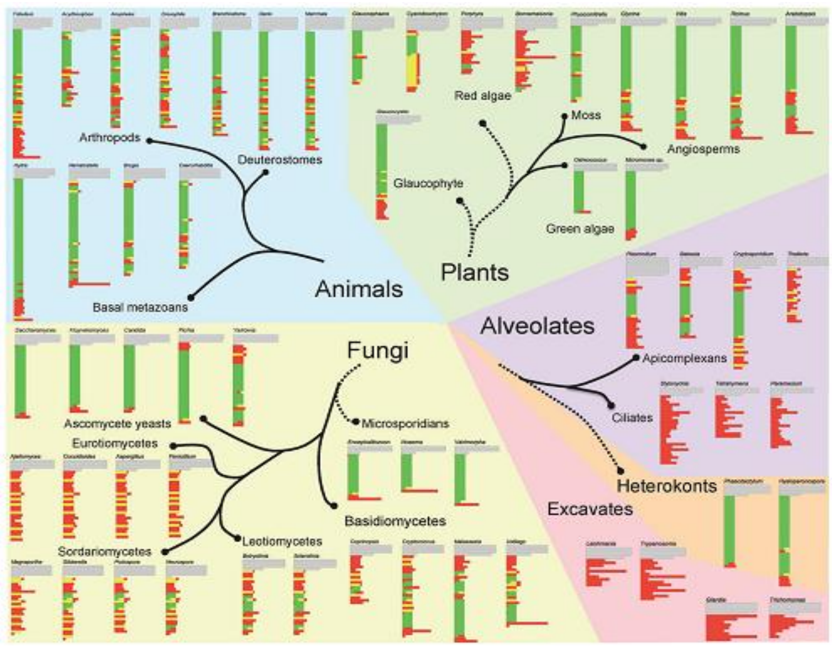

B

1	L	S	P	R	T	P	S		
2	Y	G	G	M	S	P	G	V	
3	Y	S	P	S	S	P	Q		
4	F	S	M	T	S	P	H		
5	Y	S	P	T	S	P	S		
6	Y	S	P	T	S	P	A	A	G
7	Q	S	P	V	S	P	S		
8	Y	S	P	T	S	P	S		
9	Y	S	P	T	S	P	S		
10	Y	S	P	T	S	P	S		
11	Y	S	P	T	S	P	S		
12	Y	S	P	T	S	P	S		
13	Y	S	P	T	S	P	S		
14	Y	S	P	S	S	P	S		
15	Y	S	P	S	S	P	S		
16	Y	S	P	S	S	P	R		
17	Y	S	P	T	S	P	T		
18	Y	S	P	T	S	P	T		
19	Y	S	P	T	S	P	T		
20	Y	S	P	T	S	P	T		
21	Y	S	P	T	S	P	S		
22	Y	E	S	G	G	G			
23	Y	S	P	S	S	P	K		
24	Y	S	P	S	S	P	T		
25	Y	S	P	T	S	P	S		
26	Y	S	P	T	S	P	Q		
27	Y	S	P	T	S	P	Q		
28	Y	S	P	S	S	P	T		
29	Y	T	P	S	S	P	T		
30	Y	N	P	T	S	P	R		
31	G	F		S	S	P	Q		
32	Y	S	P	T	S	P	T		
33	Y	S	P	T	S	P	S		
34	Y	T	P	S	S	P	Q		
35	Y	S	P	T	S	P	T		
36	Y	T	P	S	P	S	E		
37	Q	P	G	T	S	A	Q		
38	Y	S	P	T	S	P	T		
39	Y	S	P	S	S	P	T		
40	Y	S	P	A	S	P	S		
41	Y	S	P	S	S	P	T		
42	Y	D	P	N	S	*			

C

Y	S	P	T	S	P	S	CONSENSUS
			S			T	

Figure 1.11. Conservation of the RNA Pol II C-terminal domain across species. Shown are: (A) a schematic diagram across phyla of RNA Pol II structural C-terminal domain from Liu et al., 2010, PubMed ID: 20558594; (B) Amino acid composition of the C-terminal domain repeats in *C. elegans* AMA-1, and (C) The *C. elegans* RNA Pol II CTD repeat consensus sequence. (B & C) are taken from Bird and Riddle, 1989, PubMed ID: 2586513.

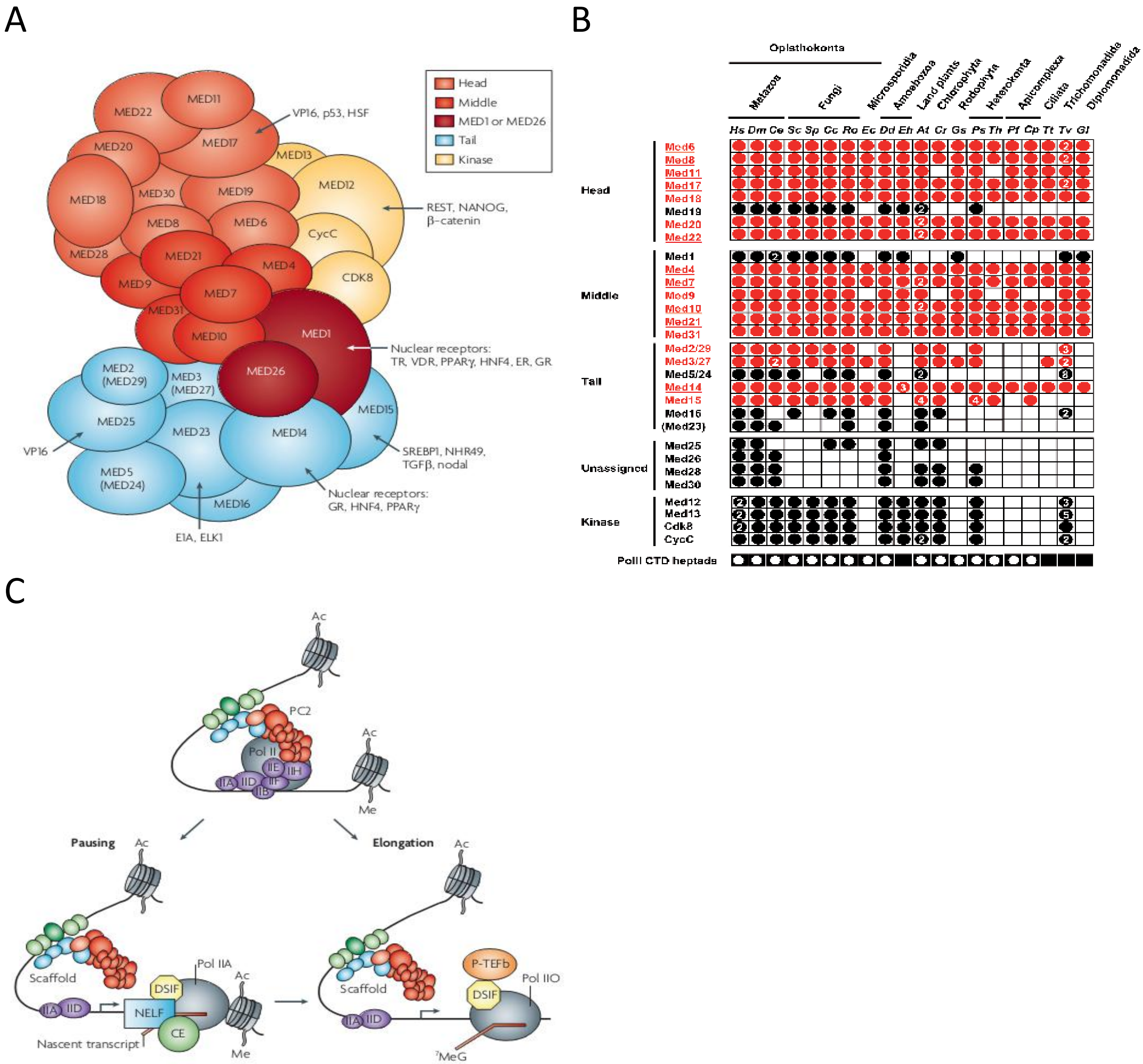

Figure 1.12. Mediator composition, conservation, and function in transcription initiation. Shown are schematic diagrams of human Mediator complex composition (A), conservation of Mediator components across species (B), and a schematic diagram of Mediator function to connect enhancer elements to the PIC for transcription initiation (C). (A & C) are taken from Malik and Roeder, 2010. (B) is taken from Bourbon, 2008, PubMed ID: 18515835.

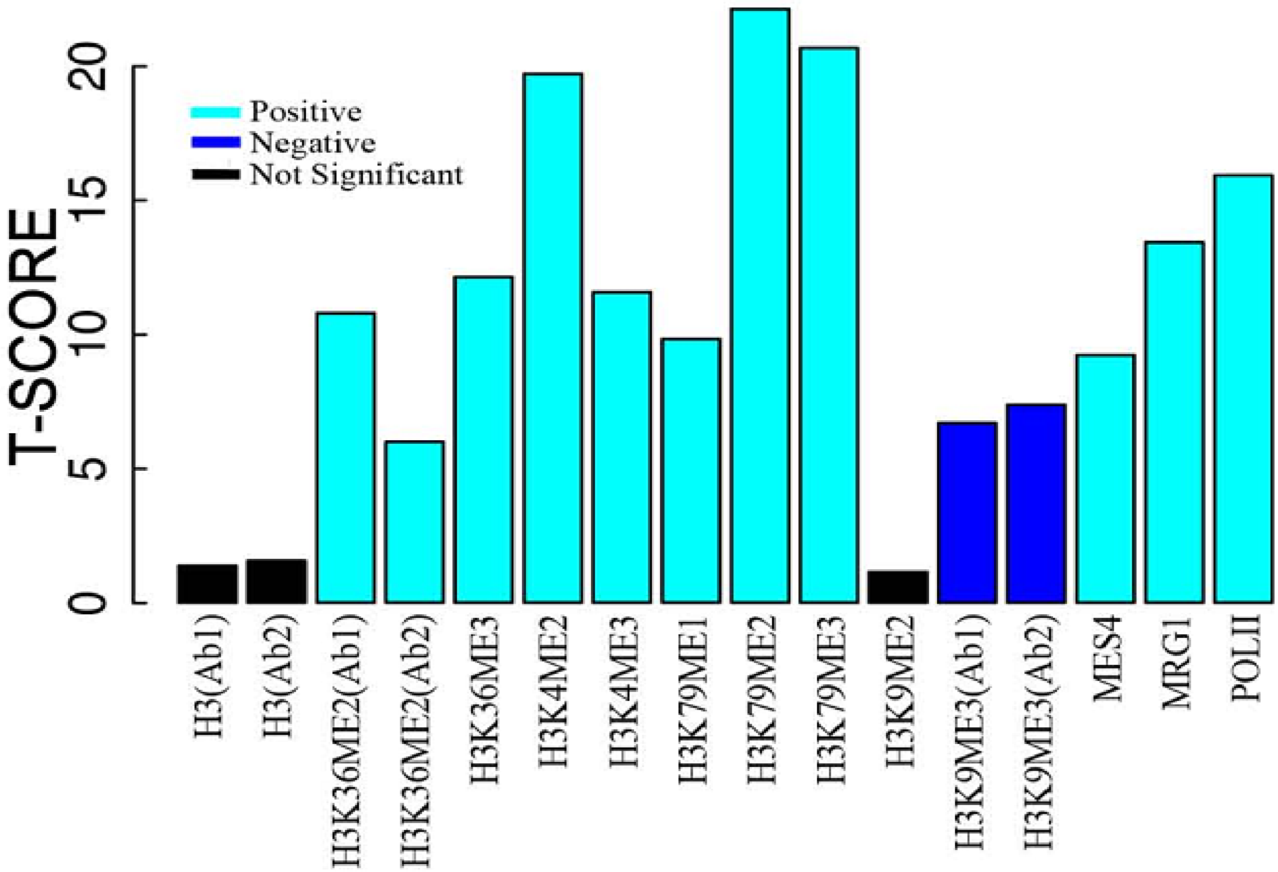

Figure 1.13. Correlation of histone modifications with transcriptional output. Shown is a graph depicting the strength of correlation (T-SCORE) between transcription (RNA-seq) and various histone modifications in *C. elegans*. This graph was taken from Cheng et al., 2011, PubMed ID: 21324173.

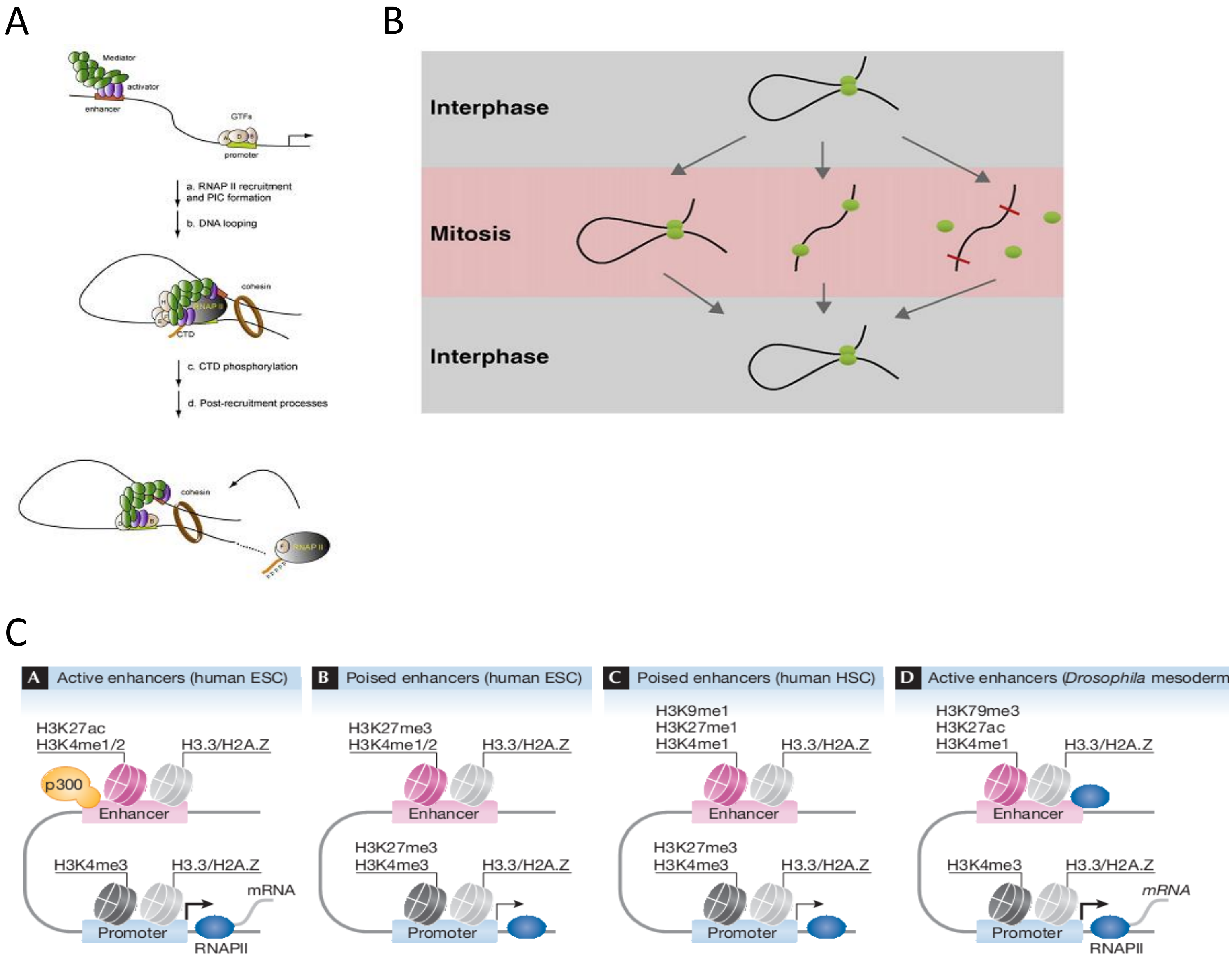

Figure 1.14. Enhancer element function. Shown are diagrams depicting basic enhancer-mediated looping (A), enhancer activity during mitosis (B), and the regulation of enhancers to control transcription (C). (A) is taken from Borggreefe and Yue, 2011, PubMed ID: 21839847. (B) is taken from Deng and Blobel, 2010, PubMed ID: 20598523. (C) is taken from Ong and Corces, 2011, PubMed ID: 22491032.

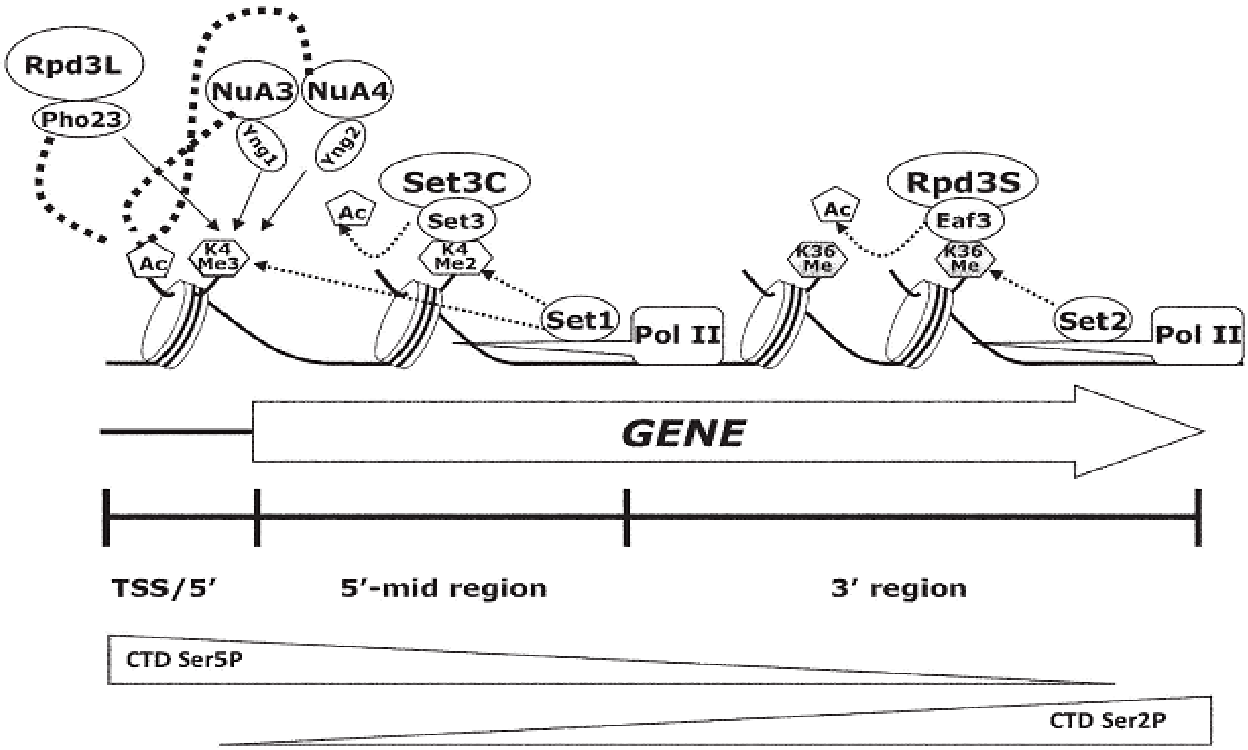

Figure 1.15. Cooperation by co-transcriptional histone methylations. Shown is a schematic diagram summarizing work indicating that co-transcriptional histone methylations are repressive in nature and help to distinguish active from repressed gene promoters. The diagram is taken from Buratowski and Kim, 2010, PubMed ID: 21447819.

References

1. Li GW, Xie XS (2011) Central dogma at the single-molecule level in living cells. Nature 475: 308-315.
2. Shapiro JA (2009) Revisiting the central dogma in the 21st century. Ann N Y Acad Sci 1178: 6-28.
3. Bustamante C, Cheng W, Mejia YX (2011) Revisiting the central dogma one molecule at a time. Cell 144: 480-497.
4. Henikoff S (2002) Beyond the central dogma. Bioinformatics 18: 223-225.
5. Cooper S (1981) The central dogma of cell biology. Cell Biol Int Rep 5: 539-549.
6. Crick F (1970) Central dogma of molecular biology. Nature 227: 561-563.
7. Schreiber SL (2005) Small molecules: the missing link in the central dogma. Nat Chem Biol 1: 64-66.
8. Robinson VL (2009) Rethinking the central dogma: noncoding RNAs are biologically relevant. Urol Oncol 27: 304-306.
9. Maydanovych O, Beal PA (2006) Breaking the central dogma by RNA editing. Chem Rev 106: 3397-3411.
10. Cooper MD, Alder MN (2006) The evolution of adaptive immune systems. Cell 124: 815-822.
11. Huston DP (1997) The biology of the immune system. JAMA 278: 1804-1814.
12. Biro JC (2004) Seven fundamental, unsolved questions in molecular biology. Cooperative storage and bi-directional transfer of biological information by nucleic acids and proteins: an alternative to "central dogma". Med Hypotheses 63: 951-962.
13. Tonegawa S (1993) The Nobel Lectures in Immunology. The Nobel Prize for Physiology or Medicine, 1987. Somatic generation of immune diversity. Scand J Immunol 38: 303-319.
14. Davis MM, Bjorkman PJ (1988) T-cell antigen receptor genes and T-cell recognition. Nature 334: 395-402.
15. Li Z, Woo CJ, Iglesias-Ussel MD, Ronai D, Scharff MD (2004) The generation of antibody diversity through somatic hypermutation and class switch recombination. Genes Dev 18: 1-11.
16. Nussenzweig MC (1998) Immune receptor editing: revise and select. Cell 95: 875-878.
17. Rawlings JS, Gatzka M, Thomas PG, Ihle JN (2011) Chromatin condensation via the condensin II complex is required for peripheral T-cell quiescence. EMBO J 30: 263-276.
18. Gosling KM, Goodnow CC, Verma NK, Fahrer AM (2008) Defective T-cell function leading to reduced antibody production in a kleisin-beta mutant mouse. Immunology 125: 208-217.
19. Seitan VC, Hao B, Tachibana-Konwalski K, Lavagnolli T, Mira-Bontenbal H, et al. (2011) A role for cohesin in T-cell-receptor rearrangement and thymocyte differentiation. Nature 476: 467-471.
20. Wood AJ, Bickmore WA (2011) A condensed view of chromatin during T cell development. EMBO J 30: 235-236.
21. Hagstrom KA, Meyer BJ (2003) Condensin and cohesin: more than chromosome compactor and glue. Nat Rev Genet 4: 520-534.
22. Hagstrom KA, Holmes VF, Cozzarelli NR, Meyer BJ (2002) C. elegans condensin promotes mitotic chromosome architecture, centromere organization, and sister chromatid segregation during mitosis and meiosis. Genes Dev 16: 729-742.
23. Wood AJ, Severson AF, Meyer BJ (2010) Condensin and cohesin complexity: the expanding repertoire of functions. Nat Rev Genet 11: 391-404.
24. Perfeito L, Ghozzi S, Berg J, Schnetz K, Lassig M (2011) Nonlinear fitness landscape of a molecular pathway. PLoS Genet 7: e1002160.

25. Dobrzynski M, Bernatowicz P, Kloc M, Kubiak JZ (2011) Evolution of bet-hedging mechanisms in cell cycle and embryo development stimulated by weak linkage of stochastic processes. Results Probl Cell Differ 53: 11-30.
26. Baryshnikova A, Costanzo M, Kim Y, Ding H, Koh J, et al. (2010) Quantitative analysis of fitness and genetic interactions in yeast on a genome scale. Nat Methods 7: 1017-1024.
27. Fontanillas P, Landry CR, Wittkopp PJ, Russ C, Gruber JD, et al. (2010) Key considerations for measuring allelic expression on a genomic scale using high-throughput sequencing. Mol Ecol 19 Suppl 1: 212-227.
28. Ohno S (1967) Sex chromosomes and sex-linked genes. Berlin, New York [etc.]: Springer-Verlag. x, 192 p. p.
29. Holmquist G (1972) Transcription rates of individual polytene chromosome bands: effects of gene dose and sex in Drosophila. Chromosoma 36: 413-452.
30. Lundgren M, Chow CM, Sabbattini P, Georgiou A, Minaee S, et al. (2000) Transcription factor dosage affects changes in higher order chromatin structure associated with activation of a heterochromatic gene. Cell 103: 733-743.
31. Epstein CJ (1990) The consequences of chromosome imbalance. Am J Med Genet Suppl 7: 31-37.
32. Cupisti S, Conn CM, Fragouli E, Whalley K, Mills JA, et al. (2003) Sequential FISH analysis of oocytes and polar bodies reveals aneuploidy mechanisms. Prenat Diagn 23: 663-668.
33. Terry J H (1986) Chromosome abnormalities in human reproductive wastage. Trends in Genetics 2: 105-110.
34. Greber-Platzer S, Schatzmann-Turhani D, Cairns N, Balcz B, Lubec G (1999) Expression of the transcription factor ETS2 in brain of patients with Down syndrome--evidence against the overexpression-gene dosage hypothesis. J Neural Transm Suppl 57: 269-281.
35. Reeves RH, Irving NG, Moran TH, Wohn A, Kitt C, et al. (1995) A mouse model for Down syndrome exhibits learning and behaviour deficits. Nat Genet 11: 177-184.
36. Murphy M, Epstein LB (1990) Down syndrome (trisomy 21) thymuses have a decreased proportion of cells expressing high levels of TCR alpha, beta and CD3. A possible mechanism for diminished T cell function in Down syndrome. Clin Immunol Immunopathol 55: 453-467.
37. Murphy M, Lempert MJ, Epstein LB (1990) Decreased level of T cell receptor expression by Down syndrome (trisomy 21) thymocytes. Am J Med Genet Suppl 7: 234-237.
38. Sarre SD, Ezaz T, Georges A (2011) Transitions between sex-determining systems in reptiles and amphibians. Annu Rev Genomics Hum Genet 12: 391-406.
39. O'Meally D, Ezaz T, Georges A, Sarre SD, Graves JA (2012) Are some chromosomes particularly good at sex? Insights from amniotes. Chromosome Res.
40. Uller T, Pen I, Wapstra E, Beukeboom LW, Komdeur J (2007) The evolution of sex ratios and sex-determining systems. Trends Ecol Evol 22: 292-297.
41. Godwin J (2009) Social determination of sex in reef fishes. Semin Cell Dev Biol 20: 264-270.
42. Livernois AM, Graves JA, Waters PD (2012) The origin and evolution of vertebrate sex chromosomes and dosage compensation. Heredity (Edinb) 108: 50-58.
43. Parma P, Radi O (2011) Molecular Mechanisms of Sexual Development. Sex Dev.
44. Salz HK (2011) Sex determination in insects: a binary decision based on alternative splicing. Curr Opin Genet Dev 21: 395-400.
45. Salz HK, Erickson JW (2010) Sex determination in Drosophila: The view from the top. Fly (Austin) 4: 60-70.
46. Matsuda M (2005) Sex determination in the teleost medaka, Oryzias latipes. Annu Rev Genet 39: 293-307.

47. Gladden JM, Farboud B, Meyer BJ (2007) Revisiting the X:A signal that specifies Caenorhabditis elegans sexual fate. Genetics 177: 1639-1654.
48. Carmi I, Meyer BJ (1999) The primary sex determination signal of Caenorhabditis elegans. Genetics 152: 999-1015.
49. Uller T, Badyaev AV (2009) Evolution of "determinants" in sex-determination: a novel hypothesis for the origin of environmental contingencies in avian sex-bias. Semin Cell Dev Biol 20: 304-312.
50. Yoshimoto S, Ito M (2011) A ZZ/ZW-type sex determination in Xenopus laevis. FEBS J 278: 1020-1026.
51. Clinton M, Zhao D, Nandi S, McBride D (2011) Evidence for avian cell autonomous sex identity (CASI) and implications for the sex-determination process? Chromosome Res.
52. Bradley KM, Breyer JP, Melville DB, Broman KW, Knapik EW, et al. (2011) An SNP-Based Linkage Map for Zebrafish Reveals Sex Determination Loci. G3 (Bethesda) 1: 3-9.
53. Meyer BJ (2010) Targeting X chromosomes for repression. Curr Opin Genet Dev 20: 179-189.
54. Cline TW (1993) The Drosophila sex determination signal: how do flies count to two? Trends Genet 9: 385-390.
55. Gempe T, Beye M (2011) Function and evolution of sex determination mechanisms, genes and pathways in insects. Bioessays 33: 52-60.
56. Sekido R, Lovell-Badge R (2009) Sex determination and SRY: down to a wink and a nudge? Trends Genet 25: 19-29.
57. Clepet C, Schafer AJ, Sinclair AH, Palmer MS, Lovell-Badge R, et al. (1993) The human SRY transcript. Hum Mol Genet 2: 2007-2012.
58. Behlke MA, Bogan JS, Beer-Romero P, Page DC (1993) Evidence that the SRY protein is encoded by a single exon on the human Y chromosome. Genomics 17: 736-739.
59. Su H, Lau YF (1993) Identification of the transcriptional unit, structural organization, and promoter sequence of the human sex-determining region Y (SRY) gene, using a reverse genetic approach. Am J Hum Genet 52: 24-38.
60. Deng X, Hiatt JB, Nguyen DK, Ercan S, Sturgill D, et al. (2011) Evidence for compensatory upregulation of expressed X-linked genes in mammals, Caenorhabditis elegans and Drosophila melanogaster. Nat Genet 43: 1179-1185.
61. Graves JA, Disteche CM (2007) Does gene dosage really matter? J Biol 6: 1.
62. Conrad T, Akhtar A (2012) Dosage compensation in Drosophila melanogaster: epigenetic fine-tuning of chromosome-wide transcription. Nat Rev Genet 13: 123-134.
63. Straub T, Becker PB (2011) Transcription modulation chromosome-wide: universal features and principles of dosage compensation in worms and flies. Curr Opin Genet Dev 21: 147-153.
64. Wells MB, Csankovszki G, Custer LM (2012) Finding a Balance: How Diverse Dosage Compensation Strategies Modify Histone H4 to Regulate Transcription. Genetics Research International 2012: 1-12.
65. Birchler J, Sun L, Fernandez H, Donohue R, Xie W, et al. (2011) Re-evaluation of the function of the male specific lethal complex in Drosophila. J Genet Genomics 38: 327-332.
66. Larschan E, Bishop EP, Kharchenko PV, Core LJ, Lis JT, et al. (2011) X chromosome dosage compensation via enhanced transcriptional elongation in Drosophila. Nature 471: 115-118.
67. Georgiev P, Chlamydas S, Akhtar A (2011) Drosophila dosage compensation: males are from Mars, females are from Venus. Fly (Austin) 5: 147-154.

68. Kadlec J, Hallacli E, Lipp M, Holz H, Sanchez-Weatherby J, et al. (2011) Structural basis for MOF and MSL3 recruitment into the dosage compensation complex by MSL1. Nat Struct Mol Biol 18: 142-149.
69. Fauth T, Muller-Planitz F, Konig C, Straub T, Becker PB (2010) The DNA binding CXC domain of MSL2 is required for faithful targeting the Dosage Compensation Complex to the X chromosome. Nucleic Acids Res 38: 3209-3221.
70. Park SW, Oh H, Lin YR, Park Y (2010) MSL cis-spreading from roX gene up-regulates the neighboring genes. Biochem Biophys Res Commun 399: 227-231.
71. Gelbart ME, Larschan E, Peng S, Park PJ, Kuroda MI (2009) Drosophila MSL complex globally acetylates H4K16 on the male X chromosome for dosage compensation. Nat Struct Mol Biol 16: 825-832.
72. Sural TH, Peng S, Li B, Workman JL, Park PJ, et al. (2008) The MSL3 chromodomain directs a key targeting step for dosage compensation of the Drosophila melanogaster X chromosome. Nat Struct Mol Biol 15: 1318-1325.
73. Kind J, Akhtar A (2007) Cotranscriptional recruitment of the dosage compensation complex to X-linked target genes. Genes Dev 21: 2030-2040.
74. Larschan E, Alekseyenko AA, Gortchakov AA, Peng S, Li B, et al. (2007) MSL complex is attracted to genes marked by H3K36 trimethylation using a sequence-independent mechanism. Mol Cell 28: 121-133.
75. Gupta V, Parisi M, Sturgill D, Nuttall R, Doctolero M, et al. (2006) Global analysis of X-chromosome dosage compensation. J Biol 5: 3.
76. Mendjan S, Taipale M, Kind J, Holz H, Gebhardt P, et al. (2006) Nuclear pore components are involved in the transcriptional regulation of dosage compensation in Drosophila. Mol Cell 21: 811-823.
77. Kotlikova IV, Demakova OV, Semeshin VF, Shloma VV, Boldyreva LV, et al. (2006) The Drosophila dosage compensation complex binds to polytene chromosomes independently of developmental changes in transcription. Genetics 172: 963-974.
78. Buscaino A, Legube G, Akhtar A (2006) X-chromosome targeting and dosage compensation are mediated by distinct domains in MSL-3. EMBO Rep 7: 531-538.
79. Legube G, McWeeney SK, Lercher MJ, Akhtar A (2006) X-chromosome-wide profiling of MSL-1 distribution and dosage compensation in Drosophila. Genes Dev 20: 871-883.
80. Fagegaltier D, Baker BS (2004) X chromosome sites autonomously recruit the dosage compensation complex in Drosophila males. PLoS Biol 2: e341.
81. Chiang PW, Kurnit DM (2003) Study of dosage compensation in Drosophila. Genetics 165: 1167-1181.
82. Birchler JA, Pal-Bhadra M, Bhadra U (2003) Dosage dependent gene regulation and the compensation of the X chromosome in Drosophila males. Genetica 117: 179-190.
83. Park Y, Mengus G, Bai X, Kageyama Y, Meller VH, et al. (2003) Sequence-specific targeting of Drosophila roX genes by the MSL dosage compensation complex. Mol Cell 11: 977-986.
84. Kageyama Y, Mengus G, Gilfillan G, Kennedy HG, Stuckenholz C, et al. (2001) Association and spreading of the Drosophila dosage compensation complex from a discrete roX1 chromatin entry site. EMBO J 20: 2236-2245.
85. Gorman M, Baker BS (1994) How flies make one equal two: dosage compensation in Drosophila. Trends Genet 10: 376-380.
86. Hilfiker A, Yang Y, Hayes DH, Beard CA, Manning JE, et al. (1994) Dosage compensation in Drosophila: the X-chromosomal binding of MSL-1 and MLE is dependent on Sxl activity. EMBO J 13: 3542-3550.

87. Gorman M, Kuroda MI, Baker BS (1993) Regulation of the sex-specific binding of the maleless dosage compensation protein to the male X chromosome in Drosophila. Cell 72: 39-49.
88. Straub T, Grimaud C, Gilfillan GD, Mitterweger A, Becker PB (2008) The chromosomal high-affinity binding sites for the Drosophila dosage compensation complex. PLoS Genet 4: e1000302.
89. Zhang Y, Malone JH, Powell SK, Periwal V, Spana E, et al. (2010) Expression in aneuploid Drosophila S2 cells. PLoS Biol 8: e1000320.
90. Yildirim E, Sadreyev RI, Pinter SF, Lee JT (2011) X-chromosome hyperactivation in mammals via nonlinear relationships between chromatin states and transcription. Nat Struct Mol Biol 19: 56-61.
91. Deakin JE, Hore TA, Koina E, Marshall Graves JA (2008) The status of dosage compensation in the multiple X chromosomes of the platypus. PLoS Genet 4: e1000140.
92. Bisoni L, Batlle-Morera L, Bird AP, Suzuki M, McQueen HA (2005) Female-specific hyperacetylation of histone H4 in the chicken Z chromosome. Chromosome Res 13: 205-214.
93. Rens W, Wallduck MS, Lovell FL, Ferguson-Smith MA, Ferguson-Smith AC (2010) Epigenetic modifications on X chromosomes in marsupial and monotreme mammals and implications for evolution of dosage compensation. Proc Natl Acad Sci U S A 107: 17657-17662.
94. Al Nadaf S, Deakin JE, Gilbert C, Robinson TJ, Graves JA, et al. (2012) A cross-species comparison of escape from X inactivation in Eutheria: implications for evolution of X chromosome inactivation. Chromosoma 121: 71-78.
95. Escamilla-Del-Arenal M, da Rocha ST, Heard E (2011) Evolutionary diversity and developmental regulation of X-chromosome inactivation. Hum Genet 130: 307-327.
96. Grimaud C, Becker PB (2010) Form and function of dosage-compensated chromosomes--a chicken-and-egg relationship. Bioessays 32: 709-717.
97. Xiong Y, Chen X, Chen Z, Wang X, Shi S, et al. (2010) RNA sequencing shows no dosage compensation of the active X-chromosome. Nat Genet 42: 1043-1047.
98. Marks H, Chow JC, Denissov S, Francoijs KJ, Brockdorff N, et al. (2009) High-resolution analysis of epigenetic changes associated with X inactivation. Genome Res 19: 1361-1373.
99. Arthold S, Kurowski A, Wutz A (2011) Mechanistic insights into chromosome-wide silencing in X inactivation. Hum Genet 130: 295-305.
100. Leeb M, Wutz A (2010) Mechanistic concepts in X inactivation underlying dosage compensation in mammals. Heredity 105: 64-70.
101. Barakat TS, Jonkers I, Monkhorst K, Gribnau J (2010) X-changing information on X inactivation. Exp Cell Res 316: 679-687.
102. Okamoto I, Patrat C, Thepot D, Peynot N, Fauque P, et al. (2011) Eutherian mammals use diverse strategies to initiate X-chromosome inactivation during development. Nature 472: 370-374.
103. Payer B, Lee JT (2008) X chromosome dosage compensation: how mammals keep the balance. Annu Rev Genet 42: 733-772.
104. Mendjan S, Akhtar A (2007) The right dose for every sex. Chromosoma 116: 95-106.
105. Heard E, Disteche CM (2006) Dosage compensation in mammals: fine-tuning the expression of the X chromosome. Genes Dev 20: 1848-1867.
106. Nguyen DK, Disteche CM (2006) Dosage compensation of the active X chromosome in mammals. Nat Genet 38: 47-53.

107. Plath K, Fang J, Mlynarczyk-Evans SK, Cao R, Worringer KA, et al. (2003) Role of histone H3 lysine 27 methylation in X inactivation. Science 300: 131-135.
108. Csankovszki G, Nagy A, Jaenisch R (2001) Synergism of Xist RNA, DNA methylation, and histone hypoacetylation in maintaining X chromosome inactivation. J Cell Biol 153: 773-784.
109. Lyon MF (1962) Sex chromatin and gene action in the mammalian X-chromosome. Am J Hum Genet 14: 135-148.
110. Splinter E, de Wit E, Nora EP, Klous P, van de Werken HJ, et al. (2011) The inactive X chromosome adopts a unique three-dimensional conformation that is dependent on Xist RNA. Genes Dev 25: 1371-1383.
111. Chang SC, Brown CJ (2010) Identification of regulatory elements flanking human XIST reveals species differences. BMC Mol Biol 11: 20.
112. Navarro P, Chantalat S, Foglio M, Chureau C, Vigneau S, et al. (2009) A role for non-coding Tsix transcription in partitioning chromatin domains within the mouse X-inactivation centre. Epigenetics Chromatin 2: 8.
113. Spencer RJ, del Rosario BC, Pinter SF, Lessing D, Sadreyev RI, et al. (2011) A boundary element between Tsix and Xist binds the chromatin insulator Ctcf and contributes to initiation of X-chromosome inactivation. Genetics 189: 441-454.
114. Sun BK, Deaton AM, Lee JT (2006) A Transient Heterochromatic State in Xist Preempts X Inactivation Choice without RNA Stabilization. Molecular Cell 21: 617-628.
115. Luikenhuis S, Wutz A, Jaenisch R (2001) Antisense transcription through the Xist locus mediates Tsix function in embryonic stem cells. Mol Cell Biol 21: 8512-8520.
116. Migeon BR, Chowdhury AK, Dunston JA, McIntosh I (2001) Identification of TSIX, encoding an RNA antisense to human XIST, reveals differences from its murine counterpart: implications for X inactivation. Am J Hum Genet 69: 951-960.
117. Stavropoulos N, Lu N, Lee JT (2001) A functional role for Tsix transcription in blocking Xist RNA accumulation but not in X-chromosome choice. Proc Natl Acad Sci U S A 98: 10232-10237.
118. Morey C, Arnaud D, Avner P, Clerc P (2001) Tsix-mediated repression of Xist accumulation is not sufficient for normal random X inactivation. Hum Mol Genet 10: 1403-1411.
119. Sado T, Wang Z, Sasaki H, Li E (2001) Regulation of imprinted X-chromosome inactivation in mice by Tsix. Development 128: 1275-1286.
120. Chaumeil J, Waters PD, Koina E, Gilbert C, Robinson TJ, et al. (2011) Evolution from XIST-independent to XIST-controlled X-chromosome inactivation: epigenetic modifications in distantly related mammals. PLoS ONE 6: e19040.
121. Chaumeil J, Le Baccon P, Wutz A, Heard E (2006) A novel role for Xist RNA in the formation of a repressive nuclear compartment into which genes are recruited when silenced. Genes Dev 20: 2223-2237.
122. Kucera KS, Reddy TE, Pauli F, Gertz J, Logan JE, et al. (2011) Allele-specific distribution of RNA polymerase II on female X chromosomes. Hum Mol Genet 20: 3964-3973.
123. Maenner S, Blaud M, Fouillen L, Savoye A, Marchand V, et al. (2010) 2-D structure of the A region of Xist RNA and its implication for PRC2 association. PLoS Biol 8: e1000276.
124. Chow JC, Ciaudo C, Fazzari MJ, Mise N, Servant N, et al. (2010) LINE-1 activity in facultative heterochromatin formation during X chromosome inactivation. Cell 141: 956-969.
125. Csankovszki G, Panning B, Bates B, Pehrson JR, Jaenisch R (1999) Conditional deletion of Xist disrupts histone macroH2A localization but not maintenance of X inactivation. Nat Genet 22: 323-324.

126. Chadwick BP, Willard HF (2004) Multiple spatially distinct types of facultative heterochromatin on the human inactive X chromosome. Proc Natl Acad Sci U S A 101: 17450-17455.
127. Prabhakaran M, Kelley RL (2010) A new strategy for isolating genes controlling dosage compensation in Drosophila using a simple epigenetic mosaic eye phenotype. BMC Biol 8: 80.
128. Prestel M, Feller C, Straub T, Mitlohner H, Becker PB (2010) The activation potential of MOF is constrained for dosage compensation. Mol Cell 38: 815-826.
129. Kind J, Vaquerizas JM, Gebhardt P, Gentzel M, Luscombe NM, et al. (2008) Genome-wide analysis reveals MOF as a key regulator of dosage compensation and gene expression in Drosophila. Cell 133: 813-828.
130. Rea S, Xouri G, Akhtar A (2007) Males absent on the first (MOF): from flies to humans. Oncogene 26: 5385-5394.
131. Akhtar A, Becker PB (2000) Activation of transcription through histone H4 acetylation by MOF, an acetyltransferase essential for dosage compensation in Drosophila. Mol Cell 5: 367-375.
132. Bell O, Conrad T, Kind J, Wirbelauer C, Akhtar A, et al. (2008) Transcription-coupled methylation of histone H3 at lysine 36 regulates dosage compensation by enhancing recruitment of the MSL complex in Drosophila melanogaster. Mol Cell Biol 28: 3401-3409.
133. Moore SA, Ferhatoglu Y, Jia Y, Al-Jiab RA, Scott MJ (2010) Structural and biochemical studies on the chromo-barrel domain of male specific lethal 3 (MSL3) reveal a binding preference for mono or dimethyl lysine 20 on histone H4. J Biol Chem.
134. Kim D, Blus BJ, Chandra V, Huang P, Rastinejad F, et al. (2010) Corecognition of DNA and a methylated histone tail by the MSL3 chromodomain. Nat Struct Mol Biol 17: 1027-1029.
135. Li F, Schiemann AH, Scott MJ (2008) Incorporation of the noncoding roX RNAs alters the chromatin-binding specificity of the Drosophila MSL1/MSL2 complex. Mol Cell Biol 28: 1252-1264.
136. Alekseyenko AA, Peng S, Larschan E, Gorchakov AA, Lee OK, et al. (2008) A sequence motif within chromatin entry sites directs MSL establishment on the Drosophila X chromosome. Cell 134: 599-609.
137. Buscaino A, Köcher T, Kind JH, Holz H, Taipale M, et al. (2003) MOF-Regulated Acetylation of MSL-3 in the Drosophila Dosage Compensation Complex. Molecular Cell 11: 1265-1277.
138. Smith ER, Allis CD, Lucchesi JC (2001) Linking global histone acetylation to the transcription enhancement of X-chromosomal genes in Drosophila males. J Biol Chem 276: 31483-31486.
139. Cai Y, Jin J, Swanson SK, Cole MD, Choi SH, et al. (2010) Subunit composition and substrate specificity of a MOF-containing histone acetyltransferase distinct from the male-specific lethal (MSL) complex. J Biol Chem 285: 4268-4272.
140. Raja SJ, Charapitsa I, Conrad T, Vaquerizas JM, Gebhardt P, et al. (2010) The nonspecific lethal complex is a transcriptional regulator in Drosophila. Mol Cell 38: 827-841.
141. Gladstein N, McKeon MN, Horabin JI (2010) Requirement of male-specific dosage compensation in Drosophila females--implications of early X chromosome gene expression. PLoS Genet 6: e1001041.
142. Franke A, Dernburg A, Bashaw GJ, Baker BS (1996) Evidence that MSL-mediated dosage compensation in Drosophila begins at blastoderm. Development 122: 2751-2760.

143. Bernstein M, Cline TW (1994) Differential effects of Sex-lethal mutations on dosage compensation early in Drosophila development. Genetics 136: 1051-1061.
144. Gergen JP (1987) Dosage Compensation in Drosophila: Evidence That daughterless and Sex-lethal Control X Chromosome Activity at the Blastoderm Stage of Embryogenesis. Genetics 117: 477-485.
145. Cline TW, Dorsett M, Sun S, Harrison MM, Dines J, et al. (2010) Evolution of the Drosophila feminizing switch gene Sex-lethal. Genetics 186: 1321-1336.
146. Erickson JW, Quintero JJ (2007) Indirect effects of ploidy suggest X chromosome dose, not the X:A ratio, signals sex in Drosophila. PLoS Biol 5: e332.
147. Penalva LOF, Sanchez L (2003) RNA Binding Protein Sex-Lethal (Sxl) and Control of Drosophila Sex Determination and Dosage Compensation. Microbiology and Molecular Biology Reviews 67: 343-359.
148. Gebauer F, Corona DF, Preiss T, Becker PB, Hentze MW (1999) Translational control of dosage compensation in Drosophila by Sex-lethal: cooperative silencing via the 5' and 3' UTRs of msl-2 mRNA is independent of the poly(A) tail. EMBO J 18: 6146-6154.
149. Bopp D, Horabin JI, Lersch RA, Cline TW, Schedl P (1993) Expression of the Sex-lethal gene is controlled at multiple levels during Drosophila oogenesis. Development 118: 797-812.
150. Horabin JI, Schedl P (1993) Sex-lethal autoregulation requires multiple cis-acting elements upstream and downstream of the male exon and appears to depend largely on controlling the use of the male exon 5' splice site. Mol Cell Biol 13: 7734-7746.
151. Keyes LN, Cline TW, Schedl P (1992) The primary sex determination signal of Drosophila acts at the level of transcription. Cell 68: 933-943.
152. Bell LR, Horabin JI, Schedl P, Cline TW (1991) Positive autoregulation of sex-lethal by alternative splicing maintains the female determined state in Drosophila. Cell 65: 229-239.
153. Bopp D, Bell LR, Cline TW, Schedl P (1991) Developmental distribution of female-specific Sex-lethal proteins in Drosophila melanogaster. Genes Dev 5: 403-415.
154. Salz HK, Maine EM, Keyes LN, Samuels ME, Cline TW, et al. (1989) The Drosophila female-specific sex-determination gene, Sex-lethal, has stage-, tissue-, and sex-specific RNAs suggesting multiple modes of regulation. Genes Dev 3: 708-719.
155. Bell LR, Maine EM, Schedl P, Cline TW (1988) Sex-lethal, a Drosophila sex determination switch gene, exhibits sex-specific RNA splicing and sequence similarity to RNA binding proteins. Cell 55: 1037-1046.
156. Csankovszki G, Petty EL, Collette KS (2009) The worm solution: a chromosome-full of condensin helps gene expression go down. Chromosome Res 17: 621-635.
157. Csankovszki G, Collette K, Spahl K, Carey J, Snyder M, et al. (2009) Three distinct condensin complexes control C. elegans chromosome dynamics. Curr Biol 19: 9-19.
158. Tsai CJ, Mets DG, Albrecht MR, Nix P, Chan A, et al. (2008) Meiotic crossover number and distribution are regulated by a dosage compensation protein that resembles a condensin subunit. Genes Dev 22: 194-211.
159. Yonker SA, Meyer BJ (2003) Recruitment of C. elegans dosage compensation proteins for gene-specific versus chromosome-wide repression. Development 130: 6519-6532.
160. Lieb JD, Capowski EE, Meneely P, Meyer BJ (1996) DPY-26, a link between dosage compensation and meiotic chromosome segregation in the nematode. Science 274: 1732-1736.
161. Hsu DR, Meyer BJ (1994) The Dpy-30 Gene Encodes an Essential Component of the Caenorhabditis-Elegans Dosage Compensation Machinery. Genetics 137: 999-1018.

162. Chuang PT, Albertson DG, Meyer BJ (1994) DPY-27:a chromosome condensation protein homolog that regulates C. elegans dosage compensation through association with the X chromosome. Cell 79: 459-474.
163. DeLong L, Casson LP, Meyer BJ (1987) Assessment of X chromosome dosage compensation in Caenorhabditis elegans by phenotypic analysis of lin-14. Genetics 117: 657-670.
164. Meyer BJ, Casson LP (1986) Caenorhabditis elegans compensates for the difference in X chromosome dosage between the sexes by regulating transcript levels. Cell 47: 871-881.
165. Plenefisch JD, DeLong L, Meyer BJ (1989) Genes that implement the hermaphrodite mode of dosage compensation in Caenorhabditis elegans. Genetics 121: 57-76.
166. Kimura K, Rybenkov VV, Crisona NJ, Hirano T, Cozzarelli NR (1999) 13S condensin actively reconfigures DNA by introducing global positive writhe: implications for chromosome condensation. Cell 98: 239-248.
167. Lieb JD, Albrecht MR, Chuang PT, Meyer BJ (1998) MIX-1: an essential component of the C. elegans mitotic machinery executes X chromosome dosage compensation. Cell 92: 265-277.
168. Hodgkin J (1983) X chromosome dosage and gene expression in <i>Caenorhabditis elegans : Two unusual dumpy genes. Molecular and General Genetics MGG 192: 452-458.
169. Chu DS, Dawes HE, Lieb JD, Chan RC, Kuo AF, et al. (2002) A molecular link between gene-specific and chromosome-wide transcriptional repression. Genes Dev 16: 796-805.
170. Dawes HE, Berlin DS, Lapidus DM, Nusbaum C, Davis TL, et al. (1999) Dosage Compensation Proteins Targeted to X Chromosomes by a Determinant of Hermaphrodite Fate. Science 284: 1800-1804.
171. Jans J, Gladden JM, Ralston EJ, Pickle CS, Michel AH, et al. (2009) A condensin-like dosage compensation complex acts at a distance to control expression throughout the genome. Genes Dev 23: 602-618.
172. Pferdehirt RR, Kruesi WS, Meyer BJ (2011) An MLL/COMPASS subunit functions in the C. elegans dosage compensation complex to target X chromosomes for transcriptional regulation of gene expression. Genes Dev 25: 499-515.
173. Ercan S, Dick LL, Lieb JD (2009) The C. elegans dosage compensation complex propagates dynamically and independently of X chromosome sequence. Curr Biol 19: 1777-1787.
174. Ercan S, Giresi PG, Whittle CM, Zhang X, Green RD, et al. (2007) X chromosome repression by localization of the C. elegans dosage compensation machinery to sites of transcription initiation. Nat Genet 39: 403-408.
175. Blauwkamp TA, Csankovszki G (2009) Two classes of dosage compensation complex binding elements along Caenorhabditis elegans X chromosomes. Mol Cell Biol 29: 2023-2031.
176. Hartman PS, Ishii N (2007) Chromosome dosage as a life span determinant in Caenorhabiditis elegans. Mech Ageing Dev 128: 437-443.
177. Hsu DR, Chuang PT, Meyer BJ (1995) Dpy-30, a Nuclear-Protein Essential Early in Embryogenesis for Caenorhabditis-Elegans Dosage Compensation. Development 121: 3323-3334.
178. Csankovszki G (2009) Condensin function in dosage compensation. Epigenetics 4: 212-215.
179. Hirano T (2005) Condensins: organizing and segregating the genome. Curr Biol 15: R265-275.
180. Legagneux V, Cubizolles F, Watrin E (2004) Multiple roles of Condensins: a complex story. Biol Cell 96: 201-213.
181. Chan RC, Severson AF, Meyer BJ (2004) Condensin restructures chromosomes in preparation for meiotic divisions. J Cell Biol 167: 613-625.

182. Hirano T, Kobayashi R, Hirano M (1997) Condensins, chromosome condensation protein complexes containing XCAP-C, XCAP-E and a Xenopus homolog of the Drosophila Barren protein. Cell 89: 511-521.
183. Lavoie BD, Hogan E, Koshland D (2002) In vivo dissection of the chromosome condensation machinery: reversibility of condensation distinguishes contributions of condensin and cohesin. J Cell Biol 156: 805-815.
184. Bazett-Jones DP, Kimura K, Hirano T (2002) Efficient supercoiling of DNA by a single condensin complex as revealed by electron spectroscopic imaging. Mol Cell 9: 1183-1190.
185. Kimura K, Hirano T (1997) ATP-dependent positive supercoiling of DNA by 13S condensin: a biochemical implication for chromosome condensation. Cell 90: 625-634.
186. Hagstrom KA, Holmes VF, Cozzarelli NR, Meyer BJ (2002) C-elegans condensin promotes mitotic chromosome architecture, centromere organization, and sister chromatid segregation during mitosis and meiosis. Genes & Development 16: 729-742.
187. Kimura K, Cuvier O, Hirano T (2001) Chromosome condensation by a human condensin complex in Xenopus egg extracts. J Biol Chem 276: 5417-5420.
188. Strick TR, Kawaguchi T, Hirano T (2004) Real-time detection of single-molecule DNA compaction by condensin I. Curr Biol 14: 874-880.
189. Cuylen S, Metz J, Haering CH (2011) Condensin structures chromosomal DNA through topological links. Nat Struct Mol Biol 18: 894-901.
190. Dej KJ, Ahn C, Orr-Weaver TL (2004) Mutations in the Drosophila condensin subunit dCAP-G: defining the role of condensin for chromosome condensation in mitosis and gene expression in interphase. Genetics 168: 895-906.
191. Bhalla N, Biggins S, Murray AW (2002) Mutation of YCS4, a budding yeast condensin subunit, affects mitotic and nonmitotic chromosome behavior. Mol Biol Cell 13: 632-645.
192. Xu Y, Leung CG, Lee DC, Kennedy BK, Crispino JD (2006) MTB, the murine homolog of condensin II subunit CAP-G2, represses transcription and promotes erythroid cell differentiation. Leukemia 20: 1261-1269.
193. Klein RD, Meyer BJ (1993) Independent domains of the Sdc-3 protein control sex determination and dosage compensation in C. elegans. Cell 72: 349-364.
194. Chuang PT, Albertson DG, Meyer BJ (1994) Dpy-27 - a Chromosome Condensation Protein Homolog That Regulates C. Elegans Dosage Compensation through Association with the X-Chromosome. Cell 79: 459-474.
195. DeLong L, Plenefisch JD, Klein RD, Meyer BJ (1993) Feedback control of sex determination by dosage compensation revealed through Caenorhabditis elegans sdc-3 mutations. Genetics 133: 875-896.
196. Nonet ML, Meyer BJ (1991) Early aspects of Caenorhabditis elegans sex determination and dosage compensation are regulated by a zinc-finger protein. Nature 351: 65-68.
197. Hsu DR, Meyer BJ (1994) The dpy-30 gene encodes an essential component of the Caenorhabditis elegans dosage compensation machinery. Genetics 137: 999-1018.
198. Petty E, Laughlin E, Csankovszki G (2011) Regulation of DCC localization by HTZ-1/H2A.Z and DPY-30 does not correlate with H3K4 methylation levels. PLoS ONE 6: e25973.
199. Hsu DR, Chuang PT, Meyer BJ (1995) DPY-30, a nuclear protein essential early in embryogenesis for Caenorhabditis elegans dosage compensation. Development 121: 3323-3334.

200. Jiang H, Shukla A, Wang X, Chen WY, Bernstein BE, et al. (2011) Role for Dpy-30 in ES cell-fate specification by regulation of H3K4 methylation within bivalent domains. Cell 144: 513-525.
201. South PF, Fingerman IM, Mersman DP, Du HN, Briggs SD (2010) A conserved interaction between the SDI domain of Bre2 and the Dpy-30 domain of Sdc1 is required for histone methylation and gene expression. J Biol Chem 285: 595-607.
202. Wang X, Lou Z, Dong X, Yang W, Peng Y, et al. (2009) Crystal structure of the C-terminal domain of human DPY-30-like protein: A component of the histone methyltransferase complex. J Mol Biol 390: 530-537.
203. Dong X, Peng Y, Peng Y, Xu F, He X, et al. (2005) Characterization and crystallization of human DPY-30-like protein, an essential component of dosage compensation complex. Biochim Biophys Acta 1753: 257-262.
204. Meneely PM, Wood WB (1987) Genetic analysis of X-chromosome dosage compensation in Caenorhabditis elegans. Genetics 117: 25-41.
205. Meneely PM, Wood WB (1984) An autosomal gene that affects X chromosome expression and sex determination in Caenorhabditis elegans. Genetics 106: 29-44.
206. Shah VC, Smart V (1996) Human chromosome Y and SRY. Cell Biol Int 20: 3-6.
207. Jager RJ, Anvret M, Hall K, Scherer G (1990) A human XY female with a frame shift mutation in the candidate testis-determining gene SRY. Nature 348: 452-454.
208. Cline TW, Meyer BJ (1996) Vive la difference: males vs females in flies vs worms. Annu Rev Genet 30: 637-702.
209. Powell JR, Jow MM, Meyer BJ (2005) The T-box transcription factor SEA-1 is an autosomal element of the X:A signal that determines C. elegans sex. Dev Cell 9: 339-349.
210. Gladden JM, Meyer BJ (2007) A ONECUT homeodomain protein communicates X chromosome dose to specify Caenorhabditis elegans sexual fate by repressing a sex switch gene. Genetics 177: 1621-1637.
211. Beckmann K, Grskovic M, Gebauer F, Hentze MW (2005) A dual inhibitory mechanism restricts msl-2 mRNA translation for dosage compensation in Drosophila. Cell 122: 529-540.
212. Hager JH, Cline TW (1997) Induction of female Sex-lethal RNA splicing in male germ cells: implications for Drosophila germline sex determination. Development 124: 5033-5048.
213. Bashaw GJ, Baker BS (1995) The msl-2 dosage compensation gene of Drosophila encodes a putative DNA-binding protein whose expression is sex specifically regulated by Sex-lethal. Development 121: 3245-3258.
214. Trent C, Purnell B, Gavinski S, Hageman J, Chamblin C, et al. (1991) Sex-specific transcriptional regulation of the C. elegans sex-determining gene her-1. Mech Dev 34: 43-55.
215. Chandler DS, McGuffin ME, Mattox W (2001) Functionally antagonistic sequences are required for normal autoregulation of Drosophila tra-2 pre-mRNA splicing. Nucleic Acids Res 29: 3012-3019.
216. Lieberman AP, Friedlich DL, Harmison G, Howell BW, Jordan CL, et al. (2001) Androgens regulate the mammalian homologues of invertebrate sex determination genes tra-2 and fox-1. Biochem Biophys Res Commun 282: 499-506.
217. Wang S, Kimble J (2001) The TRA-1 transcription factor binds TRA-2 to regulate sexual fates in Caenorhabditis elegans. EMBO J 20: 1363-1372.
218. Goodwin EB, Hofstra K, Hurney CA, Mango S, Kimble J (1997) A genetic pathway for regulation of tra-2 translation. Development 124: 749-758.

219. Kuwabara PE (1996) A novel regulatory mutation in the C. elegans sex determination gene tra-2 defines a candidate ligand/receptor interaction site. Development 122: 2089-2098.
220. Grote P, Conradt B (2006) The PLZF-like protein TRA-4 cooperates with the Gli-like transcription factor TRA-1 to promote female development in C. elegans. Dev Cell 11: 561-573.
221. Mehra A, Gaudet J, Heck L, Kuwabara PE, Spence AM (1999) Negative regulation of male development in Caenorhabditis elegans by a protein-protein interaction between TRA-2A and FEM-3. Genes Dev 13: 1453-1463.
222. Gaudet J, VanderElst I, Spence AM (1996) Post-transcriptional regulation of sex determination in Caenorhabditis elegans: widespread expression of the sex-determining gene fem-1 in both sexes. Mol Biol Cell 7: 1107-1121.
223. Hargitai B, Kutnyanszky V, Blauwkamp TA, Stetak A, Csankovszki G, et al. (2009) xol-1, the master sex-switch gene in C. elegans, is a transcriptional target of the terminal sex-determining factor TRA-1. Development 136: 3881-3887.
224. Graves LE, Segal S, Goodwin EB (1999) TRA-1 regulates the cellular distribution of the tra-2 mRNA in C. elegans. Nature 399: 802-805.
225. Harrison MM, Lu X, Horvitz HR (2007) LIN-61, one of two Caenorhabditis elegans malignant-brain-tumor-repeat-containing proteins, acts with the DRM and NuRD-like protein complexes in vulval development but not in certain other biological processes. Genetics 176: 255-271.
226. Harrison MM, Ceol CJ, Lu X, Horvitz HR (2006) Some C. elegans class B synthetic multivulva proteins encode a conserved LIN-35 Rb-containing complex distinct from a NuRD-like complex. Proc Natl Acad Sci U S A 103: 16782-16787.
227. Kelly WG, Aramayo R (2007) Meiotic silencing and the epigenetics of sex. Chromosome Res 15: 633-651.
228. Kelly WG, Schaner CE, Dernburg AF, Lee MH, Kim SK, et al. (2002) X-chromosome silencing in the germline of C. elegans. Development 129: 479-492.
229. Tabuchi TM, Deplancke B, Osato N, Zhu LJ, Barrasa MI, et al. (2011) Chromosome-biased binding and gene regulation by the Caenorhabditis elegans DRM complex. PLoS Genet 7: e1002074.
230. Bender LB, Suh J, Carroll CR, Fong Y, Fingerman IM, et al. (2006) MES-4: an autosome-associated histone methyltransferase that participates in silencing the X chromosomes in the C. elegans germ line. Development 133: 3907-3917.
231. Bender LB, Cao R, Zhang Y, Strome S (2004) The MES-2/MES-3/MES-6 complex and regulation of histone H3 methylation in C. elegans. Curr Biol 14: 1639-1643.
232. Fong Y, Bender L, Wang W, Strome S (2002) Regulation of the different chromatin states of autosomes and X chromosomes in the germ line of C. elegans. Science 296: 2235-2238.
233. Garvin C, Holdeman R, Strome S (1998) The Phenotype of mes-2, mes-3, mes-4 and mes-6, Maternal-Effect Genes Required for Survival of the Germline in Caenorhabditis elegans, Is Sensitive to Chromosome Dosage. Genetics 148: 167-186.
234. Rechtsteiner A, Ercan S, Takasaki T, Phippen TM, Egelhofer TA, et al. (2010) The histone H3K36 methyltransferase MES-4 acts epigenetically to transmit the memory of germline gene expression to progeny. PLoS Genet 6.
235. Carrozza MJ, Li B, Florens L, Suganuma T, Swanson SK, et al. (2005) Histone H3 methylation by Set2 directs deacetylation of coding regions by Rpd3S to suppress spurious intragenic transcription. Cell 123: 581-592.

236. Takasaki T, Liu Z, Habara Y, Nishiwaki K, Nakayama J, et al. (2007) MRG-1, an autosome-associated protein, silences X-linked genes and protects germline immortality in Caenorhabditis elegans. Development 134: 757-767.
237. Furuhashi H, Takasaki T, Rechtsteiner A, Li T, Kimura H, et al. (2010) Trans-generational epigenetic regulation of C. elegans primordial germ cells. Epigenetics Chromatin 3: 15.
238. Petrella LN, Wang W, Spike CA, Rechtsteiner A, Reinke V, et al. (2011) synMuv B proteins antagonize germline fate in the intestine and ensure C. elegans survival. Development 138: 1069-1079.
239. Luger K, Mader A, Richmond R, Sargent D, Richmond T (1997) Crystal structure of the nucleosome core particle at 2.8 A resolution. Nature 389: 251 - 260.
240. Giri S, Prasanth SG (2012) Replicating and transcribing on twisted roads of chromatin. Brief Funct Genomics.
241. Campos EI, Reinberg D (2009) Histones: Annotating Chromatin. Annual Review of Genetics 43: 559-599.
242. Jin J, Cai Y, Li B, Conaway RC, Workman JL, et al. (2005) In and out: histone variant exchange in chromatin. Trends Biochem Sci 30: 680-687.
243. Campos EI, Reinberg D (2009) Histones: annotating chromatin. Annu Rev Genet 43: 559-599.
244. Kouzarides T (2007) Chromatin modifications and their function. Cell 128: 693-705.
245. Bannister AJ, Kouzarides T (2011) Regulation of chromatin by histone modifications. Cell Res 21: 381-395.
246. Bartke T, Kouzarides T (2011) Decoding the chromatin modification landscape. Cell Cycle 10: 182.
247. Tan M, Luo H, Lee S, Jin F, Yang JS, et al. (2011) Identification of 67 histone marks and histone lysine crotonylation as a new type of histone modification. Cell 146: 1016-1028.
248. Ahmad W, Shabbiri K, Nazar N, Nazar S, Qaiser S, et al. (2011) Human linker histones: interplay between phosphorylation and O-beta-GlcNAc to mediate chromatin structural modifications. Cell Div 6: 15.
249. Gardner KE, Allis CD, Strahl BD (2011) Operating on chromatin, a colorful language where context matters. J Mol Biol 409: 36-46.
250. Dhall A, Chatterjee C (2011) Chemical approaches to understand the language of histone modifications. ACS Chem Biol 6: 987-999.
251. Strahl BD, Allis CD (2000) The language of covalent histone modifications. Nature 403: 41-45.
252. Lee JS, Smith E, Shilatifard A (2010) The language of histone crosstalk. Cell 142: 682-685.
253. Craig JM (2005) Heterochromatin--many flavours, common themes. Bioessays 27: 17-28.
254. Taverna SD, Li H, Ruthenburg AJ, Allis CD, Patel DJ (2007) How chromatin-binding modules interpret histone modifications: lessons from professional pocket pickers. Nat Struct Mol Biol 14: 1025-1040.
255. Suganuma T, Workman JL (2011) Signals and combinatorial functions of histone modifications. Annu Rev Biochem 80: 473-499.
256. Ruthenburg AJ, Li H, Patel DJ, Allis CD (2007) Multivalent engagement of chromatin modifications by linked binding modules. Nat Rev Mol Cell Biol 8: 983-994.
257. Ruthenburg AJ, Li H, Milne TA, Dewell S, McGinty RK, et al. (2011) Recognition of a mononucleosomal histone modification pattern by BPTF via multivalent interactions. Cell 145: 692-706.
258. Simonis M, Kooren J, de Laat W (2007) An evaluation of 3C-based methods to capture DNA interactions. Nat Meth 4: 895-901.

259. Sanyal A, Bau D, Marti-Renom MA, Dekker J (2011) Chromatin globules: a common motif of higher order chromosome structure? Curr Opin Cell Biol 23: 325-331.
260. Mirny LA (2011) The fractal globule as a model of chromatin architecture in the cell. Chromosome Res 19: 37-51.
261. Lieberman-Aiden E, van Berkum NL, Williams L, Imakaev M, Ragoczy T, et al. (2009) Comprehensive mapping of long-range interactions reveals folding principles of the human genome. Science 326: 289-293.
262. Sexton T, Yaffe E, Kenigsberg E, Bantignies F, Leblanc B, et al. (2012) Three-Dimensional Folding and Functional Organization Principles of the Drosophila Genome. Cell.
263. Umbarger MA, Toro E, Wright MA, Porreca GJ, Bau D, et al. (2011) The three-dimensional architecture of a bacterial genome and its alteration by genetic perturbation. Mol Cell 44: 252-264.
264. Dion MF, Altschuler SJ, Wu LF, Rando OJ (2005) Genomic characterization reveals a simple histone H4 acetylation code. Proc Natl Acad Sci U S A 102: 5501-5506.
265. Zhang K, Sridhar VV, Zhu J, Kapoor A, Zhu JK (2007) Distinctive core histone post-translational modification patterns in Arabidopsis thaliana. PLoS ONE 2: e1210.
266. Turner BM, O'Neill LP, Allan IM (1989) Histone H4 acetylation in human cells. Frequency of acetylation at different sites defined by immunolabeling with site-specific antibodies. FEBS Lett 253: 141-145.
267. Thorne AW, Kmiciek D, Mitchelson K, Sautiere P, Crane-Robinson C (1990) Patterns of histone acetylation. Eur J Biochem 193: 701-713.
268. Scharf AN, Barth TK, Imhof A (2009) Establishment of histone modifications after chromatin assembly. Nucleic Acids Res 37: 5032-5040.
269. Zhang K, Williams KE, Huang L, Yau P, Siino JS, et al. (2002) Histone acetylation and deacetylation: identification of acetylation and methylation sites of HeLa histone H4 by mass spectrometry. Mol Cell Proteomics 1: 500-508.
270. Garcia BA, Hake SB, Diaz RL, Kauer M, Morris SA, et al. (2007) Organismal differences in post-translational modifications in histones H3 and H4. J Biol Chem 282: 7641-7655.
271. Vaquero A, Sternglanz R, Reinberg D (2007) NAD+-dependent deacetylation of H4 lysine 16 by class III HDACs. Oncogene 26: 5505-5520.
272. Lu L, Li L, Lv X, Wu XS, Liu DP, et al. (2011) Modulations of hMOF autoacetylation by SIRT1 regulate hMOF recruitment and activities on the chromatin. Cell Res 21: 1182-1195.
273. Yang D, Arya G (2011) Structure and binding of the H4 histone tail and the effects of lysine 16 acetylation. Phys Chem Chem Phys 13: 2911-2921.
274. Allahverdi A, Yang R, Korolev N, Fan Y, Davey CA, et al. (2011) The effects of histone H4 tail acetylations on cation-induced chromatin folding and self-association. Nucleic Acids Research 39: 1680-1691.
275. Shogren-Knaak M, Ishii H, Sun JM, Pazin MJ, Davie JR, et al. (2006) Histone H4-K16 acetylation controls chromatin structure and protein interactions. Science 311: 844-847.
276. Robinson PJ, An W, Routh A, Martino F, Chapman L, et al. (2008) 30 nm chromatin fibre decompaction requires both H4-K16 acetylation and linker histone eviction. J Mol Biol 381: 816-825.
277. Balakrishnan L, Milavetz B (2010) Decoding the histone H4 lysine 20 methylation mark. Crit Rev Biochem Mol Biol 45: 440-452.
278. Fang J, Feng Q, Ketel CS, Wang H, Cao R, et al. (2002) Purification and functional characterization of SET8, a nucleosomal histone H4-lysine 20-specific methyltransferase. Curr Biol 12: 1086-1099.

279. Nishioka K, Rice JC, Sarma K, Erdjument-Bromage H, Werner J, et al. (2002) PR-Set7 is a nucleosome-specific methyltransferase that modifies lysine 20 of histone H4 and is associated with silent chromatin. Mol Cell 9: 1201-1213.
280. Beisel C, Imhof A, Greene J, Kremmer E, Sauer F (2002) Histone methylation by the Drosophila epigenetic transcriptional regulator Ash1. Nature 419: 857-862.
281. Schotta G, Lachner M, Sarma K, Ebert A, Sengupta R, et al. (2004) A silencing pathway to induce H3-K9 and H4-K20 trimethylation at constitutive heterochromatin. Genes Dev 18: 1251-1262.
282. Sakaguchi A, Karachentsev D, Seth-Pasricha M, Druzhinina M, Steward R (2008) Functional characterization of the Drosophila Hmt4-20/Suv4-20 histone methyltransferase. Genetics 179: 317-322.
283. Yang H, Pesavento JJ, Starnes TW, Cryderman DE, Wallrath LL, et al. (2008) Preferential dimethylation of histone H4 lysine 20 by Suv4-20. J Biol Chem 283: 12085-12092.
284. Rice JC, Nishioka K, Sarma K, Steward R, Reinberg D, et al. (2002) Mitotic-specific methylation of histone H4 Lys 20 follows increased PR-Set7 expression and its localization to mitotic chromosomes. Genes Dev 16: 2225-2230.
285. Kapoor-Vazirani P, Kagey JD, Vertino PM (2011) SUV420H2-mediated H4K20 trimethylation enforces RNA polymerase II promoter-proximal pausing by blocking hMOF-dependent H4K16 acetylation. Mol Cell Biol 31: 1594-1609.
286. Kohlmaier A, Savarese F, Lachner M, Martens J, Jenuwein T, et al. (2004) A chromosomal memory triggered by Xist regulates histone methylation in X inactivation. PLoS Biol 2: E171.
287. Talasz H, Lindner HH, Sarg B, Helliger W (2005) Histone H4-lysine 20 monomethylation is increased in promoter and coding regions of active genes and correlates with hyperacetylation. J Biol Chem 280: 38814-38822.
288. Vakoc CR, Sachdeva MM, Wang H, Blobel GA (2006) Profile of histone lysine methylation across transcribed mammalian chromatin. Mol Cell Biol 26: 9185-9195.
289. Barski A, Cuddapah S, Cui K, Roh TY, Schones DE, et al. (2007) High-resolution profiling of histone methylations in the human genome. Cell 129: 823-837.
290. Wakabayashi K, Okamura M, Tsutsumi S, Nishikawa NS, Tanaka T, et al. (2009) The peroxisome proliferator-activated receptor gamma/retinoid X receptor alpha heterodimer targets the histone modification enzyme PR-Set7/Setd8 gene and regulates adipogenesis through a positive feedback loop. Mol Cell Biol 29: 3544-3555.
291. Li Z, Nie F, Wang S, Li L (2011) Histone H4 Lys 20 monomethylation by histone methylase SET8 mediates Wnt target gene activation. Proc Natl Acad Sci U S A 108: 3116-3123.
292. Sims JK, Rice JC (2008) PR-Set7 establishes a repressive trans-tail histone code that regulates differentiation. Mol Cell Biol 28: 4459-4468.
293. Sims JK, Houston SI, Magazinnik T, Rice JC (2006) A trans-tail histone code defined by monomethylated H4 Lys-20 and H3 Lys-9 demarcates distinct regions of silent chromatin. J Biol Chem 281: 12760-12766.
294. Karachentsev D, Sarma K, Reinberg D, Steward R (2005) PR-Set7-dependent methylation of histone H4 Lys 20 functions in repression of gene expression and is essential for mitosis. Genes Dev 19: 431-435.
295. Congdon LM, Houston SI, Veerappan CS, Spektor TM, Rice JC (2010) PR-Set7-mediated monomethylation of histone H4 lysine 20 at specific genomic regions induces transcriptional repression. J Cell Biochem 110: 609-619.

296. Kalakonda N, Fischle W, Boccuni P, Gurvich N, Hoya-Arias R, et al. (2008) Histone H4 lysine 20 monomethylation promotes transcriptional repression by L3MBTL1. Oncogene 27: 4293-4304.
297. Trojer P, Li G, Sims RJ, 3rd, Vaquero A, Kalakonda N, et al. (2007) L3MBTL1, a histone-methylation-dependent chromatin lock. Cell 129: 915-928.
298. Scharf AN, Meier K, Seitz V, Kremmer E, Brehm A, et al. (2009) Monomethylation of lysine 20 on histone H4 facilitates chromatin maturation. Mol Cell Biol 29: 57-67.
299. Ebert A, Lein S, Schotta G, Reuter G (2006) Histone modification and the control of heterochromatic gene silencing in Drosophila. Chromosome Res 14: 377-392.
300. Ebert A, Schotta G, Lein S, Kubicek S, Krauss V, et al. (2004) Su(var) genes regulate the balance between euchromatin and heterochromatin in Drosophila. Genes Dev 18: 2973-2983.
301. Gonzalo S, Garcia-Cao M, Fraga MF, Schotta G, Peters AH, et al. (2005) Role of the RB1 family in stabilizing histone methylation at constitutive heterochromatin. Nat Cell Biol 7: 420-428.
302. Houston SI, McManus KJ, Adams MM, Sims JK, Carpenter PB, et al. (2008) Catalytic function of the PR-Set7 histone H4 lysine 20 monomethyltransferase is essential for mitotic entry and genomic stability. J Biol Chem 283: 19478-19488.
303. Grimm C, Matos R, Ly-Hartig N, Steuerwald U, Lindner D, et al. (2009) Molecular recognition of histone lysine methylation by the Polycomb group repressor dSfmbt. EMBO J 28: 1965-1977.
304. Klymenko T, Papp B, Fischle W, Kocher T, Schelder M, et al. (2006) A Polycomb group protein complex with sequence-specific DNA-binding and selective methyl-lysine-binding activities. Genes Dev 20: 1110-1122.
305. Koina E, Chaumeil J, Greaves IK, Tremethick DJ, Graves JA (2009) Specific patterns of histone marks accompany X chromosome inactivation in a marsupial. Chromosome Res 17: 115-126.
306. Filippova GN, Cheng MK, Moore JM, Truong JP, Hu YJ, et al. (2005) Boundaries between chromosomal domains of X inactivation and escape bind CTCF and lack CpG methylation during early development. Dev Cell 8: 31-42.
307. Goldman MA, Reeves PS, Wirth CM, Zupko WJ, Wong MA, et al. (1998) Comparative methylation analysis of murine transgenes that undergo or escape X-chromosome inactivation. Chromosome Res 6: 397-404.
308. Tsuchiya KD, Greally JM, Yi Y, Noel KP, Truong JP, et al. (2004) Comparative sequence and x-inactivation analyses of a domain of escape in human xp11.2 and the conserved segment in mouse. Genome Res 14: 1275-1284.
309. Disteche CM, Filippova GN, Tsuchiya KD (2002) Escape from X inactivation. Cytogenet Genome Res 99: 36-43.
310. Disteche CM (1995) Escape from X inactivation in human and mouse. Trends Genet 11: 17-22.
311. Berletch JB, Yang F, Disteche CM (2010) Escape from X inactivation in mice and humans. Genome Biol 11: 213.
312. Berletch JB, Yang F, Xu J, Carrel L, Disteche CM (2011) Genes that escape from X inactivation. Hum Genet 130: 237-245.
313. Yang F, Babak T, Shendure J, Disteche CM (2010) Global survey of escape from X inactivation by RNA-sequencing in mouse. Genome Res 20: 614-622.
314. Buscaino A, Kocher T, Kind JH, Holz H, Taipale M, et al. (2003) MOF-regulated acetylation of MSL-3 in the Drosophila dosage compensation complex. Mol Cell 11: 1265-1277.

315. Zippo A, Serafini R, Rocchigiani M, Pennacchini S, Krepelova A, et al. (2009) Histone crosstalk between H3S10ph and H4K16ac generates a histone code that mediates transcription elongation. Cell 138: 1122-1136.
316. Ivaldi MS, Karam CS, Corces VG (2007) Phosphorylation of histone H3 at Ser10 facilitates RNA polymerase II release from promoter-proximal pausing in Drosophila. Genes Dev 21: 2818-2831.
317. Regnard C, Straub T, Mitterweger A, Dahlsveen IK, Fabian V, et al. (2011) Global analysis of the relationship between JIL-1 kinase and transcription. PLoS Genet 7: e1001327.
318. Teranishi M, Shimada Y, Hori T, Nakabayashi O, Kikuchi T, et al. (2001) Transcripts of the MHM region on the chicken Z chromosome accumulate as non-coding RNA in the nucleus of female cells adjacent to the DMRT1 locus. Chromosome Research 9: 147-165.
319. Petty EL, Collette KS, Cohen AJ, Snyder MJ, Csankovszki G (2009) Restricting dosage compensation complex binding to the X chromosomes by H2A.Z/HTZ-1. PLoS Genet 5: e1000699.
320. Whittle CM, McClinic KN, Ercan S, Zhang X, Green RD, et al. (2008) The genomic distribution and function of histone variant HTZ-1 during C. elegans embryogenesis. PLoS Genet 4: e1000187.
321. Tolstorukov MY, Kharchenko PV, Goldman JA, Kingston RE, Park PJ (2009) Comparative analysis of H2A.Z nucleosome organization in the human and yeast genomes. Genome Res 19: 967-977.
322. Petter M, Lee CC, Byrne TJ, Boysen KE, Volz J, et al. (2011) Expression of P. falciparum var genes involves exchange of the histone variant H2A.Z at the promoter. PLoS Pathog 7: e1001292.
323. Zilberman D, Coleman-Derr D, Ballinger T, Henikoff S (2008) Histone H2A.Z and DNA methylation are mutually antagonistic chromatin marks. Nature 456: 125-129.
324. Raisner RM, Hartley PD, Meneghini MD, Bao MZ, Liu CL, et al. (2005) Histone Variant H2A.Z Marks the 52 Ends of Both Active and Inactive Genes in Euchromatin. Cell 123: 233-248.
325. Mavrich TN, Jiang C, Ioshikhes IP, Li X, Venters BJ, et al. (2008) Nucleosome organization in the Drosophila genome. Nature 453: 358-362.
326. Guillemette B, Bataille AR, Gévry N, Adam M, Blanchette M, et al. (2005) Variant Histone H2A.Z Is Globally Localized to the Promoters of Inactive Yeast Genes and Regulates Nucleosome Positioning. PLoS Biol 3: e384.
327. Jiang D, Kong NC, Gu X, Li Z, He Y (2011) Arabidopsis COMPASS-like complexes mediate histone H3 lysine-4 trimethylation to control floral transition and plant development. PLoS Genet 7: e1001330.
328. Mohan M, Herz HM, Smith ER, Zhang Y, Jackson J, et al. (2011) The COMPASS family of H3K4 methylases in Drosophila. Mol Cell Biol 31: 4310-4318.
329. Wang P, Lin C, Smith ER, Guo H, Sanderson BW, et al. (2009) Global analysis of H3K4 methylation defines MLL family member targets and points to a role for MLL1-mediated H3K4 methylation in the regulation of transcriptional initiation by RNA polymerase II. Mol Cell Biol 29: 6074-6085.
330. Shilatifard A (2008) Molecular implementation and physiological roles for histone H3 lysine 4 (H3K4) methylation. Curr Opin Cell Biol 20: 341-348.
331. Takahashi YH, Westfield GH, Oleskie AN, Trievel RC, Shilatifard A, et al. (2011) Structural analysis of the core COMPASS family of histone H3K4 methylases from yeast to human. Proc Natl Acad Sci U S A 108: 20526-20531.
332. Takahashi YH, Shilatifard A (2010) Structural basis for H3K4 trimethylation by yeast Set1/COMPASS. Adv Enzyme Regul 50: 104-110.

333. Liu T, Rechtsteiner A, Egelhofer TA, Vielle A, Latorre I, et al. (2011) Broad chromosomal domains of histone modification patterns in C. elegans. Genome Res 21: 227-236.
334. Gerstein MB, Lu ZJ, Van Nostrand EL, Cheng C, Arshinoff BI, et al. (2010) Integrative analysis of the Caenorhabditis elegans genome by the modENCODE project. Science 330: 1775-1787.
335. Wells MB, Snyder MJ, Custer LM, Csankovszki G (2012) Caenorhabditis elegans dosage compensation regulates histone H4 chromatin state on X chromosomes. Mol Cell Biol 32: 1710-1719.
336. Nechaev S, Adelman K (2010) Pol II waiting in the starting gates: Regulating the transition from transcription initiation into productive elongation. Biochim Biophys Acta.
337. Venters BJ, Pugh BF (2009) How eukaryotic genes are transcribed. Crit Rev Biochem Mol Biol 44: 117-141.
338. van Hijum SAFT, Medema MH, Kuipers OP (2009) Mechanisms and Evolution of Control Logic in Prokaryotic Transcriptional Regulation. Microbiology and Molecular Biology Reviews 73: 481-509.
339. Ishihama A (2010) Prokaryotic genome regulation: multifactor promoters, multitarget regulators and hierarchic networks. FEMS Microbiology Reviews 34: 628-645.
340. Finzi L, Dunlap DD (2010) Single-molecule Approaches to Probe the Structure, Kinetics, and Thermodynamics of Nucleoprotein Complexes That Regulate Transcription. Journal of Biological Chemistry 285: 18973-18978.
341. Larson MH, Landick R, Block SM (2011) Single-Molecule Studies of RNA Polymerase: One Singular Sensation, Every Little Step It Takes. Molecular Cell 41: 249-262.
342. Tie F, Banerjee R, Stratton CA, Prasad-Sinha J, Stepanik V, et al. (2009) CBP-mediated acetylation of histone H3 lysine 27 antagonizes Drosophila Polycomb silencing. Development 136: 3131-3141.
343. Fry CJ, Peterson CL (2002) Transcription. Unlocking the gates to gene expression. Science 295: 1847-1848.
344. Ranish JA, Yudkovsky N, Hahn S (1999) Intermediates in formation and activity of the RNA polymerase II preinitiation complex: holoenzyme recruitment and a postrecruitment role for the TATA box and TFIIB. Genes Dev 13: 49-63.
345. Aso T, Conaway JW, Conaway RC (1994) Role of core promoter structure in assembly of the RNA polymerase II preinitiation complex. A common pathway for formation of preinitiation intermediates at many TATA and TATA-less promoters. J Biol Chem 269: 26575-26583.
346. Wallenfang MR, Seydoux G (2002) cdk-7 Is required for mRNA transcription and cell cycle progression in Caenorhabditis elegans embryos. Proc Natl Acad Sci U S A 99: 5527-5532.
347. Hong SW, Hong SM, Yoo JW, Lee YC, Kim S, et al. (2009) Phosphorylation of the RNA polymerase II C-terminal domain by TFIIH kinase is not essential for transcription of Saccharomyces cerevisiae genome. Proc Natl Acad Sci U S A 106: 14276-14280.
348. Egly JM, Coin F (2011) A history of TFIIH: two decades of molecular biology on a pivotal transcription/repair factor. DNA Repair (Amst) 10: 714-721.
349. Helenius K, Yang Y, Tselykh TV, Pessa HK, Frilander MJ, et al. (2011) Requirement of TFIIH kinase subunit Mat1 for RNA Pol II C-terminal domain Ser5 phosphorylation, transcription and mRNA turnover. Nucleic Acids Res 39: 5025-5035.
350. Guzman E, Lis JT (1999) Transcription factor TFIIH is required for promoter melting in vivo. Mol Cell Biol 19: 5652-5658.
351. Egloff S, Murphy S (2008) Cracking the RNA polymerase II CTD code. Trends Genet 24: 280-288.

352. Bird DM, Riddle DL (1989) Molecular cloning and sequencing of ama-1, the gene encoding the largest subunit of Caenorhabditis elegans RNA polymerase II. Mol Cell Biol 9: 4119-4130.
353. Seifart KH, Sekeris CE (1969) Alpha-amanitin, a specific inhibitor of transcription by mammalian RNA-polymerase. Z Naturforsch B 24: 1538-1544.
354. Liu P, Kenney JM, Stiller JW, Greenleaf AL (2010) Genetic Organization, Length Conservation, and Evolution of RNA Polymerase II Carboxyl-Terminal Domain. Molecular Biology and Evolution 27: 2628-2641.
355. Bowman EA, Riddle DL, Kelly W (2011) Amino Acid Substitutions in the Caenorhabditis elegans RNA Polymerase II Large Subunit AMA-1/RPB-1 that Result in α-Amanitin Resistance and/or Reduced Function. G3: Genes, Genomes, Genetics 1: 411-416.
356. Rogalski TM, Bullerjahn A, Riddle DL (1988) Lethal and Amanitin-Resistance Mutations in the Caenorhabditis elegans ama-1 and ama-2 Genes. Genetics 120: 409-422.
357. Sanford T, Golomb M, Riddle DL (1983) RNA polymerase II from wild type and alpha-amanitin-resistant strains of Caenorhabditis elegans. Journal of Biological Chemistry 258: 12804-12809.
358. Shim EY, Walker AK, Shi Y, Blackwell TK (2002) CDK-9/cyclin T (P-TEFb) is required in two postinitiation pathways for transcription in the C. elegans embryo. Genes Dev 16: 2135-2146.
359. Liu X, Bushnell DA, Silva D-A, Huang X, Kornberg RD (2011) Initiation Complex Structure and Promoter Proofreading. Science 333: 633-637.
360. Wada T, Takagi T, Yamaguchi Y, Ferdous A, Imai T, et al. (1998) DSIF, a novel transcription elongation factor that regulates RNA polymerase II processivity, is composed of human Spt4 and Spt5 homologs. Genes Dev 12: 343-356.
361. Wada T, Orphanides G, Hasegawa J, Kim DK, Shima D, et al. (2000) FACT relieves DSIF/NELF-mediated inhibition of transcriptional elongation and reveals functional differences between P-TEFb and TFIIH. Mol Cell 5: 1067-1072.
362. Yankulov KY, Pandes M, McCracken S, Bouchard D, Bentley DL (1996) TFIIH functions in regulating transcriptional elongation by RNA polymerase II in Xenopus oocytes. Mol Cell Biol 16: 3291-3299.
363. Yamaguchi Y, Wada T, Watanabe D, Takagi T, Hasegawa J, et al. (1999) Structure and function of the human transcription elongation factor DSIF. J Biol Chem 274: 8085-8092.
364. Conaway RC, Conaway JW (1994) Transcription : mechanisms and regulation. New York: Raven Press. xix, 570 p. p.
365. Rahl PB, Lin CY, Seila AC, Flynn RA, McCuine S, et al. (2010) c-Myc regulates transcriptional pause release. Cell 141: 432-445.
366. Cheng B, Li T, Rahl PB, Adamson TE, Loudas NB, et al. (2012) Functional Association of Gdown1 with RNA Polymerase II Poised on Human Genes. Mol Cell 45: 38-50.
367. Core LJ, Waterfall JJ, Lis JT (2008) Nascent RNA sequencing reveals widespread pausing and divergent initiation at human promoters. Science 322: 1845-1848.
368. Gilchrist DA, Dos Santos G, Fargo DC, Xie B, Gao Y, et al. (2010) Pausing of RNA polymerase II disrupts DNA-specified nucleosome organization to enable precise gene regulation. Cell 143: 540-551.
369. Lis JT (2007) Imaging Drosophila gene activation and polymerase pausing in vivo. Nature 450: 198-202.
370. Core LJ, Lis JT (2008) Transcription regulation through promoter-proximal pausing of RNA polymerase II. Science 319: 1791-1792.

371. Chopra VS, Hendrix DA, Core LJ, Tsui C, Lis JT, et al. (2011) The polycomb group mutant esc leads to augmented levels of paused Pol II in the Drosophila embryo. Mol Cell 42: 837-844.
372. Gilmour DS (2009) Promoter proximal pausing on genes in metazoans. Chromosoma 118: 1-10.
373. Peterlin BM, Price DH (2006) Controlling the elongation phase of transcription with P-TEFb. Mol Cell 23: 297-305.
374. Ping YH, Rana TM (2001) DSIF and NELF interact with RNA polymerase II elongation complex and HIV-1 Tat stimulates P-TEFb-mediated phosphorylation of RNA polymerase II and DSIF during transcription elongation. J Biol Chem 276: 12951-12958.
375. Wada T, Takagi T, Yamaguchi Y, Watanabe D, Handa H (1998) Evidence that P-TEFb alleviates the negative effect of DSIF on RNA polymerase II-dependent transcription in vitro. EMBO J 17: 7395-7403.
376. Bres V, Yoh SM, Jones KA (2008) The multi-tasking P-TEFb complex. Curr Opin Cell Biol 20: 334-340.
377. Fujita T, Schlegel W (2010) Promoter-proximal pausing of RNA polymerase II: an opportunity to regulate gene transcription. J Recept Signal Transduct Res 30: 31-42.
378. Lin X, Taube R, Fujinaga K, Peterlin BM (2002) P-TEFb containing cyclin K and Cdk9 can activate transcription via RNA. J Biol Chem 277: 16873-16878.
379. Yamada T, Yamaguchi Y, Inukai N, Okamoto S, Mura T, et al. (2006) P-TEFb-mediated phosphorylation of hSpt5 C-terminal repeats is critical for processive transcription elongation. Mol Cell 21: 227-237.
380. Fujita T, Piuz I, Schlegel W (2009) The transcription elongation factors NELF, DSIF and P-TEFb control constitutive transcription in a gene-specific manner. FEBS Lett 583: 2893-2898.
381. Fay A, Misulovin Z, Li J, Schaaf CA, Gause M, et al. (2011) Cohesin selectively binds and regulates genes with paused RNA polymerase. Curr Biol 21: 1624-1634.
382. Wang Z, Rana TM (1997) DNA damage-dependent transcriptional arrest and termination of RNA polymerase II elongation complexes in DNA template containing HIV-1 promoter. Proc Natl Acad Sci U S A 94: 6688-6693.
383. Awrey DE, Weilbaecher RG, Hemming SA, Orlicky SM, Kane CM, et al. (1997) Transcription elongation through DNA arrest sites. A multistep process involving both RNA polymerase II subunit RPB9 and TFIIS. J Biol Chem 272: 14747-14754.
384. Komissarova N, Kashlev M (1997) Transcriptional arrest: Escherichia coli RNA polymerase translocates backward, leaving the 3' end of the RNA intact and extruded. Proc Natl Acad Sci U S A 94: 1755-1760.
385. Gu W, Wind M, Reines D (1996) Increased accommodation of nascent RNA in a product site on RNA polymerase II during arrest. Proc Natl Acad Sci U S A 93: 6935-6940.
386. Sen R, Nagai H, Shimamoto N (2000) Polymerase arrest at the lambdaP(R) promoter during transcription initiation. J Biol Chem 275: 10899-10904.
387. Dvir A, Conaway RC, Conaway JW (1996) Promoter escape by RNA polymerase II. A role for an ATP cofactor in suppression of arrest by polymerase at promoter-proximal sites. J Biol Chem 271: 23352-23356.
388. Samkurashvili I, Luse DS (1996) Translocation and transcriptional arrest during transcript elongation by RNA polymerase II. J Biol Chem 271: 23495-23505.
389. Hawryluk PJ, Ujvari A, Luse DS (2004) Characterization of a novel RNA polymerase II arrest site which lacks a weak 3' RNA-DNA hybrid. Nucleic Acids Res 32: 1904-1916.

390. Luse DS, Spangler LC, Ujvari A (2011) Efficient and rapid nucleosome traversal by RNA polymerase II depends on a combination of transcript elongation factors. J Biol Chem 286: 6040-6048.
391. Izban MG, Luse DS (1992) Factor-stimulated RNA polymerase II transcribes at physiological elongation rates on naked DNA but very poorly on chromatin templates. J Biol Chem 267: 13647-13655.
392. Chang CH, Luse DS (1997) The H3/H4 tetramer blocks transcript elongation by RNA polymerase II in vitro. J Biol Chem 272: 23427-23434.
393. Ujvari A, Hsieh FK, Luse SW, Studitsky VM, Luse DS (2008) Histone N-terminal tails interfere with nucleosome traversal by RNA polymerase II. J Biol Chem 283: 32236-32243.
394. Izban MG, Luse DS (1993) The increment of SII-facilitated transcript cleavage varies dramatically between elongation competent and incompetent RNA polymerase II ternary complexes. J Biol Chem 268: 12874-12885.
395. Keene RG, Luse DS (1999) Initially transcribed sequences strongly affect the extent of abortive initiation by RNA polymerase II. J Biol Chem 274: 11526-11534.
396. Pal M, Luse DS (2003) The initiation-elongation transition: lateral mobility of RNA in RNA polymerase II complexes is greatly reduced at +8/+9 and absent by +23. Proc Natl Acad Sci U S A 100: 5700-5705.
397. Bondarenko VA, Steele LM, Ujvari A, Gaykalova DA, Kulaeva OI, et al. (2006) Nucleosomes can form a polar barrier to transcript elongation by RNA polymerase II. Mol Cell 24: 469-479.
398. Knezetic JA, Luse DS (1986) The presence of nucleosomes on a DNA template prevents initiation by RNA polymerase II in vitro. Cell 45: 95-104.
399. Jin J, Bai L, Johnson DS, Fulbright RM, Kireeva ML, et al. (2010) Synergistic action of RNA polymerases in overcoming the nucleosomal barrier. Nat Struct Mol Biol 17: 745-752.
400. Palangat M, Renner DB, Price DH, Landick R (2005) A negative elongation factor for human RNA polymerase II inhibits the anti-arrest transcript-cleavage factor TFIIS. Proc Natl Acad Sci U S A 102: 15036-15041.
401. Taft RJ, Kaplan CD, Simons C, Mattick JS (2009) Evolution, biogenesis and function of promoter-associated RNAs. Cell Cycle 8: 2332-2338.
402. Taft RJ, Simons C, Nahkuri S, Oey H, Korbie DJ, et al. (2010) Nuclear-localized tiny RNAs are associated with transcription initiation and splice sites in metazoans. Nat Struct Mol Biol 17: 1030-1034.
403. Cserzo M, Turu G, Varnai P, Hunyady L (2010) Relating underrepresented genomic DNA patterns and tiRNAs: the rule behind the observation and beyond. Biology Direct 5: 56.
404. Taft RJ, Glazov EA, Cloonan N, Simons C, Stephen S, et al. (2009) Tiny RNAs associated with transcription start sites in animals. Nat Genet 41: 572-578.
405. Takagi T, Walker AK, Sawa C, Diehn F, Takase Y, et al. (2003) The Caenorhabditis elegans mRNA 5'-capping enzyme. In vitro and in vivo characterization. J Biol Chem 278: 14174-14184.
406. Srinivasan P, Piano F, Shatkin AJ (2003) mRNA capping enzyme requirement for Caenorhabditis elegans viability. J Biol Chem 278: 14168-14173.
407. Fabrega C, Shen V, Shuman S, Lima CD (2003) Structure of an mRNA Capping Enzyme Bound to the Phosphorylated Carboxy-Terminal Domain of RNA Polymerase II. Molecular Cell 11: 1549-1561.
408. Mandal SS, Chu C, Wada T, Handa H, Shatkin AJ, et al. (2004) Functional interactions of RNA-capping enzyme with factors that positively and negatively regulate promoter

escape by RNA polymerase II. Proceedings of the National Academy of Sciences of the United States of America 101: 7572-7577.
409. Meinhart A, Cramer P (2004) Recognition of RNA polymerase II carboxy-terminal domain by 3[prime]-RNA-processing factors. Nature 430: 223-226.
410. Ai N, Hu X, Ding F, Yu B, Wang H, et al. (2011) Signal-induced Brd4 release from chromatin is essential for its role transition from chromatin targeting to transcriptional regulation. Nucleic Acids Res 39: 9592-9604.
411. Zhang Z, Klatt A, Gilmour DS, Henderson AJ (2007) Negative elongation factor NELF represses human immunodeficiency virus transcription by pausing the RNA polymerase II complex. J Biol Chem 282: 16981-16988.
412. Schneider J, Wood A, Lee JS, Schuster R, Dueker J, et al. (2005) Molecular regulation of histone H3 trimethylation by COMPASS and the regulation of gene expression. Mol Cell 19: 849-856.
413. Ivanovska I, Jacques PE, Rando OJ, Robert F, Winston F (2011) Control of chromatin structure by spt6: different consequences in coding and regulatory regions. Mol Cell Biol 31: 531-541.
414. Hartzog GA, Wada T, Handa H, Winston F (1998) Evidence that Spt4, Spt5, and Spt6 control transcription elongation by RNA polymerase II in Saccharomyces cerevisiae. Genes Dev 12: 357-369.
415. Belotserkovskaya R, Reinberg D (2004) Facts about FACT and transcript elongation through chromatin. Curr Opin Genet Dev 14: 139-146.
416. Andrulis ED, Guzman E, Doring P, Werner J, Lis JT (2000) High-resolution localization of Drosophila Spt5 and Spt6 at heat shock genes in vivo: roles in promoter proximal pausing and transcription elongation. Genes Dev 14: 2635-2649.
417. Sapountzi V, Logan IR, Robson CN (2006) Cellular functions of TIP60. Int J Biochem Cell Biol 38: 1496-1509.
418. Verdone L, Caserta M, Mauro ED (2005) Role of histone acetylation in the control of gene expression. Biochemistry and Cell Biology 83: 344-353.
419. Li B, Carey M, Workman JL (2007) The Role of Chromatin during Transcription. Cell 128: 707-719.
420. Bourbon HM (2008) Comparative genomics supports a deep evolutionary origin for the large, four-module transcriptional mediator complex. Nucleic Acids Res 36: 3993-4008.
421. Malik S, Roeder RG (2010) The metazoan Mediator co-activator complex as an integrative hub for transcriptional regulation. Nat Rev Genet 11: 761-772.
422. Svejstrup JQ, Li Y, Fellows J, Gnatt A, Bjorklund S, et al. (1997) Evidence for a mediator cycle at the initiation of transcription. Proceedings of the National Academy of Sciences 94: 6075-6078.
423. Max T, Søgaard M, Svejstrup JQ (2007) Hyperphosphorylation of the C-terminal Repeat Domain of RNA Polymerase II Facilitates Dissociation of Its Complex with Mediator. Journal of Biological Chemistry 282: 14113-14120.
424. Malik S, Barrero MJ, Jones T (2007) Identification of a Regulator of Transcription Elongation as an Accessory Factor for the Human Mediator Coactivator. Proceedings of the National Academy of Sciences of the United States of America 104: 6182-6187.
425. Yoda A, Kouike H, Okano H, Sawa H (2005) Components of the transcriptional Mediator complex are required for asymmetric cell division in C. elegans. Development 132: 1885-1893.
426. Nguyen AT, Zhang Y (2011) The diverse functions of Dot1 and H3K79 methylation. Genes Dev 25: 1345-1358.

427. Mohan M, Herz HM, Takahashi YH, Lin C, Lai KC, et al. (2010) Linking H3K79 trimethylation to Wnt signaling through a novel Dot1-containing complex (DotCom). Genes Dev 24: 574-589.
428. Cheng C, Yan KK, Yip KY, Rozowsky J, Alexander R, et al. (2011) A statistical framework for modeling gene expression using chromatin features and application to modENCODE datasets. Genome Biol 12: R15.
429. Iyer LM, Anantharaman V, Wolf MY, Aravind L (2008) Comparative genomics of transcription factors and chromatin proteins in parasitic protists and other eukaryotes. Int J Parasitol 38: 1-31.
430. San-Segundo PA, Roeder GS (2000) Role for the Silencing Protein Dot1 in Meiotic Checkpoint Control. Molecular Biology of the Cell 11: 3601-3615.
431. Kolasinska-Zwierz P, Down T, Latorre I, Liu T, Liu XS, et al. (2009) Differential chromatin marking of introns and expressed exons by H3K36me3. Nat Genet 41: 376-381.
432. Wagner EJ, Carpenter PB (2012) Understanding the language of Lys36 methylation at histone H3. Nat Rev Mol Cell Biol 13: 115-126.
433. Guenther MG, Levine SS, Boyer LA, Jaenisch R, Young RA (2007) A chromatin landmark and transcription initiation at most promoters in human cells. Cell 130: 77-88.
434. Chantalat S, Depaux A, Hery P, Barral S, Thuret JY, et al. (2011) Histone H3 trimethylation at lysine 36 is associated with constitutive and facultative heterochromatin. Genome Res 21: 1426-1437.
435. Adelman K, La Porta A, Santangelo TJ, Lis JT, Roberts JW, et al. (2002) Single molecule analysis of RNA polymerase elongation reveals uniform kinetic behavior. Proc Natl Acad Sci U S A 99: 13538-13543.
436. Davenport RJ, Wuite GJ, Landick R, Bustamante C (2000) Single-molecule study of transcriptional pausing and arrest by E. coli RNA polymerase. Science 287: 2497-2500.
437. Guertin MJ, Petesch SJ, Zobeck KL, Min IM, Lis JT (2010) Drosophila Heat Shock System as a General Model to Investigate Transcriptional Regulation. Cold Spring Harbor Symposia on Quantitative Biology 75: 1-9.
438. Zobeck KL, Buckley MS, Zipfel WR, Lis JT (2010) Recruitment timing and dynamics of transcription factors at the Hsp70 loci in living cells. Mol Cell 40: 965-975.
439. Guertin MJ, Lis JT (2010) Chromatin Landscape Dictates HSF Binding to Target DNA Elements. PLoS Genet 6: e1001114.
440. Petesch SJ, Lis JT (2008) Rapid, transcription-independent loss of nucleosomes over a large chromatin domain at Hsp70 loci. Cell 134: 74-84.
441. Petesch SJ, Lis JT (2012) Activator-Induced Spread of Poly(ADP-Ribose) Polymerase Promotes Nucleosome Loss at Hsp70. Mol Cell 45: 64-74.
442. Heale JT, Ball AR, Jr., Schmiesing JA, Kim JS, Kong X, et al. (2006) Condensin I interacts with the PARP-1-XRCC1 complex and functions in DNA single-strand break repair. Mol Cell 21: 837-848.
443. Xing H, Wilkerson DC, Mayhew CN, Lubert EJ, Skaggs HS, et al. (2005) Mechanism of hsp70i gene bookmarking. Science 307: 421-423.
444. Borggrefe T, Yue X (2011) Interactions between subunits of the Mediator complex with gene-specific transcription factors. Semin Cell Dev Biol 22: 759-768.
445. Deng W, Blobel GA (2010) Do chromatin loops provide epigenetic gene expression states? Curr Opin Genet Dev 20: 548-554.
446. Ong CT, Corces VG (2011) Enhancer function: new insights into the regulation of tissue-specific gene expression. Nat Rev Genet 12: 283-293.

447. Buratowski S, Kim T (2010) The role of cotranscriptional histone methylations. Cold Spring Harb Symp Quant Biol 75: 95-102.
448. Reeves WM, Hahn S (2005) Targets of the Gal4 transcription activator in functional transcription complexes. Mol Cell Biol 25: 9092-9102.
449. Morillon A, Karabetsou N, Nair A, Mellor J (2005) Dynamic lysine methylation on histone H3 defines the regulatory phase of gene transcription. Mol Cell 18: 723-734.
450. Taverna SD, Ilin S, Rogers RS, Tanny JC, Lavender H, et al. (2006) Yng1 PHD Finger Binding to H3 Trimethylated at K4 Promotes NuA3 HAT Activity at K14 of H3 and Transcription at a Subset of Targeted ORFs. Molecular Cell 24: 785-796.
451. Terzi N, Churchman LS, Vasiljeva L, Weissman J, Buratowski S (2011) H3K4 trimethylation by Set1 promotes efficient termination by the Nrd1-Nab3-Sen1 pathway. Mol Cell Biol 31: 3569-3583.
452. Kim T, Buratowski S (2009) Dimethylation of H3K4 by Set1 recruits the Set3 histone deacetylase complex to 5' transcribed regions. Cell 137: 259-272.
453. Keogh MC, Kurdistani SK, Morris SA, Ahn SH, Podolny V, et al. (2005) Cotranscriptional set2 methylation of histone H3 lysine 36 recruits a repressive Rpd3 complex. Cell 123: 593-605.
454. Buratowski S, Kim T (2011) The Role of Cotranscriptional Histone Methylations. Cold Spring Harbor Symposia on Quantitative Biology.
455. Quan TK, Hartzog GA (2010) Histone H3K4 and K36 methylation, Chd1 and Rpd3S oppose the functions of Saccharomyces cerevisiae Spt4-Spt5 in transcription. Genetics 184: 321-334.
456. Burgio G, La Rocca G, Sala A, Arancio W, Di Gesu D, et al. (2008) Genetic identification of a network of factors that functionally interact with the nucleosome remodeling ATPase ISWI. PLoS Genet 4: e1000089.
457. Sala A, Toto M, Pinello L, Gabriele A, Di Benedetto V, et al. (2011) Genome-wide characterization of chromatin binding and nucleosome spacing activity of the nucleosome remodelling ATPase ISWI. EMBO J 30: 1766-1777.
458. Alkhatib SG, Landry JW (2011) The nucleosome remodeling factor. FEBS Lett 585: 3197-3207.
459. Clapier CR, Nightingale KP, Becker PB (2002) A critical epitope for substrate recognition by the nucleosome remodeling ATPase ISWI. Nucleic Acids Res 30: 649-655.
460. Clapier CR, Langst G, Corona DF, Becker PB, Nightingale KP (2001) Critical role for the histone H4 N terminus in nucleosome remodeling by ISWI. Mol Cell Biol 21: 875-883.
461. Corona DF, Clapier CR, Becker PB, Tamkun JW (2002) Modulation of ISWI function by site-specific histone acetylation. EMBO Rep 3: 242-247.
462. Kia SK, Gorski MM, Giannakopoulos S, Verrijzer CP (2008) SWI/SNF mediates polycomb eviction and epigenetic reprogramming of the INK4b-ARF-INK4a locus. Mol Cell Biol 28: 3457-3464.
463. Diebold ML, Koch M, Loeliger E, Cura V, Winston F, et al. (2010) The structure of an Iws1/Spt6 complex reveals an interaction domain conserved in TFIIS, Elongin A and Med26. EMBO J 29: 3979-3991.
464. Morillon A, Karabetsou N, O'Sullivan J, Kent N, Proudfoot N, et al. (2003) Isw1 chromatin remodeling ATPase coordinates transcription elongation and termination by RNA polymerase II. Cell 115: 425-435.
465. Euskirchen GM, Auerbach RK, Davidov E, Gianoulis TA, Zhong G, et al. (2011) Diverse roles and interactions of the SWI/SNF chromatin remodeling complex revealed using global approaches. PLoS Genet 7: e1002008.

466. Marenda DR, Zraly CB, Dingwall AK (2004) The Drosophila Brahma (SWI/SNF) chromatin remodeling complex exhibits cell-type specific activation and repression functions. Dev Biol 267: 279-293.
467. Batsche E, Yaniv M, Muchardt C (2006) The human SWI/SNF subunit Brm is a regulator of alternative splicing. Nat Struct Mol Biol 13: 22-29.
468. Brown CR, Mao C, Falkovskaia E, Law JK, Boeger H (2011) In Vivo Role for the Chromatin-remodeling Enzyme SWI/SNF in the Removal of Promoter Nucleosomes by Disassembly Rather Than Sliding. J Biol Chem 286: 40556-40565.
469. Montecino M, Stein JL, Stein GS, Lian JB, van Wijnen AJ, et al. (2007) Nucleosome organization and targeting of SWI/SNF chromatin-remodeling complexes: contributions of the DNA sequence. Biochem Cell Biol 85: 419-425.
470. Peterson CL, Workman JL (2000) Promoter targeting and chromatin remodeling by the SWI/SNF complex. Curr Opin Genet Dev 10: 187-192.
471. Mulholland N, Xu Y, Sugiyama H, Zhao K (2012) SWI/SNF-mediated chromatin remodeling induces Z-DNA formation on a nucleosome. Cell Biosci 2: 3.
472. Moller A, Avila FW, Erickson JW, Jackle H (2005) Drosophila BAP60 is an essential component of the Brahma complex, required for gene activation and repression. J Mol Biol 352: 329-337.
473. Zhang B, Chambers KJ, Faller DV, Wang S (2007) Reprogramming of the SWI/SNF complex for co-activation or co-repression in prohibitin-mediated estrogen receptor regulation. Oncogene 26: 7153-7157.
474. Zhang, Yinghua L (2011) The Expanding Mi-2/NuRD Complexes: A Schematic Glance. Proteomics Insights: 79.
475. Erkina TY, Zou Y, Freeling S, Vorobyev VI, Erkine AM (2010) Functional interplay between chromatin remodeling complexes RSC, SWI/SNF and ISWI in regulation of yeast heat shock genes. Nucleic Acids Research 38: 1441-1449.
476. Shivaswamy S, Iyer VR (2008) Stress-dependent dynamics of global chromatin remodeling in yeast: dual role for SWI/SNF in the heat shock stress response. Mol Cell Biol 28: 2221-2234.
477. Altaf M, Auger A, Monnet-Saksouk J, Brodeur J, Piquet S, et al. (2010) NuA4-dependent acetylation of nucleosomal histones H4 and H2A directly stimulates incorporation of H2A.Z by the SWR1 complex. J Biol Chem 285: 15966-15977.
478. Santisteban MS, Kalashnikova T, Smith MM (2000) Histone H2A.Z regulats transcription and is partially redundant with nucleosome remodeling complexes. Cell 103: 411-422.
479. Hassan AH, Neely KE, Vignali M, Reese JC, Workman JL (2001) Promoter targeting of chromatin-modifying complexes. Front Biosci 6: D1054-1064.
480. Passannante M, Marti CO, Pfefferli C, Moroni PS, Kaeser-Pebernard S, et al. (2010) Different Mi-2 complexes for various developmental functions in Caenorhabditis elegans. PLoS ONE 5: e13681.
481. Drouin S, Laramee L, Jacques PE, Forest A, Bergeron M, et al. (2010) DSIF and RNA polymerase II CTD phosphorylation coordinate the recruitment of Rpd3S to actively transcribed genes. PLoS Genet 6: e1001173.
482. Li B, Jackson J, Simon MD, Fleharty B, Gogol M, et al. (2009) Histone H3 lysine 36 dimethylation (H3K36me2) is sufficient to recruit the Rpd3s histone deacetylase complex and to repress spurious transcription. J Biol Chem 284: 7970-7976.
483. Churchman LS, Weissman JS (2011) Nascent transcript sequencing visualizes transcription at nucleotide resolution. Nature 469: 368-373.

484. Stevens JR, O'Donnell AF, Perry TE, Benjamin JJ, Barnes CA, et al. (2011) FACT, the Bur kinase pathway, and the histone co-repressor HirC have overlapping nucleosome-related roles in yeast transcription elongation. PLoS ONE 6: e25644.
485. Belotserkovskaya R, Saunders A, Lis JT, Reinberg D (2004) Transcription through chromatin: understanding a complex FACT. Biochim Biophys Acta 1677: 87-99.
486. Winkler DD, Muthurajan UM, Hieb AR, Luger K (2011) Histone Chaperone FACT Coordinates Nucleosome Interaction through Multiple Synergistic Binding Events. J Biol Chem 286: 41883-41892.
487. Winkler DD, Luger K (2011) The histone chaperone FACT: structural insights and mechanisms for nucleosome reorganization. J Biol Chem 286: 18369-18374.
488. Anderson DM, Beres BJ, Wilson-Rawls J, Rawls A (2009) The homeobox gene Mohawk represses transcription by recruiting the sin3A/HDAC co-repressor complex. Dev Dyn 238: 572-580.
489. Calvo D, Victor M, Gay F, Sui G, Po-Shan Luke M, et al. (2001) A POP-1 repressor complex restricts inappropriate cell type-specific gene transcription during Caenorhabditis elegans embryogenesis. EMBO J 20: 7197-7208.
490. Ruiz-Roig C, Vieitez C, Posas F, de Nadal E (2010) The Rpd3L HDAC complex is essential for the heat stress response in yeast. Mol Microbiol 76: 1049-1062.
491. Deckert J, Struhl K (2002) Targeted recruitment of Rpd3 histone deacetylase represses transcription by inhibiting recruitment of Swi/Snf, SAGA, and TATA binding protein. Mol Cell Biol 22: 6458-6470.
492. Chang KT, Min K-T (2002) Regulation of lifespan by histone deacetylase. Ageing Research Reviews 1: 313-326.
493. Pile LA, Wassarman DA (2000) Chromosomal localization links the SIN3-RPD3 complex to the regulation of chromatin condensation, histone acetylation and gene expression. EMBO J 19: 6131-6140.
494. Rajendran R, Garva R, Krstic-Demonacos M, Demonacos C (2011) Sirtuins: molecular traffic lights in the crossroad of oxidative stress, chromatin remodeling, and transcription. J Biomed Biotechnol 2011: 368276.
495. Imai S, Johnson FB, Marciniak RA, McVey M, Park PU, et al. (2000) Sir2: an NAD-dependent histone deacetylase that connects chromatin silencing, metabolism, and aging. Cold Spring Harb Symp Quant Biol 65: 297-302.
496. Dali-Youcef N, Lagouge M, Froelich S, Koehl C, Schoonjans K, et al. (2007) Sirtuins: The ‘magnificent seven’, function, metabolism and longevity. Annals of Medicine 39: 335-345.
497. Gao L, Gross DS (2008) Sir2 silences gene transcription by targeting the transition between RNA polymerase II initiation and elongation. Mol Cell Biol 28: 3979-3994.
498. Haeusler RA, Pratt-Hyatt M, Good PD, Gipson TA, Engelke DR (2008) Clustering of yeast tRNA genes is mediated by specific association of condensin with tRNA gene transcription complexes. Genes Dev 22: 2204-2214.
499. Morales V, Straub T, Neumann MF, Mengus G, Akhtar A, et al. (2004) Functional integration of the histone acetyltransferase MOF into the dosage compensation complex. EMBO J 23: 2258-2268.

CHAPTER 2

Caenorhabditis elegans Dosage Compensation Regulates Histone H4 Chromatin State on X Chromosomes

This Chapter was published as Wells et al. (2012) in Molecular and Cellular Biology as "*Caenorhabditis elegans* Dosage Compensation Regulates Histone H4 Chromatin State on X Chromosomes." I conducted the experiments and image analysis for data shown in all figures, with two exceptions. The images shown in Figure 2.2B were acquired by M. Snyder, and the Western blots shown in Figure 2.6B were conducted by L. Custer. Figures 2.8 (Martha Snyder) and 2.9 (Laura Custer) were generated to address reviewer comments and concerns. Figure 2.10 was generated by me to confirm that the genetically rescued male worms were, in fact, males.

ABSTRACT

Dosage compensation equalizes X-linked gene expression between the sexes. This process is achieved in *Caenorhabditis elegans* by hermaphrodite-specific, dosage compensation complex (DCC)-mediated, two-fold X-downregulation. How the DCC downregulates gene expression is not known. By analyzing the distribution of histone modifications in nuclei using quantitative fluorescence microscopy, we found that H4K16ac is underrepresented and H4K20me1 is enriched on hermaphrodite X chromosomes in a DCC-dependent manner. Depletion of H4K16ac also requires the conserved histone deacetylase SIR-2.1, while enrichment of H4K20me1 requires the activities of the histone methyltransferases SET-1 and SET-4. Our data suggests that the mechanism of dosage compensation in *C. elegans* involves redistribution of chromatin modifying activities leading to a depletion of H4K16ac and an enrichment of H4K20me1 on the X chromosome. These results support conserved roles for histone H4

chromatin modification in worm dosage compensation analogous to that of flies, using similar elements and opposing strategies to achieve differential two-fold changes in X-linked gene expression.

Introduction

Higher eukaryotes require a balanced karyotype. Most aneuploidies are not tolerated, and those that are have detrimental phenotypic consequences. However, a difference in sex chromosome dose is well tolerated in many species due to dosage compensation. Dosage compensation equalizes both sex chromosome-linked gene expression to autosomes and sex-linked gene expression between the sexes [1]. In the fly *Drosophila melanogaster*, XY males upregulate the single X chromosome two-fold, a mechanism which results in each sex having the functional equivalent of two X chromosomes and two sets of autosomes and therefore a balance of gene expression [2,3]. X upregulation is thought to occur in both sexes in mammals and worms [4-6], resulting in the need to prevent X-linked hyperexpression in females/hermaphrodites. To achieve that, in mammals, XX females inactivate one of the two X chromosomes [7-9], while in the worm *C. elegans*, XX hermaphrodites downregulate both X chromosomes two-fold [10,11].

Dosage compensation mechanisms in mammals and flies involve changes in chromatin. Mammalian X-inactivation is initiated by the *Xist* non-coding RNA and is accomplished by spreading facultative heterochromatin over the entire inactive X (Xi) [7-9]. The active X (Xa) and the Xi can be distinguished by unique sets of activating and repressive epigenetic marks, respectively. The Xi is depleted of H3K4me2/3, acetylation of H3K9, H4K5, K8, K12 and K16, H3R17me2, and H3R26me, but is enriched for H3K9me2/3, H3K27me3, H4R3me2, H4K20me1, H2AK119ub1, and macroH2A, relative to the active X and autosomes [7-9]. To achieve upregulation of the X chromosome in flies, the male-specific lethal (MSL) complex loads across the single X chromosome in males, dependent on *msl-2* expression [12]. The histone acetyltransferase activity of MOF (a subunit of the MSL complex) leads to hyperacetylation of histone H4 lysine 16, a chromatin mark widely associated with gene activation [13-15]. Another histone mark, phosphorylation of histone H3 serine 10 by JIL-1 kinase, also contributes to fly dosage compensation [16-18].

In worms, the dosage compensation complex (DCC) binds to both X chromosomes in hermaphrodites to downregulate gene expression. The DCC consists of condensin I^{DC}, which contains two SMC (structural maintenance of chromosomes) proteins (DPY-27 and MIX-1) and three CAP (chromosome-associated polypeptide) proteins (DPY-26, DPY-28, and CAPG-1), and a recruitment complex, composed of SDC-1, SDC-2, SDC-3 and the associated proteins DPY-30 and DPY-21 [10,11,19-24]. The DCC is thought to load across X in a two-part manner: binding to a group of high-affinity recruitment sites (rex) and spreading in a transcription-dependent, DNA sequence-independent manner to sites unable to recruit on their own (dox) [25,26]. Some rex sites are only able to recruit as extrachromosomal arrays, but not as part of a duplication of a small region of X (waystations) [27]. Condensin I^{DC} is homologous to condensin, the highly conserved mitotic chromosome organization and segregation machinery, suggesting that dosage compensation in the worm is achieved by partial condensation of the X chromosomes. Whether this is accompanied by DCC-mediated changes in chromatin structure at the level of the nucleosome, analogous to those documented in mammals and flies, is not known.

Previous studies reported a decrease in HTZ-1 (histone H2A variant) occupancy [28,29] and decreased levels of H3K4me3 on dosage compensated X chromosomes [30]. Other work has shown an increase in nucleosome occupancy at X-linked gene promoters that is sequence-, and not DCC-, dependent [31]. Genome-wide mapping of chromatin marks by the modEncode project revealed a small decrease in activating marks and a small increase in repressive marks on the X, as well as a large increase in the repressive mark H4K20me1 [32,33]. Whether these chromatin changes are a result of DCC action in worms remains unknown.

In this study, we present evidence that the mechanism of dosage compensation in *C. elegans* involves genome-wide redistribution of chromatin marks, including depletion of H4K16ac and enrichment of H4K20me1 on the X as compared to autosomes. These results suggest that regulation of H4K16ac is a conserved feature of *Drosophila* and *C. elegans* dosage compensation, both of which involve a two-fold regulation of transcript levels from the dosage compensated chromosome. In addition, H4K20me1 enrichment, indicative of transcriptional repression, is conserved in dosage compensation between mammals and *C. elegans*, despite the difference in the degree of transcriptional repression during these processes.

Results

Dosage compensation-dependent changes in chromatin

To look for evidence for the involvement of histone modifications in rebalancing chromosome dosage effects in *C. elegans*, we used immunofluorescence (IF) to assay levels of various histone modifications. To mark the X chromosome territory, we used either IF with antibodies to DCC components (CAPG-1 or DPY-27) or fluorescence *in situ* hybridization with X chromosome probes (Xpaint). We chose this method because IF offers a rapid method to test many antibodies/modifications with relative ease at single cell resolution (so that we can focus on the dosage compensated soma). Microscopy can also be used on the limited amount of starting material obtained from mutants where chromatin immunoprecipiation (ChIP) analysis would not be possible. We analyzed intestinal nuclei, which are 32-ploid, facilitating easier visualization and quantification of antibody staining. We quantified the ratio of average histone modification staining on X versus the entire nucleus using intensity-based masks (see Methods), similar to methods used previously in other systems [34-36]. Because dosage compensation in *C.*

elegans involves a downregulation of gene expression on both hermaphrodite X chromosomes, we expected some activating histone modifications to be underrepresented, some repressive modifications to be enriched, or a combination of both.

We observed significant depletion of H4K16ac and confirmed enrichment of H4K20me1 on hermaphrodite X chromosomes (Fig. 2.1) [32,33]. H4K5ac, H4K8ac, H4K12ac, H3K9ac, and H3K27me3 staining is not statistically different on the hermaphrodite X (Fig. 2.1, data not shown). We observed similar depletion of H4K16ac and enrichment of H4K20me1 whether we used DCC antibodies or X paint FISH to mark the X chromosome (Figs. 2.1A-B), indicating that the harsh fixation conditions involved in FISH did not affect our quantification. Since the H4K16ac and H4K20me1 modifications lie very close to each other on the histone tail, we performed peptide blocking IF experiments to ensure that binding to one modification was not inhibited by the presence of the other (Fig. 2.8). Signal from the H4K16ac antibody was blocked by both a K16ac acetylated peptide and a peptide modified on both residues, but not by a K20me1 peptide, indicating that the antibody is able to bind a K16 acetylated histone tail, whether or not K20 is monomethylated. Similarly, signal from the H4K20me1 antibody was blocked by both a K20me1 peptide and dimodified peptide, but not a K16ac peptide (Fig. 2.8).

We next asked whether the observed depletion of H4K16ac on hermaphrodite X chromosomes were dependent on the hermaphrodite-specific activity of the DCC by analyzing wild type male worms and hermaphrodites carrying mutations in DCC subunits (see Materials and Methods). In both males (Fig. 2.1C) and DCC mutant hermaphrodites (Fig. 2.2), H4K16ac was no longer depleted on the X. In fact, it was enriched on the Xs of DCC mutant hermaphrodites. Similar results were obtained when we used IF to mark the X chromosomes in *sdc-1* or *dpy-21* animals (DCC function is compromised in these strains, but the DCC still loads onto the X chromosomes) (Fig. 2.2A), as well as when we used Xpaint FISH in all mutants analyzed (Figs.

2.2B-C). H4K16ac levels are enriched on the X in dosage compensation mutant hermaphrodites, but not on the X in wild type males (Fig. 2.1C), suggesting the existence of additional sex-specific differences in X chromatin regulatory mechanisms beyond DCC function.

Mutations in DCC subunits either reduced or eliminated H4K20me1 enrichment (Fig. 2.3). Interestingly, in dosage compensation mutants, H4K20me1 signal intensity appeared to increase on autosomes. This is consistent with the idea that in these mutants X chromosome expression increases while autosomal expression decreases [25]. These data indicate that DCC function is necessary both for reduction of H4K16ac and enrichment of H4K20me1 on hermaphrodite X chromosomes.

To gain further insight into how DCC activity may relate to these chromatin changes, we also made use of publically available ChIP-chip datasets produced by the modEncode consortium (http://www.modencode.org) [32,33] for high-resolution analysis of H4K16ac, H4K20me1, and DPY-27 occupancy across the genome. Using Cistrome [37], a web-based platform for high-throughput data analysis, we constructed metagene profiles (Fig. 2.4) for each feature at two time-points, early-biased mixed embryonic stages and larval stage L3 or L4. No larval dataset is currently available for H4K16ac. We compared average ChIP signal profiles of all 2,778 X-linked genes and 17,143 autosomal genes identified in genome build ce4 (WS170). We also compared profiles of X-linked genes subjected to dosage compensation (DC genes) and X-linked genes whose expression is not influenced by the DCC (non-DC genes). DC genes are defined as the 365 genes whose expression is elevated at least 1.5-fold in dosage compensation mutant embryos, and non-DC genes are defined as the 287 genes whose expression does not change significantly in these samples [25]. The ChIP-chip data confirms that H4K16ac is underrepresented and H4K20me1 and DPY-27 are enriched on X-linked genes compared to autosomes (Fig. 2.4). Unexpectedly, there is not a substantial difference between the distribution of DPY-27 and H4K20me1 on DC versus non-DC genes (Fig. 2.4). This is consistent with previous observations that DPY-27 occupancy is not predictive of dosage compensation status [25]. However, H4K16ac levels are considerably higher on non-DC genes than DC genes (Fig. 2.4, row 1), both at the promoter and throughout the gene body, suggesting that lower levels of this mark may be a distinguishing feature of dosage compensation.

SIR-2.1, SET-1 and SET-4 mediate changes on the dosage compensated X chromosomes

We next set out to determine which histone modifying activity is responsible for the reduction of H4K16ac levels on the X chromosomes. Budding yeast Sir2 and its homologs in other organisms are conserved H4K16 deacetylases [38]. Depletion or mutation of *sir-2.1*, a *C. elegans* Sir2 homolog [39], led to the loss of the H4K16ac depletion seen in control vector RNAi-treated worms (Fig. 2.5). Depletion of the other HDACs [*sir-2.2, sir-2.3, sir-2.4, hda-1* (RPD3 homolog)*, hda-2*, *hda-3*, *hda-4*, *hda-5*, *hda-6*, *hda-10*, or *hda-11*] did not show a similar increase in H4K16ac levels on the X chromosomes. We conclude that SIR-2.1 is responsible, at least in part, for the reduction in H4K16ac observed on dosage compensated X chromosomes. However, we cannot rule out the possibility that additional factors, including decreased histone acetyltransferase activity on X, also contribute to the depletion of H4K16ac.

Next we wanted to determine which histone methyltransferase is responsible for the enrichment of H4K20me1 on the X. We tested two candidates: SET-1, the *C. elegans* gene most closely related to PR-SET-7, the enzyme which monomethylates H4K20 [40]; and SET-4, the gene annotated as the *C. elegans* homolog of SUV4-20, the methyltransferase which mediates di- and tri-methylation of H4K20 (Wormbase, [http://www.wormbase.org], release WS222). By IF and western blot analysis, H4K20me1 levels were eliminated in *set-1* mutants or after *set-1* RNAi (Fig. 2.6), consistent with SET-1 depositing this mark. In *set-4(n4600)* mutants [41], or after *set-4*

RNAi, overall H4K20me1 levels increased, and the signal was evenly distributed across the nucleus (Fig. 2.6), suggesting that SET-4 may antagonize H4K20 monomethylation on autosomes. This finding is consistent with the observed increase in H4K20me1 levels in flies carrying a mutation in the *set*-4 homolog *Suv4-20* [42]. Western blot analysis also revealed that SET-4 activity is needed for wild type levels of H4K20me3 (Fig. 2.6B). Confirmation of Western blot results was done using quantitative Western blot analysis (Fig. 2.9). IF experiments using antibodies specific to H4K20me2 and H4K20me3 only produced low level nuclear staining which was not dependent on the presence of SET-4 (data not shown), possibly due to cross-reactivity with another protein. This finding prevented us from assessing the spatial distribution of H4K20me3 in the nucleus. The X enrichment of H4K20me1 was reduced or eliminated in both *set-1* or *set-4* mutant/depleted worms, indicating that X enrichment of this marks requires the activities of both SET-1 and SET-4.

Previous studies suggested that H4K20me1 antagonizes H4K16ac [43]. Consistent with this model, knockdown of *set-1* or mutation of *set-4* abrogated both the enrichment of H4K20me1 and the H4K16ac reduction on the X chromosomes (Figs. 2.5, 2.6A). Conversely, mutation in *sir-2.1* only affected depletion of H4K16ac and did not alter H4K20me1 enrichment on the X chromosomes (Figs. 2.5, 2.6), suggesting that SIR-2.1 may act downstream of SET-1 and SET-4 (see discussion).

Genetic requirements for dosage compensation

We further asked whether *set-1*, *set-4*, and *sir-2.1* are genetically required for dosage compensation. In the *him-8(e1489)*; *xol-1(y9) sex-1(y263)* strain, males die due to inappropriate activation of the DCC, but can be rescued by RNAi depletion of factors necessary for dosage compensation [28]. Significant male rescue was observed after knockdown of the DCC subunit

DPY-27 or consecutive depletion of *set-4* and *set-1* (Fig. 7A). We further analyzed *set-4 set-1* treated worms usng immunoFISH (Fig. 2.10). The DCC bound X chromosomes in both sexes, consistent with the genotype of the strain (Fig. 2.10, rows 1-2). We confirmed the maleness of rescued male worms through identification of the characteristic lagging X chromosome phenotype in male spermatid anaphase I (Fig. 2.10, row 3). Finally, we hypothesized that male rescue was a consequence of X chromosome de-repression. In line with this hypothesis, levels of H4K20me1 were low and similar across the nucleus in both *set-4 set-1* RNAi-treated males and hermaphrodites (Fig. 2.10, rows 4 & 5). Depletion of *set-4* alone led to less, but still significant rescue (Fig. 2.7A), indicating a genetic requirement for these factors in dosage compensation. However, SIR-2.1 rescued males at levels similar to vector RNAi (0.78%; Fig. 2.7A), indicating that SIR-2.1 depletion is not sufficient to disrupt dosage compensation. Since these chromatin factors affect histone modifications globally, and are not specific to dosage compensation, low levels of male rescue should not be interpreted as lack of a dosage compensation role. *set-1* RNAi singly caused 95% lethality among progeny; however, male rescue of 3.6% was seen using a shortened RNAi treatment beginning with L4 stage worms (data not shown).

Discussion

In this study, we searched for evidence of X chromosome histone modification differences in *C. elegans*. We established that levels of H4K16ac levels are reduced, but H4K20me1 levels are enriched, on the dosage compensated X chromosomes in *C. elegans* hermaphrodites (Fig. 2.1). These changes depend both on DCC function and the function of the chromatin modifiers SET-1, SET-4 and SIR-2.1 (Fig. 2.5).

DCC-mediated chromatin changes

Sex chromosome dosage compensation in worms is thought to involve two mechanisms. First, X chromosome expression is upregulated in both sexes compared to autosomes by an unknown mechanism [4,5], followed by hermaphrodite-specific downregulation of both Xs [10,11]. Our data indicates that in the absence of DCC activity, H4K16ac is enriched on hermaphrodite X chromosomes, suggesting that this mark may be involved in the X upregulation process. However, our data in males shows no X enrichment of H4K16ac, indicating that this mark is not responsible for general X upregulation. These observations suggest that other sex-specific, but not DCC-mediated, mechanisms may regulate the X:A gene dosage balance in worms. These additional processes may involve feedback mechanisms between sex determination and chromosome dosage regulatory mechanisms reported previously [44-47]. Indeed, males carrying mutations in DCC genes have X chromosomes similar to wild type males (not enriched for H4K16ac), while karyotypically male (XO) animals transformed into hermaphrodites by a genetic mutation and carrying mutations in DCC genes [*dpy-28(s939); xol-1(y9)* and *her-1(e1520); sdc-3(y126) xol-1(y9)*] had X chromosomes enriched for H4K16ac, similar to DCC mutant hermaphrodites (data not shown).

A mechanistically better understood aspect of the regulation of chromosome dosage effects is the two-fold down-regulation of the X chromosomes in hermaphrodites. Extensive genetic studies demonstrated that the DCC is essential for this process [10,19-24]. Mutations in genes encoding DCC subunits lead to an increase in mRNA levels from the X chromosomes [25,48]. How the DCC regulates transcription is not known, but our results show that the mechanism of transcriptional downregulation by the DCC likely involves the decreased levels of H4K16ac and increased levels of H4K20me1 observed on X. Based on our data, we propose the following model (Fig. 2.7B). First, DCC activity via the function of SET-1 and SET-4 leads to an enrichment of H4K20me1 on the X chromosome. How the DCC influences SET-1 and SET-4 function is unclear. One possibility is that DCC activity leads to an enrichment of the SET-1 protein on X, leading to increased levels of H4K20me1. Alternatively, or in addition, DCC activity (directly or indirectly) may lead to enrichment of SET-4 on autosomes, causing reduced levels of H4K20me1 on autosomes. SET-1 and SET-4 may act in the same pathway and/or in parallel pathways to regulate H4K20me1 levels. Second, DCC activity, via the function of SIR-2.1, leads to a depletion of H4K16ac levels on X. Our results suggest that H4K20me1 regulation is upstream of H4K16ac regulation (Figs. 2.5-2.6), indicating that H4K20me1 may antagonizes H4K16ac. Previous work suggested that H4K20me1 and H4K16ac are mutually antagonistic [43], but other studies find that this may not always be the case [49,50]. Our data suggests a similar dichotomy. In hermaphrodites, H4K20me1 antagonizes H4K16ac on X, because we see loss of H4K16ac depletion when H4K20me1 is no longer X-enriched (Fig. 2.5). In males (Fig. 2.1) and in *set-4* mutant hermaphrodites (Fig. 2.6), however, both marks coexist across the entire nucleus, suggesting that H4K16ac does not antagonize H4K20me1 in our system, at least at the level of whole chromosomes. Furthermore, H4K16ac is distributed uniformly in the nucleus both in the absence (*set-1* mutants) and the presence of uniformly high levels of H4K20me1 (*set-4* mutants), indicating a more complex relationship. The possibility remains that additional parallel chromatin pathways regulate H4K16ac and H4K20me1, perhaps through regulation of H4K16 acetyltransferase(s).

It is worth noting that loss of DPY-21 had the greatest effect on both H4K16ac and H4K20me1 levels on hermaphrodite X chromosomes (Figs. 2.2, 2.3A). To date, the mechanistic contribution of DPY-21 to dosage compensation in *C. elegans* has not been well characterized. Previous studies indicated that DPY-21 is enriched on X in a DCC-dependent manner and regulates gene expression both inside and outside the context of the DCC [24,51,52]. However, severe loss-of-function mutations in *dpy-21* do not lead to hermaphrodite-specific lethality, while mutations in most other DCC components do [24,52]. Taken together, these observations suggest that other mechanisms beyond modulation of H4K20me1 and H4K16ac levels contribute to *C. elegans* dosage compensation. It will be interesting to determine whether these or other histone modifications contribute to gene expression changes on the X chromosomes.

Our results indicate that modulation of H4K16ac is a conserved feature of fly and worm dosage compensation. Enrichment of H4K16ac on the X chromosome in male flies leads to increased transcriptional output [13-15,53], while depletion of H4K16ac on the X chromosomes in hermaphrodite worms leads to a chromatin environment repressive to transcription. H4K16ac can inhibit formation of the 30nm fiber without recruiting accessory chromatin proteins [54], and perhaps this feature makes it well suited for two-fold modulation of gene expression. Both the fly and the worm dosage compensation chromatin regulation mechanisms appear largely different than the chromatin profile associated with X inactivation in mammals. While fly and worm dosage compensation leads to a two-fold adjustment in gene expression levels, X inactivation leads to complete silencing of many genes on the affected chromosome(s). The inactive mammalian X chromosome is enriched for many repressive histone marks and is depleted of many activating histone marks [9]. In contrast, activating chromatin marks are still present on each of the two dosage compensated X chromosomes in worms, and the repressive modification H3K27me3 is not enriched on the dosage compensated X chromosomes (data not shown). This work demonstrates that a similar, but opposite, mechanism than is observed in the fly for transcriptional control during dosage compensation is at work in *C. elegans* and that modulation of histone H4 chromatin state is uniquely well-suited for schemes of two-fold gene regulation.

Transcriptional regulation

Changes in chromatin structure may affect RNA production to achieve dosage compensation in several ways, including different stages of transcription as well as co- and post-transcriptional processing. During mammalian X-inactivation, RNA polymerase II (Pol II) is almost completely excluded from the inactive X chromosome territory early in the X inactivation process leading to transcriptional silencing [55,56]. In *Drosophila*, upregulation of male X is thought to be achieved by increased transcriptional elongation facilitated by H4K16ac enriched in gene bodies [57-63]. The most compelling evidence for increased elongation comes from a recent study gathered using global run-on sequencing to map active transcription across the *Drosophila* genome [60]. The results support a model in which the MSL complex facilitates transcriptional elongation through gene bodies.

Studies in other systems have revealed a link between H4K16ac and regulation of transcriptional elongation by RNA polymerase II. H4K16ac, together with H3S10ph, creates a binding site for the bromodomain protein BRD4, which in turn leads to recruitment of P-TEFb and productive elongation [53,63]. Consistent with this, SIR silencing at the yeast mating type loci has been linked to H4K16 deacetylation and Pol II stalling [64,65]. It is tempting to speculate that regulation of transcription elongation may be involved in *C. elegans* dosage compensation as well. H4K20me1 has been correlated with transcriptional repression in other contexts [66-68].

Comparison of high-resolution chromatin profiles of X-linked and autosomal genes (Fig. 2.4) [32] provide additional insight into potential dosage compensation mechanisms. H4K16ac levels on X-linked genes peak near the transcription start site (TSS) and are very low around the transcription termination site (TTS). In contrast, autosomal genes have higher H4K16ac levels across the TSS and much higher H4K16ac levels near the TTS [32], consistent with increased elongation on autosomes as compared to the X. However, the greatest H4K16ac signal is near the TSS, which is different from the gene body enrichment that has been observed in flies [61,69]. In addition the greatest difference in H4K16ac between DC and non-DC genes is in the promoter region suggesting that regulation of transcription initiation is another possibility.

It is important to acknowledge the strengths and weaknesses of the assays we employed in this study. The often low standard deviations seen in our fluorescence intensity quantification suggest that the technique and our raw data are quite reproducible, and the large changes in X:nucleus signal ratio (0.76 to 1.29 comparing H4K16ac in WT and *dpy-21* mutants, Fig. 2A) indicates the power of this assay to detect differences. However, due to the nature of the technique, this quantification method is best suited to making relative comparisons, not absolute quantification of protein or modification occupancy.

Condensin and chromatin regulation

The exact mechanism of how DCC function leads to the observed chromatin changes remains unknown. We did not observe a physical interaction between the DCC subunits and SIR-2.1, SET-1, or SET-4 by proteomics approaches [19]. However, the interaction may be weak and need not be direct. DPY-21 interacts only weakly with other members of the DCC [24], but may represent a link between SET-1, SET-4, SIR-2.1 and the DCC. It is also possible that other linker proteins are involved, or that DCC action influences SET-1, SET-4, and SIR-2.1 localization or activity indirectly by modulating the higher order structure of the X chromosomes. Condensin is thought to influence higher-order chromosome architecture, and it is possible that condensin-mediated changes in the folding path of the chromatin fiber affect the binding or the activity of other chromosomal proteins. It is worth noting that condensin II recognizes H4K20me1 for chromosomal binding during mitosis in HeLa cells [70], suggesting a connection between condensin and this chromatin modification.

Condensin regulation of Sir2 and transcription has been previously documented in other systems. Condensin regulates Sir2 localization and Sir2-mediated rDNA silencing in budding yeast [71]. Outside of worms, condensin has been implicated in transcriptional regulation in budding yeast and *Drosophila* [72,73]. Therefore, our studies of *C. elegans* condensin I^{DC} function may shed further light on the mechanism of gene repression by condensin in other organisms, as well.

Materials and Methods

Strains

Animals were maintained on NG agar plates using standard methods. The following strains were used in this study:

MT14911 *set-4(n4600)* II

SS1075 *set-1(tm1821)* III/ hT2g

TY0420 *dpy-27(y57)* III

TY1140 *sdc-2(y46)* X

TY1724 *sdc-3(y129)* V

TY1936 *dpy-30(y228)* V/ nt1 [*unc-? (n754) let-?*] (IV; V)

TY2386 wild type (N2)

TY4381 *dpy-28(s939)* III/qC1 III

TY3936 *dpy-21(e428)*

TY4161 *sdc-1(y415)* X

TY4341 *dpy-26(n199) unc-30(e191)* IV/nT1 [qIs51] (III;IV)

TY4403 *him-8(e1489)* IV; *xol-1(y9) sex-1(y263)* X

VC199 *sir-2.1(ok434)* IV

Strains defective in dosage compensation

We analyzed worms homozygous for strong loss-of-function alleles descended from heterozygous mothers (m+z-, *dpy-26(n199)*, *dpy-28(s939)*, *dpy-30(y228)*); worms homozygous for weaker loss-of-function alleles, in which the function of the gene was further depleted by RNAi (*sdc-2(y46, RNAi)*; *dpy-27(y57*, *RNAi)*); worms homozygous for a weak loss-of-function allele in *sdc-3(y129)*, and worms homozygous for strong loss-of-function alleles in the two exceptional dosage compensation genes which do not lead to hermaphrodite lethality (*dpy-21(e428)*, *sdc-1(y415)*).

RNA Interference

RNA interference by feeding was performed with the Ahringer lab RNAi feeding library [74]. Concentrated RNAi (*dpy-27(y57)* on *dpy-27 RNAi*, WT on *set-1* RNAi) was performed as follows: 100mL of LB was inoculated with the RNAi construct-containing bacteria from the Ahringer library in the presence of ampicillin and tetracycline and grown 16 hours at 37°C. IPTG (20% v/w) was added at a dilution of 1:1000 and incubation continued for 2 hours at 37°C. The culture was spun down at 4000rpm for 10 minutes and resuspended in 700 uL of LB. 100uL was plated onto NGM plates containing ampicillin and IPTG and used for RNAi beginning the following day. One generation feeding RNAi [*sdc-2(y46)* grown on *sdc-2 RNAi*] was performed as follows: L1-stage larvae were placed on plates seeded with RNAi bacteria and grown to adulthood. Three generation feeding RNAi (WT on concentrated set-1 RNAi) was performed as follows: P_0 adults from above were transferred to fresh RNAi plates and allowed to lay eggs; L4-stage larvae from this F_1 generation were transferred to a third set of new RNAi plates, allowed to lay embryos, and these worms (the “F_2” generation) were grown to adulthood and examined. Two generation feeding RNAi (all other analyses) was performed as follows: P_0 adults from 1 generation feeding RNAi were transferred to fresh RNAi plates and allowed to lay eggs, and these progeny (''F_1'' generation) were grown to adulthood and examined. Multiple RNAi knockouts (Fig. 2.6) were performed sequentially [similar to [75]]. P_0 adults grown from L1-stage larvae on plates spotted with RNAi against the first factor were moved to plates seeded with RNAi against the second factor and allowed to lay eggs. The progeny ("F_1" generation) were grown to adulthood and examined. RNAi was conducted in the order shown in the data row label.

Antibodies

Antibodies specific to DPY-27 and CAPG-1 were described previously (Csankovszki et al., 2009). Commercial antibodies used for IF analysis were: H3K9ac (1:100, rabbit, Abcam ab4441); H4K16ac (1:500, rabbit, Millipore 07-329); H4K20me1 (1:100, rabbit, Abcam ab9051); H4K20me2 (1:100, rabbit, Millipore 07-367); H4K20me3 (1:100, rabbit, Abcam ab9053); H3K27me3 (1:100, rabbit, Millipore 07-449). Secondary antibodies were purchased from Jackson ImmunoResearch. Antibody specificity was tested using the following peptides: H4K20me1 (Abcam ab17043), H4K16ac (Millipore 12-346). The dimodified H4K16acK20me1 peptide with sequence KGGAK(ac)RHRK(me1)VLRDNIQ was synthesized by Biomatik.

Microscopy

Antibody staining of dissected adults, immunoFISH, and detergent extraction, were performed as described previously [28,76]. Images were captured with a Hamamatsu ORCA-ERGA CCD camera mounted on an Olympus BX61 motorized Z-drive microscope using a 60x APO oil immersion objective. These images are projections of optical sections with a Z spacing of 0.2 microns. Scale bars were added using ImageJ (available at http://rsb.info.nih.gov/ij; developed by Wayne Rasband, National Institutes of Health, Bethesda, MD) and a template image created in Slidebook.

Image Analysis

3D image stacks were collected for each nucleus analyzed at 0.2 micrometer Z-spacing. Fluorescence intensity quantification for histone modifications staining was completed in Slidebook, similarly to methods used previously by other groups in a variety of experimental systems [34-36]. Images were collected by setting exposure times such that the fluorescence intensity for each channel fell within the dynamic range of detection, approximately 2/3 of the maximal intensity for the sample.

For each image, masks were set using the “mask -> segment” function. The mask is established by a user-defined intensity threshold value applied over an image in order to distinguish real signal from background signal and autofluorescence. The same standard of background signal exclusion was applied to all nuclei from the same worm, based upon the levels of background signal and autofluorescence observed. Average signal intensity within a mask, calculated in three dimensions and for each channel individually, is measured by Slidebook calculating the intensity value of each pixel within a masked volume and averaging all values within this mask. This is done for each channel of an image, and histone modification staining average intensity values were recorded for both the “X chromosome(s)” mask and the “histone modification (whole nucleus)” mask. The “whole nucleus” mask was calculated from the histone modification signal, not the DAPI signal. For each histone modification, the ratio of “average X chromosome(s) histone modification intensity” to “whole nucleus histone modification intensity” was then calculated for each nucleus within an experimental set. This ratio was then averaged over all nuclei within an experimental set to calculate the final

“X:nucleus” mean histone modification intensity values shown on each graph. Descriptive statistics (standard deviation and sample size) were also calculated. Sample sizes are listed in each figure. Values shown are means +/- 1 standard deviation of the mean. Fluorescence intensity differences were evaluated by Student’s T-test using MINITAB 12 Student Release.

High-resolution ChIP-chip Metagene Analysis

Chromatin and DCC ChIP-chip datasets (H4K16ac EE: DCC id 3182; H4K20me1 EE: DCC id 2765; H4K20me1 L3: DCC id 2784; DPY-27 EE: DCC id 3435; DPY-27 L4: DCC id 630) were downloaded from modMine 25 (modEncode; intermine.modencode.org). EE refers to early-biased embryo samples composed of roughly 50% dosage compensated and 50% non-dosage compensated tissue [77]. The unzipped raw data and annotation files were then uploaded to the Cistrome/Galaxy server [37], referenced to the ce4 (WS170) genome, for analysis. First, we ran each experiment using MA2C [78] and default settings to call peak regions of signal. Then, the MA2C output files were used in CEAS [79] analysis. We ran CEAS using default settings, but with the addition of four gene lists to the analysis (DC genes, non-DC genes, Autosomes, and X Chromosome). The “All” gene list includes both the expressed and non-expressed genes included in WS170. The DC and non-DC gene lists were constructed from the lists of 373 dosage compensated and 290 non-dosage compensated genes defined previously [25]. The autosomal and X chromosome gene lists were compiled from a WS226 genome download from WormMart (http://caprica.caltech.edu:9002/biomart/martview/). Cistrome recognizes all 17,143 genes on autosomes and all 2,778 genes on X in the WS170 genome build from these autosome and X gene lists. The “Average Gene Profiles” were extracted from each CEAS output report. The X axis (shown in bp) marks the 3kb-scaled metagene body and 1kb upstream and downstream of the transcript start and stop sites. The Y axis represents the average normalized signal from two replicate ChIP-chip experiments (4 replicates for DPY-27 L4 data).

Western blot analysis

Embryos were collected from mutant or RNAi-treated gravid adults. Lysates were prepared by sonicating embryos for ten 15-s bursts in homogenization buffer (50 mM HEPES pH 7.6, 1 mM EDTA, 140 mM KCl, 0.5% NP-40, 10% glycerol, and protease inhibitor cocktail [Calbiochem]). Cellular debris was pelleted by centrifugation at 5000g at 4° C for 15 min. Equal amounts of each sample (7.5 µg) were loaded into 15% acrylamide gels for SDS-PAGE. Proteins were transferred to nitrocellulose and blotted with the following antibodies: H4K20me1 (Abcam ab9051) at 1:10,000 or H4K20me3 (Abcam ab9053) at 1:1000 and α-tubulin (Sigma T6199) at 1:1000.

Acknowledgments

We thank Anna Cacciaglia for laboratory assistance, Susan Strome for the *set-1* mutant strain, as well as Ken Cadigan, Ray Chan, Yali Dou, Anuj Kumar, Kentaro Nabeshima, Andrzej Wierzbicki, and several members of the worm modENCODE consortium for insightful project discussions. The *sir-2.1(ok434)* strain was generated by the C. elegans Reverse Genetics Core Facility at UBC, which is part of the International C. elegans Gene Knockout Consortium. The *set-1(tm1821)* allele was generated by the Mitani lab (National Bioresource Project, Japan), and backcrossed and balanced to generate the SS1075 strain in the laboratory of Susan Strome (UC Santa Cruz).

This work was supported by National Institutes of Health grant RO1 GM079533 (to G.C.), National Science Foundation grant #MCB 1021013 (to G.C.), and the Biological Sciences Scholars Program at the University of Michigan. Some nematode strains used in this work were provided by the Caenorhabditis Genetics Center, which is funded by the NIH National Center for Research Resources.

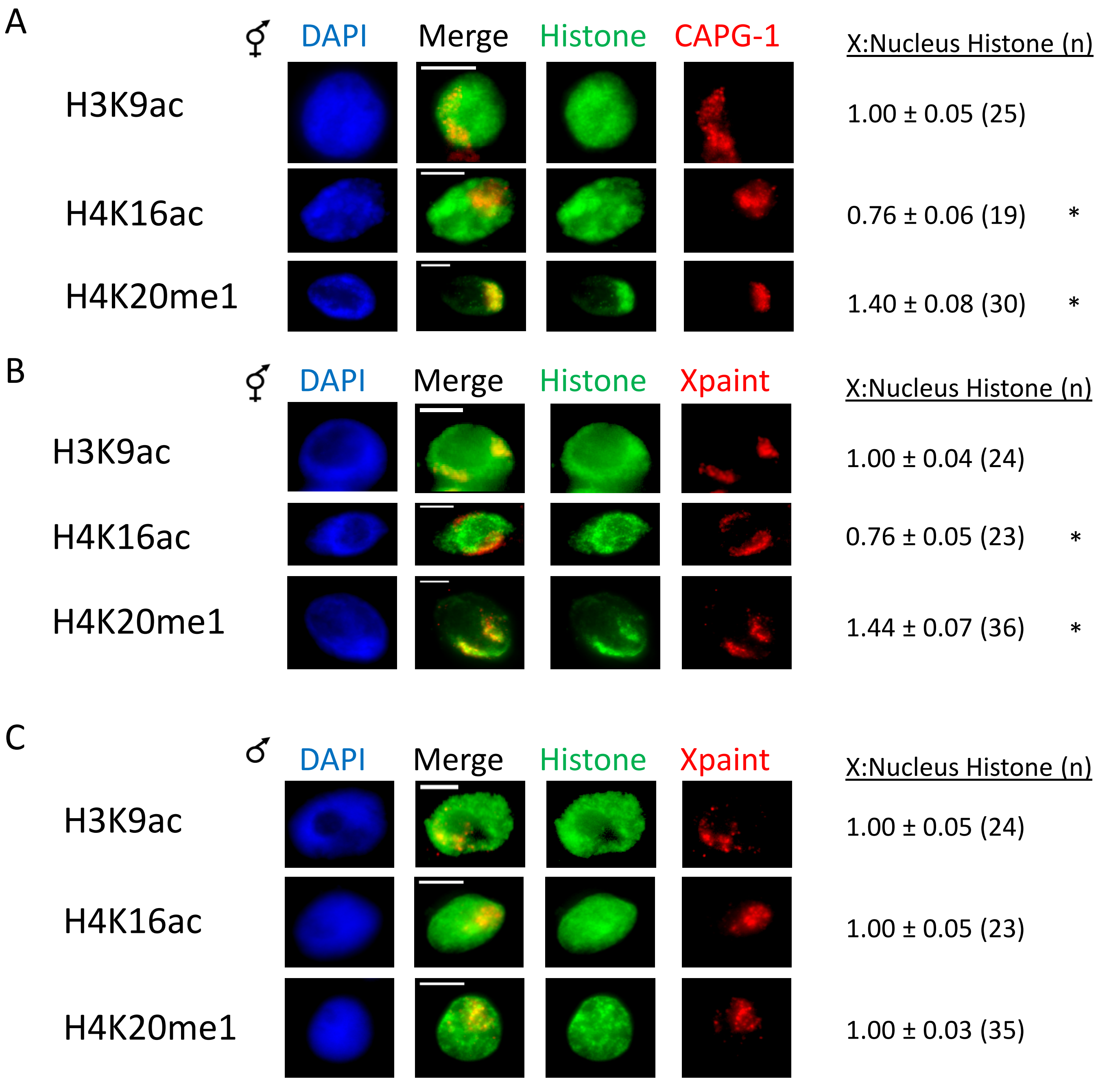

Figure 2.1. Histone modification differences on hermaphrodite X chromosomes. Representative IF images of intestinal nuclei from WT hermaphrodites or males stained with antibodies against H3K9ac, H4K16ac, or H4K20me1 (green) and DCC subunit CAPG-1 (A, red) or probed with Xpaint fluorescent *in situ* hybridization probes (FISH, B-C, red) to mark the X chromosomes. DNA (DAPI) is shown in blue. Scale bars = 5 microns. (right) Fluorescence intensity quantification for (A-C). Average green intensity was determined in both the green and red channels. The ratio of "histone modification staining in X chromosome channel" to "histone modification staining in histone modification channel" was determined and averaged over many nuclei. Mean values +/- 1 standard deviation and sample size (n) are indicated. Asterisks indicate results statistically significant at $p < 0.001$ as compared to males. H4K16ac was reduced by about 25% and H4K20me1 was enriched by 40% on the WT hermaphrodite X chromosomes compared to whole nucleus average.

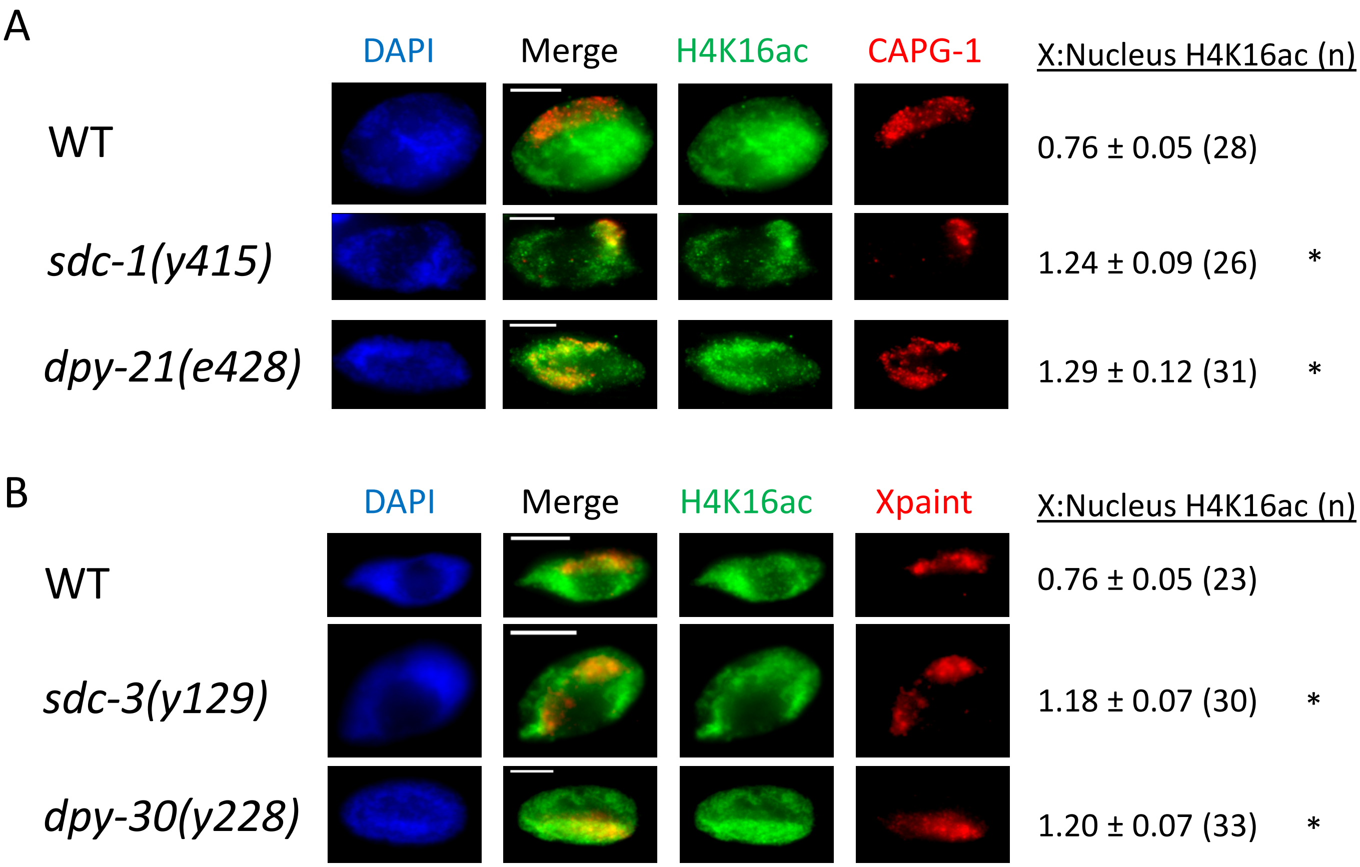

C

Strain	Hermaphrodite (H4K16ac, FISH)	n	Strain	Hermaphrodite (H4K16ac, FISH)	n
dpy-21(e428)	1.29 ± 0.07 *	32	***dpy-28(s939)***	1.23 ± 0.06 *	31
dpy-26(n199)	1.20 ± 0.07 *	25	***sdc-1(y415)***	1.21 ± 0.06 *	32
dpy-27(y57, RNAi)	1.22 ± 0.06 *	33	***sdc-2(y46, RNAi)***	1.22 ± 0.08 *	30

Figure 2.2. H4K16ac depletion is lost in dosage compensation mutants. (A) (left) Representative images of intestinal nuclei from WT hermaphrodite and dosage compensation mutant worms stained with antibodies against H4K16ac (green). The X chromosomes (red) are marked either with antibodies against CAPG-1 (A) or Xpaint FISH (B). DNA, DAPI is shown in blue. Scale bar = 5 microns. (C) Fluorescence intensity quantification for additional DC mutant strains analyzed by H4K16ac IF and Xpaint FISH; images not shown. Asterisks in all panels indicate results statistically significant at $p < 0.001$ as compared to control WT hermaphrodites. Fluorescence intensity quantification (right) shows enrichment of H4K16ac on the X chromosome in all DCC mutants tested. *dpy-21(e428)* shows the greatest degree of enrichment.

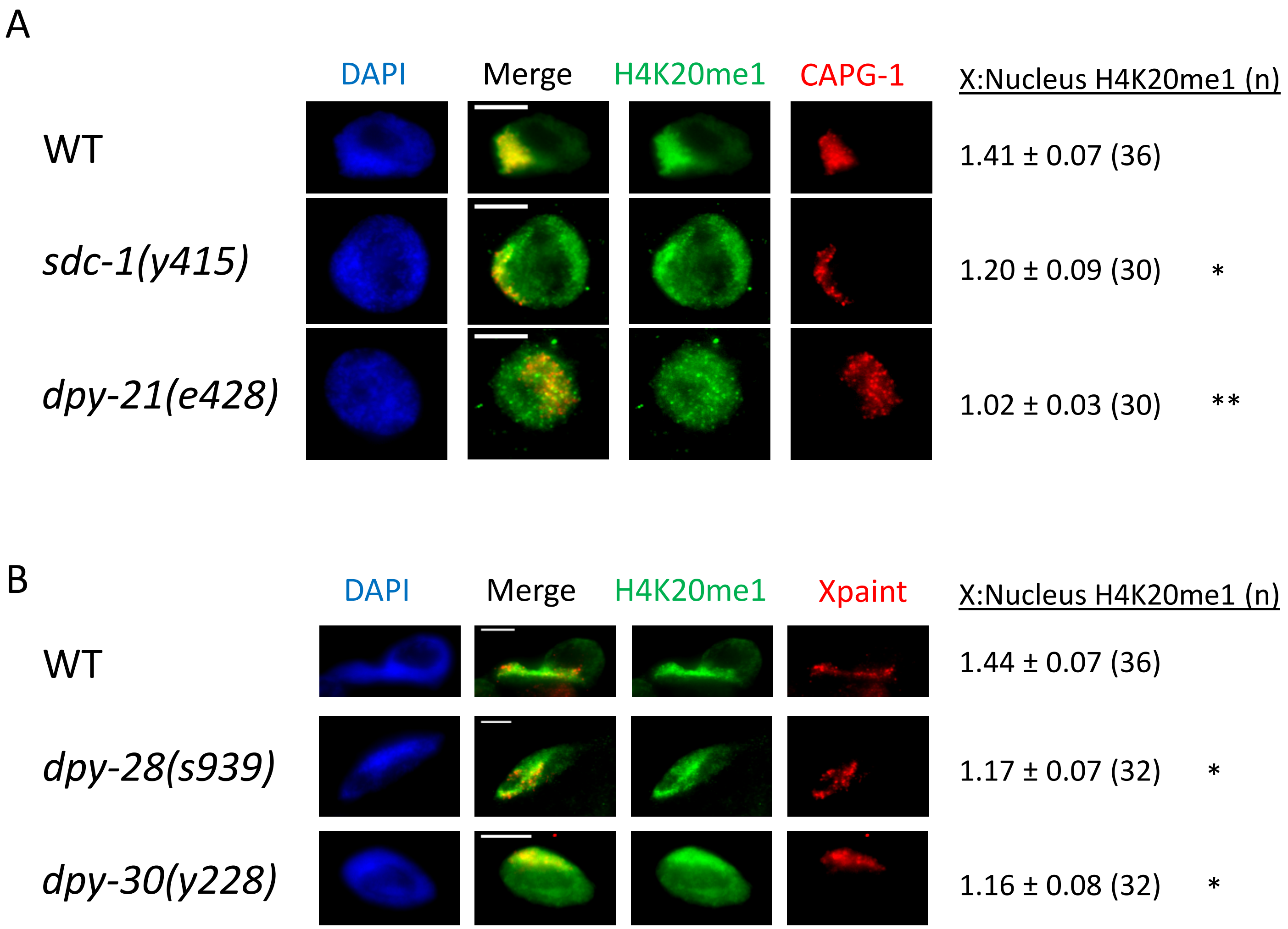

Figure 2.3. H4K20me1 enrichment is lost in dosage compensation mutants. (left) Representative images of intestinal nuclei from WT hermaphrodite and dosage compensation mutant worms stained with antibodies against H4K20me1 (green); the X chromosomes (red) are marked by anti-CAPG-1 (A) or Xpaint FISH (B). DNA, DAPI is shown in blue. Scale bar = 5 microns. Asterisks indicate results statistically significant at $p < 0.001$ as compared to control WT hermaphrodites (one asterisk) or both WT and *sdc-1(y415)* hermaphrodites (two asterisks). Fluorescence intensity quantification (right) shows that the enrichment of H4K20me1 on the X chromosome is reduced in DCC mutants, except in *dpy-21(e428)* where no enrichment is seen.

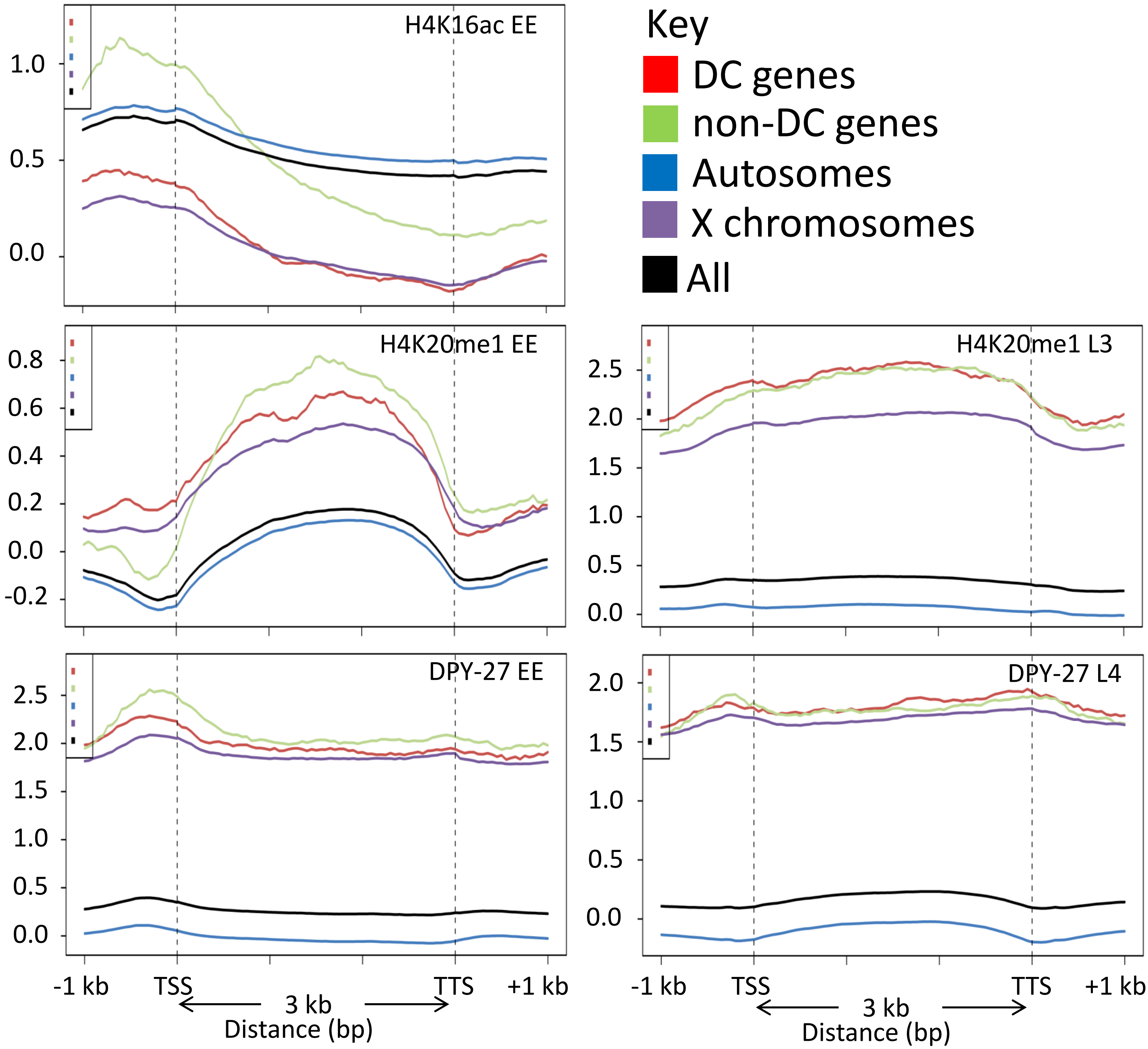

Figure 2.4. High-resolution analysis of chromatin regulation during development. Metagene profiles illustrating H4K16ac, H4K20me1, and DPY-27 ChIP-chip analysis, obtained from modEncode.org or NCBI GEO, conducted on either WT early-biased (EE) embryos (left column) and L3 or L4 stage WT larval tissue (right column). The X axis consists of a 3kb scaled gene body with 1kb upstream and downstream of the transcribed region. The Y axis shows the average ChIP-chip profile values. "All", X-linked, and autosomal genes includes both expressed and not expressed genes from genome build ce4 (WS170), while DC and non-DC genes only include expressed X-linked genes. X to A comparison confirms our IF results concerning H4K16ac and H4K20me1. Further, these results suggest that H4K16ac, but not H4K20me1 or DPY-27 occupancy, may be a predictor of dosage compensation status on X.

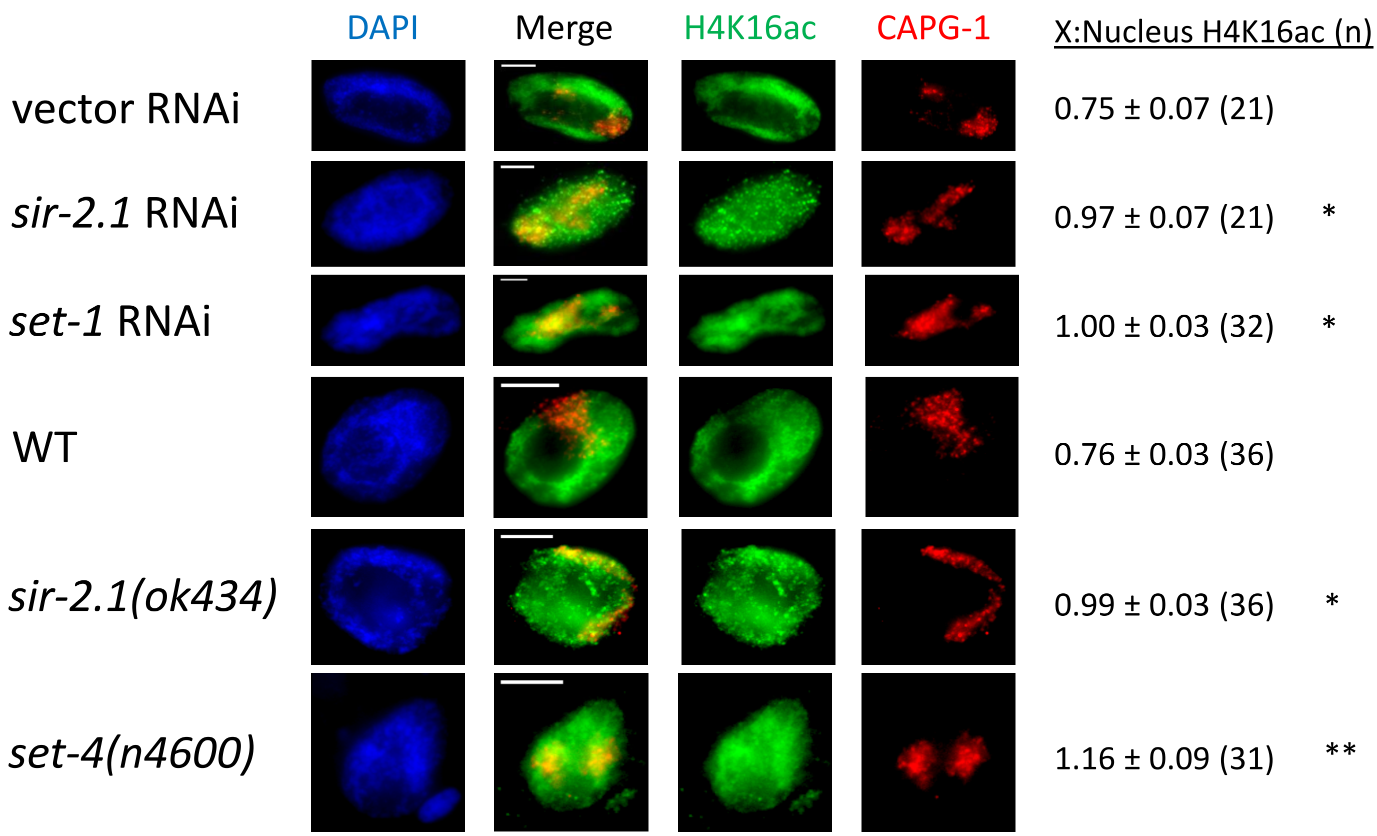

Figure 2.5. The activities of SIR-2, SET-1, and SET-4 are needed for the depletion of H4K16ac on the X chromosomes. (left) Representative immunofluorescence images of intestinal nuclei from worms treated with control vector, *sir-2.1* or *set-1* RNAi, as well as WT, *sir-2.1(ok434),* and *set-4(n4600)* worms stained with antibodies against CAPG-1 (red) and H4K16ac (green). DNA (DAPI) is shown in blue. Scale bars = 5 microns. (right) Fluorescence intensity quantification. Asterisks indicate results statistically significant at $p < 0.001$ as compared to control WT or vector RNAi-treated hermaphrodites (one asterisk) or both WT and *sir-2.1(ok434)* (two asterisks). *sir-2.1* and *set-1* RNAi and/or mutation abolishes the partial H4K16ac depletion; while *set-4* mutation may lead to enrichment of H4K16ac on the X chromosomes similar to most DCC mutants.

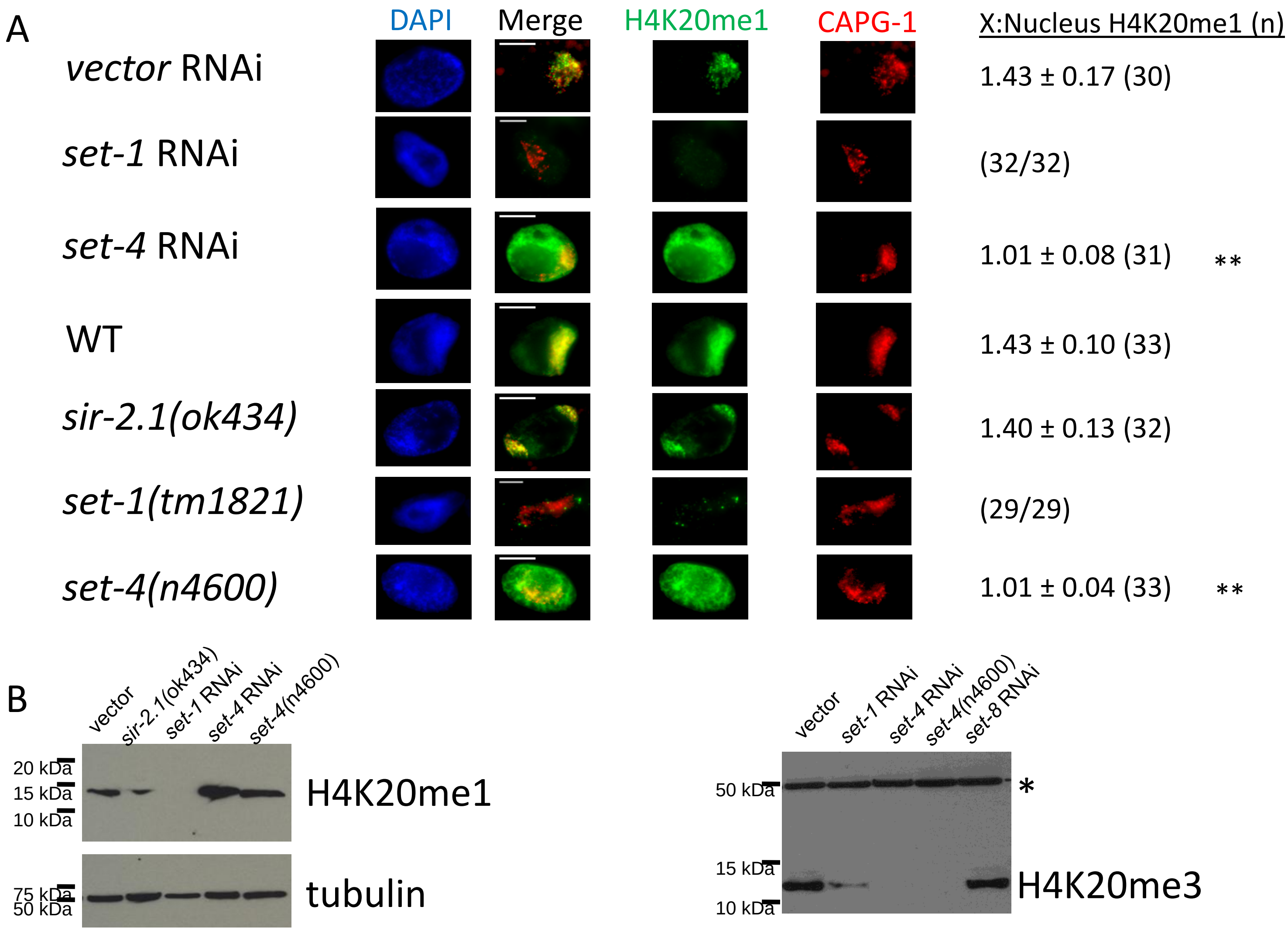

Figure 2.6. Enrichment of H4K20me1 on dosage compensated X chromosomes requires the function of SET-1 and SET-4, but not SIR-2.1. (A, left) Representative immunofluorescence images of intestinal nuclei from worms treated with control vector, *sir-2.1* or *set-1* RNAi, as well as WT, *sir-2.1(ok434),* and *set-4(n4600)* worms stained with antibodies against CAPG-1 (red) and H4K20me1 (green). DNA (DAPI) is shown in blue. Scale bars = 5 microns. (right) Fluorescence intensity quantification. Asterisks indicate results statistically significant at $p < 0.001$ as compared to control WT or vector RNAi controls. *set-1* and *set-4* RNAi and/or mutation abolishes the enrichment of H4K20me1 on the X chromosomes, but a mutation in *sir-2.1* does not. (B) Western blot analysis of H4K20me1 (left) and me3 (right) levels. Shown are embryonic extracts derived from vector, *set-1*, *set-4, or set-8* (a methyltransferase not involved in H4K20 methylation) RNAi-treated WT worms or *set-4(n4600)* or *sir-2.1(ok434)* strains probed with anti-H4K20me1, H4K20me3, and anti-tubulin antibodies. Whereas *set-4* RNAi and mutation increase H4K20me1 as compared to vector controls, *set-1* RNAi abrogated H4K20me1 and *sir-2.1* mutation did not significantly affect H4K20me1. Tubulin is shown as a loading control. H4K20me3 levels diminish after *set-1* RNAi, and are undetectable after *set-4* RNAi or in *set-4(n4600).* Note that the H4K20me3 specific antibody cross-reacts with a higher molecular weight protein (marked by *).

A

B

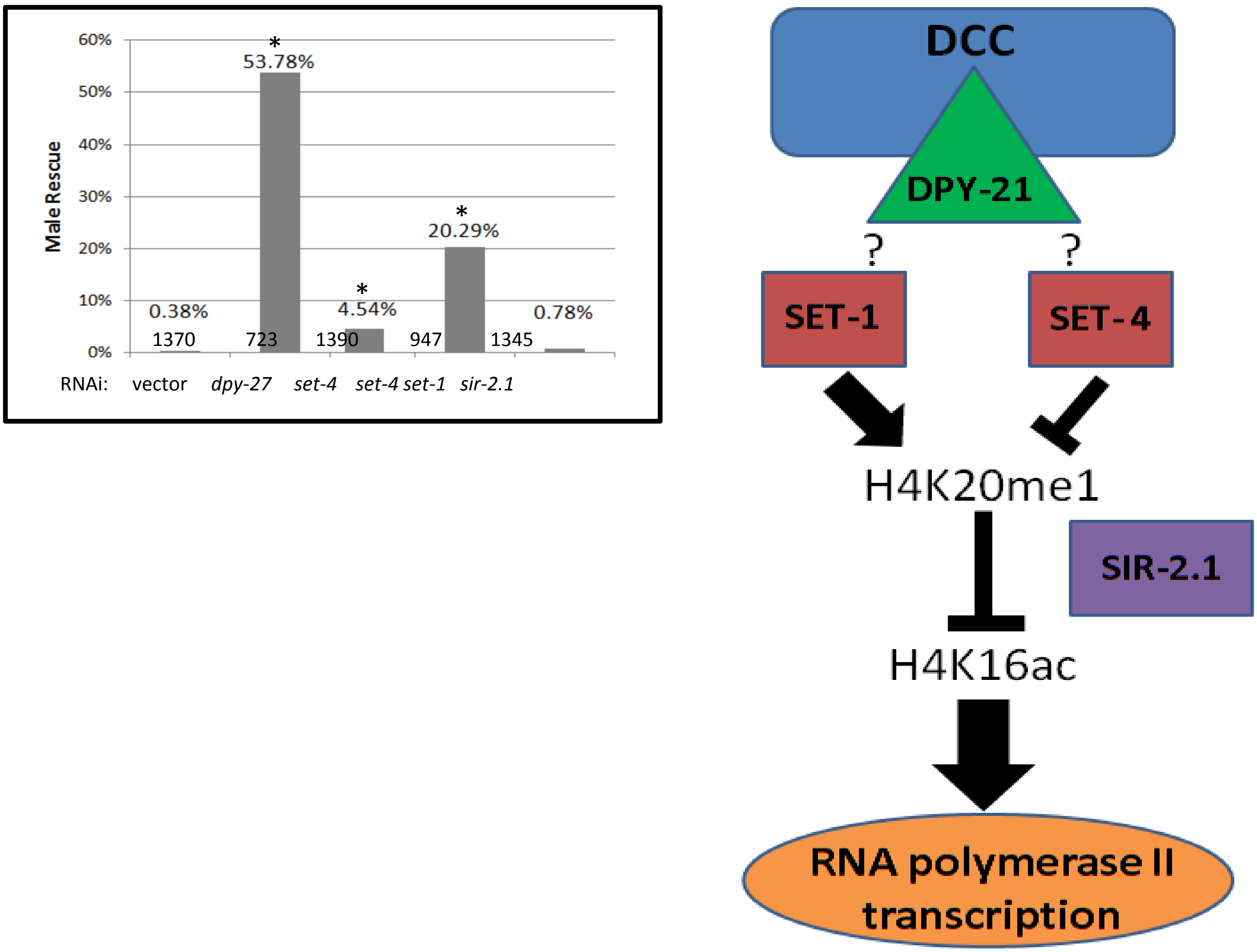

Figure 2.7. Chromatin regulators function in dosage compensation. (A) Male rescue assay for dosage compensation function. Knockdown of the DCC component *dpy-27* rescued 54% of the expected number of male progeny. Sequential RNAi against *set-4* and *set-1* rescued about 21%, and *set-4* RNAi singly rescued 4.5%, of expected males. Sample sizes are listed at the bottom of each bar in the graph and represent a combination of the total embryos laid from three independent trials conducted simultaneously. (B) Proposed model of chromatin regulation of transcription during *C. elegans* dosage compensation. Graphical cartoon illustrating DCC, SET-1, SET-4, and SIR-2.1 effects on X-linked transcription in hermaphrodites. DCC function, through SET-1 and SET-4, leads to an enrichment of H4K20me1 on the X chromosome, which in turn, through SIR-2.1 function, reduces H4K16ac and creates an environment repressive to transcription.

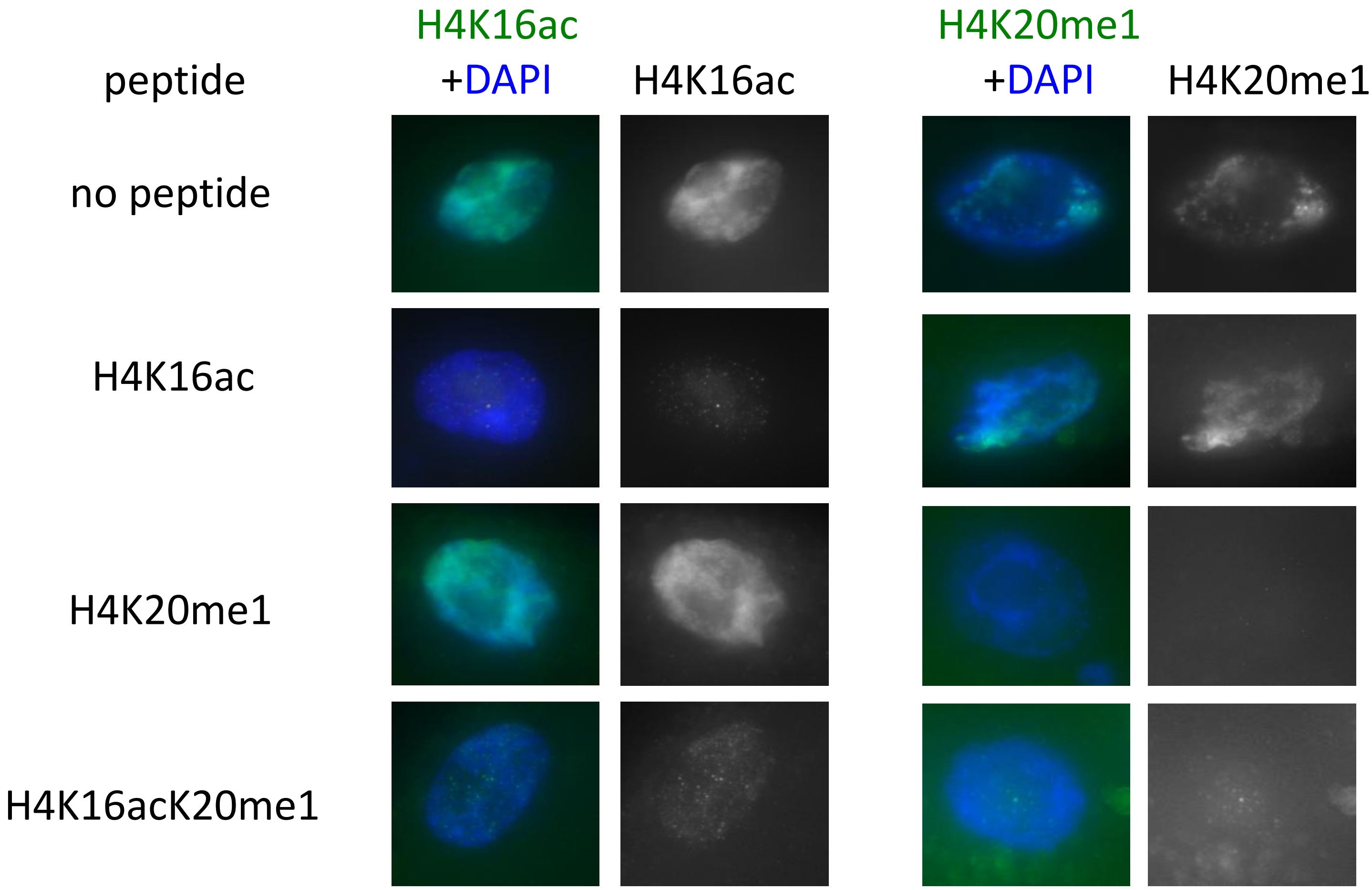

Figure 2.8. Test of antibody specificity. Intestinal nuclei were stained with either H4K16ac specific antibodies (left), or H4K20me1 specific antibodies (right). Prior to staining, the antibody was pre-incubated with excess peptide corresponding to the H4 N terminal tail with various modifications. The K16ac and the K16acK20me1 peptides effectively competed out the H4K16ac signal, indicating that the antibody is able to bind a K16-acetylated tail regardless of the methylation status of K20. Similarly, the K20me1 and the K16acK20me1 peptides competed out the H4K20me1 signal, indicating that the antibody is able bind K20me1 tail, regardless of the acetylation status of the K16. All images with the same antibody were taken using identical exposure times, Z stacks were collected and projected into a single plane, but further manipulations (such as deconvolution or contrast enhancement) were not performed.

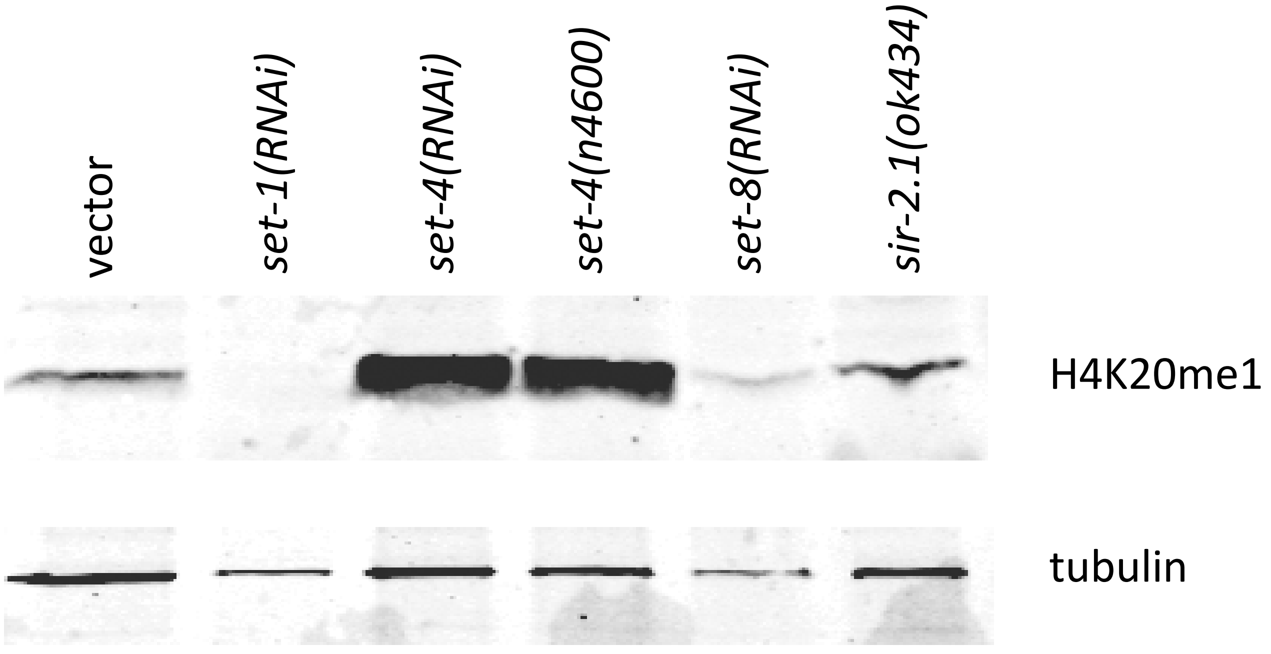

Figure 2.9. A Western blot similar to Figure 2.6B. Embryonic extracts from various genetic background or RNAi-treated worms were analyzed for H4K20me1 levels. Tubulin was used as loading control. H4K20me1 was undetectable in s*et-1* RNAi, increased after *set-4* RNAi or in set-4 mutants, but was comparable to vector control levels in *sir-2.1* mutants. Note that the *set-8(RNAi)* lane is under-loaded. *set-8* encodes an unrelated histone methyltransferase. Quantification of H4K20me1 levels actually showed a slight increase in the *sir-2.1* background.

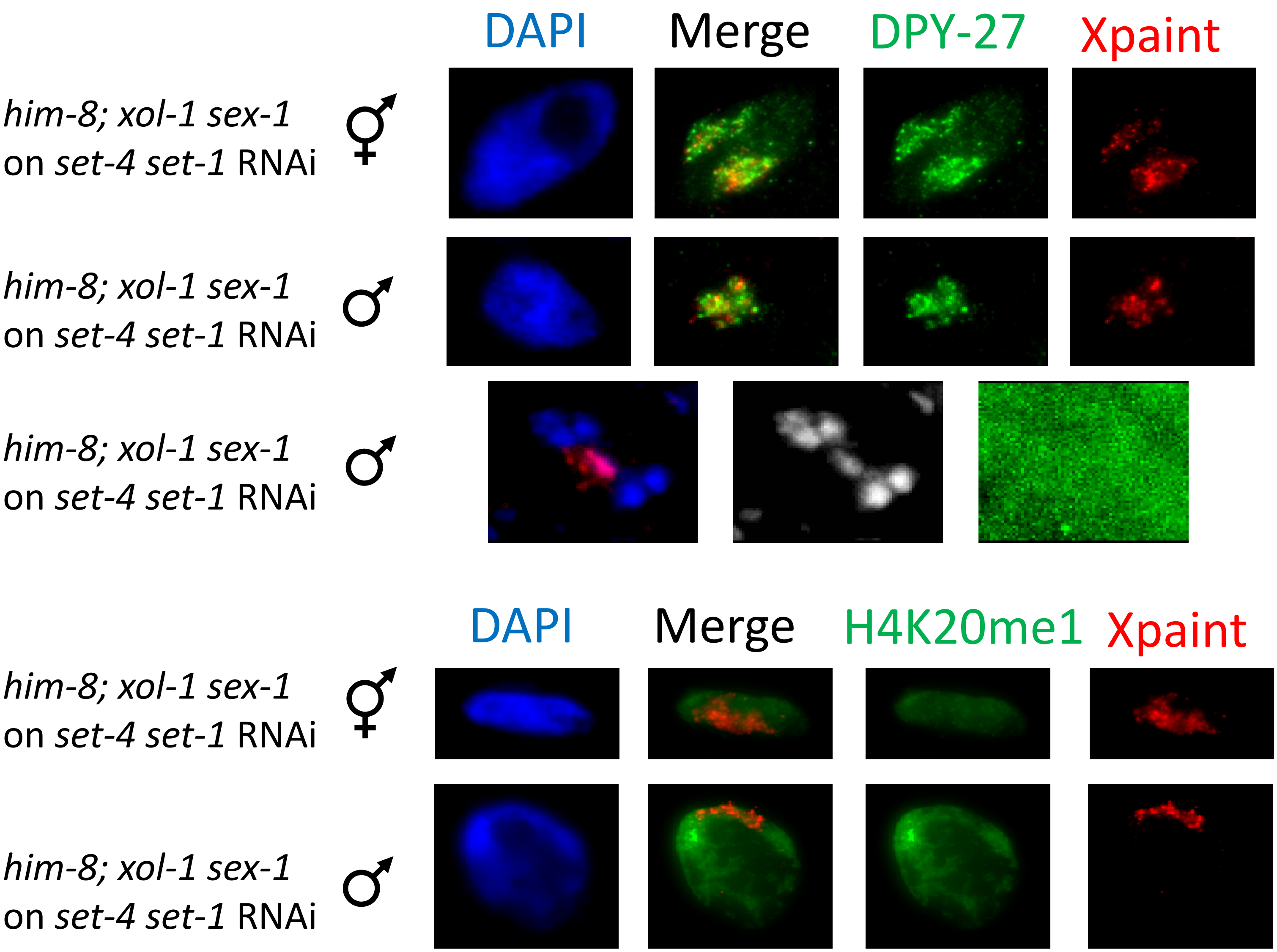

Figure 2.10. Validation of the maleness of RNAi-rescued male worms. Shown are representative Xpaint (red), anti-DPY-27/anti-H4K20me1 (green) immunoFISH images from *him-8*; *xol-1 sex-1* hermaphrodite or rescued male worms following treatment with *set-4 set-1* sequential RNAi. DAPI (DNA) is shown in blue. Results show moderate levels of DPY-27 bound to the X chromosomes in hermaphrodites and rescued males (lines 1-2), consistent with no role for SET-1 and SET-4 in DCC localization. Rescued males were males, as determined by the characteristic lagging X chromosome in male sperm meiosis I (line 3). Also, H4K20me1 levels are very low and similar across the nucleus in both hermaphrodites and rescued males (lines 4-5), consistent with loss of DCC-directed repression downstream of DCC loading.

References

1. Ohno S (1967) Sex chromosomes and sex-linked genes. Berlin, New York [etc.]: Springer-Verlag. x, 192 p. p.
2. Gelbart ME, Kuroda MI (2009) Drosophila dosage compensation: a complex voyage to the X chromosome. Development 136: 1399-1410.
3. Straub T, Becker PB (2007) Dosage compensation: the beginning and end of generalization. Nat Rev Genet 8: 47-57.
4. Gupta V, Parisi M, Sturgill D, Nuttall R, Doctolero M, et al. (2006) Global analysis of X-chromosome dosage compensation. J Biol 5: 3.
5. Deng X, Hiatt JB, Nguyen DK, Ercan S, Sturgill D, et al. (2011) Evidence for compensatory upregulation of expressed X-linked genes in mammals, Caenorhabditis elegans and Drosophila melanogaster. Nat Genet.
6. Nguyen DK, Disteche CM (2006) Dosage compensation of the active X chromosome in mammals. Nat Genet 38: 47-53.
7. Payer B, Lee JT (2008) X chromosome dosage compensation: how mammals keep the balance. Annu Rev Genet 42: 733-772.
8. Leeb M, Wutz A (2010) Mechanistic concepts in X inactivation underlying dosage compensation in mammals. Heredity 105: 64-70.
9. Heard E, Disteche CM (2006) Dosage compensation in mammals: fine-tuning the expression of the X chromosome. Genes Dev 20: 1848-1867.
10. Meyer BJ (2010) Targeting X chromosomes for repression. Curr Opin Genet Dev 20: 179-189.
11. Csankovszki G, Petty EL, Collette KS (2009) The worm solution: a chromosome-full of condensin helps gene expression go down. Chromosome Res 17: 621-635.
12. Kelley RL, Solovyeva I, Lyman LM, Richman R, Solovyev V, et al. (1995) Expression of msl-2 causes assembly of dosage compensation regulators on the X chromosomes and female lethality in Drosophila. Cell 81: 867-877.
13. Smith ER, Pannuti A, Gu W, Steurnagel A, Cook RG, et al. (2000) The drosophila MSL complex acetylates histone H4 at lysine 16, a chromatin modification linked to dosage compensation. Mol Cell Biol 20: 312-318.
14. Bone JR, Lavender J, Richman R, Palmer MJ, Turner BM, et al. (1994) Acetylated histone H4 on the male X chromosome is associated with dosage compensation in Drosophila. Genes Dev 8: 96-104.
15. Akhtar A, Becker PB (2000) Activation of transcription through histone H4 acetylation by MOF, an acetyltransferase essential for dosage compensation in Drosophila. Mol Cell 5: 367-375.
16. Jin Y, Wang Y, Johansen J, Johansen KM (2000) JIL-1, a chromosomal kinase implicated in regulation of chromatin structure, associates with the male specific lethal (MSL) dosage compensation complex. J Cell Biol 149: 1005-1010.
17. Lerach S, Zhang W, Deng H, Bao X, Girton J, et al. (2005) JIL-1 kinase, a member of the male-specific lethal (MSL) complex, is necessary for proper dosage compensation of eye pigmentation in Drosophila. Genesis 43: 213-215.
18. Regnard C, Straub T, Mitterweger A, Dahlsveen IK, Fabian V, et al. (2011) Global analysis of the relationship between JIL-1 kinase and transcription. PLoS Genet 7: e1001327.
19. Csankovszki G, Collette K, Spahl K, Carey J, Snyder M, et al. (2009) Three distinct condensin complexes control C. elegans chromosome dynamics. Curr Biol 19: 9-19.
20. Chuang PT, Albertson DG, Meyer BJ (1994) Dpy-27 - a Chromosome Condensation Protein Homolog That Regulates C. Elegans Dosage Compensation through Association with the X-Chromosome. Cell 79: 459-474.

21. Hsu DR, Meyer BJ (1994) The Dpy-30 Gene Encodes an Essential Component of the Caenorhabditis-Elegans Dosage Compensation Machinery. Genetics 137: 999-1018.
22. Lieb JD, Capowski EE, Meneely P, Meyer BJ (1996) DPY-26, a link between dosage compensation and meiotic chromosome segregation in the nematode. Science 274: 1732-1736.
23. Tsai CJ, Mets DG, Albrecht MR, Nix P, Chan A, et al. (2008) Meiotic crossover number and distribution are regulated by a dosage compensation protein that resembles a condensin subunit. Genes Dev 22: 194-211.
24. Yonker SA, Meyer BJ (2003) Recruitment of C. elegans dosage compensation proteins for gene-specific versus chromosome-wide repression. Development 130: 6519-6532.
25. Jans J, Gladden JM, Ralston EJ, Pickle CS, Michel AH, et al. (2009) A condensin-like dosage compensation complex acts at a distance to control expression throughout the genome. Genes Dev 23: 602-618.
26. Ercan S, Dick LL, Lieb JD (2009) The C. elegans dosage compensation complex propagates dynamically and independently of X chromosome sequence. Curr Biol 19: 1777-1787.
27. Blauwkamp TA, Csankovszki G (2009) Two classes of dosage compensation complex binding elements along Caenorhabditis elegans X chromosomes. Mol Cell Biol 29: 2023-2031.
28. Petty EL, Collette KS, Cohen AJ, Snyder MJ, Csankovszki G (2009) Restricting dosage compensation complex binding to the X chromosomes by H2A.Z/HTZ-1. PLoS Genet 5: e1000699.
29. Whittle CM, McClinic KN, Ercan S, Zhang X, Green RD, et al. (2008) The genomic distribution and function of histone variant HTZ-1 during C. elegans embryogenesis. PLoS Genet 4: e1000187.
30. Petty E, Laughlin E, Csankovszki G (2011) Regulation of DCC Localization by HTZ-1/H2A.Z and DPY-30 Does not Correlate with H3K4 Methylation Levels. PLoS ONE 6: e25973.
31. Ercan S, Lubling Y, Segal E, Lieb JD (2011) High nucleosome occupancy is encoded at X-linked gene promoters in C. elegans. Genome Res 21: 237-244.
32. Liu T, Rechtsteiner A, Egelhofer TA, Vielle A, Latorre I, et al. (2011) Broad chromosomal domains of histone modification patterns in C. elegans. Genome Res 21: 227-236.
33. Gerstein MB, Lu ZJ, Van Nostrand EL, Cheng C, Arshinoff BI, et al. (2010) Integrative Analysis of the Caenorhabditis elegans Genome by the modENCODE Project. Science.
34. Mouron S, de Carcer G, Seco E, Fernandez-Miranda G, Malumbres M, et al. (2010) RINGO C is required to sustain the spindle-assembly checkpoint. J Cell Sci 123: 2586-2595.
35. Han Z, Saam JR, Adams HP, Mango SE, Schumacher JM (2003) The C. elegans Tousled-like kinase (TLK-1) has an essential role in transcription. Curr Biol 13: 1921-1929.
36. Strukov YG, Sural TH, Kuroda MI, Sedat JW (2011) Evidence of activity-specific, radial organization of mitotic chromosomes in Drosophila. PLoS Biol 9: e1000574.
37. Liu T, Ortiz JA, Taing L, Meyer CA, Lee B, et al. (2011) Cistrome: an integrative platform for transcriptional regulation studies. Genome Biol 12: R83.
38. Imai S, Armstrong CM, Kaeberlein M, Guarente L (2000) Transcriptional silencing and longevity protein Sir2 is an NAD-dependent histone deacetylase. Nature 403: 795-800.
39. Tissenbaum HA, Guarente L (2001) Increased dosage of a sir-2 gene extends lifespan in Caenorhabditis elegans. Nature 410: 227-230.
40. Fang J, Feng Q, Ketel CS, Wang H, Cao R, et al. (2002) Purification and functional characterization of SET8, a nucleosomal histone H4-lysine 20-specific methyltransferase. Curr Biol 12: 1086-1099.
41. Andersen EC, Horvitz HR (2007) Two C. elegans histone methyltransferases repress lin-3 EGF transcription to inhibit vulval development. Development 134: 2991-2999.

42. Sakaguchi A, Karachentsev D, Seth-Pasricha M, Druzhinina M, Steward R (2008) Functional characterization of the Drosophila Hmt4-20/Suv4-20 histone methyltransferase. Genetics 179: 317-322.
43. Nishioka K, Rice JC, Sarma K, Erdjument-Bromage H, Werner J, et al. (2002) PR-Set7 is a nucleosome-specific methyltransferase that modifies lysine 20 of histone H4 and is associated with silent chromatin. Mol Cell 9: 1201-1213.
44. Hargitai B, Kutnyanszky V, Blauwkamp TA, Stetak A, Csankovszki G, et al. (2009) xol-1, the master sex-switch gene in C. elegans, is a transcriptional target of the terminal sex-determining factor TRA-1. Development 136: 3881-3887.
45. Delong L, Plenefisch JD, Klein RD, Meyer BJ (1993) Feedback-Control of Sex Determination by Dosage Compensation Revealed through Caenorhabditis-Elegans Sdc-3 Mutations. Genetics 133: 875-896.
46. Hodgkin J (2002) Exploring the Envelope: Systematic Alteration in the Sex-Determination System of the Nematode Caenorhabditis elegans. Genetics 162: 767-780.
47. Grote P, Conradt B (2006) The PLZF-like protein TRA-4 cooperates with the Gli-like transcription factor TRA-1 to promote female development in C. elegans. Dev Cell 11: 561-573.
48. Meyer BJ, Casson LP (1986) Caenorhabditis Elegans Compensates for the Difference in X-Chromosome Dosage between the Sexes by Regulating Transcript Levels. Cell 47: 871-881.
49. Oda H, Okamoto I, Murphy N, Chu J, Price SM, et al. (2009) Monomethylation of histone H4-lysine 20 is involved in chromosome structure and stability and is essential for mouse development. Mol Cell Biol 29: 2278-2295.
50. Talasz H, Lindner HH, Sarg B, Helliger W (2005) Histone H4-lysine 20 monomethylation is increased in promoter and coding regions of active genes and correlates with hyperacetylation. J Biol Chem 280: 38814-38822.
51. Meneely PM, Wood WB (1987) Genetic analysis of X-chromosome dosage compensation in Caenorhabditis elegans. Genetics 117: 25-41.
52. Meneely PM, Wood WB (1984) An autosomal gene that affects X chromosome expression and sex determination in Caenorhabditis elegans. Genetics 106: 29-44.
53. Zippo A, Serafini R, Rocchigiani M, Pennacchini S, Krepelova A, et al. (2009) Histone crosstalk between H3S10ph and H4K16ac generates a histone code that mediates transcription elongation. Cell 138: 1122-1136.
54. Shogren-Knaak M, Ishii H, Sun JM, Pazin MJ, Davie JR, et al. (2006) Histone H4-K16 acetylation controls chromatin structure and protein interactions. Science 311: 844-847.
55. Chaumeil J, Le Baccon P, Wutz A, Heard E (2006) A novel role for Xist RNA in the formation of a repressive nuclear compartment into which genes are recruited when silenced. Genes Dev 20: 2223-2237.
56. Okamoto I, Otte AP, Allis CD, Reinberg D, Heard E (2004) Epigenetic dynamics of imprinted X inactivation during early mouse development. Science 303: 644-649.
57. Greenberg AJ, Yanowitz JL, Schedl P (2004) The Drosophila GAGA factor is required for dosage compensation in males and for the formation of the male-specific-lethal complex chromatin entry site at 12DE. Genetics 166: 279-289.
58. Lee C, Li X, Hechmer A, Eisen M, Biggin MD, et al. (2008) NELF and GAGA factor are linked to promoter-proximal pausing at many genes in Drosophila. Mol Cell Biol 28: 3290-3300.
59. Smith ER, Winter B, Eissenberg JC, Shilatifard A (2008) Regulation of the transcriptional activity of poised RNA polymerase II by the elongation factor ELL. Proc Natl Acad Sci U S A 105: 8575-8579.

60. Larschan E, Bishop EP, Kharchenko PV, Core LJ, Lis JT, et al. (2011) X chromosome dosage compensation via enhanced transcriptional elongation in Drosophila. Nature 471: 115-118.
61. Kind J, Vaquerizas JM, Gebhardt P, Gentzel M, Luscombe NM, et al. (2008) Genome-wide analysis reveals MOF as a key regulator of dosage compensation and gene expression in Drosophila. Cell 133: 813-828.
62. Smith ER, Allis CD, Lucchesi JC (2001) Linking global histone acetylation to the transcription enhancement of X-chromosomal genes in Drosophila males. J Biol Chem 276: 31483-31486.
63. Ivaldi MS, Karam CS, Corces VG (2007) Phosphorylation of histone H3 at Ser10 facilitates RNA polymerase II release from promoter-proximal pausing in Drosophila. Genes Dev 21: 2818-2831.
64. Gao L, Gross DS (2008) Sir2 silences gene transcription by targeting the transition between RNA polymerase II initiation and elongation. Mol Cell Biol 28: 3979-3994.
65. Rudner AD, Hall BE, Ellenberger T, Moazed D (2005) A nonhistone protein-protein interaction required for assembly of the SIR complex and silent chromatin. Mol Cell Biol 25: 4514-4528.
66. Kohlmaier A, Savarese F, Lachner M, Martens J, Jenuwein T, et al. (2004) A chromosomal memory triggered by Xist regulates histone methylation in X inactivation. PLoS Biol 2: E171.
67. Karachentsev D, Sarma K, Reinberg D, Steward R (2005) PR-Set7-dependent methylation of histone H4 Lys 20 functions in repression of gene expression and is essential for mitosis. Genes Dev 19: 431-435.
68. Balakrishnan L, Milavetz B (2010) Decoding the histone H4 lysine 20 methylation mark. Crit Rev Biochem Mol Biol 45: 440-452.
69. Gelbart ME, Larschan E, Peng S, Park PJ, Kuroda MI (2009) Drosophila MSL complex globally acetylates H4K16 on the male X chromosome for dosage compensation. Nat Struct Mol Biol 16: 825-832.
70. Liu W, Tanasa B, Tyurina OV, Zhou TY, Gassmann R, et al. (2010) PHF8 mediates histone H4 lysine 20 demethylation events involved in cell cycle progression. Nature 466: 508-512.
71. Machin F, Paschos K, Jarmuz A, Torres-Rosell J, Pade C, et al. (2004) Condensin regulates rDNA silencing by modulating nucleolar Sir2p. Curr Biol 14: 125-130.
72. Bhalla N, Biggins S, Murray AW (2002) Mutation of YCS4, a budding yeast condensin subunit, affects mitotic and nonmitotic chromosome behavior. Mol Biol Cell 13: 632-645.
73. Dej KJ, Ahn C, Orr-Weaver TL (2004) Mutations in the Drosophila condensin subunit dCAP-G: defining the role of condensin for chromosome condensation in mitosis and gene expression in interphase. Genetics 168: 895-906.
74. Kamath RS, Ahringer J (2003) Genome-wide RNAi screening in Caenorhabditis elegans. Methods 30: 313-321.
75. Shapira M, Hamlin BJ, Rong J, Chen K, Ronen M, et al. (2006) A conserved role for a GATA transcription factor in regulating epithelial innate immune responses. Proc Natl Acad Sci U S A 103: 14086-14091.
76. Csankovszki G, McDonel P, Meyer BJ (2004) Recruitment and spreading of the C-elegans dosage compensation complex along X chromosomes. Science 303: 1182-1185.
77. Rechtsteiner A, Ercan S, Takasaki T, Phippen TM, Egelhofer TA, et al. (2010) The histone H3K36 methyltransferase MES-4 acts epigenetically to transmit the memory of germline gene expression to progeny. PLoS Genet 6.

78. Song JS, Johnson WE, Zhu X, Zhang X, Li W, et al. (2007) Model-based analysis of two-color arrays (MA2C). Genome Biol 8: R178.
79. Shin H, Liu T, Manrai AK, Liu XS (2009) CEAS: cis-regulatory element annotation system. Bioinformatics 25: 2605-2606.

CHAPTER 3

Cataloguing of Histone Modification and Protein Occupancy Relationships Reveals a Role for Histone Acetyltransferases in Proper DCC Localization via Action at Enhancer-like Recruitment Sites

Abstract

Recent work in *Caenorhabditis elegans* has focused on realizing a greater understanding of the transcriptome and epigenome through high-throughput, high-resolution studies. The datasets generated are now becoming available to the broader research community for further application to particular research interests. Dosage compensation in *C. elegans* is achieved by the DCC, which downregulates transcription from both hermaphrodite X chromosomes by half. The mechanism(s) of action, as well as the upstream and downstream DCC interactors, are not known. The current work defines a more accurate set of dosage compensated and non-dosage compensated genes on the X chromosomes, active genes on all chromosomes in embryos, and seeks to relate an ever-growing database of chromatin modification and transcription factor ChIP-chip and ChIP-seq datasets with each other and with *C. elegans* dosage compensation occupancy and function. We made use of Cistrome, a user-friendly web-based platform, to perform these analyses across more than 35 embryonic datasets. Most strikingly, we have uncovered an enhancer-like chromatin signature representative of DCC binding elements (*rex* sites, *dox* sites, and waystations) and defined over 300 additional candidate rex/*dox* sites. We also characterize numerous novel protein and chromatin differences between dosage compensated and non-dosage compensated genes on X, as well as at active genes on X and autosomes. We go on to correlate across all pairs of datasets, across the genome, by dosage

compensation status, or by DCC binding element characteristics, to give a true picture of the relationship each mark has to the others and to the process of dosage compensation. H3K27ac, H4K16ac, and CBP-1 occupancy suggested that HAT proteins may play a role in DCC binding, and this is indeed the case. DCC mislocalization to autosomes, PSer2 accumulation on X, and loss of DCC-mediated chromatin repression were seen with HAT RNAi or mutation. These revelations lead to a model by which the DCC functions, dependent upon HAT protein action, to regulate enhancer function, RNA Pol II recruitment, and perhaps downstream RNA Pol II elongation. Our compendium serves both as a reference for researchers interested in chromatin state organization in *C. elegans* and as a hypothesis generating tool for further research into the mechanisms of transcription and signaling, chromatin regulation, and dosage compensation in the worm.

Introduction

Dosage compensation is the mechanism that equalizes X-linked gene expression between the sexes of many species [1-7]. This process is accomplished using different mechanisms across species [2,3,6,7], but two common themes have emerged: evidence from the three primary model systems in which dosage compensation is studied (flies, mammals, and worms) indicates that dosage compensation-directed gene regulation is achieved by chromatin and transcriptional regulation [2,3,8-10].

Fly dosage compensation is achieved by two-fold transcriptional upregulation of the single male X chromosome [11-21], driven by MSL complex-mediated H4K16 hyperacetylation [22-24]. Mammalian dosage compensation involves transcriptional inactivation of one of the two X chromosomes in females by the non-coding RNA *Xist* and the repressive co-factors it recruits (including Polycomb-mediated H3K27me3) [25-28]. Finally, in worms, expression from both hermaphrodite X chromosomes is halved by the action of a dosage compensation complex

(DCC) [6,7,29-37], which contains a Condensin-like complex (Condensin I^{DC}) [38]. Elucidation of the molecular mechanism of *C. elegans* dosage compensation is only now beginning. Our previous work indicates that the DCC establishes a repressive chromatin environment on X through modulation of histone H4 chromatin modifications [39], and other work has indicated that the DCC regulates levels of RNA polymerase II on DNA [40]. However, the general mechanism of condensin regulation of interphase gene expression [41-45] remains to be characterized.

An important question in *C. elegans* dosage compensation subject to ongoing studies has been targeting of the complex to hermaphrodite X chromosomes. Establishment of X inactivation in mammals [1,3-5] and MSL complex assembly on the single male X in flies [46-55] have been well characterized. In worms, it is thought that a sequence element known as the MEX motif [56], which is mildly enriched on X and at DCC-recruitment elements, is involved in DCC targeting. Other studies have shown that RNA Pol II transcription is important for the spreading of the complex across the X chromosomes [57]. However, these factors alone are not sufficient to fully explain DCC targeting. It has been hypothesized that chromatin may contribute to DCC recruitment, and it is known that the histone variant HTZ-1 acts as a barrier element to DCC loading on autosomes [58,59], but further roles for chromatin in DCC localization have not yet been revealed.

Recent work from various groups [40,60,61], has produced high-resolution, genome-wide ChIP-chip, ChIP-seq, and RNA-seq datasets interrogating *C. elegans* histone modification levels, protein occupancy, or transcript production at various developmental stages. We saw the release of this data as an opportunity to learn more about the chromatin and protein occupancy "character" of the hermaphrodite X chromosomes, dosage compensated, and non-dosage compensated genes. We made use of publicly-available online tools (MEME Suite [62-64] and

Cistrome [65]) to conduct our analysis. The aims of this study are: 1) to refine DC and non-DC gene lists; 2) to define an active gene list for embryos from RNA-seq data; 3) to investigate DCC binding elements for a distinct chromatin signature; 4) to determine histone modification levels and protein occupancy states at dosage compensated and non-dosage compensated genes; 5) to determine the relationships between histone modifications or proteins across the genome and at sites of interest; and 6) to address whether histone acetyltransferases and/or acetylation are important for DC loading.

Results

We began this study with two goals, to define updated lists of dosage compensated and non-dosage compensated genes and to define a list of all genes active in late embryo samples. Using Cistrome [65] and the microarray datasets used for the initial classifications [56], we reanalyzed this data using statistical methods that account for mismatch probe bias, global hybridization trends, and the effects of multiple t-testing (See Methods). The results (Figure 3.1; Tables 3.2, 3.3) showed both significant overlap and divergence between the two sets of lists. Further, while the previous lists contained questionable entries (declassified and non-expressed genes), our revised lists do not. We are confident that these identified genes represent more accurate sets of dosage compensated and non-dosage compensated genes. Again using Cistrome, we cross-referenced values from a late embryo RNA-seq wiggle file with the ce6 refseq gene list to determine which genes are expressed (Table 3.1). Results show that over 90% of all genes are expressed at this stage.

We next asked whether DCC recruitment elements possess a distinct chromatin signature. Genome browser visualization of available histone modification and protein ChIP-chip datasets [60,61] indeed revealed such a distinct profile at all known DCC recruitment elements. We found that all 38 *rex* sites [42], all 49 *dox* sites [42], and the four known waystations [66] are enriched for H3K4me1, H3K27ac, H4K16ac, and CBP-1, and depleted of H3K27me3 (Figure 3.2) as compared to sites without DPY-27 peaks (Figure 3.9). Defined in previous work, *rex* sites are capable of recruiting the DCC as multi-copy transgenic arrays, *dox* sites are unable to recruit as multi-copy transgenic arrays, and waystations are DPY-27 peaks unable to recruit as single copy duplications [42,66]. These features suggest that DCC binding elements possess enhancer-like chromatin, and might be enhancers. H3K4me1 at these sites had one of two shapes, monomodal or bimodal, suggesting a poised and an active enhancer state, respectively [67,68]. Figures 3.2B-D depict the proportions of *rex* sites, *dox* sites, and waystations with active enhancer, poised enhancer, or off (no activating marks accompanying H3K4me1 enrichment) enhancer characteristics. We extended this analysis using feature-centric analysis (SitePro) within Cistrome, which identified differences between active and poised DCC binding elements and *rex* and *dox* sites for SDC-2, SDC-3, CBP-1, and HCP-3, but not DPY-27 (Figure 3.3). This analysis suggests that many features, but not Condensin I^{DC}, are found at distinctly different levels which serve to distinguish disparate categories of DCC binding elements.

We next asked whether DNA sequence, histone modifications, and protein occupancy analysis could be used to define novel DCC recruitment elements. Using 39 *rex* site DNA sequences and MEME-ChIP [63] running with settings to find 12nt sequences, we were able to identify 13 instances of a motif (Figure 3.4A) that matches up well with the published *rex* site MEX motif [56]. The low number of hits is consistent with the severe degeneracy of the MEX motif. Using FIMO [62], running at a significance value of less than $1*10^{-5}$, we identified 3,555 instances of this MEX motif genome-wide. Using Cistrome, we selected among these MEX motifs or a list of all called DPY-27 ChIP-seq peaks from http://www.modencode.org by selecting for positive H3K4me1, H3K27ac, H4K16ac, and SDC-2. We found that a frame of reference (MEX sites or DPY-27 peaks), as well as an SDC-2 selection step, were both necessary to obtain high quality results lists of candidate DCC recruitment elements possessing enhancer-like chromatin (data not shown). As compared to the profiles of these histone modifications and SDC-2 at known DCC recruitment sites (Figures 3.4B-C), levels at our more than 300 candidate sites were quite similar (Figures 3.4D-E), reinforcing the quality of these candidates. Although none of these candidates were tested for DCC recruitment ability, we see no differences between our candidate sites and the known recruitment sites. Table 3.4 contains the signal values for each selection feature at each candidate DCC recruitment site identified. It is tempting to speculate that DCC function at different classes of sites (*rex* vs. *dox*, candidate MEX-containing vs. candidate non-MEX-containing) could represent two sides of the same 3D interaction (recruitment at distal enhancer/rex sites vs. binding in a loop that encompasses promoter *dox* sites or intronic regions), given that the chromatin signal is maintained, but *dox* sites are unable to recruit the DCC on their own.

We next sought to create a compendium illustrating the inter-relationships between histone modifications or protein occupancy across the genome, at DCC recruitment elements, or at HTZ-1 peaks on X. Figure 3.7 shows histone modification or protein cross-correlation tables created in Cistrome across the entire genome at 20kb resolution. Figures 3.8-3.16 show cross-correlation tables and SitePro analysis based on DCC recruitment site type, DCC recruitment site enhancer character, or control sites. Figure 3.17 shows cross-correlation tables and SitePro analysis at all HTZ-1 peaks on X. HTZ-1 has been previously shown to play an important role in restricting DCC binding to the X chromosomes [59].

The second half of our compendium is focused on the use of metagene analysis in Cistrome to plot levels of histone modifications and protein occupancy for comparison between dosage compensated (DC) and non-dosage compensated (non-DC), active X-linked and active autosomal genes, or DC and non-DC genes based on expression level divisions (low, medium, or high). The results of this extensive analysis are shown in Table 3.5, and the metagenes are found in Figures 3.18 through 3.62. In these figures, parts A and B are metagenes, parts C and D are concatenated exon profiles, parts A and C compare DC, non-DC, active X, and active autosomal genes, and parts B and D compare DC and non-DC genes binned by expression level. In total, this compendium of histone modification and protein occupancy emphasizing *C. elegans* dosage compensation has revealed numerous differences between gene groups and underscores the effectiveness of Cistrome as a user-friendly tool to categorize regions of interest.

During creation of our compendium, this analysis generated many testable hypotheses. The most striking of which we chose to follow-up on in great detail. Shown in Figure 3.5, at DCC recruitment elements, the DCC colocalizes, and positively correlates, with H3K27ac, H4K16ac, and the histone acetyltransferase CBP-1 (Figures 3.5A-D). This association, and previous reports [69], suggested that histone acetylation and acetyltransferases may be important for proper DCC loading or localization. Using immunoFISH microscopy and quantification, we asked whether HAT gene RNAi alters DCC localization confinement to the X chromosomes (Figure 3.5E). As compared to control *vector* or *sir-2.1* RNAi, in which DCC correlation with Xpaint is high, knockdown of *cbp-1*, *mys-1*, and *mys-4* individually led to decreased DCC to Xpaint correlation values. Furthermore, sequential RNAi against any two of these HAT gene transcripts led to a further decrease in correlation between the DCC and Xpaint. Also, *hda-1* knockdown led to severe X chromosome structure changes and very poor DCC to Xpaint colocalization. Other data suggests that in *C. elegans*, *hda-1*, a known histone deacetylase [70], is acting as a positive regulator of H4K16ac (Figure 3.65), possibly through promoting HAT protein function [71,72]. We confirmed the importance of HAT protein function for DCC localization using DPY-27, Xpaint immunoFISH microscopy in *mys-1* or one of two *cbp-1* mutants with or without HAT gene transcript RNAi of the same type (Figure 3.6). Results show that HAT gene mutation leads to defects in X chromosome structure and DCC mislocalization, especially in *cbp-1(ok1491)*. Addition of RNAi against the HAT gene in the mutant strain led to greater DCC mislocalization from X than mutation.

We further investigated effects of HAT RNAi on histone modifications and RNA Pol II activity (Figures 3.63-3.67). PSer2 marks elongating RNA Pol II, while 4H8 marks hypo-phosphorylated (recruited and initiated) RNA Pol II. H3K36me3 is a mark commonly associated with transcriptional elongation [73], H4 acetylation is associated with active chromatin, and H4K20me1 is a mark of repressive chromatin. MYS-1 and MYS-4 contribute to H4K16ac (Figures 3.66-3.67). H4K20me1 (marking DCC-mediated repression on X [39]) and H3K36me3 were largely unchanged (Figures 3.63-3.67). Strikingly, though, PSer2 levels were punctate and enriched on X compared to *vector* RNAi in *cbp-1*, *hda-1*, *mys-1*, and *mys-4* RNAi. These data strongly indicate that HAT proteins promote proper RNA Pol II elongation, which is necessary for proper DCC localization and perhaps contributes to X chromosome structure.

Discussion

This study seeks to thoroughly understand the chromatin and protein occupancy profile of dosage compensated X chromosomes in *C. elegans*, primarily through the use of an online portal for high-resolution data analysis, Cistrome [65] and publically-available datasets [40,56,60,61]. Using publically available RNA-seq data, we constructed a list of all genes in *C. elegans* active in a late embryo stage-biased sample (Table 3.1). We have also created a more accurate list of dosage compensated and non-dosage compensated genes on X (Tables 3.2, 3.3) by using up-to-date statistical methodology (MAT) that avoids mismatch probe bias and corrects for multiple testing [74]. Our revised DC and non-DC gene lists do not contain any decommissioned or non-expressed genes found in the lists from the previous study [42] and have both substantial overlap and divergence from the previous study's classifications (Figure 3.1; Tables 3.2, 3.3).

Genome browsing using publically available datasets detailing chromatin modification and protein occupancy across the genome [40,60,75] revealed that dosage compensation complex recruitment and binding elements (known as *rex* sites, *dox* sites, and waystations) possess an enhancer-like chromatin signature (Figure 3.2A): enrichment of H3K4me1 and H3K27ac, and depletion of H3K27me3. We noticed that these enhancers were a mixture (Figure 3.2B) of active (bimodal H3K4me1), poised (monomodal H3K4me1), and off (no activating marks, such as H3K27ac or H4K16ac, accompanying H3K4me1 enrichment) [67,68].

Using Cistrome [65], we first determined protein occupancy that could differentiate between *rex* and *dox* sites (Figure 3.3). Our results indicate that SDC-2, SDC-3, CBP-1, and HCP-3 (*C. elegans* histone H3 variant CENP-A homolog), but not DPY-27, binding could distinguish these classes of sites. Using MEME [63,64] and FIMO [62], we identified all occurrences of the MEX motif, thought to partially distinguish *rex* from *dox* sites, across the genome. We then refined this list and a list of all DPY-27 ChIP-seq peak calls using H3K4me1, H3K27ac, H4K16ac, and SDC-2. With these refinements, we have discovered more than 300 additional candidate DCC binding elements, greatly expanding upon the known list of about 90 sites (Table 3.4).

We also employed Cistrome to create a genome-wide compendium of histone modification and protein occupancy inter-relationships and correlations to control "no peak" regions, DPY-27 binding peaks, DCC binding peak categories, or enhancer status. The genome wide cross-correlation tables are shown in Figure 3.7, while the tables and feature-centric (SitePro) analyses are shown in Figures 3.8 - 3.16. Correlations and SitePro analysis within all HTZ-1 peaks on X are shown in Figure 3.17. Expanding this study, we categorized histone modification and protein occupancy with respect to dosage compensation status, X versus autosomal location, or transcriptional output. The results of this metagene analysis, shown in Figures 3.18-3.62, are summarized in Table 3.5. This work greatly contributes to our knowledge of the chromatin and protein complement associated with dosage compensation and X chromosome status and has identified numerous novel differences between DC and non-DC genes as well as X chromosomes versus autosomes. This epigenomic and proteomic "character profile" of the X chromosomes stands as an essential manual for future experimental approaches to further dissecting DCC function.

A unique co-binding of the DCC, histone acetylation, and CBP-1 suggests that HAT proteins may play a role in proper DCC recruitment or localization (Figures 3.5A-D). The role and importance of HAT proteins in worm dosage compensation has been a topic of open and unresolved debate for some time [69]. RNA interference against the histone acetyltransferase-encoding genes *cbp-1*, *mys-1*, and *mys-4* each resulted in diminished colocalization of the DCC with X and spreading of the DCC to autosomes (Figure 3.5E). Further, knockdown of any two of these resulted in increased mislocalization of the DCC away from X (Figure 3.5E). Intriguingly, knockdown of the histone deacetylase *hda-1*, which we characterize as having an overall net positive effect on H4K16ac levels (but not the H4K16 deacetylase-encoding *sir-2.1*), also leads to severe loss of DCC to X chromosome colocalization (Figure 3.5E). Further analysis revealed that similar DCC localization and X chromosome structure defects were seen when visualizing HAT mutant worms, and DCC spreading to autosomes was seen primarily when these mutants were additionally treated with RNAi to the mutated gene (Figure 3.6). Staining for histone modifications and RNA Pol II activity (Figures 3.63-3.67) showed that PSer2 (RNA Pol II elongation) is enriched on the X chromosomes with HAT or *hda-1* knockdown, but marks of DCC-mediated repression and other features of elongation appear un- or inconsistently perturbed. Given the known role for RNA Pol II transcriptional elongation in proper DCC localization [57], these results suggest that HAT proteins and HDA-1 contribute to proper DCC localization and X chromosome structure and allow for proper RNA Pol II elongation, which has been shown to be important for DCC localization [57].

These results further highlight enhancer elements [76-80] and HAT proteins [81-86] as critical regulators of gene expression. Our study suggests that enhancers represent a critical regulatory point for *C. elegans* dosage compensation, allowing perhaps for regulation of RNA Pol II loading/re-loading, initiation, and/or early elongation.

Another unanswered question in *C. elegans* dosage compensation is the meaning of the MEX motif [56], thought to contribute to DCC loading on X. The MEX motif is highly degenerate. In fact, MEME retrieved only 13 instances from 39 *rex* sites defined previously to each have multiple occurrences, and no instances of the most highly-represented consensus sequence (TCGCGCAGGGAG) can be found by BLAST search (data not shown). In order to begin to address the significance of the MEX motif, we hypothesized that it is a combination of two half sites (TCGCG) and (CAGGG). Literature searching identified TCGCG as indicative of binding to the minor groove of the DNA backbone [87,88]. Further investigation suggested that CAGGG is a sequence element (G4 motif) important for complex DNA hairpin loop [89-91]. Loops of this type are known to regulate transcription in humans through promoter-proximal RNA Pol II pausing [92-94]. We hypothesize that the DCC may stabilize DNA hairpin loops, along with auxiliary binding to the minor groove of the DNA backbone, to contribute to RNA Pol II transcription regulation.

This work stands as a case study of data analysis refinement and a prime example of what additional knowledge can be gained from interrogation of public data with powerful, user-friendly online tools. We sincerely hope that support for this type of work, as a means of hypothesis generation and confirmation of prior results, will continue to grow in the future.

Methods

Strains

MH2430 *cbp-1(ku258)* III

MT13172 *mys-1(n4075)* V/nT1[qIs51] (IV;V)

TY2386 wild type (WT) (N2)

VC1006 *cbp-1(ok1491)* III/ht2[bli-4(e937) let-?(q782) qIs48] (I; III)

Nematode strains used in this work were provided by the Caenorhabditis Genetics Center, which is funded by the NIH National Center for Research Resources.

RNAi Treatment

RNAi treatment was performed over two generations as described previously [39].

Public Datasets

Downloaded from http://www.modencode.org or (http://www.ncbi.nlm.nih.gov/geo/).

Format: Dataset ID (GSE denotes NCBI GEO), Description (Stage), Array (if applicable)

3432, AMA-1 ME, 080922

334, DPY-26 ME, 7685

3435, DPY-27 EE, 080922

578, DPY-27 ME, 7685

644, DPY-28 ME, 080922

GSE25834, DPY-30 ME, 8134

GSE25834, MIX-1 ME, 8134

645, SDC-2 ME, 080922

553 & 575, SDC-3 ME, 7685

2767, CBP-1 ME, 080922

3438, HPL-2 LE, 080922

3439, LIN-15B LE, 080922

911, MES-4 EE, 080922

897, MRG-1 EE, 080922

2738, NPP-13 ME, 080922

2969, ZFP-1 ME, 080922

3206, H3 EE, 080922

2726, H3K4me1 EE, 080922

GSE22741, H3K4me2 EE, 080922

GSE22721, H3K4me3 EE, 080922

2646, H3K9me1 EE, 080922

2444, H3K9me2 EE, 080922

982, H3K9me3 EE, 080922

2727, H3K27ac EE, 080922

3179, H3K27me1 EE, 080922

3171, H3K27me3 EE, 080922

2604, H3K36me1 EE, 080922

909, H3K36me2 EE, 080922

973, H3K36me3 EE, 080922

2410, H3K79me1 EE, 080922

2442, H3K79me2 EE, 080922

2443, H3K79me3 EE, 080922

3181, H4K8ac EE, 080922

3182, H4K16ac EE, 080922

2765, H4K20me1 EE, 080922

2766, H4tetraAc EE, 080922

GSE25834, RNA Pol II (8WG16 on vector or *sdc-2* RNAi), 8134

2436, AMA-1::GFP LE ChIP-seq

2416, DPY-27 ME ChIP-seq

3977, WT EE RNA-seq

3978, WT LE RNA-seq

43, HTZ-1 ME, direct wiggle file download

Notes: 1) Many experiments have dyeswaps, which are not always properly annotated on modencode.org. 2) Number of replicates varies from one to four. 3) Inconsistent or poor quality replicates were discarded.

Cistrome Analysis

Cistrome [65] can be accessed at: http://cistrome.org/ap/root.

Definition of DC and non-DC genes

Using the microarray datasets from [42] loaded into Cistrome, statistically significant changes in gene expression were determined by comparing WT to: A) *dpy-27(y57)*, B) *sdc-2(y93)*, or C) *her-1(hv1y101); xol-1(y9) sdc-2(y74) unc-9(e101)* samples using MAT with default settings and "calculate differential expression" using default settings, except a Benjamini-Hochberg FDR Type II error control at a maximum p-value of 0.05 and a minimum fold-change of 1.5. Qualifications for dosage compensated and non-dosage compensated gene status were the same as in [42]. Dosage compensated genes will change expression in (A) and (B), but not (C) as compared to WT, and non-dosage compensated genes will change expression in (C), but not (A) or (B) as compared to WT.

Definition of active X, A genes

Early (modENCODE_3977; mis-coded as late on modencode.org dataset browser, correct on FTP site) or late (modENCODE_3978) embryo sample FASTQ read files were used as input for TopHat alignment to ce6, followed by transcript discovery by Cufflinks and BAM file creation with SAMtools (Rich McEachin, University of Michigan). The BAM file was uploaded to Galaxy (https://main.g2.bx.psu.edu/) and used to generate a pileup file ("Generate pileup" function), then an interval file ("Pileup-to-Interval" function). The interval file was downloaded and uploaded to a different instance of Galaxy (http://bifx-core.bio.ed.ac.uk:8080 /root?tool_id=int2wig). The interval file was used to generate a wiggle file ("Int2Wig" function). This wiggle file was then uploaded to Cistrome and compared to output obtained with wiggle files downloaded from the modENCODE FTP site for each dataset. Results showed the wiggle files to be virtually identical, so the modENCODE wiggle files were used in downstream analysis. RNA-seq wiggle file overlap with the ce6 refseq gene table was found ("Intersect" function). Common gene names, and their genomic coordinates, with RNA-seq reads were copied and used to assemble active (<0 RPKM) X chromosome and autosome gene lists for the WT early and late embryo stages.

Wiggle file creation and metagene profiles

All .wig files were created with respect to the ce6 genome build. For ChIP-chip datasets, raw pair, ndf, and pos files were downloaded from modencode.org or NCBI Accession #GSE25834. These files were uploaded and used as input for MA2C normalization in Cistrome using default settings. This results in creation of a .wig file, which was used for metagene profiling. For RNA-seq metagenes, the generated wiggle file detailed above was used for metagene profiling. Wiggle files and gene lists [MW dosage compensated, MW non-dosage compensated, active X (late embryo), active A (late embryo), low RPKM (1-49.5) MW DC or non-

DC, mid RPKM (50-149) MW DC or non-DC, and high RPKM (150 to max) MW DC or non-DC] were used as input for metagene profiling ("CEAS: Enrichment on chromosome and annotation" function) using the appropriate profiling resolution (either 50bp or 86bp, depending on the array design).

BED file creation

BED files representing rex sites, dox sites, waystations, these three site types combined, all DPY-27 ChIP-seq peaks, no DPY-27 peak control sites from [66], active enhancer (bimodal H3K4me1) *rex* and *dox* sites, poised enhancer (monomodal H3K4me1) *rex* and *dox* sites, off (no H4K16ac signal) enhancer *rex* and *dox* sites, or HTZ-1 peaks on X) were generated by hand in Microsoft Excel 2007 or download as modencode.org peak call files.

Cross-correlation plots

Wiggle files were used as input to generate cross-correlation tables in Cistrome relating any two datasets ("Multiple wiggle files correlation" or "Multiple wiggle files correlation in given regions" function) either at 20kb resolution or within specified bed files.

Ordering of the samples along the diagonal within cross-correlation tables is as follows (from upper left to lower right):

Histone modifications: H4K16ac EE, H3K4me2 EE, H3K27ac EE, H4K20me1 EE, H3K4me1 EE, H3 EE, H3K4me3 EE, H3K9me2 EE, H3K9me3 EE, H3K27me1 EE, H3K36me1 EE, H3K36me2 EE, H3K36me3 EE, H3K79me1 EE, H3K79me2 EE, H3K79me3 EE, H4K8ac EE, H4tetraAc EE, H3K9me1 EE, H3K27me3 EE. **Protein occupancy:** 8WG16 EE, AMA-1 ME, CBP-1, ME, DPY-27 EE, DPY-28 ME, HPL-2 LE, LEM-2 EE, LIN-15B LE, MES-4 EE, NPP-13 ME, DOT-1 ME, ZFP-1 ME, HCP-3 EE, MRG-1 EE. **Pferdehirt et al., 2011:** WT 8WG16 ME, *sdc-2* 8WG16 ME, ASH-2 ME, Bentley RNA Pol II ME, DPY-27 ME, DPY-30 ME, SMC-4 ME.

SitePro analysis

Wiggle files and bed files explained above were used as input for SitePro (feature-centric) analysis using a span of 1000bp and the appropriate profiling resolution (either 50bp or 86bp, depending on the array design).

Venn Diagram, Pie Charts, and Tables

Venn diagram, pie charts, and tables were created using Microsoft Excel 2007.

Browser Screenshots

The applicable WIG (wiggle) public dataset tracks were loaded into the Integrated Genome Viewer (IGV; Broad Institute). Screenshots were taken of regions of interest using the "print screen" and "paste" functions in Windows 7 and Microsoft PowerPoint 2007. *rex* and *dox* sites were labeled as referenced in [42].

Motif Construction (MEME) and Genome Occurrences (FIMO)

FASTA sequences corresponding to all 39 *rex* sites were obtained from Cistrome ("fetch sequences" feature). The resulting FASTA file was used as input for MEME-ChIP (http://meme.sdsc.edu/meme/cgi-bin/meme-chip.cgi) with the following settings: any number of repetitions per FASTA sequence, MOTIF width of 12 positions. 39 instances of a MEX-like motif comparable to that found previously [42] were identified. The resulting MEX-like motif was used as input for FIMO (http://meme.nbcr.net/meme/cgi-bin/fimo.cgi), which identified 3,555 instances of this motif across the genome at a significance of $p < 1*10^{-5}$. This level was chosen because it was the most significant level to include all 39 identified instances of the MEX motif used as input.

ImmunoFISH and Immunofluorescence Microscopy

FISH, immunostaining, and imaging were conducted as described previously [39]. Quantification was performed as previously described [39], with the following change: 1)

Pearson correlation coefficients were determined between FITC (DCC) mask overlap with CY3 (Xpaint) signal masks.

Acknowledgements

I would like to thank Rich McEachin for RNA-seq dataset analysis assistance.

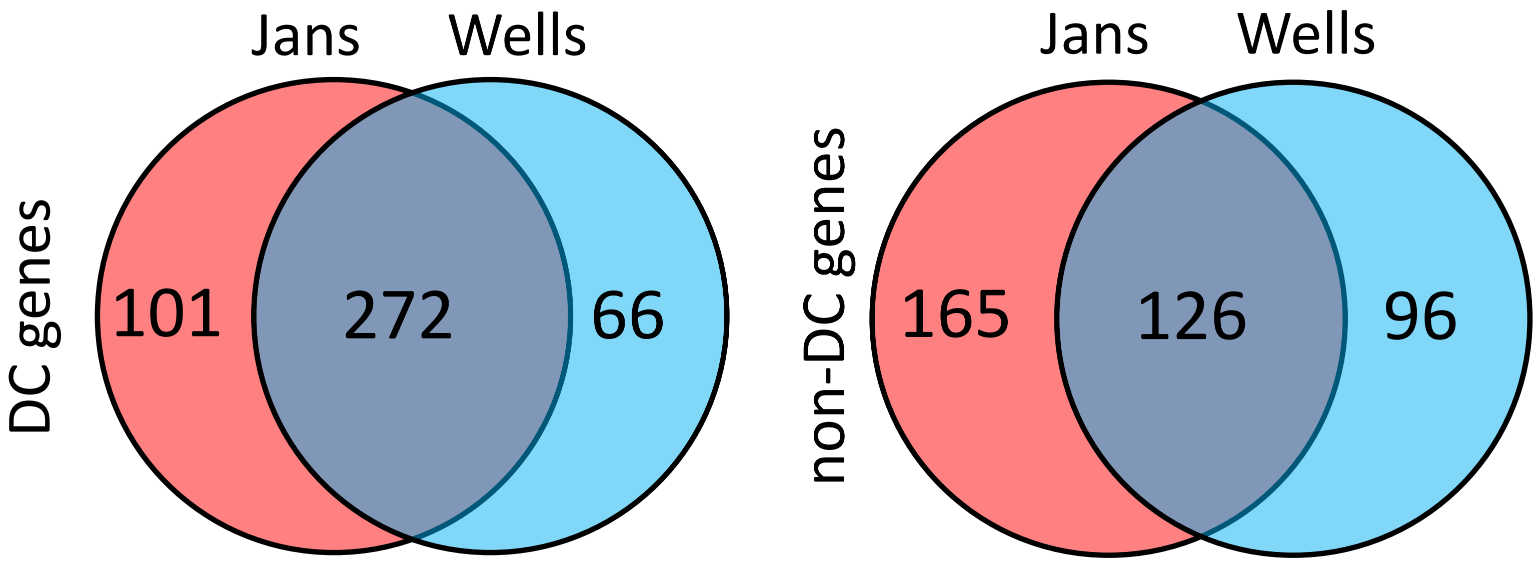

Figure 3.1. Overlap between Jans et al., 2009 and the updated lists of dosage compensated and non-dosage compensated genes. Shown are Venn diagrams comparing the DC and non-DC gene lists from Jans et al., 2009 to the same lists derived in this work. Results demonstrate substantial overlap and divergence between called gene lists. The current study uses the same classification strategy employed in the previous study, but employ refined statistical methods that account for multiple testing and mismatch probe bias to derive a more accurate list of true gene expression changes from WT within each comparison (See Methods).

Table 3.1. X and autosomal gene activity using late embryo RNA-seq data.

All genes (ce6)		
	Autosomes	17,144
	X chromosomes	2,779
Active genes (greater than 0 RPKM)		
Hermaphrodite late embryo RNA-seq		
	Autosomes	15,547 (90.7%)
	X chromosomes	2,622 (94.4%)

Table 3.2 MW revised dosage compensated gene list.

MBW DC genes

gene name	chromosome	tx start	tx end
R04A9.5	chrX	384382	388797
ugt-46	chrX	525933	530177
F28C10.3	chrX	531885	535750
mrp-2	chrX	563724	572702
mrp-1	chrX	576318	587483
F13C5.1	chrX	601574	604922
ncam-1	chrX	695065	702537
aex-3	chrX	752710	759731
T04G9.1	chrX	788351	796141
daf-3	chrX	817925	823840
mab-7	chrX	892239	898068
stau-1	chrX	1027669	1035241
F55A4.8	chrX	1038540	1044378
K03E6.7	chrX	1084223	1088147
F49E7.2	chrX	1095543	1097010
tsp-9	chrX	1246011	1247494
zfp-3	chrX	1440367	1446571
T26C11.4	chrX	1840560	1845531
ceh-41	chrX	1846670	1848669
ceh-39	chrX	1853926	1856166
F52D2.7	chrX	1962566	1966164
Y102A11A.3	chrX	2019164	2025731
Y102A11A.2	chrX	2026646	2031004
acl-4	chrX	2066547	2070435
lsy-2	chrX	2089659	2093240
AH9.1	chrX	2243594	2247001
T10H10.2	chrX	2294742	2298144
F47G3.3	chrX	2375990	2378646
C43H6.7	chrX	2398805	2402045
C43H6.4	chrX	2404017	2407352
C43H6.3	chrX	2407460	2409558
fox-1	chrX	2445492	2450501
syg-1	chrX	2509329	2515310
tbc-12	chrX	2525206	2532430
F52H2.5	chrX	2557980	2559553
F54G2.1	chrX	2621287	2629680
T14G11.1	chrX	2688985	2691989
T02C5.1	chrX	2694914	2698083
igcm-3	chrX	2698253	2705850
cgef-1	chrX	2793928	2799236
C14A11.9	chrX	2807909	2809624
F53B3.5	chrX	2872800	2879612

Y71H10A.2	chrX	2933351	2937731
Y41G9A.5	chrX	2946841	2948940
osm-5	chrX	2984268	2991366
M02F4.3	chrX	3036423	3040723
F52E4.5	chrX	3085885	3087330
K10B3.6	chrX	3109923	3111332
mai-1	chrX	3113429	3116587
rgl-1	chrX	3210966	3220282
ddr-2	chrX	3315309	3323952
clc-3	chrX	3373234	3374728
T27A10.2	chrX	3585943	3586853
R11G1.6	chrX	3639490	3644493
sax-1	chrX	3646310	3650137
F35A5.1	chrX	3807448	3816392
ceh-18	chrX	3844764	3857777
R02E12.4	chrX	4003508	4007611
R02E4.1	chrX	4103420	4104495
ZK470.2	chrX	4135106	4147801
nck-1	chrX	4148630	4153417
ZK470.1	chrX	4163620	4169764
mrp-6	chrX	4177880	4186421
rab-37	chrX	4228501	4231346
coel-1	chrX	4265856	4270523
cka-2	chrX	4287546	4291335
F14H12.3	chrX	4344224	4345609
lst-2	chrX	4378002	4383339
dpy-23	chrX	4389337	4393768
dop-1	chrX	4411563	4413898
ncr-1	chrX	4472256	4480049
dgk-2	chrX	4496298	4504360
spr-3	chrX	4514068	4516862
ham-2	chrX	4554662	4558827
C05E11.3	chrX	4579476	4581627
C46C11.1	chrX	4637410	4643273
K02G10.5	chrX	4687757	4691286
lon-2	chrX	4738931	4749051
mig-13	chrX	4796420	4799590
R08E3.3	chrX	4818566	4821676
tsp-14	chrX	4867079	4871028
ZC8.6	chrX	4972567	4997565
lfi-1	chrX	4984044	4992822
ZC449.3	chrX	5018361	5020624
ZC449.2	chrX	5021181	5024223
ZC449.5	chrX	5034994	5037742
C24H10.1	chrX	5072003	5074198

tbc-7	chrX	5138957	5146253
pqn-62	chrX	5197749	5204207
Y34B4A.4	chrX	5264294	5271753
C26B9.1	chrX	5344830	5347927
jkk-1	chrX	5368430	5372019
C25F6.7	chrX	5445033	5447554
dlg-1	chrX	5479663	5484671
C25F6.1	chrX	5486459	5488063
mec-2	chrX	5582568	5584618
unc-97	chrX	5593091	5594924
T22B7.4	chrX	5638539	5641321
set-19	chrX	5675203	5680183
set-20	chrX	5680306	5684699
W01C8.5	chrX	5694432	5696216
cyp-43A1	chrX	5714236	5717535
tag-294	chrX	5760253	5763334
sft-4	chrX	5778834	5780704
hbl-1	chrX	5823025	5826319
puf-9	chrX	5841549	5845925
W06B11.1	chrX	5849061	5851858
ctbp-1	chrX	5862714	5873278
flp-7	chrX	5885822	5886781
F49E10.2	chrX	5890363	5894715
tbc-16	chrX	5897348	5902095
mig-23	chrX	5945778	5948827
C45B2.6	chrX	6053057	6057300
gln-1	chrX	6058211	6060187
C45B2.2	chrX	6084696	6085146
C45B2.8	chrX	6087942	6088321
C15H9.11	chrX	6102838	6103390
tag-275	chrX	6142450	6150499
W05H9.4	chrX	6263604	6266866
W05H9.2	chrX	6267005	6271008
mom-1	chrX	6293082	6298151
gar-1	chrX	6479592	6484765
cdf-1	chrX	6499891	6504557
glr-8	chrX	6506838	6509837
ets-4	chrX	6519061	6522603
ilys-5	chrX	6535478	6536755
T14E8.1	chrX	6553242	6559368
T14E8.4	chrX	6559524	6562226
T28B4.1	chrX	6588754	6596088
T28B4.4	chrX	6597872	6598821
F38B6.6	chrX	6684416	6690038
F38B6.1	chrX	6700263	6700778
nas-11	chrX	6713529	6716275

nas-11	chrX	6713529	6716275
abts-4	chrX	6747315	6761691
sgca-1	chrX	6787208	6789505
M03A8.3	chrX	6800640	6803658
F41B4.1	chrX	6823846	6825790
C53B7.3	chrX	6844706	6845852
rig-3	chrX	6853569	6860867
unc-6	chrX	6889640	6897087
otpl-3	chrX	6921618	6924403
F14B8.5	chrX	6924768	6928655
tsp-16	chrX	6994733	6996742
tyra-2	chrX	6996809	7001937
ist-1	chrX	7132155	7139599
alh-10	chrX	7140454	7143591
lam-2	chrX	7143867	7151090
syd-9	chrX	7218275	7226766
F46H5.2	chrX	7265600	7267829
unc-10	chrX	7272283	7280267
clc-2	chrX	7431416	7433481
C01C10.2	chrX	7435583	7437899
acl-12	chrX	7439356	7442523
sox-2	chrX	7458962	7463682
F48E3.2	chrX	7490360	7493066
F48E3.8	chrX	7507829	7517639
adt-2	chrX	7586052	7593757
F27D9.2	chrX	7672932	7676221
stn-2	chrX	7676470	7680569
C53C9.2	chrX	7686585	7689159
K09F5.6	chrX	7719211	7725457
ZK154.6	chrX	7790395	7792197
R03G5.7	chrX	7805622	7806750
sek-1	chrX	7816673	7820983
C39D10.6	chrX	7896234	7897691
zig-4	chrX	7925379	7926462
zig-3	chrX	7930680	7931747
tnt-3	chrX	7937580	7944991
C18A11.2	chrX	8067627	8067963
C17H11.1	chrX	8173849	8180805
M60.4	chrX	8232294	8236253
kqt-2	chrX	8243074	8246308
M60.6	chrX	8248145	8252397
cutl-29	chrX	8262378	8270960
ksr-1	chrX	8275095	8283238
R09F10.3	chrX	8294562	8296602
tbc-18	chrX	8378494	8382638

wrk-1	chrX	8387901	8392520
tth-1	chrX	8422416	8423671
F16F9.1	chrX	8447211	8450344
flp-5	chrX	8528187	8530971
nlp-7	chrX	8593133	8593750
rig-1	chrX	8669229	8671294
F53A9.8	chrX	8718503	8718846
tag-130	chrX	8792097	8795728
R04E5.8	chrX	8802507	8803123
R04E5.9	chrX	8806053	8810973
sec-15	chrX	8831684	8835653
C06E2.1	chrX	8872871	8874572
twk-18	chrX	8988072	8991897
tsp-11	chrX	9163097	9165903
C35B8.3	chrX	9213913	9216788
vav-1	chrX	9217390	9232003
gpa-12	chrX	9246937	9248848
gly-13	chrX	9293605	9296553
B0416.7	chrX	9296966	9297863
B0416.1	chrX	9303654	9310362
oga-1	chrX	9343674	9347309
pkc-2	chrX	9376201	9385657
ZK899.1	chrX	9446594	9447543
F49E2.2	chrX	9567228	9573656
F34H10.3	chrX	9633229	9634979
T14B1.1	chrX	9664434	9668688
rrc-1	chrX	9823712	9831181
F47A4.5	chrX	9833311	9837971
R07B1.8	chrX	9870817	9872531
C17G1.5	chrX	9941561	9944705
F19C6.2	chrX	10000870	10004831
mkk-4	chrX	10027787	10030061
ZC373.4	chrX	10062400	10069715
unc-58	chrX	10105029	10109799
unc-115	chrX	10147175	10153071
erd-2	chrX	10156788	10160369
R07E3.4	chrX	10330647	10331803
rme-4	chrX	10373169	10374768
acr-8	chrX	10412692	10416560
syd-2	chrX	10549050	10555167
nhx-5	chrX	10576887	10580982
sdn-1	chrX	10589707	10593262
flp-19	chrX	10604737	10605755
abl-1	chrX	10606125	10624112

daf-12	chrX	10664332	10665408
F13E6.2	chrX	10668206	10674220
F13E6.5	chrX	10695233	10697762
R07A4.2	chrX	10744281	10746413
sma-9	chrX	10769212	10781815
plc-1	chrX	10794795	10812459
F47B10.8	chrX	10905172	10906505
T21B6.3	chrX	10945077	10948894
lge-1	chrX	10966568	10969704
ver-3	chrX	10992433	10997753
F59F3.4	chrX	11004914	11008105
ttr-31	chrX	11008189	11008994
clc-1	chrX	11047444	11049156
F13D2.1	chrX	11163881	11175072
hst-2	chrX	11204072	11207016
C34F6.6	chrX	11207412	11208049
C34F6.7	chrX	11210040	11215395
C03A3.1	chrX	11257444	11260150
F38B2.2	chrX	11278617	11279293
F08G12.1	chrX	11301999	11305799
ttyh-1	chrX	11368644	11374272
F08B12.1	chrX	11385040	11392705
slo-2	chrX	11394531	11401473
C35C5.9	chrX	11536490	11537045
C35C5.3	chrX	11545332	11547486
mig-2	chrX	11548530	11550107
lev-8	chrX	11560837	11563620
frm-3	chrX	11576177	11581649
F52D10.2	chrX	11589641	11591641
T04F8.6	chrX	11667080	11672223
rsd-3	chrX	11798423	11803576
C34E11.2	chrX	11805283	11811386
tag-241	chrX	11826637	11836037
F55G7.2	chrX	11929820	11931568
set-6	chrX	11969951	11974598
tsp-20	chrX	12031519	12033945
W03G11.3	chrX	12100125	12103723
F57G12.1	chrX	12169020	12171605
cab-1	chrX	12199485	12212971
C23H4.6	chrX	12235542	12240703
E01G6.3	chrX	12241637	12244559
nekl-3	chrX	12389553	12391394
F17E5.2	chrX	12394186	12399412
lin-2	chrX	12399439	12413947
atf-6	chrX	12480869	12484809

R09A8.5	chrX	12638413	12640409
nhr-17	chrX	12663762	12667772
rgs-2	chrX	12712571	12727533
pgp-14	chrX	12744641	12749500
gei-3	chrX	12796229	12797508
bcat-1	chrX	12877399	12880248
gpc-1	chrX	12881509	12884909
pqn-18	chrX	12907751	12919458
nhr-25	chrX	13008413	13013134
F17H10.2	chrX	13114085	13115989
nlp-3	chrX	13177774	13178375
skr-19	chrX	13223537	13224629
C29F7.6	chrX	13436375	13441805
srd-51	chrX	13482569	13484690
sad-1	chrX	13489374	13500472
cdk-4	chrX	13515970	13517674
pab-2	chrX	13522189	13525743
F18H3.4	chrX	13529007	13531952
unc-84	chrX	13584694	13589710
nlg-1	chrX	13625353	13631015
C04A11.1	chrX	13660438	13662883
pix-1	chrX	13727218	13734270
obr-3	chrX	13798560	13803493
dyc-1	chrX	14049455	14063776
lgc-21	chrX	14064354	14067598
C33G3.6	chrX	14080310	14084246
F28H6.6	chrX	14117008	14125795
akt-2	chrX	14147620	14151990
ceh-37	chrX	14197356	14209074
K06G5.1	chrX	14214893	14218966
K04C1.3	chrX	14241492	14243318
tag-172	chrX	14284755	14291230
T14C1.1	chrX	14406096	14411101
M163.1	chrX	14502416	14503760
H01A20.2	chrX	14568795	14570343
C44H4.1	chrX	14572638	14576028
F54E4.3	chrX	14632012	14636327
C26G2.2	chrX	14665303	14671220
epn-1	chrX	14816544	14818426
flp-8	chrX	14881337	14881986
daf-6	chrX	14888413	14894179
nac-1	chrX	14895063	14898371
mrp-5	chrX	14938859	14946235
C18B12.4	chrX	15036614	15040520
Y15E3A.4	chrX	15330882	15333869

C33A11.1	chrX	15355156	15363782
C02C6.3	chrX	15546688	15547342
ent-2	chrX	15600984	15603683
rab-14	chrX	15604685	15606555
nipi-3	chrX	15607888	15611731
F59D12.1	chrX	15666680	15672283
F59F4.3	chrX	15842344	15847508
csb-1	chrX	15861278	15865831
F53H4.4	chrX	15866329	15868616
ZK1073.1	chrX	16123863	16128782
sgk-1	chrX	16254928	16261966
ace-1	chrX	16367144	16373698
ztf-19	chrX	16536749	16540111
K08B5.1	chrX	16558358	16562224
F59C12.3	chrX	16603300	16609439
tag-343	chrX	16665350	16672518
C10E2.6	chrX	16767094	16770415
T01C8.2	chrX	16786358	16787535
fbxb-114	chrX	16921767	16922776
F35B3.4	chrX	17019537	17020720
C33E10.1	chrX	17305259	17306220
osm-11	chrX	17420134	17421380
C36E6.2	chrX	17452304	17455769
nhr-1	chrX	17518356	17524658
F31A3.5	chrX	17554915	17561376
C16H3.3	chrX	17601887	17604523
T23E7.2	chrX	17670939	17680687

Note: red gene names were similarly classified in Jans et al., 2009.

Table 3.3 MW revised non-dosage compensated gene list.

MBW nonDC genes

gene name	chromosome	tx start	tx end
R57.2	chrX	297247	299177
R57.1	chrX	301831	308231
sor-3	chrX	353619	357933
pqn-40	chrX	450463	457545
B0310.2	chrX	501965	506943
ifd-2	chrX	813850	815928
igcm-1	chrX	845729	851506
ZC13.3	chrX	882964	888392
F53H8.3	chrX	938512	942605
F55A4.4	chrX	1024642	1026173
H42K12.3	chrX	1311595	1316625
W05H7.1	chrX	1450762	1452233
D1005.1	chrX	1479536	1484393
Y75D11A.3	chrX	1745262	1746212
Y102A11A.8	chrX	2039415	2046340
F49H12.5	chrX	2074441	2075936
F53B1.2	chrX	2108975	2111714
F53B1.6	chrX	2114622	2118251
T24C12.3	chrX	2196517	2203887
hex-1	chrX	2223475	2226612
rpl-11.2	chrX	2241748	2242613
crn-4	chrX	2256082	2258074
T01B6.1	chrX	2335676	2348615
R04B3.1	chrX	2467343	2470284
aat-3	chrX	2554224	2557708
tra-4	chrX	2853688	2857596
nmy-1	chrX	2909546	2918027
wrt-2	chrX	3092385	3094363
sec-3	chrX	3095438	3099828
spc-1	chrX	3117431	3127064
K10B3.1	chrX	3135483	3136636
C15C7.7	chrX	3165786	3167570
F28B4.3	chrX	3227494	3235397
F40F4.7	chrX	3243891	3245969
lbp-3	chrX	3257439	3258052
fbxb-71	chrX	3262922	3264150
K09C4.10	chrX	3276041	3280188
F11D5.1	chrX	3344678	3347012
C12D12.1	chrX	3501154	3505224
T27A10.6	chrX	3588843	3596447
C18B2.5	chrX	3606726	3611079
tag-18	chrX	3731904	3733443

F35A5.4	chrX	3789741	3792799
sup-12	chrX	3904569	3907650
T22B2.1	chrX	3926083	3929470
lin-18	chrX	3958474	3961884
vha-12	chrX	4191065	4193111
hpk-1	chrX	4210556	4217264
taf-11.1	chrX	4255143	4256781
col-165	chrX	4353590	4354784
F02E8.4	chrX	4454100	4457271
C07A12.7	chrX	4517868	4521019
pqn-65	chrX	4617498	4620394
F16H11.3	chrX	4647496	4649165
glit-1	chrX	4712247	4715047
rpl-25.1	chrX	4715144	4715767
M03F4.6	chrX	4964054	4969326
ZC449.1	chrX	5024386	5028105
C31H2.4	chrX	5155130	5159628
T03G11.6	chrX	5177492	5179163
H28G03.2	chrX	5213802	5215523
Y34B4A.5	chrX	5257263	5258351
Y34B4A.8	chrX	5271807	5275247
C26B9.5	chrX	5329419	5332302
C26B9.2	chrX	5340303	5341974
pfn-2	chrX	5353067	5354109
chtl-1	chrX	5355861	5363757
ddr-1	chrX	5461220	5466027
hog-1	chrX	5851991	5853327
R07E4.5	chrX	5949500	5953132
R07E4.1	chrX	5963358	5969896
inx-3	chrX	5996113	5998201
F22F4.1	chrX	6004440	6007001
C09B8.4	chrX	6018438	6019894
hsp-25	chrX	6034432	6039454
hsp-3	chrX	6088972	6092082
C14F11.1	chrX	6240911	6242663
C03B1.13	chrX	6335297	6337711
C03B1.7	chrX	6342111	6345601
T22E5.3	chrX	6385439	6387818
nhr-173	chrX	6655501	6659705
asg-2	chrX	6841209	6842034
C16E9.2	chrX	6938361	6938769
F46H5.4	chrX	7245025	7254510
atg-11	chrX	7334748	7340134
C07D8.6	chrX	7341454	7342722
mek-1	chrX	7479193	7480258

F46C8.3	chrX	7525517	7527198
F46C8.8	chrX	7551208	7554371
sto-1	chrX	7562780	7564749
apy-1	chrX	7568087	7569666
F26A10.2	chrX	7632033	7637028
pcca-1	chrX	7657477	7660926
ref-2	chrX	7744178	7749907
mec-7	chrX	7774798	7776622
ZK154.5	chrX	7783130	7787875
sfxn-2	chrX	7956161	7958246
C34D10.1	chrX	8029440	8031396
dim-1	chrX	8050417	8052623
C46F2.1	chrX	8077685	8079827
vem-1	chrX	8087675	8089619
cdd-1	chrX	8208715	8211088
F13B9.1	chrX	8287198	8294055
R09F10.8	chrX	8325071	8326391
H03E18.1	chrX	8507813	8514064
tag-233	chrX	8554068	8555834
tag-279	chrX	8570987	8574975
F18E9.3	chrX	8586104	8589950
K09E2.3	chrX	8676565	8677869
F53A9.3	chrX	8708303	8709309
F53A9.9	chrX	8720253	8720697
tnt-2	chrX	8721702	8723491
ifd-1	chrX	8820663	8824386
C28G1.5	chrX	8826733	8828425
cyn-8	chrX	8911322	8913771
tmbi-4	chrX	9150627	9160580
B0416.4	chrX	9278892	9279774
tbb-4	chrX	9434400	9436824
nuc-1	chrX	9539837	9542363
ifp-1	chrX	9675775	9680101
him-4	chrX	9717557	9753501
F36G3.2	chrX	9792333	9794205
mrp-4	chrX	9884254	9889636
C17G1.7	chrX	9952512	9954472
ZC373.1	chrX	10054212	10057456
W07E11.1	chrX	10083936	10103994
F21A10.2	chrX	10181740	10194307
nucb-1	chrX	10197635	10200286
R07E3.6	chrX	10317651	10321772
cut-5	chrX	10333945	10338119
C39B10.1	chrX	10460475	10463510

F13E6.3	chrX	10680554	10682683
R07A4.4	chrX	10751691	10754704
F47B10.1	chrX	10897602	10900041
pbo-4	chrX	10954057	10958153
pxn-2	chrX	10972109	10979189
lpr-4	chrX	11065056	11066732
C03A3.2	chrX	11262770	11266237
pgp-4	chrX	11359093	11363965
pek-1	chrX	11410108	11414737
sdc-2	chrX	11522635	11533373
hnd-1	chrX	11684649	11685568
col-180	chrX	11711299	11712202
F54F7.6	chrX	11865463	11866749
sams-1	chrX	11965902	11969706
C49F5.3	chrX	11982712	11983821
F57G12.2	chrX	12156392	12159961
C04B4.2	chrX	12283242	12285201
W06D11.3	chrX	12298612	12299941
F19H6.4	chrX	12365609	12367037
T18D3.1	chrX	12454666	12457866
tag-147	chrX	12624592	12634276
col-182	chrX	12636074	12636533
chd-3	chrX	12846352	12852521
C34E7.4	chrX	12932158	12934897
F11C1.5	chrX	12991395	12999492
K03A11.1	chrX	13051716	13055257
R04D3.3	chrX	13288916	13290549
C49F8.3	chrX	13386074	13387469
C29F7.2	chrX	13415999	13418137
R01E6.2	chrX	13565536	13566357
R01E6.7	chrX	13567360	13569874
aakb-1	chrX	13755693	13758858
M03B6.2	chrX	13852827	13857246
M03B6.3	chrX	13861211	13864214
meg-1	chrX	13926963	13929553
pqn-39	chrX	13965657	13969489
C04C11.1	chrX	14020706	14022330
ceh-36	chrX	14183369	14185518
K04C1.2	chrX	14238628	14241265
E02H4.6	chrX	14250641	14252057
sel-7	chrX	14332713	14340401
F23D12.2	chrX	14416198	14421392
F23D12.4	chrX	14444921	14446044
gfi-3	chrX	14480491	14484576
D1025.2	chrX	14514111	14514991

sym-1	chrX	14581575	14584290
F40E10.5	chrX	14701709	14703601
F40E10.6	chrX	14703623	14706776
C05G5.1	chrX	14734388	14740007
C05G5.4	chrX	14753944	14756378
Y16B4A.2	chrX	14761884	14771770
rgs-11	chrX	14964500	14965851
F20D1.1	chrX	14968821	14970191
tbc-1	chrX	14970668	14974681
F20D1.3	chrX	14976034	14978630
F20D1.9	chrX	15002013	15003750
H40L08.1	chrX	15080699	15084004
dhhc-1	chrX	15097984	15100323
mlt-9	chrX	15101704	15107885
ucr-2.2	chrX	15173821	15178040
T10B10.4	chrX	15190040	15192985
tag-97	chrX	15369916	15377604
pqn-36	chrX	15409095	15413304
R03A10.1	chrX	15429929	15431034
nkat-3	chrX	15441649	15443412
eat-20	chrX	15516574	15523859
dyn-1	chrX	15568835	15573613
K09A9.6	chrX	15580519	15586668
gas-1	chrX	15586733	15590317
erv-46	chrX	15613724	15616441
F59D12.2	chrX	15672767	15675642
F53H4.5	chrX	15882018	15885062
R11.1	chrX	16189779	16194913
R11.4	chrX	16210218	16210566
F23A7.1	chrX	16217307	16217582
sdc-1	chrX	16275683	16282351
F59C12.4	chrX	16602359	16602632
C06G1.1	chrX	16633277	16637548
F22H10.4	chrX	16684328	16685622
F41G4.1	chrX	16841019	16842833
T20F7.1	chrX	16872840	16878202
F39F10.4	chrX	16902305	16904247
F52G3.1	chrX	16963783	16972726
F52G3.5	chrX	16973208	16976045
C08A9.6	chrX	17094217	17096451
cnp-3	chrX	17135923	17138026
mdt-1.2	chrX	17151435	17154461
B0302.5	chrX	17193214	17195032
F10D7.5	chrX	17388185	17391527
C36E6.1	chrX	17434358	17436282
H18N23.2	chrX	17623726	17640654

Note: red gene names were similarly classified in Jans et al., 2009.

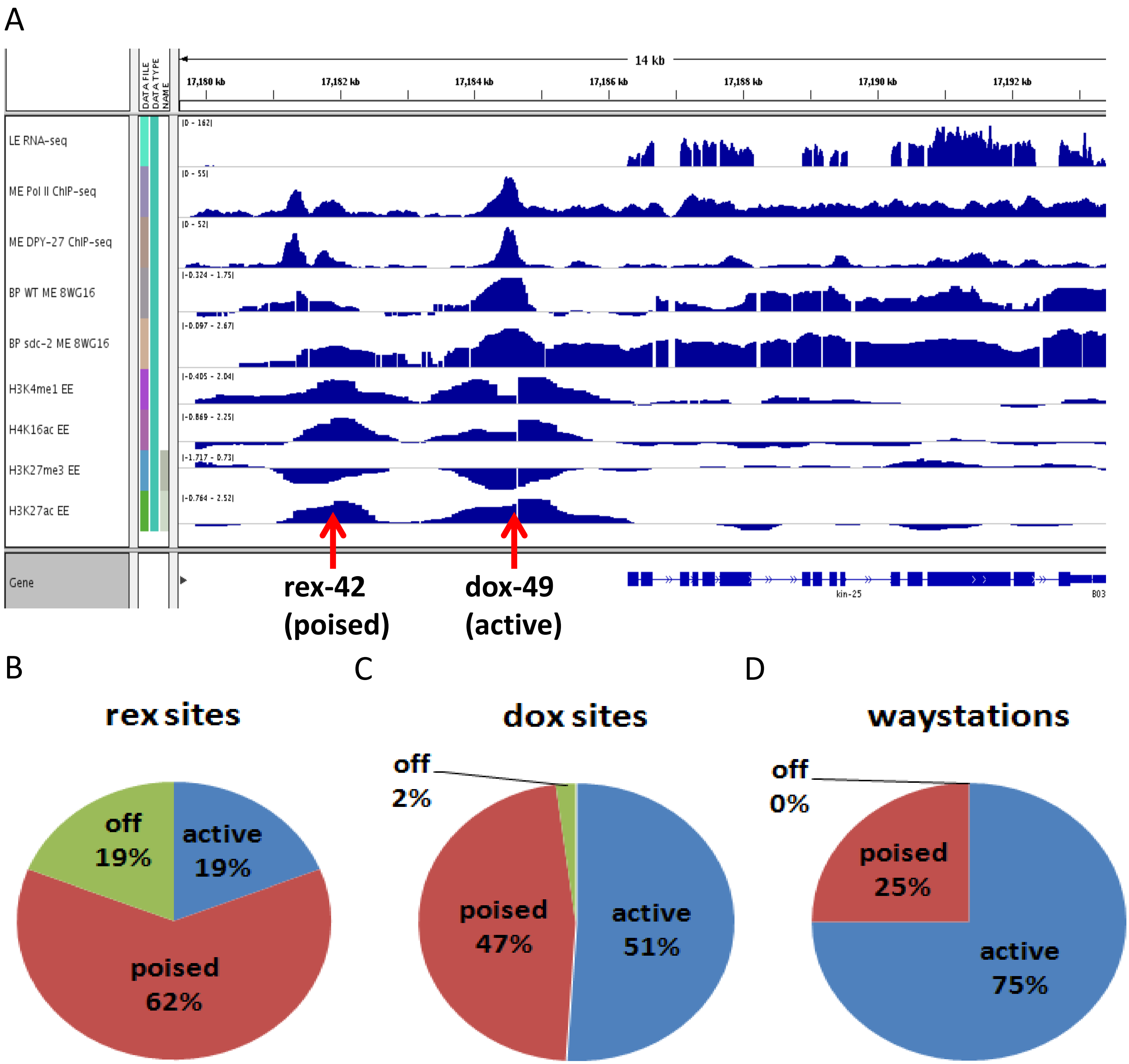

Figure 3.2. DCC binding and recruitment elements possess enhancer-like chromatin. Shown are a genome browser screenshot of two representative DCC binding elements (A) and pie charts summarizing the distribution of enhancer state among three classes of DCC binding elements (B-D). Results demonstrate: A) that defined DCC recruitment (*rex*) and binding (*dox*) sites possess enhancer-like chromatin modifications. B-D) *rex* sites (n=38), *dox* sites (n=49), and waystations (n=4) show different proportions of active, poised, and off enhancer activity. All known DCC binding elements (*rex* sites, *dox* sites, and waystations) possess the enhancer-like chromatin signature, so all are included in this analysis.

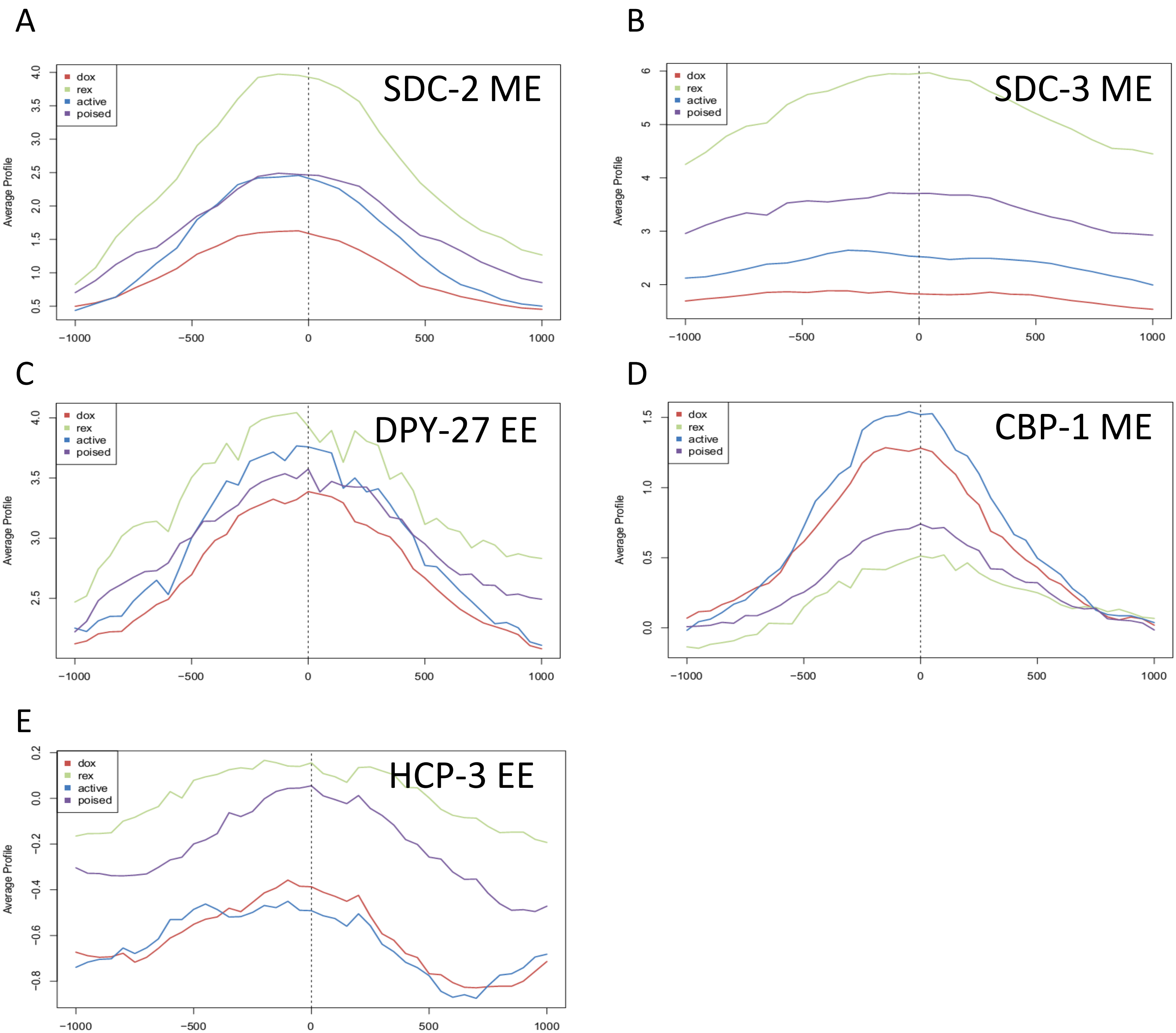

Figure 3.3. Indicators of *rex* site over *dox* site classification. SitePro analysis of five representative enriched proteins at DCC binding elements. All but DPY-27 (C) [including SDC-2 (A), SDC-3 (B), and HCP-3 (E)] show a clear enrichment at *rex* sites over *dox* sites. (D) CBP-1 shows an enrichment at *dox* sites over *rex* sites.

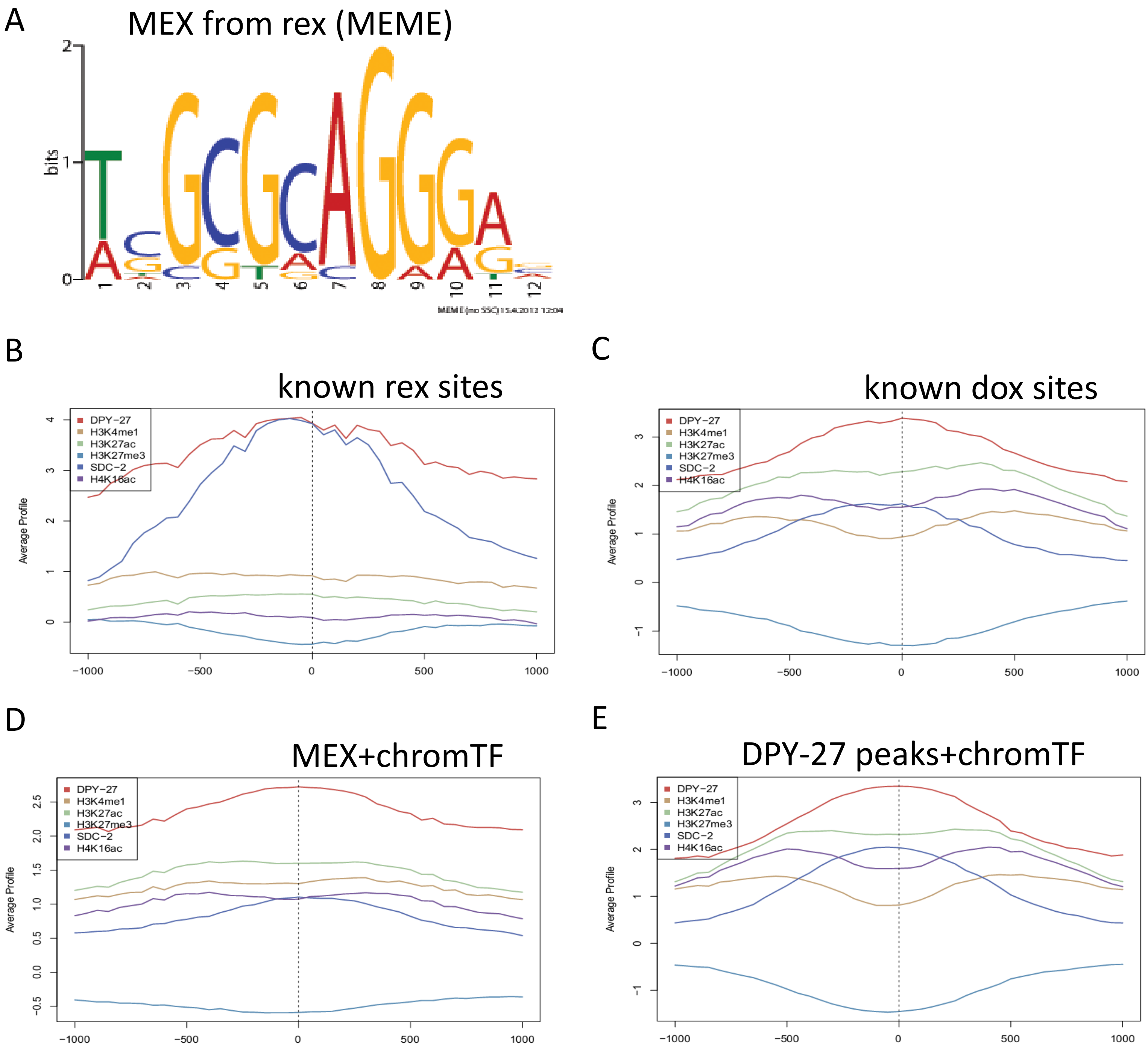

Figure 3.4. Chromatin signature across all known and predicted DCC binding elements. Shown are: (A) MEME-derived MEX motif from *rex* sites; SitePro analysis of DCC and enhancer chromatin occupancy at known *rex* sites (B), known *dox* sites (C), FIMO-derived MEX occurrences filtered in Cistrome by enhancer chromatin enrichment (D), or DPY-27 ChIP-seq peaks filtered in CIstrome by enhancer chromatin enrichment (E). Results show that the enhancer-like chromatin state is across known DCC binding elements and extends to over 300 additional sites. This suggests that the true number of DCC binding elements is much larger than currently defined.

Table 3.4A. Additional enhancer-like DCC binding elements identified from MEX motif instances.

chromosome	start	stop	known?	ele type	H3K4me1 max	H3K27ac max	H4K16ac min	SDC-2 max	DPY-27 min
chrI	7500592	7500603	~	active	0.235827	3.220791	0.962293	3.220791	2.341042
chrI	12065532	12065543	~	active	1.253599	3.486584	2.164847	3.486584	1.823387
chrII	2220078	2220089	~	active	1.827783	3.953937	3.042383	3.953937	1.845122
chrII	12551082	12551093	~	poised	1.61408	1.359033	0.400069	4.193869	1.810697
chrII	14804580	14804591	~	active	1.050795	2.715515	1.188403	2.715515	2.02639
chrIII	4281021	4281032	~	active	0.802852	3.213548	1.213034	3.213548	2.067004
chrIII	9176083	9176094	~	poised	1.279208	3.24921	1.242661	3.24921	1.700373
chrIII	10460830	10460841	~	poised	1.194172	3.937715	3.103079	3.937715	2.158347
chrIV	3233017	3233028	~	active	0.814955	3.388084	1.673222	3.582584	2.268637
chrIV	4277886	4277897	~	poised	2.272632	2.238716	1.539009	2.238716	1.734795
chrX	373783	373794	~	poised	1.420112	0.620456	0.022709	0.765682	1.950051
chrX	382950	382961	~	active	2.005524	3.449735	2.773189	3.449735	3.499937
chrX	647226	647237	~	poised	0.500331	0.676114	0.060592	1.005102	1.710105
chrX	678938	678949	~	poised	2.89077	2.015134	0.964325	2.015134	2.234935
chrX	900566	900577	~	poised	0.534033	0.015029	0.034387	0.542774	1.993424
chrX	954906	954917	~	active	0.805811	3.223496	2.264749	3.223496	3.179078
chrX	1223907	1223918	~	active	2.319075	3.136947	0.673972	3.136947	3.180429
chrX	1682742	1682753	rex	poised	1.336883	0.605274	0.27879	2.024613	3.632825
chrX	1962054	1962065	~	active	2.272538	1.542396	0.362245	3.842289	3.183019
chrX	1962108	1962119	~	nes	2.272538	1.35896	0.304795	3.659776	3.106035
chrX	1977824	1977835	~	poised	1.807083	1.569598	1.337203	1.569598	3.267088
chrX	2045241	2045252	~	nes	1.124892	3.221759	1.41899	3.221759	2.717643
chrX	2211842	2211853	~	poised	2.705833	1.42103	0.500221	1.42103	2.058081
chrX	2522849	2522860	~	poised	3.112784	1.398901	0.256624	1.398901	2.049625
chrX	2543698	2543709	~	poised	1.72808	0.735982	0.121192	1.098437	1.703149
chrX	2590905	2590916	~	poised	1.741708	1.553894	0.631365	1.553894	1.81221
chrX	2668052	2668063	~	poised	1.610486	2.140347	1.212372	2.140347	2.38784
chrX	2791567	2791578	~	poised	2.475801	1.494962	0.73525	1.494962	2.396333
chrX	2852293	2852304	~	poised	3.087223	2.627376	1.890881	3.629713	3.229354
chrX	3067145	3067156	~	poised	2.978484	1.468195	0.296841	1.468195	2.549525
chrX	3200843	3200854	rex	poised	2.823021	1.430822	0.015404	1.430822	2.3592
chrX	3332561	3332572	~	poised	2.195613	1.479566	0.384396	1.479566	2.067197
chrX	3456673	3456684	~	poised	2.449955	1.278648	0.070337	1.27905	2.990137
chrX	3466457	3466468	~	poised	2.251779	2.872315	1.132987	2.872315	2.608318
chrX	3575190	3575201	~	poised	0.903022	1.373397	0.300107	1.373397	1.761407
chrX	3698312	3698323	~	poised	1.381047	0.565278	0.63527	1.174284	1.797736
chrX	3791106	3791117	~	poised	2.653921	0.793208	0.330912	0.793208	2.057771
chrX	3898931	3898942	~	poised	1.864114	1.992557	0.88136	1.992557	2.40553
chrX	4010695	4010706	rex	poised	2.106272	2.615016	1.719063	2.615016	2.778086
chrX	4152113	4152124	~	poised	1.985417	2.416741	1.485077	2.416741	2.519274
chrX	4219297	4219308	~	poised	2.188487	1.632598	0.317645	1.632598	2.569818
chrX	4512786	4512797	~	active	1.707252	3.201525	2.143272	3.201525	2.374888
chrX	4520050	4520061	~	poised	1.77858	1.425551	0.87575	1.425551	2.316138
chrX	4699842	4699853	~	active	1.162912	3.159537	1.86269	3.159537	3.498756
chrX	4699848	4699859	~	active	1.162912	3.159537	1.86269	3.159537	3.498756
chrX	4744201	4744212	~	poised	2.804159	0.974899	0.021653	0.974899	2.016955
chrX	4960921	4960932	~	poised	1.685304	3.696536	2.022047	3.696536	4.078779
chrX	4969333	4969344	~	poised	1.306836	1.713384	0.573295	1.713384	2.877473
chrX	4978307	4978318	~	active	2.485848	0.794847	0.28942	0.922047	2.521086
chrX	5060713	5060724	~	poised	1.261391	1.307994	0.505016	1.307994	2.099073
chrX	5123061	5123072	~	poised	2.732014	3.031193	1.773434	3.031193	2.503316
chrX	5208104	5208115	~	poised	2.326082	1.573506	0.667292	1.573506	1.807841
chrX	5354154	5354165	~	poised	2.485788	2.310325	1.509094	2.57142	2.648913
chrX	5368413	5368424	~	poised	1.600192	0.255847	0.372539	1.556761	2.205582
chrX	5586465	5586476	~	poised	1.939646	0.84799	0.089607	0.84799	2.259873
chrX	5764003	5764014	~	active	1.219519	2.907707	1.028339	2.907707	2.507041
chrX	6247615	6247626	~	poised	1.604389	0.709046	0.120054	0.709046	1.633249
chrX	6250272	6250283	~	poised	2.129712	1.597067	0.608415	1.597067	2.335869
chrX	6263369	6263380	~	active	0.538314	3.080464	1.899727	3.080464	3.974692

chrX	6384356	6384367	~	poised	1.471737	0.893852	0.270522	0.893852	1.53155
chrX	6618142	6618153	~	poised	1.145021	1.028758	0.048663	1.809976	3.517945
chrX	6742348	6742359	~	poised	2.555953	2.598639	1.291936	2.729637	3.430921
chrX	6747433	6747444	~	poised	1.830712	1.284827	0.961623	1.284827	1.90272
chrX	6778217	6778228	~	poised	1.610356	0.917787	0.129691	0.917787	2.047694
chrX	6892151	6892162	~	poised	3.741837	1.236038	0.395872	1.236038	2.937467
chrX	7152569	7152580	~	poised	2.217863	3.577948	2.24049	3.577948	2.778905
chrX	7809728	7809739	~	active	0.584038	3.214953	1.698967	3.961398	3.31078
chrX	7916260	7916271	~	poised	2.421319	3.439317	1.923465	3.439317	2.127095
chrX	7961990	7962001	~	active	1.627075	2.944548	1.503346	2.944548	3.008701
chrX	8268335	8268346	~	poised	2.090053	2.369846	0.97135	2.369846	2.12418
chrX	8285520	8285531	~	poised	1.06598	0.773123	0.585514	0.823613	1.651944
chrX	8298748	8298759	~	poised	1.205668	1.774679	0.864945	1.774679	2.216075
chrX	8568425	8568436	~	poised	2.40476	3.102159	1.487703	3.102159	2.470585
chrX	8806947	8806958	~	poised	2.39326	1.235238	0.692784	1.235238	2.240112
chrX	8807051	8807062	~	poised	2.04571	1.235238	0.60268	1.235238	2.144999
chrX	8811050	8811061	rex	active	1.502965	3.517948	2.127518	3.517948	3.535136
chrX	9089776	9089787	~	active	2.215529	2.935254	0.876535	2.935254	2.891005
chrX	9403550	9403561	~	poised	1.609024	1.233474	0.724535	1.233474	1.842567
chrX	9404143	9404154	~	poised	1.609024	1.233474	0.197636	1.233474	2.181191
chrX	9406332	9406343	~	poised	1.103274	1.562804	0.349521	1.562804	1.935933
chrX	9410537	9410548	~	poised	1.643599	1.827626	0.67649	1.827626	2.326008
chrX	9637417	9637428	~	active	1.463253	3.015239	1.595357	3.858602	3.560544
chrX	9667046	9667057	~	poised	1.227293	1.170251	0.134364	1.170251	1.969276
chrX	10075054	10075065	~	poised	2.073145	3.041513	2.061139	3.041513	1.752459
chrX	10201460	10201471	~	poised	1.374079	1.951503	0.222329	1.951503	2.619253
chrX	10435587	10435598	~	active	1.414872	2.719808	0.693739	3.072937	3.119188
chrX	10596701	10596712	~	poised	1.0995	3.316604	0.481095	3.316604	3.351424
chrX	10597700	10597711	dox	active	1.49958	3.73109	1.332257	3.73109	3.288671
chrX	10637950	10637961	dox	active	0.979387	0.628135	0.278693	0.980362	1.695915
chrX	10767737	10767748	~	poised	2.425783	3.16791	1.183211	3.16791	2.886682
chrX	10990487	10990498	~	poised	2.316397	2.62143	0.574143	2.739176	2.794718
chrX	11031964	11031975	~	active	2.712011	3.656303	2.921233	3.656303	2.771168
chrX	11509820	11509831	~	off	0.224001	0.05372	0.072313	0.05372	2.120871
chrX	11546587	11546598	~	active	0.226302	3.261203	1.779392	3.261203	2.708459
chrX	11666762	11666773	~	poised	1.666657	2.845315	1.754834	2.845315	2.98792
chrX	12407593	12407604	~	poised	1.900175	1.358055	0.181917	1.526016	2.259906
chrX	12410255	12410266	~	poised	1.826355	0.695144	0.085083	0.695144	2.044016
chrX	12474529	12474540	~	poised	1.202114	0.081845	0.084181	0.935985	1.951849
chrX	12507630	12507641	~	poised	2.128709	1.855993	0.753446	1.855993	3.010579
chrX	12522731	12522742	~	poised	0.896498	0.33484	0.060239	1.050999	1.713548
chrX	12721437	12721448	~	poised	1.522601	0.609211	0.186216	1.560488	2.688336
chrX	12721689	12721700	~	poised	1.522601	0.609211	0.186216	1.560488	3.09077
chrX	12781387	12781398	~	poised	0.914693	0.969541	0.043075	1.305729	1.841977
chrX	12860823	12860834	~	poised	0.599757	3.053098	2.082301	3.053098	3.123703
chrX	12932690	12932701	~	poised	0.792172	0.778242	0.144353	1.483298	2.126059
chrX	13397463	13397474	~	poised	1.006226	1.419866	1.014157	1.419866	2.342475
chrX	13526505	13526516	~	active	1.252275	3.359606	1.645465	3.359606	3.308986
chrX	13584916	13584927	~	active	1.069932	3.500319	1.602051	3.500319	3.672792
chrX	13670331	13670342	~	poised	1.229576	2.630075	0.853811	2.630075	2.82211
chrX	13712986	13712997	~	active	1.125373	0.36747	0.045935	0.449198	2.529454
chrX	13871836	13871847	~	poised	0.732562	0.754831	0.030165	0.754831	2.635473
chrX	13936975	13936986	~	poised	1.82462	1.139018	0.24185	1.139018	1.967433
chrX	13968529	13968540	~	poised	1.918584	2.382567	0.596996	2.382567	2.05428
chrX	14104451	14104462	~	poised	1.978975	1.063956	1.248485	1.063956	2.319194
chrX	14168821	14168832	~	poised	1.522257	2.425572	0.680112	2.425572	2.431879
chrX	14169266	14169277	~	poised	1.387873	3.286123	2.335101	3.286123	2.686333
chrX	14495301	14495312	~	poised	1.049559	0.948992	0.120803	0.948992	1.765383
chrX	14504575	14504586	~	poised	3.038366	2.682747	1.437043	2.682747	3.181927
chrX	14515575	14515586	~	poised	1.169773	0.634484	0.465111	0.732336	2.243169
chrX	14712163	14712174	~	poised	1.28351	2.668783	0.514989	2.668783	2.182399
chrX	14755782	14755793	~	poised	1.766077	0.753195	0.381981	0.753195	2.273116

chrX	[illegible]	[illegible]		poised	[illegible]	[illegible]	[illegible]	[illegible]	[illegible]
chrX	14852891	14852902	~	poised	1.86307	1.931083	1.309749	1.931083	1.784185
chrX	15274921	15274932	~	poised	3.201719	2.529284	1.085105	3.883119	3.596562
chrX	15736600	15736611	~	poised	1.048162	0.4281	0.005508	7.207876	1.525262
chrX	15795725	15795736	~	poised	1.246472	0.323881	0.506779	0.92002	1.816724
chrX	15798659	15798670	~	poised	1.345576	2.37519	1.920675	2.37519	2.883915
chrX	15866234	15866245	~	active	1.431577	2.379932	1.989637	2.379932	3.472413
chrX	16400412	16400423	~	poised	1.392206	0.642143	0.034257	2.008971	3.054121
chrX	16417034	16417045	~	poised	1.24845	0.573776	0.254783	0.573776	1.677552
chrX	16527918	16527929	~	poised	1.449031	1.085378	0.087237	1.147836	2.003136
chrX	16794982	16794993	~	poised	1.558493	0.615907	0.684797	0.849013	1.54424
chrX	16997408	16997419	~	poised	1.44403	0.674514	0.124551	0.923833	1.88478
chrX	17001580	17001591	~	poised	1.642475	0.531713	0.205675	0.531713	1.694462
chrX	17105252	17105263	~	poised	2.532552	1.630743	1.060014	1.630743	1.863131
chrX	17105674	17105685	~	poised	2.028305	0.785896	0.467585	0.915582	1.583835
chrX	17221990	17222001	~	active	0.588305	2.851526	1.23865	2.851526	3.220868
chrX	17472959	17472970	~	poised	1.050639	1.072263	0.36826	1.895188	1.848904

Table 3.4B Additional enhancer-like DCC binding elements identified from DPY-27 ChIP-seq peaks.

chromosome	start	stop	known?	ele type	H3K4me1 max	H3K27ac max	H4K16ac min	SDC-2 min
chrI	7214602	7215407	~	poised	2.819681	1.461904	0.302246	0.134732
chrII	11884229	11884523	~	poised	2.087381	2.632066	1.41277	0.488526
chrII	11960564	11960897	~	active	2.086116	1.040199	0.912975	0.944171
chrIII	352284	352494	~	poised	3.004247	2.8675	2.876318	0.382666
chrIII	11054570	11054943	~	poised	1.966063	2.288088	2.117288	0.912572
chrIII	12738010	12738294	~	poised	0.469568	0.856544	0.628204	1.078421
chrIII	13673705	13673949	~	poised	2.770301	1.193975	0.924046	0.606567
chrIV	4405385	4406481	~	active	2.798995	3.351641	2.14544	1.548864
chrIV	8252933	8253189	~	poised	0.678784	0.534317	-0.084223	0.556021
chrIV	8927033	8927325	~	poised	1.242358	2.361955	1.465692	1.197651
chrIV	9191211	9191502	~	active	1.210886	0.467869	-0.081898	0.172032
chrIV	11025970	11026386	~	active	0.644031	3.352595	1.793109	2.988894
chrIV	11549789	11550042	~	active	1.61881	0.217099	0.408148	0.992747
chrIV	16388187	16389266	~	poised	3.093372	2.648451	1.358904	1.115477
chrV	4498842	4499800	~	poised	2.747655	1.76016	-0.451105	1.476704
chrV	6470543	6470742	~	poised	2.317508	3.602374	2.23528	0.006141
chrV	7774262	7774591	~	active	1.488981	1.606126	1.305687	0.554024
chrV	11314022	11314339	~	active	1.640637	1.016949	0.321642	1.372545
chrV	12001919	12002297	~	active	1.524459	2.202688	0.955671	0.342874
chrV	12303454	12303749	~	active	2.113107	0.736565	0.787855	1.179997
chrV	13374528	13374736	~	poised	1.903896	2.12433	1.420062	0.723976
chrV	13655332	13655698	~	poised	2.005848	2.334083	1.341896	1.389049
chrV	13818865	13819042	~	active	1.516765	3.609574	2.794252	0.008566
chrV	18808499	18809067	~	poised	1.602114	3.239587	1.56247	0.4858
chrV	19643034	19643322	~	active	1.788547	3.401548	0.819302	1.3922
chrX	348210	348480	~	poised	1.869188	2.634616	1.897913	0.346379
chrX	353186	353501	~	poised	1.706894	2.069905	1.400602	0.883764
chrX	382538	383012	~	active	1.4256	3.449735	2.946871	0.8169
chrX	409955	410813	~	active	2.024381	1.067771	-0.146031	4.783406
chrX	535798	536180	~	active	2.44461	2.653073	1.062727	0.756118
chrX	768082	768397	~	poised	1.052283	3.008384	2.029601	1.873768
chrX	788039	788298	~	poised	2.042824	2.51968	2.091378	0.756931
chrX	870955	871383	~	active	0.711852	3.385614	1.117906	2.32963
chrX	876992	877304	~	poised	1.843369	2.94661	1.87398	1.898344
chrX	915459	915816	~	active	1.602323	3.015662	2.242317	1.21532
chrX	949470	949860	~	active	0.69904	3.596118	1.147253	2.474589
chrX	1093212	1093497	~	active	1.987253	2.821031	1.13428	1.851233

chrX	1103710	1104020	~	active	2.303023	3.590396	2.141722	0.04011
chrX	1128560	1128817	~	active	1.695657	2.811423	1.816804	1.413979
chrX	1302301	1302625	~	active	0.974779	1.945934	0.511519	2.185186
chrX	1319804	1320122	~	poised	1.949991	2.612837	1.30982	2.464673
chrX	1446792	1447133	~	active	0.515337	3.142849	1.636309	2.009531
chrX	1454367	1454775	~	active	2.706662	2.380555	1.501362	2.454616
chrX	1524678	1524978	~	active	2.655546	2.025685	0.637842	0.287455
chrX	1845573	1845759	~	poised	1.90723	2.720684	2.023166	0.696706
chrX	1856219	1856589	~	active	1.779669	2.919546	1.428396	2.942744
chrX	1961363	1961609	~	poised	2.108049	2.803983	1.165695	4.157329
chrX	2242852	2243109	~	active	0.338313	3.469257	1.825462	1.269959
chrX	2368196	2368938	~	active	1.703794	3.475068	2.111758	2.469546
chrX	2401946	2402336	~	active	0.106127	3.294262	0.873973	1.254493
chrX	2439316	2439550	~	poised	2.459086	2.913494	2.215539	0.383663
chrX	2536373	2536783	~	active	1.972945	3.158324	1.235022	2.458543
chrX	2667847	2668086	~	poised	1.610486	2.140347	1.205337	0.17609
chrX	2687206	2687466	~	poised	2.22048	2.842188	1.779424	0.512443
chrX	2688617	2688818	~	poised	1.630187	2.812929	2.186549	0.747765
chrX	2802537	2803073	~	poised	2.245234	2.142573	1.010875	1.626888
chrX	2852379	2852913	~	poised	3.048523	2.627376	1.62297	3.15821
chrX	2924365	2924660	~	poised	2.892096	1.905057	-0.167492	0.592164
chrX	3090050	3090380	~	poised	1.206414	3.749137	2.571859	1.644033
chrX	3099981	3100081	~	active	0.812269	2.597856	2.136423	1.114107
chrX	3127560	3128098	~	active	0.73302	3.601403	1.537353	2.916403
chrX	3245842	3246077	~	active	0.655028	3.26926	2.007245	1.377658
chrX	3605780	3606014	~	active	1.057497	3.109058	2.236337	1.488879
chrX	3914159	3914601	~	active	1.687278	0.617238	0.319342	0.923754
chrX	3969890	3970213	~	poised	1.677181	0.805295	-0.02125	1.746532
chrX	4157882	4158266	~	active	2.080136	3.513551	2.003754	0.913519
chrX	4190584	4190913	~	active	0.237325	3.603617	2.010495	1.277804
chrX	4214644	4214908	~	poised	2.021919	2.865764	0.813905	1.720372
chrX	4222338	4223334	~	active	1.17924	3.079835	0.494356	1.720668
chrX	4388818	4389252	dox	active	0.219838	3.11479	1.115749	2.980027
chrX	4444165	4444365	~	poised	1.801225	0.590726	0.228917	1.162511
chrX	4469311	4469581	~	poised	0.915857	2.237308	1.361035	0.903568
chrX	4523715	4524230	~	active	1.559184	3.485678	0.993298	2.534964
chrX	4635722	4635956	~	active	2.103706	3.336712	2.920596	1.044291
chrX	4890229	4890449	~	poised	1.463169	2.261023	1.97078	0.96069
chrX	4961468	4962586	~	poised	1.812909	3.134846	1.945372	3.195109
chrX	5085519	5085855	~	poised	1.448188	3.505025	0.443128	2.360008
chrX	5275292	5275555	~	active	1.073309	2.766614	2.293241	1.050461
chrX	5319324	5319551	~	poised	1.051649	0.433373	-0.096072	0.955461
chrX	5336507	5336841	~	poised	1.289398	2.299631	1.047988	1.31299
chrX	5407344	5407574	~	poised	1.436784	0.376804	-0.002016	1.144599
chrX	5475018	5475587	~	active	1.792458	3.117767	0.944253	2.638929
chrX	5686031	5686501	~	active	2.392153	3.00086	1.127596	1.369468
chrX	5764764	5765077	~	active	2.086235	3.444248	1.491145	2.501161
chrX	5781945	5782385	~	active	1.201992	3.603807	2.694052	0.750935
chrX	5812025	5812447	dox	active	2.215749	2.897469	1.257574	2.528112
chrX	5840975	5841422	~	active	0.261261	3.296333	1.370223	2.667921
chrX	5984572	5984824	~	poised	1.800123	2.424636	1.645709	0.909397
chrX	6097605	6097866	~	active	1.843766	2.353614	1.541312	0.793943
chrX	6207617	6207993	~	active	1.250192	2.540516	0.783791	1.842231
chrX	6292743	6293050	~	poised	1.80701	2.533349	1.310857	1.12405
chrX	6371165	6371466	~	poised	2.198479	1.721071	-0.107602	0.213847

chrX	6377988	6378666	~	poised	1.027323	3.558023	2.416481	1.417534
chrX	6804963	6805162	~	poised	2.364805	1.881327	1.071458	0.867845
chrX	6806492	6806869	~	poised	2.276007	3.263169	1.624034	1.390754
chrX	7264700	7265283	~	active	0.601503	3.443641	1.013566	2.334396
chrX	7334189	7334660	~	active	0.404983	3.585712	1.824064	1.22167
chrX	7475054	7475331	~	active	1.71687	3.096373	2.520981	0.474322
chrX	7782369	7782693	~	active	1.783221	2.786631	2.456882	0.578734
chrX	7787979	7788314	~	active	2.029667	3.104972	2.475638	0.888637
chrX	7823054	7823402	~	active	0.885587	3.143859	2.214288	1.398233
chrX	7951494	7951843	~	active	1.350679	3.568206	1.41682	2.590145
chrX	8029076	8029346	dox	poised	1.476081	3.044145	1.801895	0.726652
chrX	8103906	8104167	~	active	0.735905	3.251555	1.376047	2.305558
chrX	8156034	8156273	~	active	1.617134	1.793922	0.889429	1.456125
chrX	8286772	8287077	~	active	0.772945	3.519823	2.023153	0.805434
chrX	8565765	8566317	~	poised	2.22604	1.976018	1.365066	0.634914
chrX	8646240	8646450	~	poised	1.335284	0.731446	-0.131251	0.882325
chrX	8810936	8811448	rex	active	1.961613	3.577046	2.127518	2.695664
chrX	8835564	8836197	~	active	0.97643	2.683145	1.277732	1.275724
chrX	8911085	8911391	~	active	1.018221	2.645155	1.967001	0.241317
chrX	9271960	9272275	dox	active	1.785994	3.168053	2.869111	1.477656
chrX	9337756	9338087	dox	active	1.258424	3.373678	1.268292	1.425033
chrX	9347546	9347927	~	active	1.189585	2.708947	2.556437	0.675253
chrX	9441493	9441777	~	active	2.090606	2.935358	2.529424	1.001435
chrX	9637105	9637901	~	active	1.494315	3.059324	1.595357	2.486651
chrX	9822620	9822884	~	active	1.29361	3.619514	2.059399	1.555403
chrX	9838211	9838373	~	active	1.396947	2.721903	1.928522	0.533338
chrX	9899723	9900052	~	active	1.511059	3.168925	1.933099	1.187521
chrX	9932290	9932754	~	active	1.637177	3.484519	1.383394	2.880893
chrX	9958438	9958902	~	active	1.713223	3.376185	2.372735	1.309442
chrX	9999059	10000076	~	active	1.055301	3.267287	1.350626	1.730193
chrX	10146591	10146931	~	active	1.657117	2.734175	1.475875	2.022212
chrX	10188373	10188765	dox	active	2.027597	3.461523	1.636278	2.313844
chrX	10372690	10372892	~	active	1.053079	3.284056	1.0992	1.039698
chrX	10377653	10377955	~	poised	1.905907	2.748164	1.914245	0.800666
chrX	10435435	10435976	~	active	1.414872	2.376314	0.693739	2.280111
chrX	10963657	10963889	~	poised	1.22592	0.583484	0.00406	0.775229
chrX	11030958	11031666	~	active	1.892183	3.576705	0.673983	2.997789
chrX	11206951	11207229	dox	active	0.607408	3.100925	2.397525	0.503043
chrX	11299557	11299950	rex/dox	active	1.69712	3.804456	1.769279	1.876426
chrX	11344921	11345200	~	poised	1.374812	0.729599	0.001932	1.01961
chrX	11367584	11367840	dox	poised	2.660923	2.08367	1.091813	0.447126
chrX	11522032	11522288	~	active	0.448145	3.426668	1.154598	2.771406
chrX	11605855	11606142	~	active	3.02341	3.204909	1.496469	2.830999
chrX	11798050	11798263	~	active	0.68271	3.315638	1.732365	1.9177
chrX	11947092	11947391	~	poised	1.705842	3.781678	2.043526	2.167783
chrX	12017923	12018184	~	poised	1.698128	2.165641	1.849273	0.781624
chrX	12393724	12394119	dox	active	1.325366	3.254386	2.316629	0.653526
chrX	12480411	12480674	~	active	1.305905	2.842531	1.634879	1.526355
chrX	12670333	12670688	~	active	2.176203	3.102305	1.416724	2.233707
chrX	13121090	13121443	~	active	1.685617	1.753166	1.006356	1.867605
chrX	13264553	13264875	~	poised	1.116262	0.182733	0.113178	1.308604
chrX	13396543	13396817	~	poised	1.590105	2.297543	1.98508	0.62812
chrX	13419853	13420099	~	active	1.917808	3.283223	2.145444	2.018729
chrX	13518998	13519344	~	active	0.780042	3.109038	0.857142	2.583441
chrX	13583763	13584274	~	active	1.298953	3.612964	1.479251	2.035724

chrX	13596008	13596291	~	active	1.908015	3.011012	2.074821	0.803184
chrX	13653579	13653778	~	active	1.966362	1.092276	0.19052	0.30695
chrX	13686971	13687386	~	active	1.839501	3.352131	2.057392	1.729687
chrX	13726906	13727124	~	active	1.455931	2.962776	1.887632	0.594631
chrX	13950511	13951004	~	active	1.315867	2.682957	1.071794	2.422613
chrX	13969449	13969872	~	active	1.84633	3.32027	1.955647	2.44253
chrX	13977374	13977737	~	active	1.169635	3.248529	2.363432	1.173546
chrX	14102016	14102240	~	active	1.135466	3.27913	2.567891	2.048147
chrX	14169653	14169981	~	active	1.119544	3.14673	2.660182	0.850786
chrX	14243502	14243776	~	active	1.811577	3.516181	1.736243	0.228962
chrX	14312365	14312647	~	active	0.79547	3.075937	0.545838	1.085939
chrX	14489914	14490304	~	active	0.307683	3.531141	1.643213	2.009736
chrX	14602605	14602927	~	active	1.111996	3.354193	2.023625	1.932355
chrX	14610386	14610649	~	active	1.14646	2.961697	1.377136	1.699395
chrX	14708181	14708467	~	active	1.443671	2.897993	2.010907	1.335351
chrX	14753507	14753790	~	active	0.964113	3.142158	1.825457	1.095199
chrX	14810712	14810945	~	poised	1.972007	2.628335	1.613434	1.33129
chrX	14818587	14819300	~	active	1.60943	3.9054	1.328	3.410499
chrX	14853799	14854084	~	active	1.56783	2.904047	2.567913	1.280674
chrX	15100570	15100853	~	active	0.879023	3.456075	1.792274	1.076703
chrX	15148500	15149048	~	poised	2.111159	0.910948	-0.147627	0.599409
chrX	15181391	15181673	~	active	1.782425	3.352326	2.022705	1.613637
chrX	15281164	15281463	~	poised	2.038363	3.145682	1.703559	1.123498
chrX	15353953	15354213	~	poised	1.813819	1.662592	1.075459	0.712831
chrX	15515572	15516008	~	poised	1.939261	0.54805	0.332477	0.337238
chrX	15568016	15568480	~	active	1.057203	3.024297	1.767264	2.058808
chrX	15606805	15607225	~	active	1.364124	3.17316	1.785637	2.735928
chrX	15689276	15689524	~	active	1.002673	3.353056	2.132297	0.143662
chrX	15707194	15707770	~	active	1.747407	2.509431	0.450363	1.635117
chrX	15736423	15736752	~	poised	1.048162	0.4281	0.005508	3.692006
chrX	15841091	15841370	~	active	0.149708	3.437329	1.666278	2.533057
chrX	15849338	15849576	~	poised	0.933565	2.304866	1.522655	1.575641
chrX	16147409	16148047	~	active	1.174644	3.031233	0.438687	2.01424
chrX	16156854	16157285	~	poised	3.060908	1.461969	0.307743	1.494799
chrX	16202167	16202512	~	active	1.427687	1.144647	0.201053	3.708138
chrX	16275278	16275509	~	active	0.840923	3.087415	1.853289	1.092199
chrX	16445833	16446186	~	active	1.003049	2.876611	1.072101	2.055689
chrX	16612172	16612954	~	active	0.698964	3.244167	0.705001	2.793402
chrX	16704073	16704398	~	active	1.567144	2.894289	1.771888	0.709492
chrX	16726634	16727149	~	active	1.481195	2.622764	0.919564	2.36656
chrX	16929432	16930528	~	active	0.797144	3.791422	1.964627	3.759633
chrX	16961306	16961663	~	active	0.791155	3.409375	1.371887	1.354473
chrX	17151136	17151425	~	active	1.060904	3.562175	2.381364	1.237075
chrX	17181164	17181845	~	poised	1.663242	1.731197	-0.177587	5.165961
chrX	17184333	17184674	dox	active	2.036549	2.51838	0.880784	1.397085
chrX	17392189	17392416	~	active	1.737618	2.982369	2.364773	1.032649
chrX	17451359	17451623	~	active	1.069595	3.056188	1.75073	0.621094
chrX	17479827	17480378	~	active	2.075798	3.076252	1.189255	2.853988
chrX	17505722	17506130	~	active	2.57565	1.792353	1.169087	1.093266
chrX	17513431	17513838	~	active	1.525378	3.26968	1.864744	2.042648

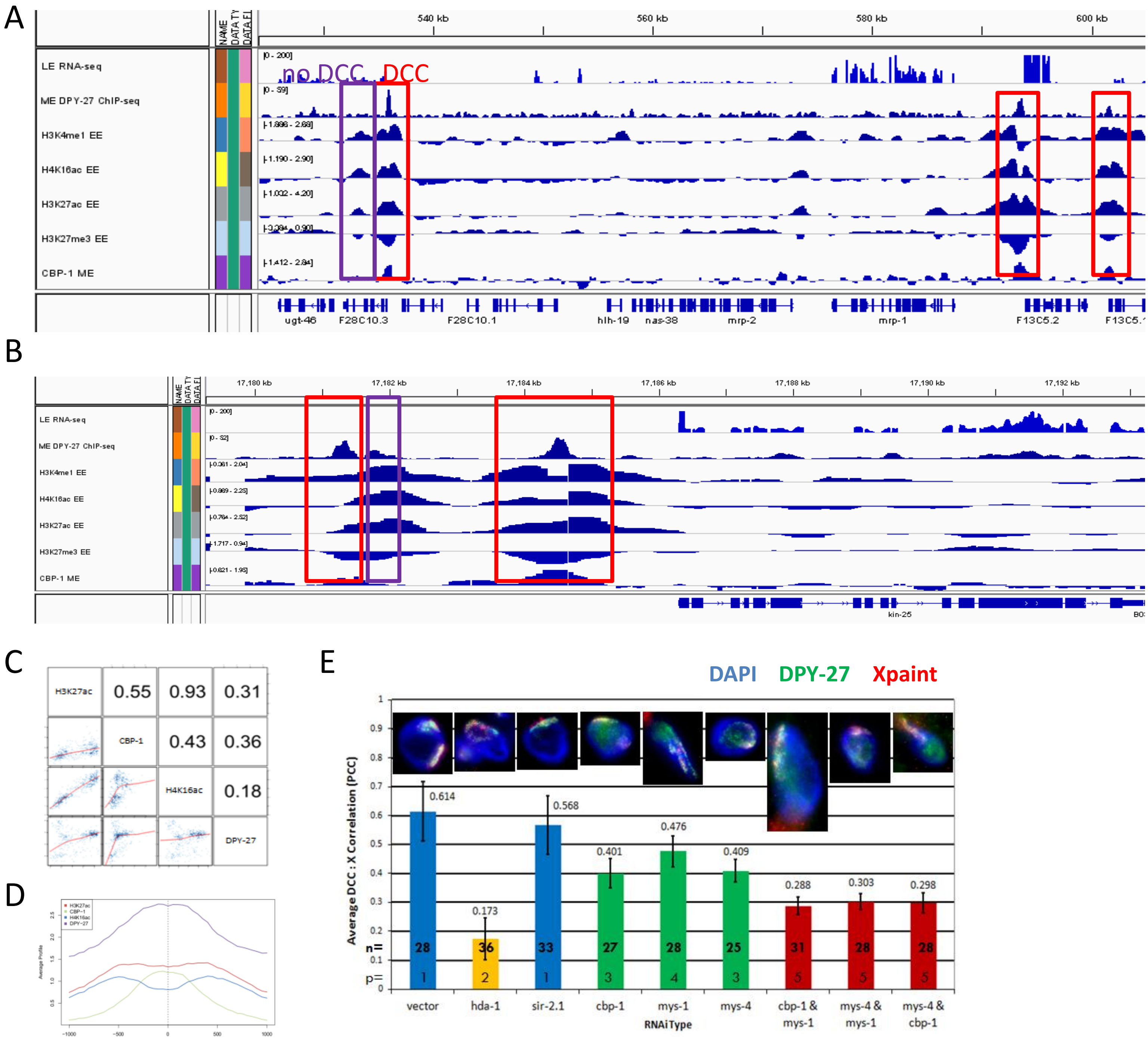

Figure 3.5. A role for histone acetyltransferases in DCC localization. Shown are: browser screenshots demonstrating H4K16ac, H3K27ac, and CBP-1 enrichment at known DCC binding elements (A & B); cross-correlation tables of the factors shown in A & B (C); SitePro analysis of the factors analyzed in A, B, and C across all known DCC binding elements (D); Pearson correlation coefficient averages across WT worms treated with vector, HDAc, HAT, or combination RNAi (E). Images in (E) are representative intestinal nuclei from each condition Xpaint FISH probes and stained with DPY-27 antibodies. DAPI (DNA) is shown in blue. Results show that H4K16ac (by MYS-1, MYS-4; data not shown), H3K27ac (by CBP-1), and CBP-1 are enriched at known DCC binding elements (A-D), and that MYS-1, MYS-4, and CBP-1 activity is needed for proper DCC localization to the X chromosomes (E).

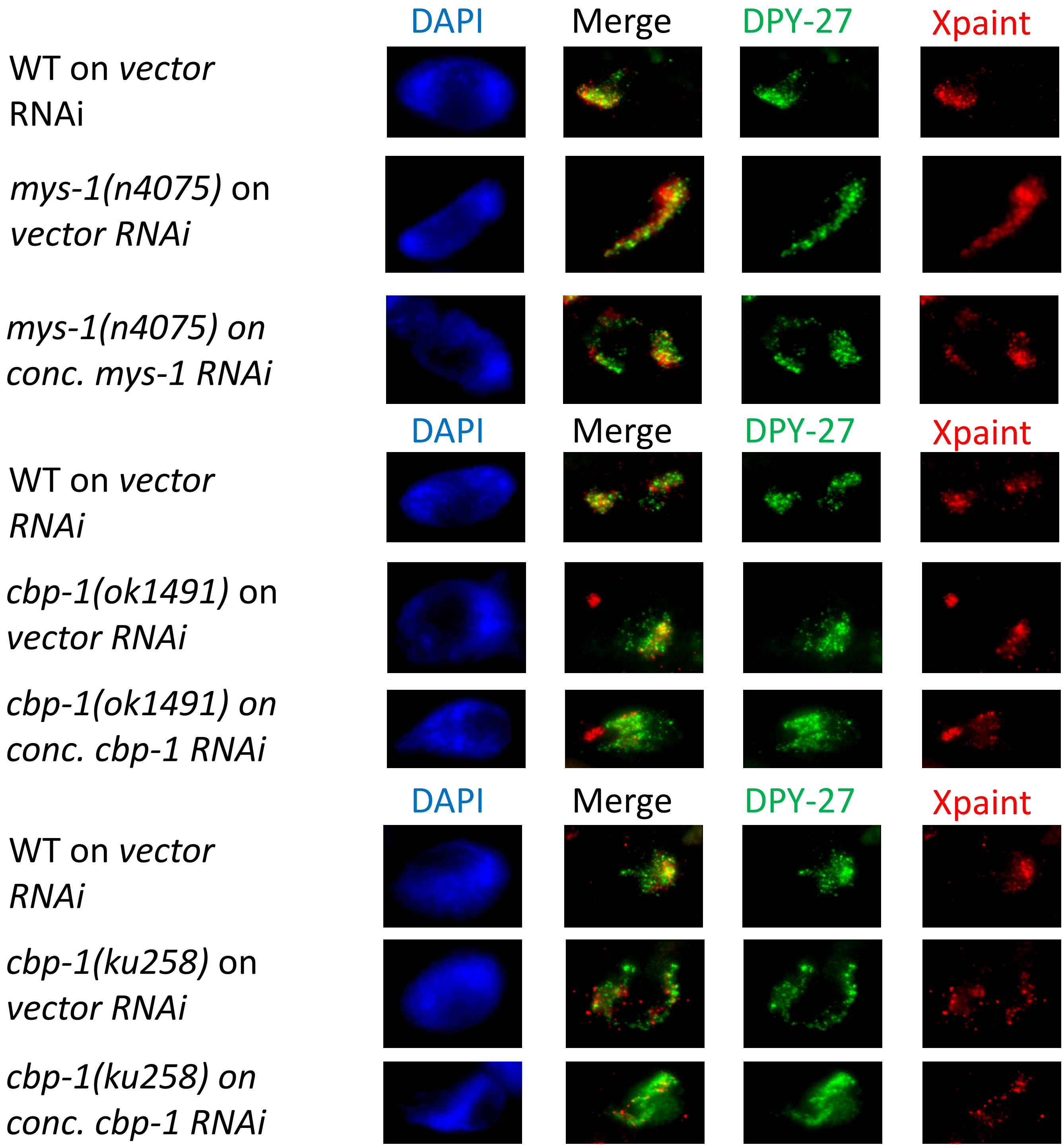

Figure 3.6. Confirmation of changes in X chromosome structure and DCC mislocalization. Shown are representative intestinal nucleus images from HAT mutant worms with or without HAT RNAi treatment processed with Xpaint and anti-DPY-27 immunoFISH. DAPI (DNA) is shown in blue. Results show that stronger loss of HAT protein function leads to disruptions in X chromosome structure, while addition of HAT RNAi against the same gene led to spreading of the DCC signal away from the X chromosomes. Interestingly, loss of CBP-1 led to drastic changes in X chromosome structure. *cbp-1(ok1491)* shows a unique highly condensed X grouping and a highly uncondensed X chromosome grouping. Dissimilarly, all X chromosome groups show severely disrupted structure in *cbp-1(ku258)*.

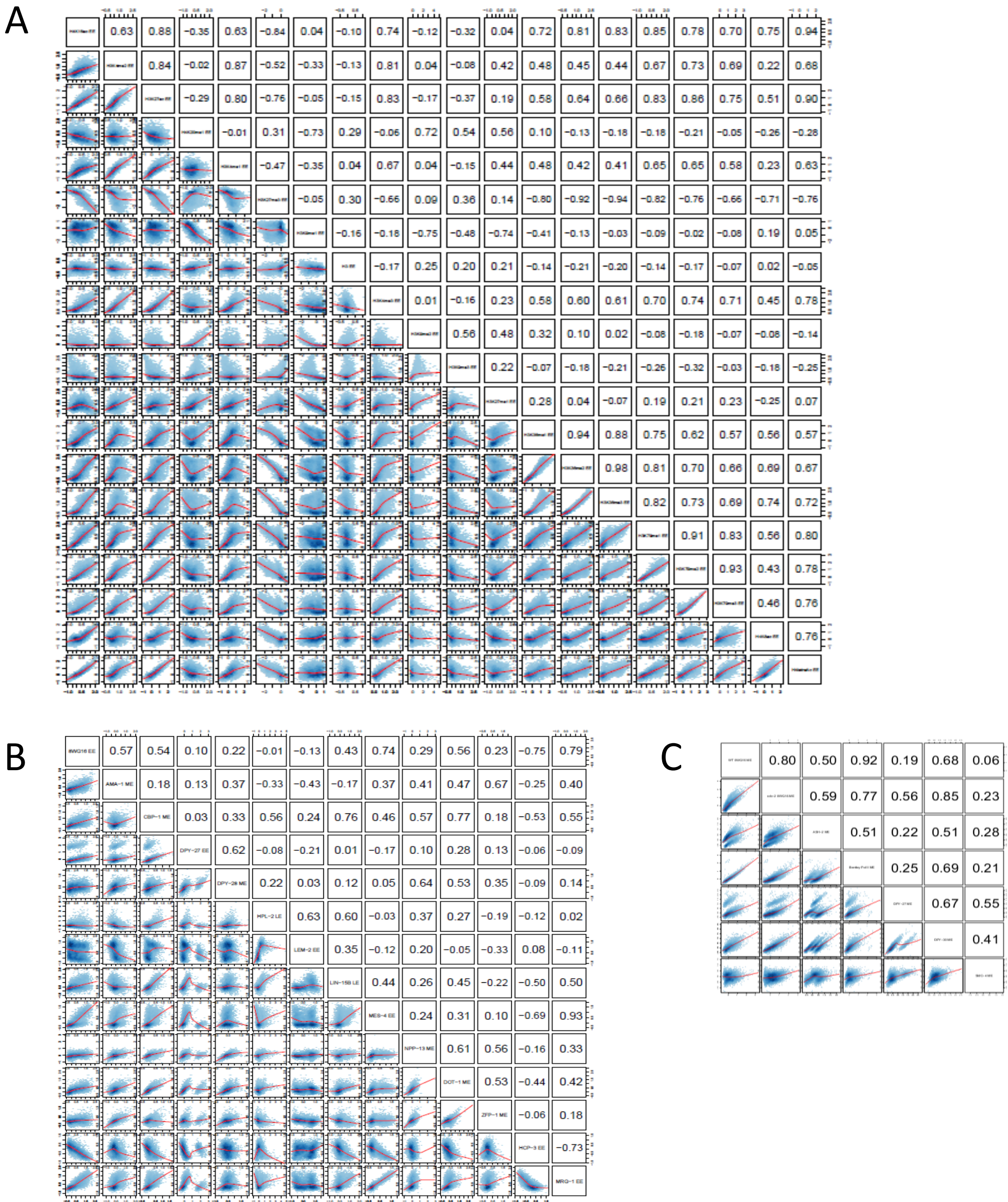

Figure 3.7. Genome-wide correlations of *Caenorhabditis elegans* embryonic chromatin modifications and protein occupancy. Shown are genome-wide cross-correlation tables of the data surveyed in this study at 20kb resolution. Results show conservation of known groupings of histone modification and protein occupancy.

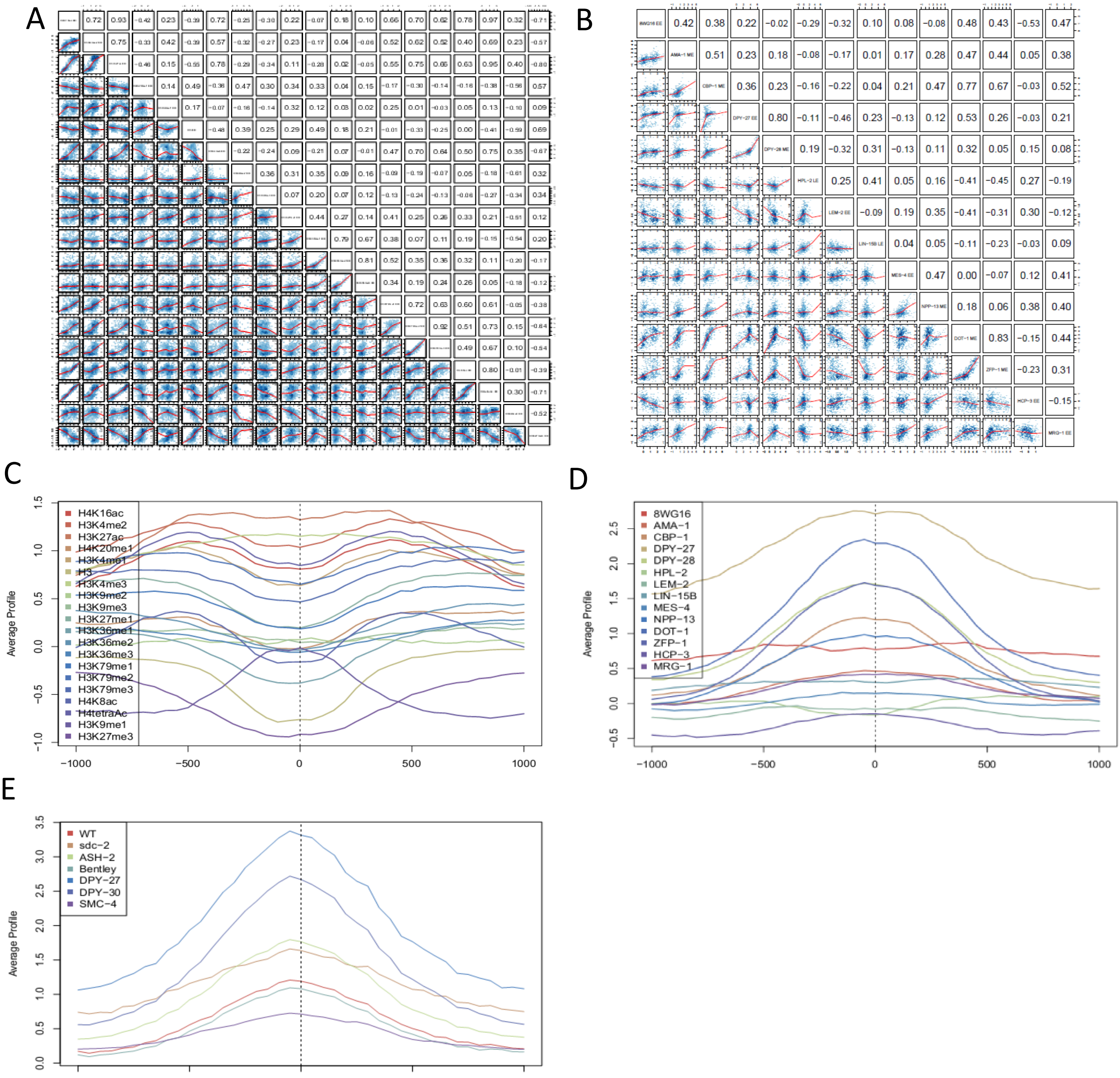

Figure 3.8. Histone modification and protein occupancy at all DPY-27 ChIP-seq peaks. Shown are histone modification (A) and protein (B) cross-correlation tables or histone modification (C), protein (D), or COMPASS/DCC complex (E) SitePro analysis. Results show histone modification or protein cross-correlation tables, DPY-27 mid-peaks are generally at the center of bimodal peaks of many histone modifications (C) and DPY-27 peaks with several transcription factors (including other DCC components and CBP-1; D & E).

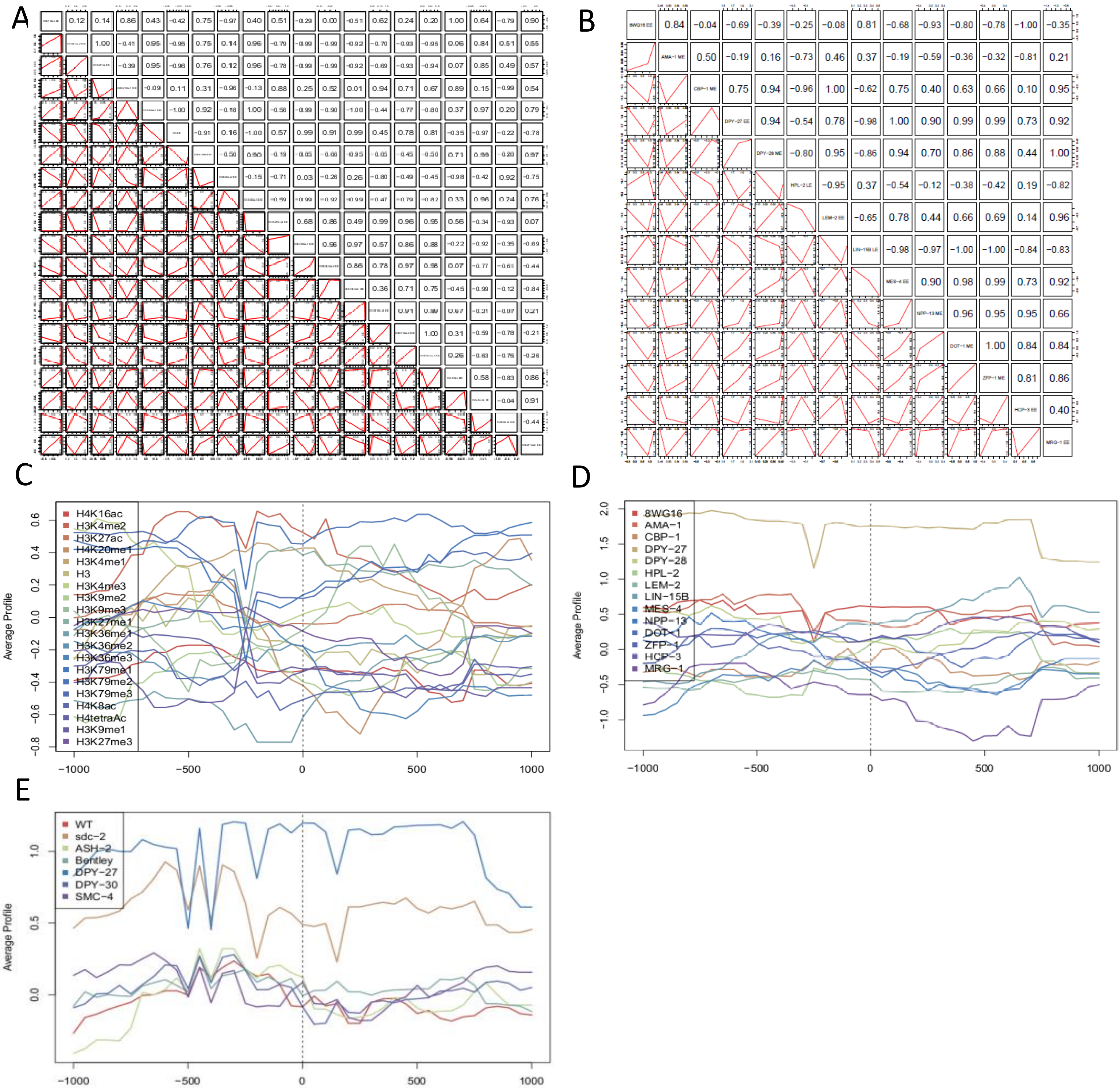

Figure 3.9. Histone modification and protein occupancy at control regions lacking DPY-27 peaks. Shown are histone modification (A) and protein (B) cross-correlation tables or histone modification (C), protein (D), or COMPASS/DCC complex (E) SitePro analysis. Results show, as expected, no strong general trends among different modifications or proteins (A-D) and no enrichment of DCC components, as expected (D &E).

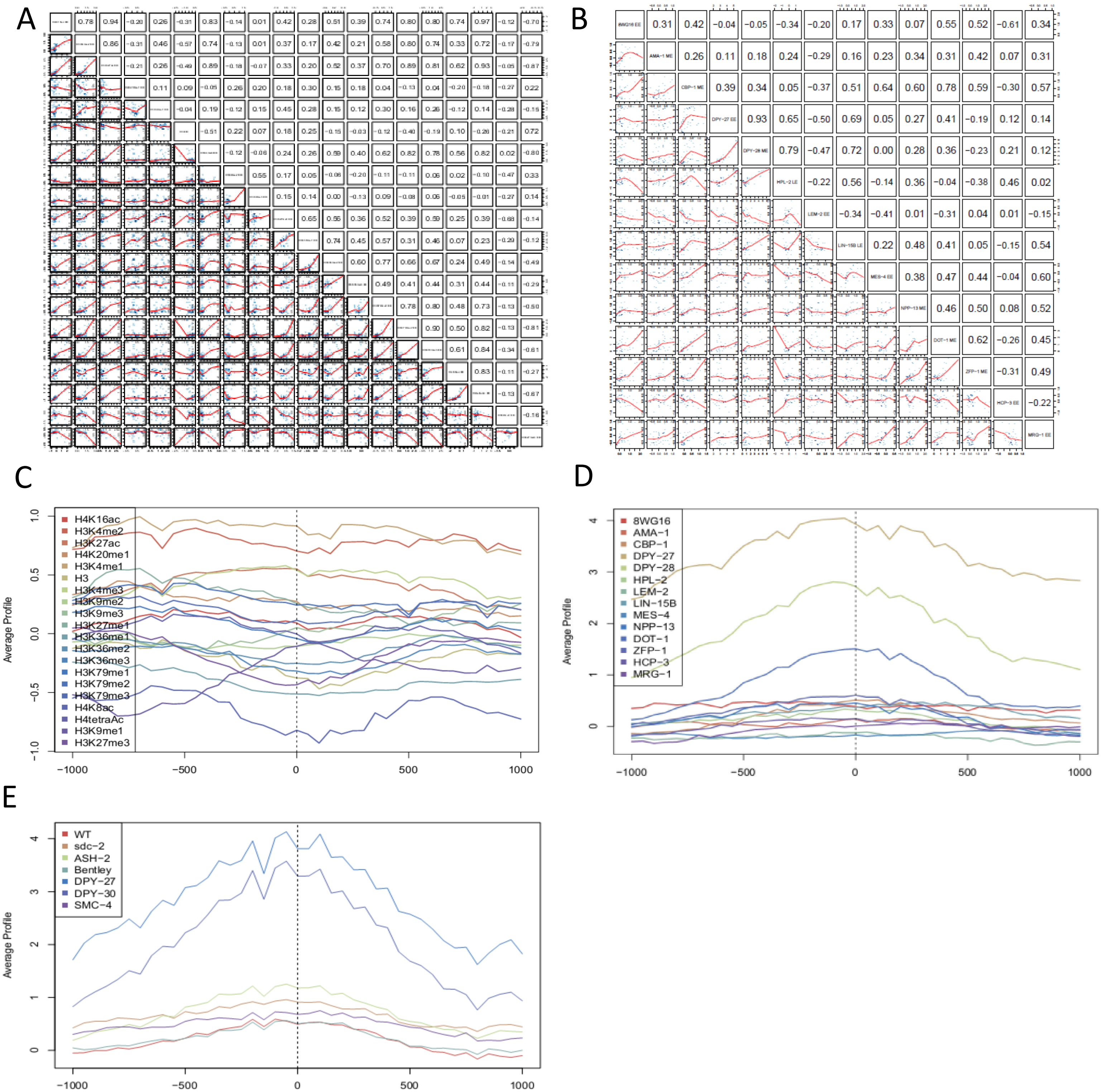

Figure 3.10. Histone modification and protein occupancy at all *rex* sites. Shown are histone modification (A) and protein (B) cross-correlation tables or histone modification (C), protein (D), or COMPASS/DCC complex (E) SitePro analysis. Results show H3K27me3 depletion and weak bimodal distribution of other marks around *rex* sites (C); DCC and NPP-13 enrichment are also seen (D & E).

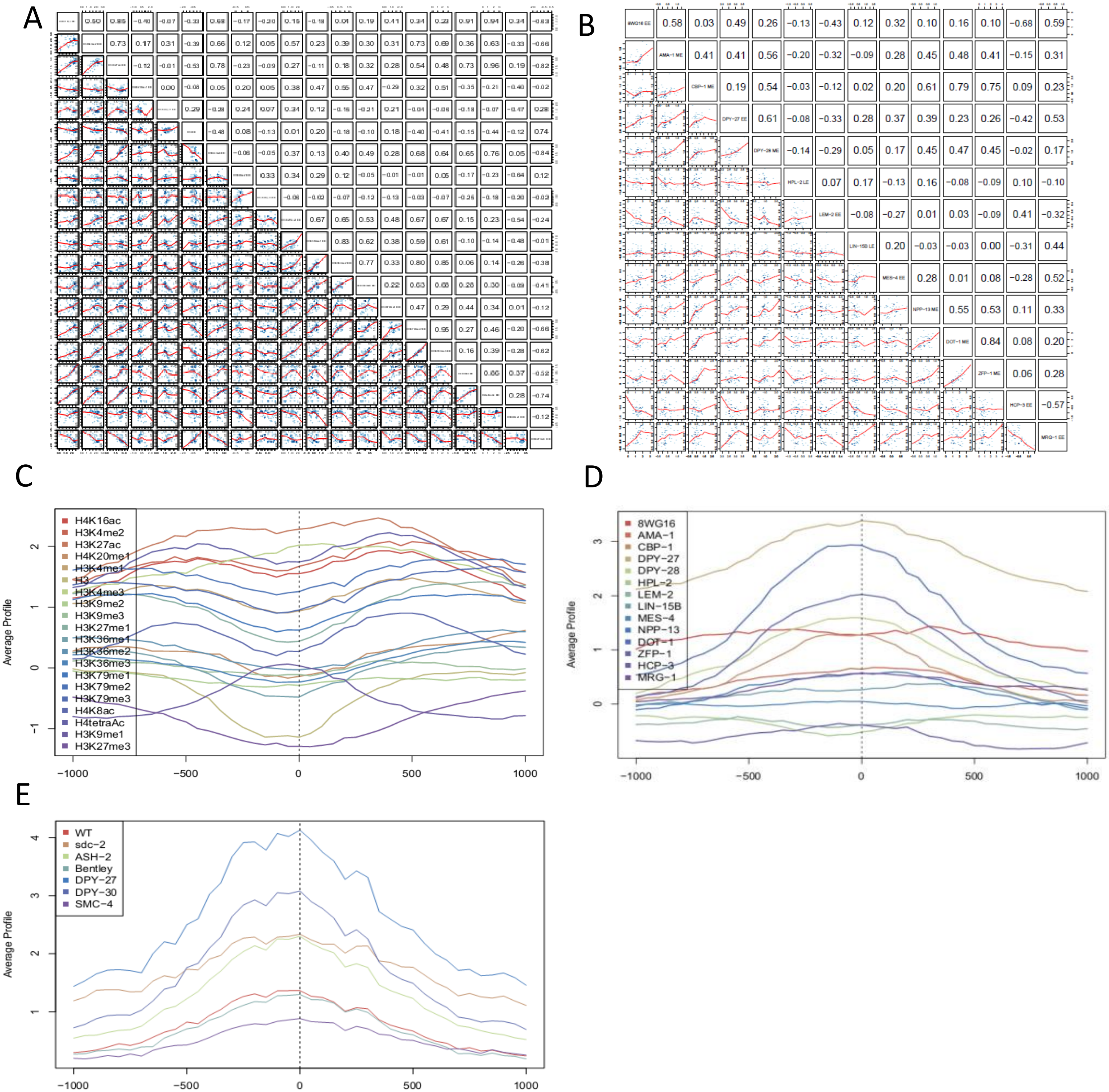

Figure 3.11. Histone modification and protein occupancy at all *dox* sites. Shown are histone modification (A) and protein (B) cross-correlation tables or histone modification (C), protein (D), or COMPASS/DCC complex (E) SitePro analysis. Results show H3K27me3 depletion and bimodal peaks of many histone modifications, as well as enrichment of many proteins, including CBP-1, ZFP-1 (zinc finger transcription factor) and NPP-13 (a member of the nuclear pore complex).

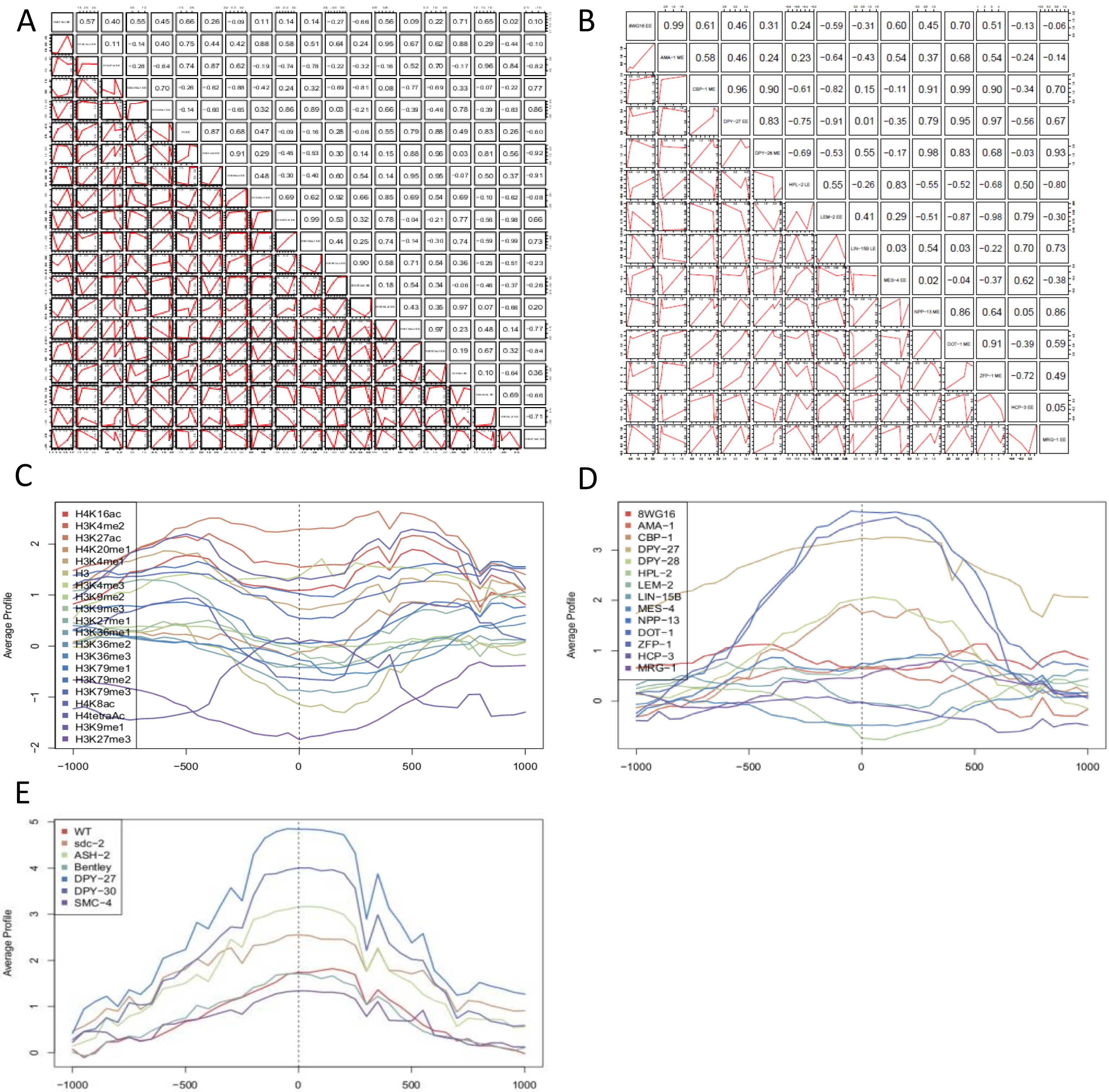

Figure 3.12. Histone modification and protein occupancy at all DCC waystations. Shown are histone modification (A) and protein (B) cross-correlation tables or histone modification (C), protein (D), or COMPASS/DCC complex (E) SitePro analysis. Results show H3K27me3 depletion and bimodal distribution of many histone modifications, COMPASS and DCC enrichment, as well as CBP-1, NPP-13, and ZFP-1 enrichment.

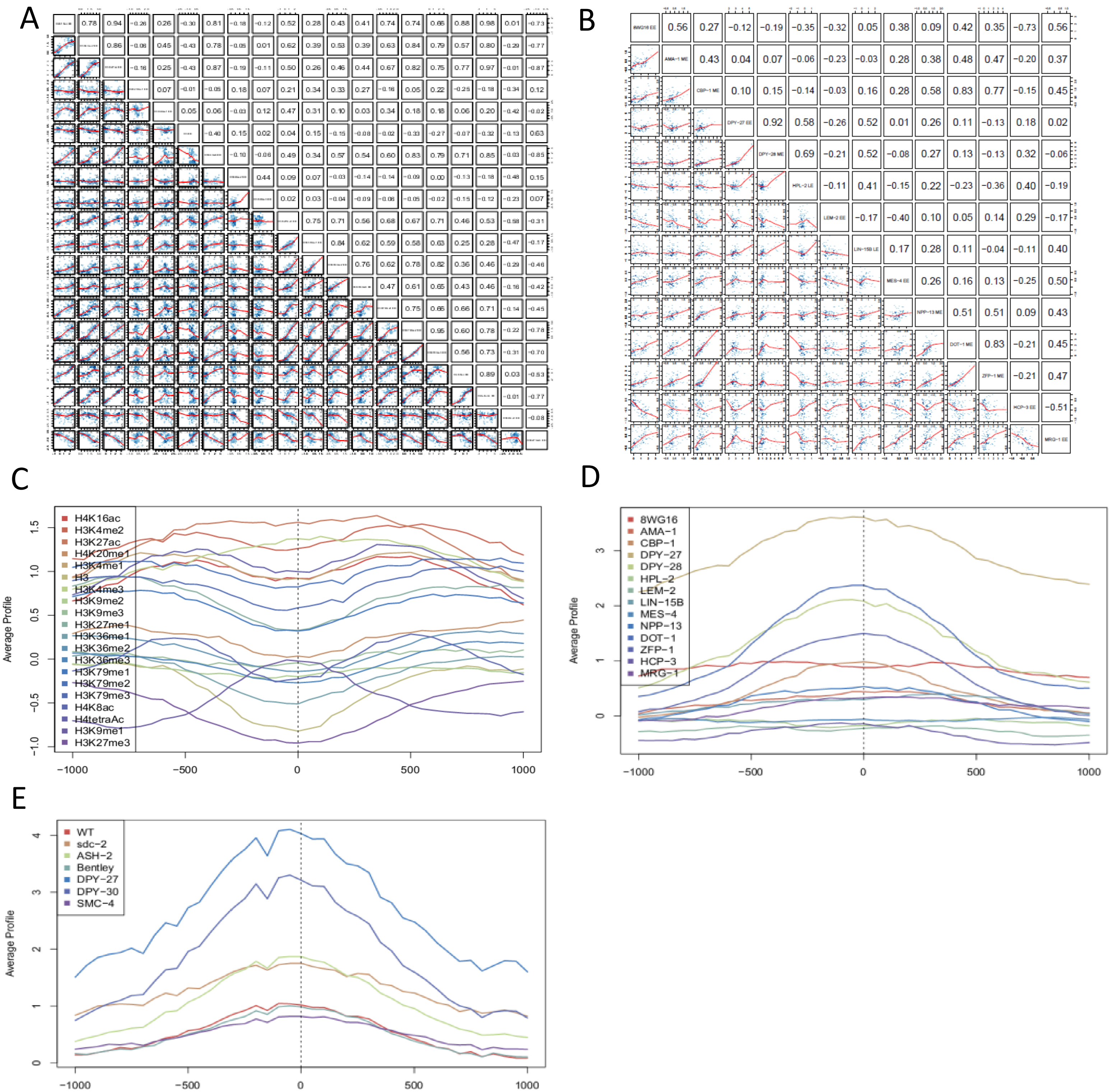

Figure 3.13. Histone modification and protein occupancy at all *rex* sites, *dox* sites, and waystations. Shown are histone modification (A) and protein (B) cross-correlation tables or histone modification (C), protein (D), or COMPASS/DCC complex (E) SitePro analysis. Results show H3K27me3 depletion and bimodal distribution of many histone modifications; also, enrichment of DCC and CBP-1, NPP-13, and ZFP-1.

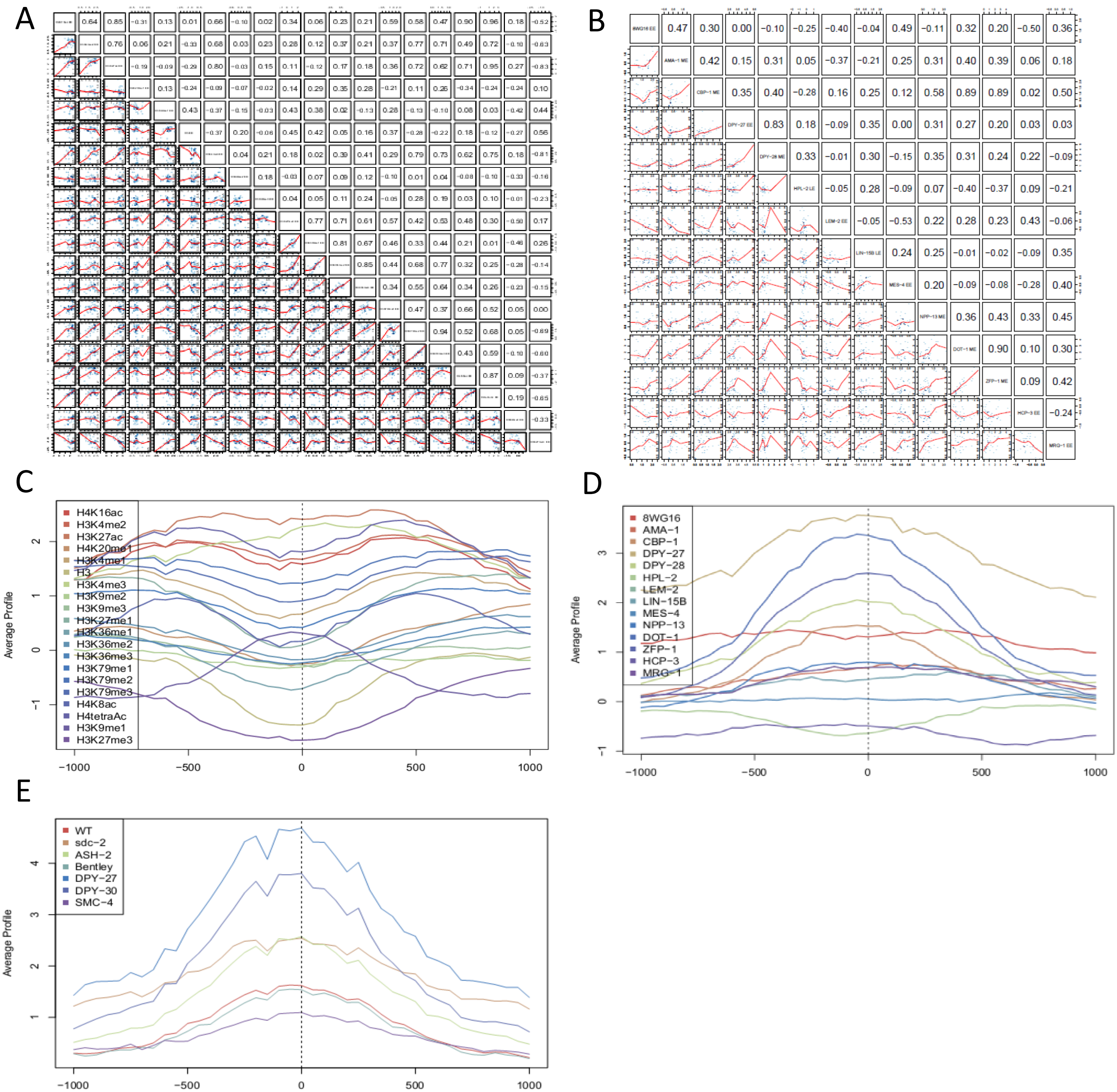

Figure 3.14. Histone modification and protein occupancy at all active enhancer-like DCC binding elements. Shown are histone modification (A) and protein (B) cross-correlation tables or histone modification (C), protein (D), or COMPASS/DCC complex (E) SitePro analysis. Results show strong H3K27me3 depletion and bimodal distribution of many histone modifications; also, COMPASS and DCC enrichment, as well as CBP-1, NPP-13, and ZFP-1 enrichment and LEM-2 (a component of the nuclear lamin) reduction.

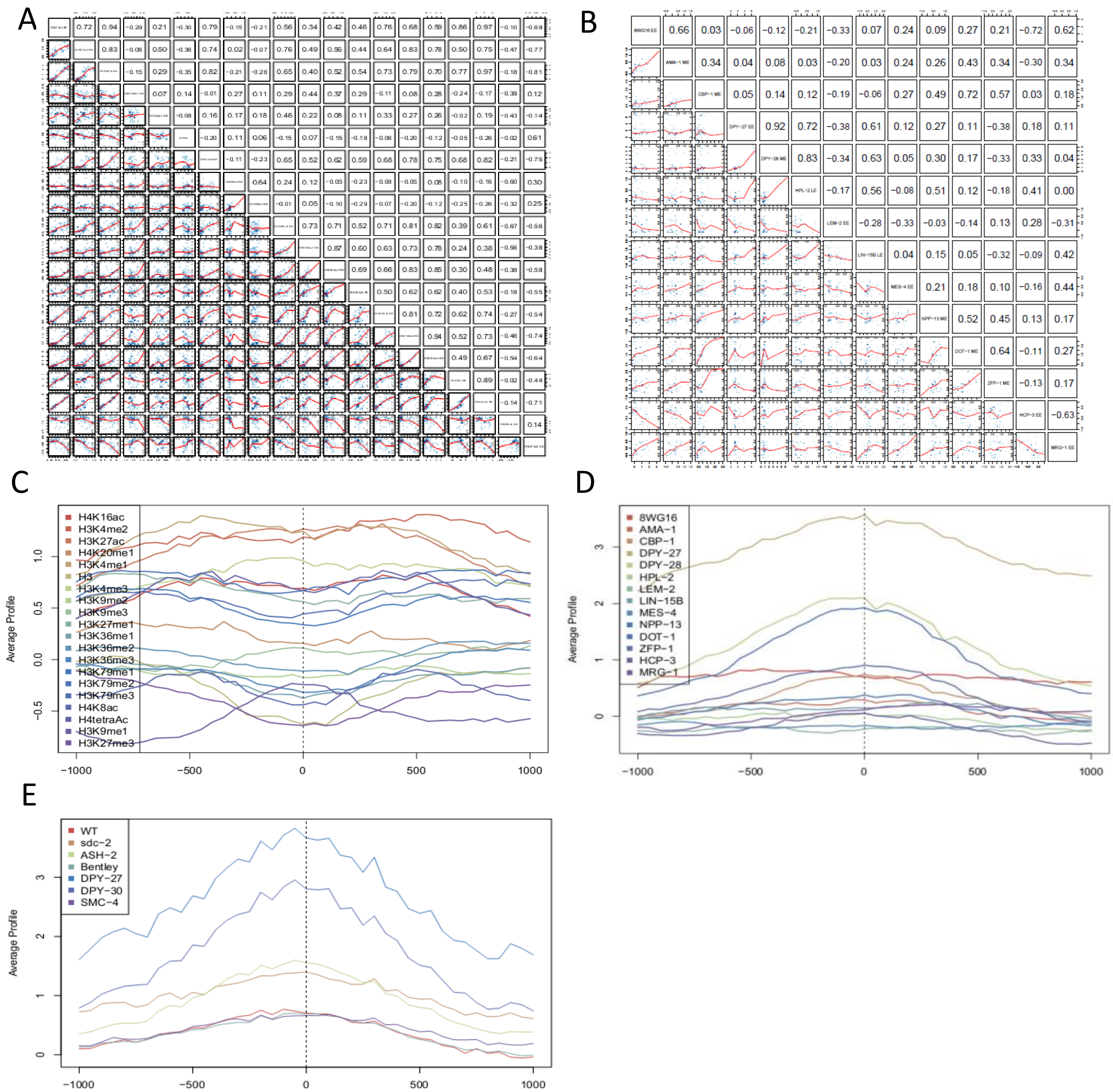

Figure 3.15. Histone modification and protein occupancy at all poised enhancer-like DCC binding elements. Shown are histone modification (A) and protein (B) cross-correlation tables or histone modification (C), protein (D), or COMPASS/DCC complex (E) SitePro analysis. Results show H3K27me3 depletion, many flat histone modification profiles, as well as DCC and NPP-13 enrichment.

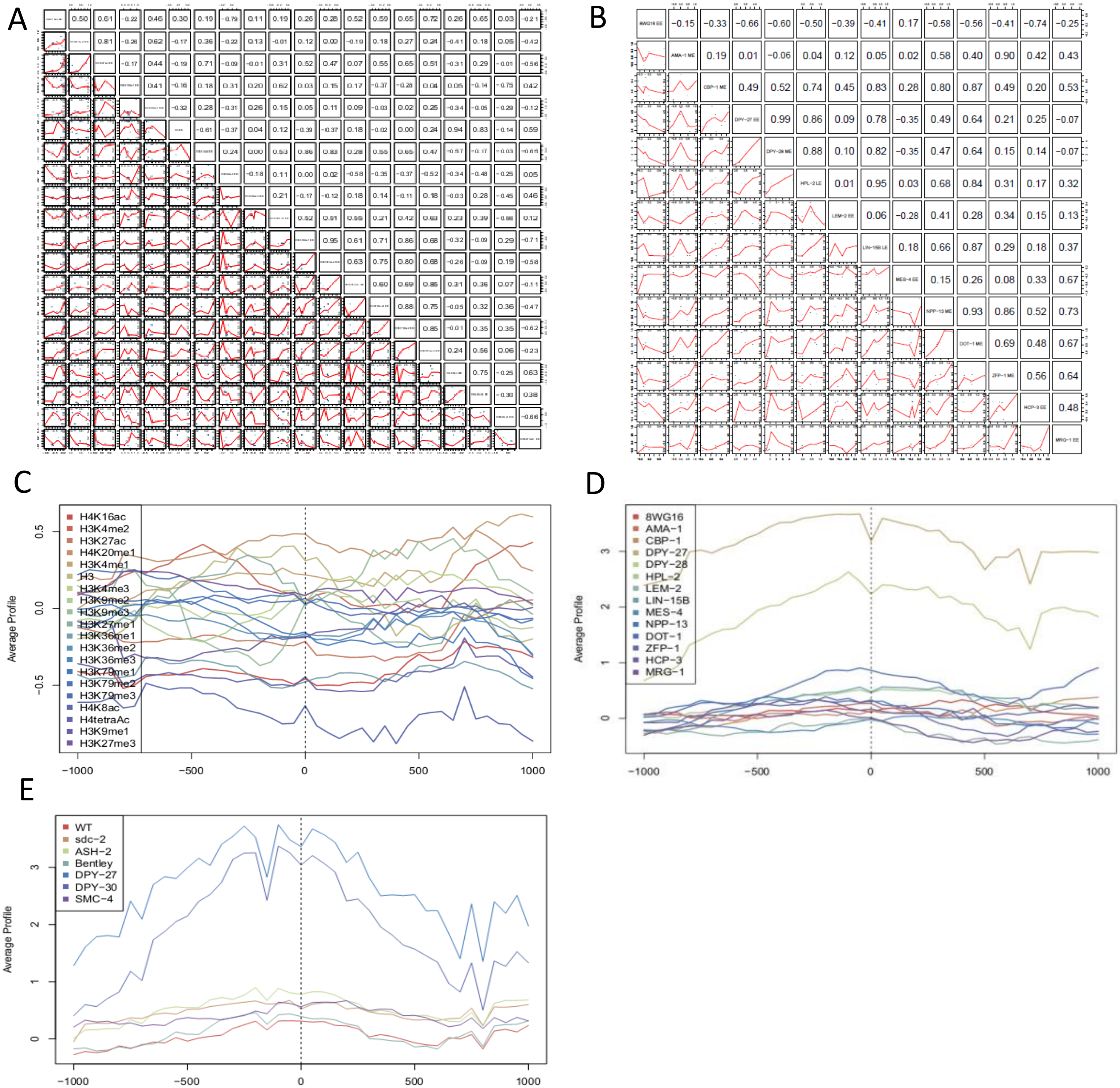

Figure 3.16. Histone modification and protein occupancy at all off enhancer-like DCC binding elements. Shown are histone modification (A) and protein (B) cross-correlation tables or histone modification (C), protein (D), or COMPASS/DCC complex (E) SitePro analysis. Results show DCC enrichment only, consistent with the off state of the enhancer-like regions.

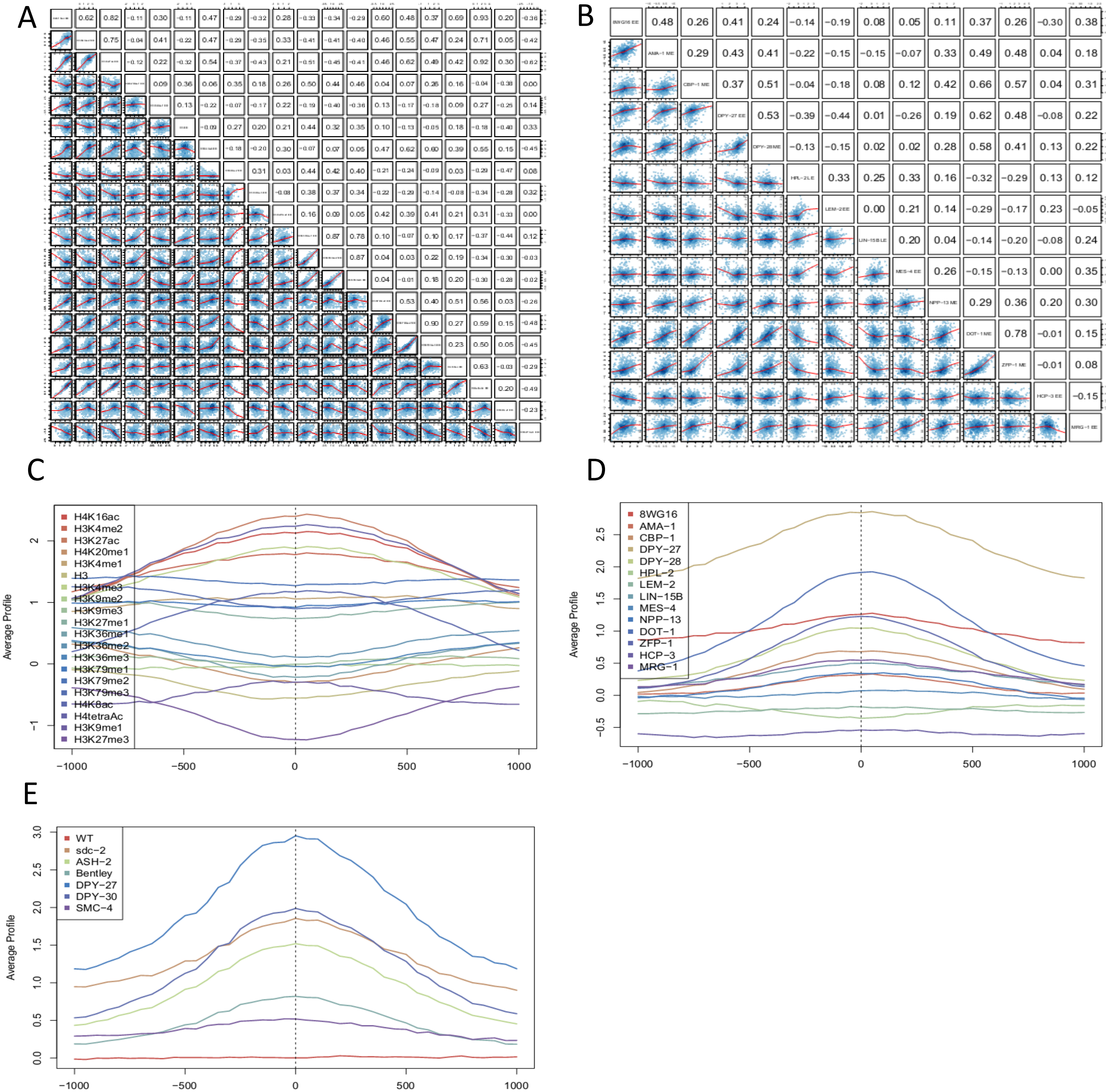

Figure 3.17. Histone modification and protein occupancy at all HTZ-1 peaks on X. Shown are histone modification (A) and protein (B) cross-correlation tables or histone modification (C), protein (D), or COMPASS/DCC complex (E) SitePro analysis. Results show broad co-associated histone modification peaks (C) and enrichments of several proteins, including: DPY-27, NPP-13, and DOT-1 (D & E).

Table 3.5. Summary of trends in metagene analysis.

Figure	Feature	Stage	DC genes	non-DC genes	Active Xs	Active As	Follows RNA-seq?
3.18	H4K16ac	EE	Lower	Higher	Lower	Higher	Yes
3.19	H3K4me2	EE	Lower	Higher	Similar	Similar	Yes
3.20	WT 8WG16	ME	Similar	Similar	Lower	Higher	Yes
3.21	*sdc-2* 8WG16	ME	Similar	Similar	Higher	Lower	Yes
3.22	H3K27ac	EE	Lower	Higher	Lower	Higher	Yes
3.23	H4K20me1	EE	Lower	Higher	Higher	Lower	Yes
3.24	H3K27me3	EE	Similar	Similar	Higher	Lower	Yes
3.25	H3K4me1	EE	Lower	Higher	Higher	Lower	Yes
3.26	ASH-2	ME	Similar	Similar	Higher	Lower	Yes
3.27	Bentley RNA Pol II	ME	Lower	Higher	Lower	Higher	Yes
3.28	DPY-27	ME	Similar	Similar	Higher	Lower	Yes
3.29	DPY-30	ME	Similar	Similar	Higher	Lower	Yes
3.30	SMC-4	ME	Lower	Higher	Higher	Lower	Yes
3.31	DPY-27	EE	Similar	Similar	Higher	Lower	Yes
3.32	H3	EE	Similar	Similar	Higher	Lower	No
3.33	H3K4me3	EE	Lower	Higher	Lower	Higher	Yes
3.34	H3K9me1	EE	Higher	Lower	Lower	Higher	Yes
3.35	H3K9me2	EE	Similar	Similar	Lower	Higher	No
3.36	H3K9me3	EE	Lower	Higher	Lower	Higher	No
3.37	H3K27me1	EE	Lower	Higher	Higher	Lower	Yes
3.38	H3K36me1	EE	Lower	Higher	Lower	Higher	Yes
3.39	H3K36me2	EE	Lower	Higher	Lower	Higher	Yes
3.40	H3K36me3	EE	Lower	Higher	Lower	Higher	Yes
3.41	H3K79me1	EE	Lower	Higher	Lower	Higher	Yes
3.42	H3K79me2	EE	Lower	Higher	Lower	Higher	Yes
3.43	H3K79me3	EE	Lower	Higher	Lower	Higher	Yes
3.44	H4K8ac	EE	Lower	Higher	Lower	Higher	Yes
3.45	H4tetraAc	EE	Lower	Higher	Lower	Higher	Yes
3.46	HCP-3	EE	Higher	Lower	Higher	Lower	Yes
3.47	HPL-2	LE	Similar	Similar	Lower	Higher	No
3.48	LEM-2	EE	Higher	Lower	Lower	Higher	Yes
3.49	LIN-15B	LE	Similar	Similar	Lower	Higher	No
3.50	MES-4	EE	Lower	Higher	Lower	Higher	Yes
3.51	MRG-1	EE	Lower	Higher	Lower	Higher	Yes
3.52	NPP-13	ME	Lower	Higher	Lower	Higher	Yes
3.53	Y39G10AR.18 (Dot1p)	ME	Similar	Similar	Higher	Lower	Yes
3.54	ZFP-1	ME	Similar	Similar	Higher	Lower	Yes
3.55	AMA-1	ME	Similar	Similar	Similar	Similar	Yes
3.56	CBP-1	ME	Similar	Similar	Lower	Higher	Yes
3.57	DPY-26	ME	Similar	Similar	Higher	Lower	Yes
3.58	DPY-28	ME	Similar	Similar	Higher	Lower	Yes
3.59	MIX-1	ME	Similar	Similar	Higher	Lower	Yes
3.60	SDC-2 ME	ME	Similar	Similar	Higher	Lower	Yes
3.61	SDC-3 ME	ME	Similar	Similar	Higher	Lower	Yes
3.62	8WG16	EE	Lower	Higher	Lower	Higher	Yes

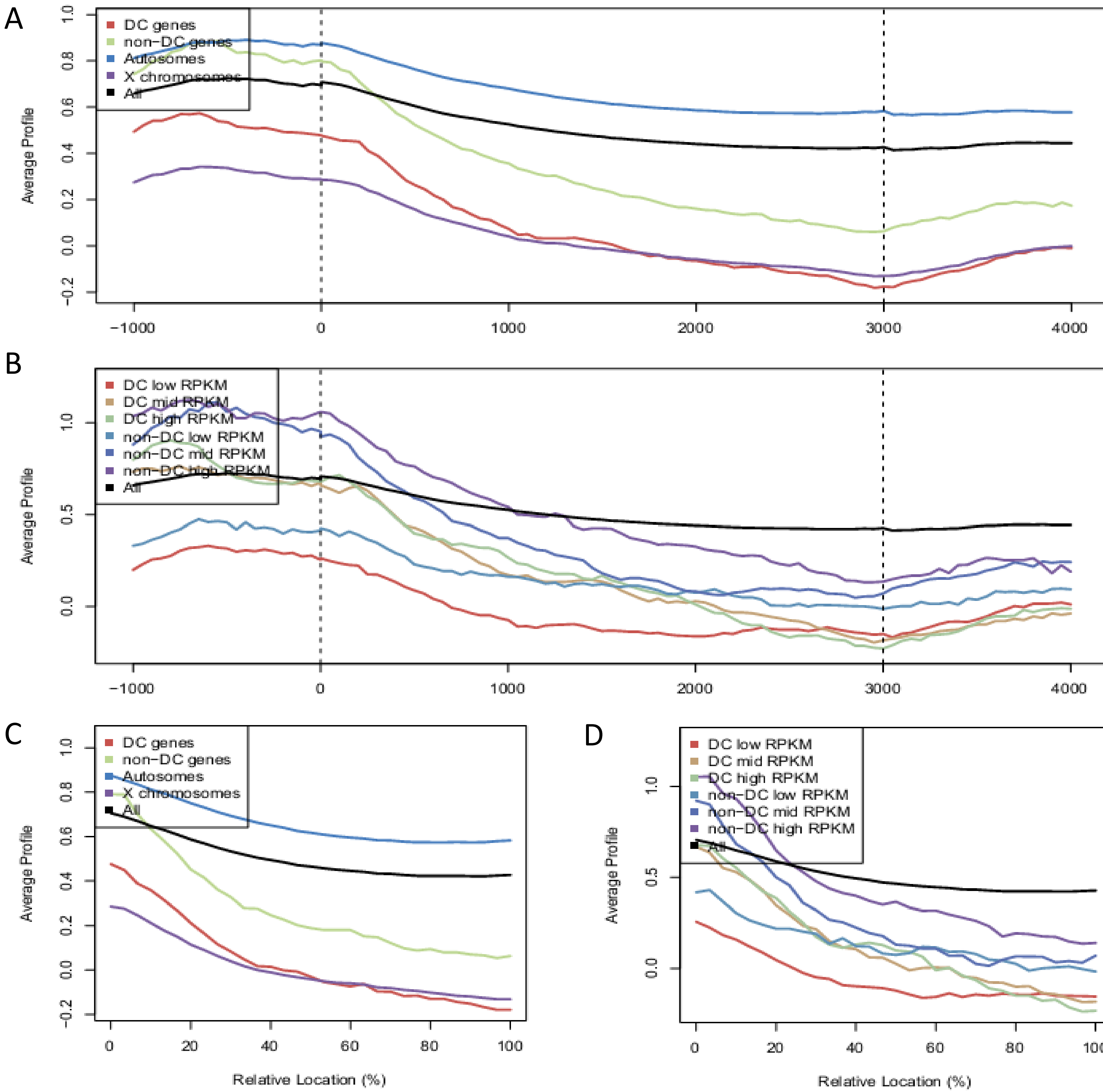

Figure 3.18. H4K16ac EE gene group and transcription level metagene analysis. Shown are metagenes (A & B) or concatenated exon signal profiles (C & D) for dosage compensated, non-dosage compensated, active autosomal, or active X-linked genes (A & C) or low, medium, and high expression dosage compensated and non-dosage compensated gene groups (B & D). Results show low levels on DC and X genes compared to non-DC and autosomal genes that positively correlate with level of transcription.

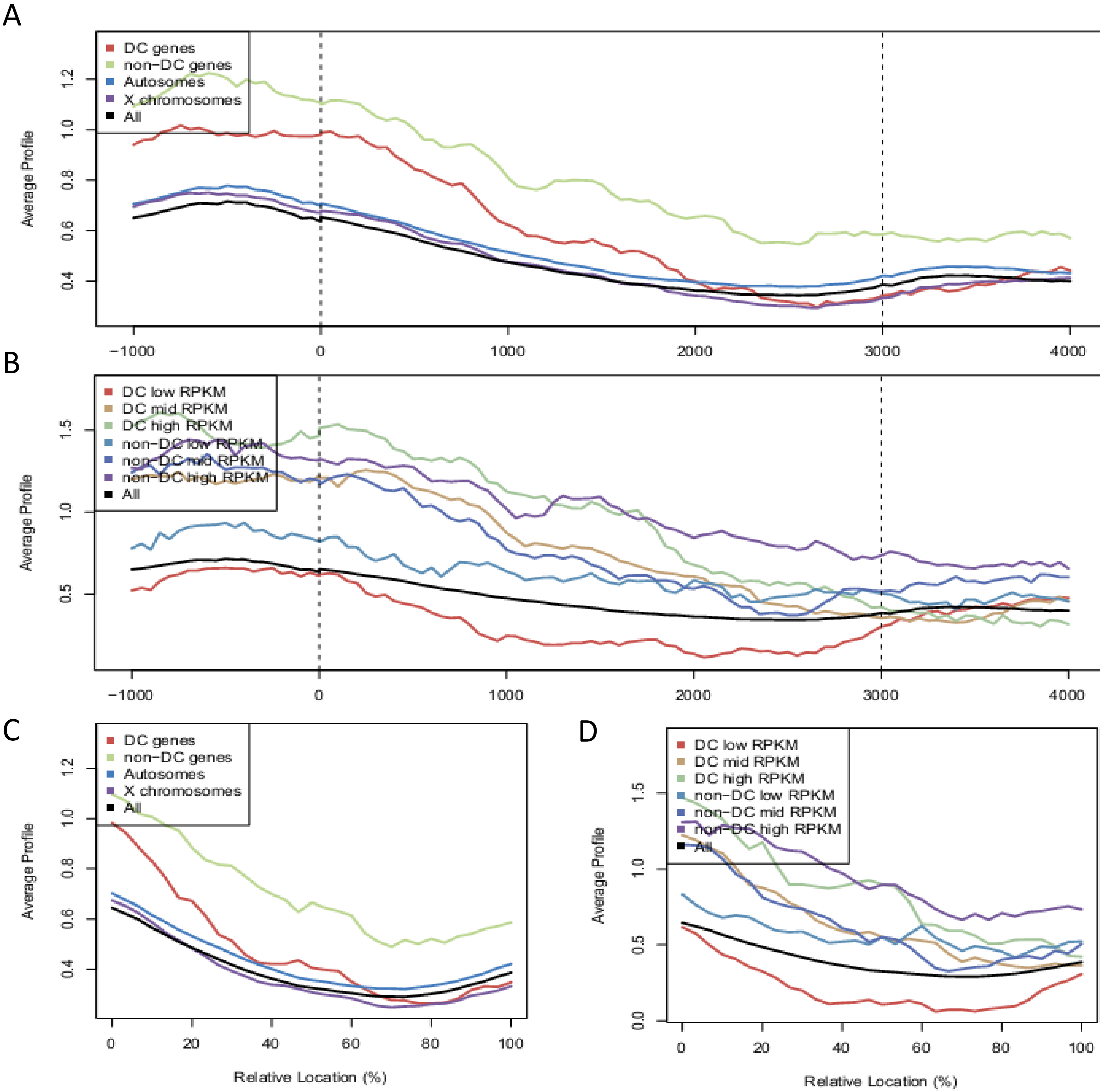

Figure 3.19. H3K4me2 EE gene group and transcription level metagene analysis. Shown are metagenes (A & B) or concatenated exon signal profiles (C & D) for dosage compensated, non-dosage compensated, active autosomal, or active X-linked genes (A & C) or low, medium, and high expression dosage compensated and non-dosage compensated gene groups (B & D). Results show higher levels at non-DC genes over DC genes that loosely correlate with transcription level.

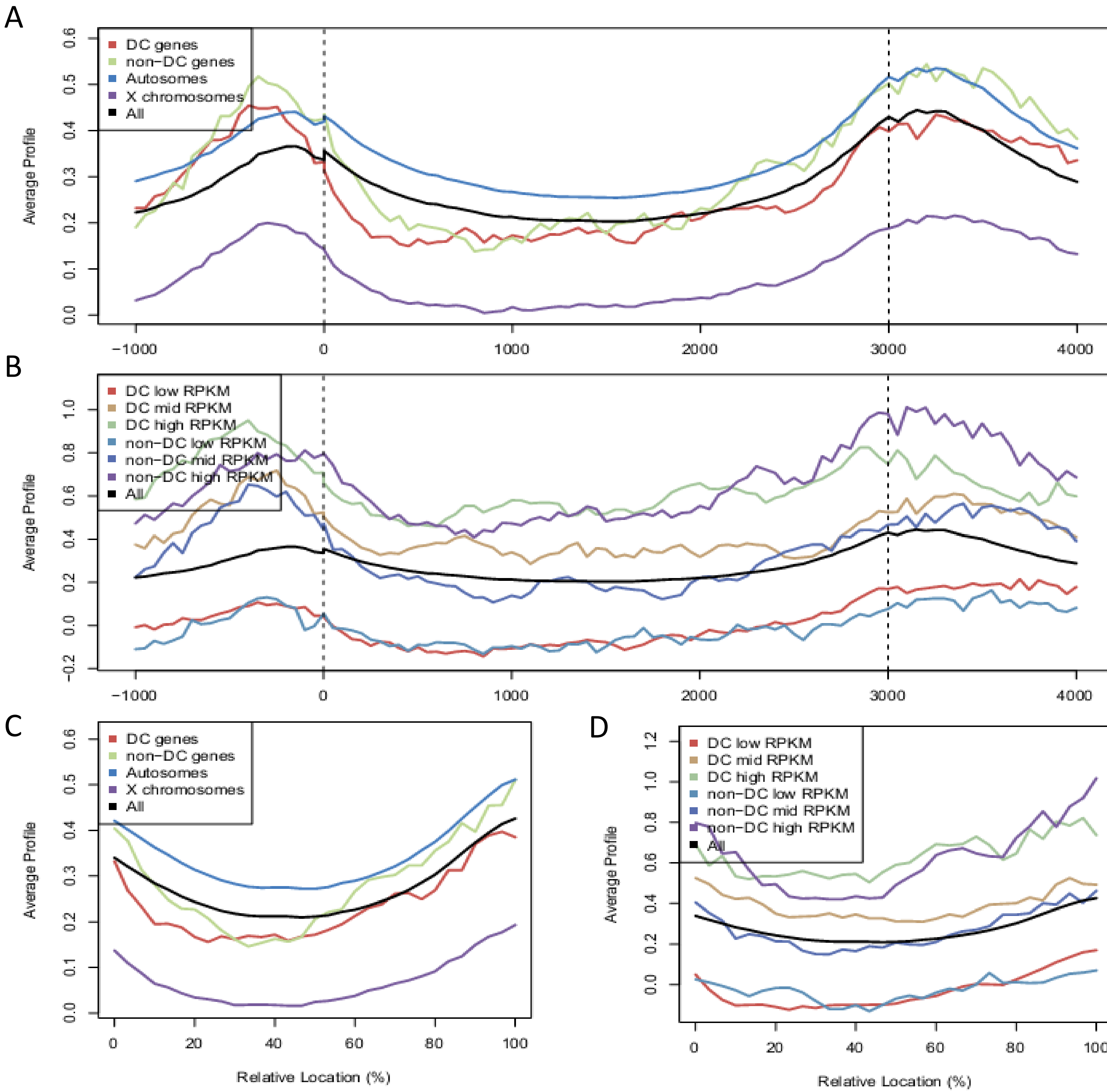

Figure 3.20. WT ME 8WG16 (hypo-phosphorylated RNA Pol II) gene group and transcription level metagene analysis. Shown are metagenes (A & B) or concatenated exon signal profiles (C & D) for dosage compensated, non-dosage compensated, active autosomal, or active X-linked genes (A & C) or low, medium, and high expression dosage compensated and non-dosage compensated gene groups (B & D). Results show lower levels of 8WG16 on X than autosomes that correlates loosely with transcription level.

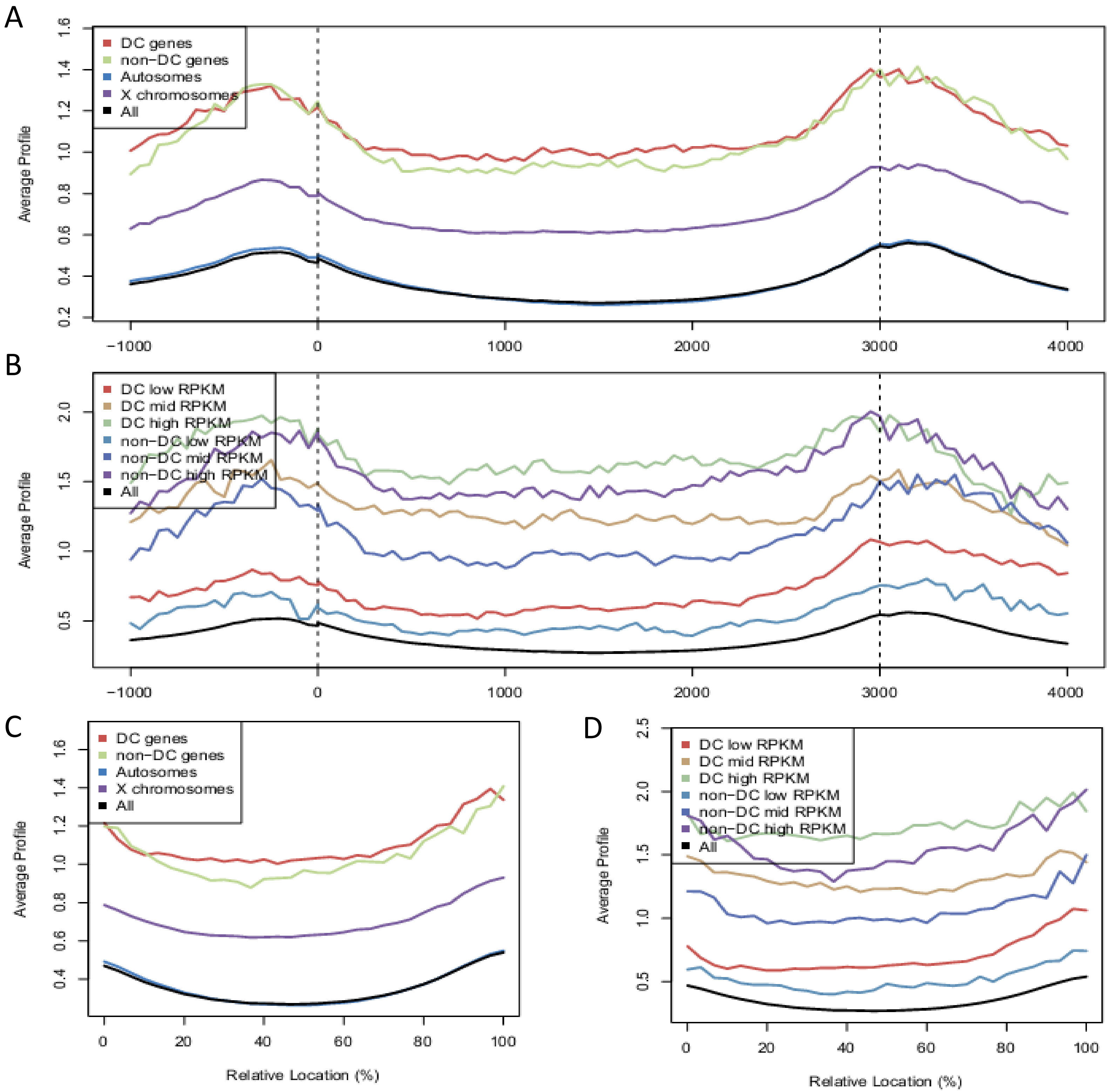

Figure 3.21. *sdc-2* ME 8WG16 (hypo-phosphorylated RNA Pol II) gene group and transcription level metagene analysis. Shown are metagenes (A & B) or concatenated exon signal profiles (C & D) for dosage compensated, non-dosage compensated, active autosomal, or active X-linked genes (A & C) or low, medium, and high expression dosage compensated and non-dosage compensated gene groups (B & D). Results show high levels of 8WG16 on X that correlates well with transcription level.

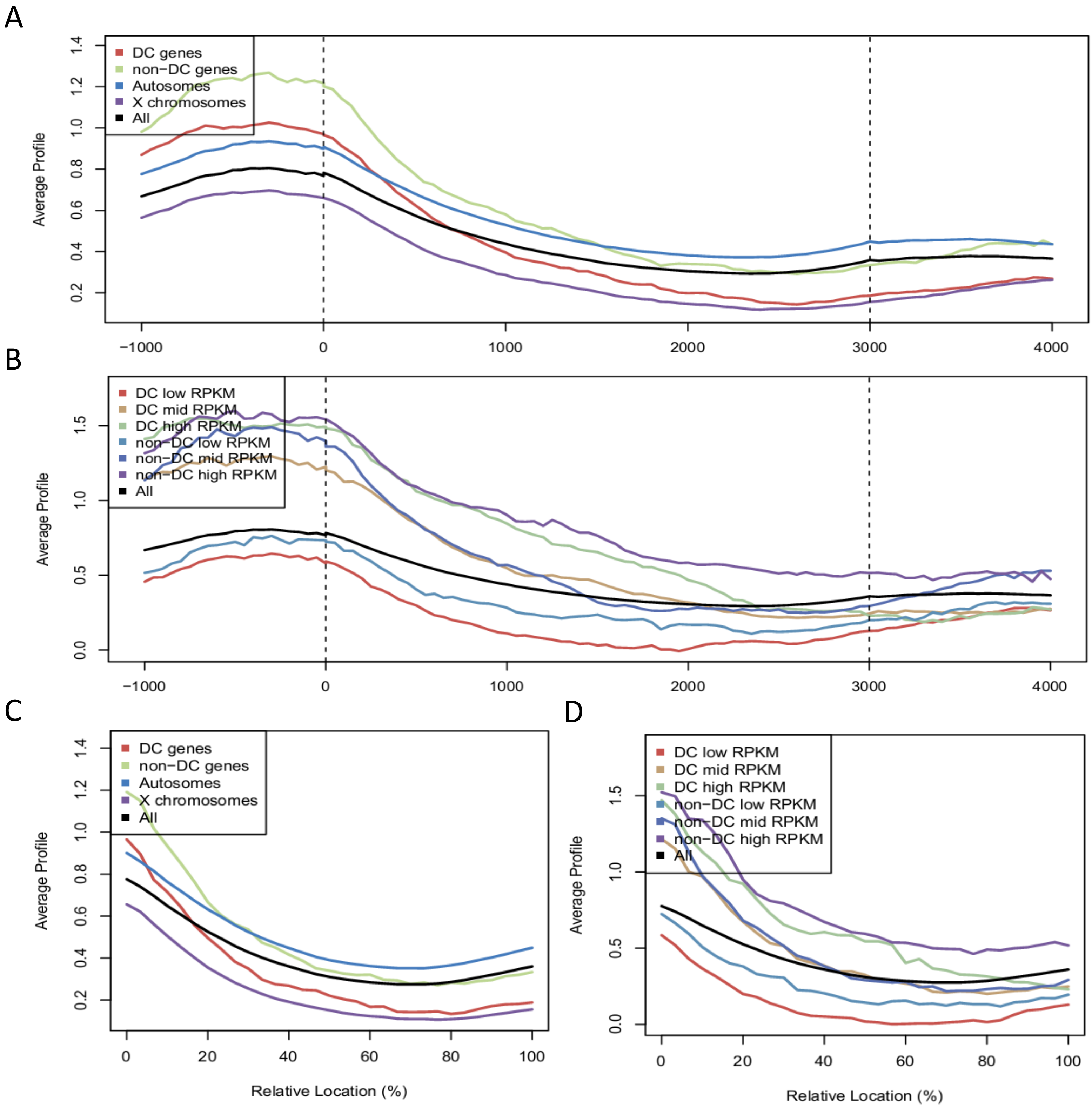

Figure 3.22. H3K27ac EE gene group and transcription level metagene analysis. Shown are metagenes (A & B) or concatenated exon signal profiles (C & D) for dosage compensated, non-dosage compensated, active autosomal, or active X-linked genes (A & C) or low, medium, and high expression dosage compensated and non-dosage compensated gene groups (B & D). Results show small increases in signal at non-DC and autosomal genes over DC and X-linked genes that loosely correlates with transcriptional level.

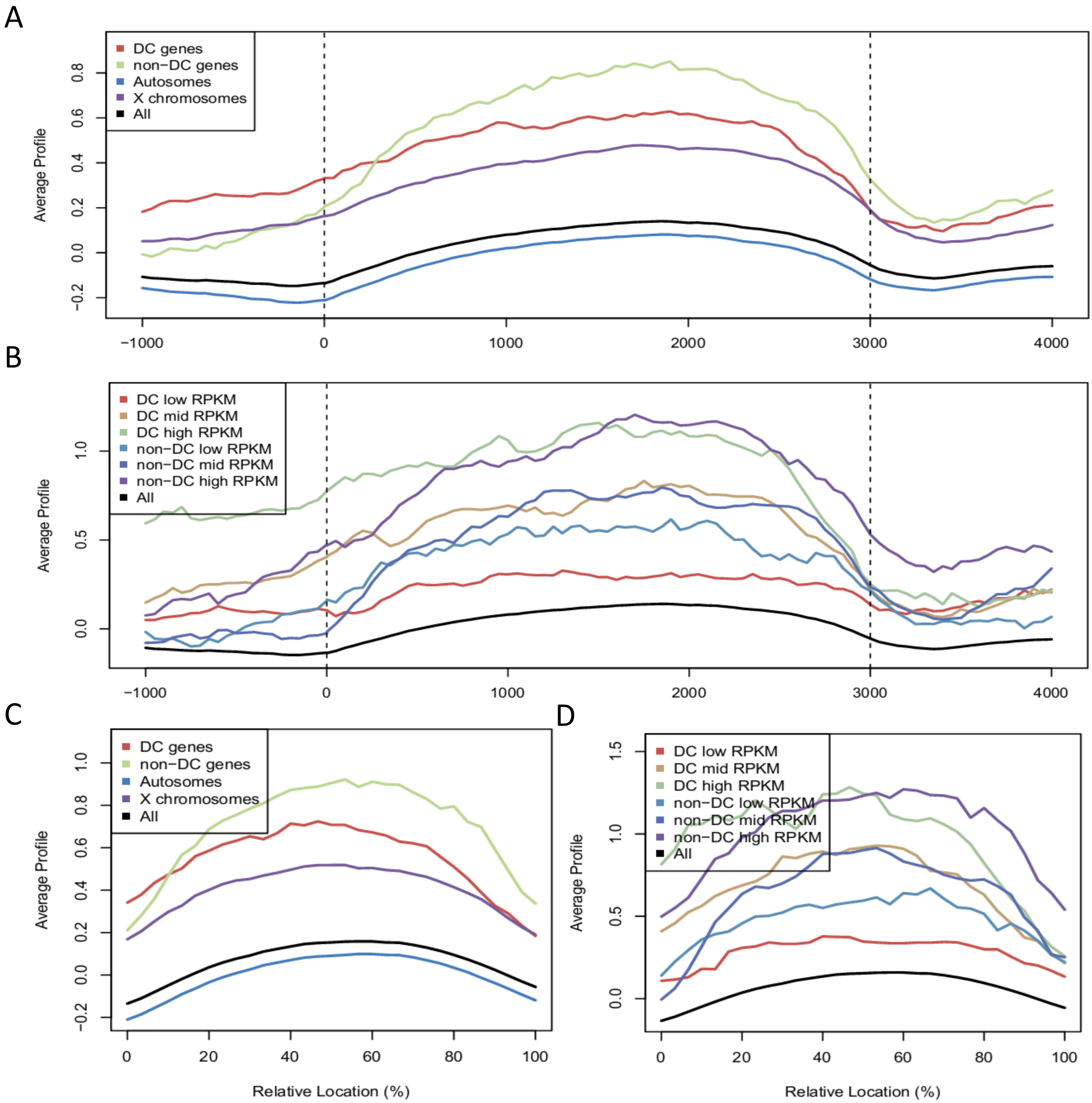

Figure 3.23. H4K20me1 EE gene group and transcription level metagene analysis. Shown are metagenes (A & B) or concatenated exon signal profiles (C & D) for dosage compensated, non-dosage compensated, active autosomal, or active X-linked genes (A & C) or low, medium, and high expression dosage compensated and non-dosage compensated gene groups (B & D). Results show enrichment on X over autosomes that correlates well with transcriptional level.

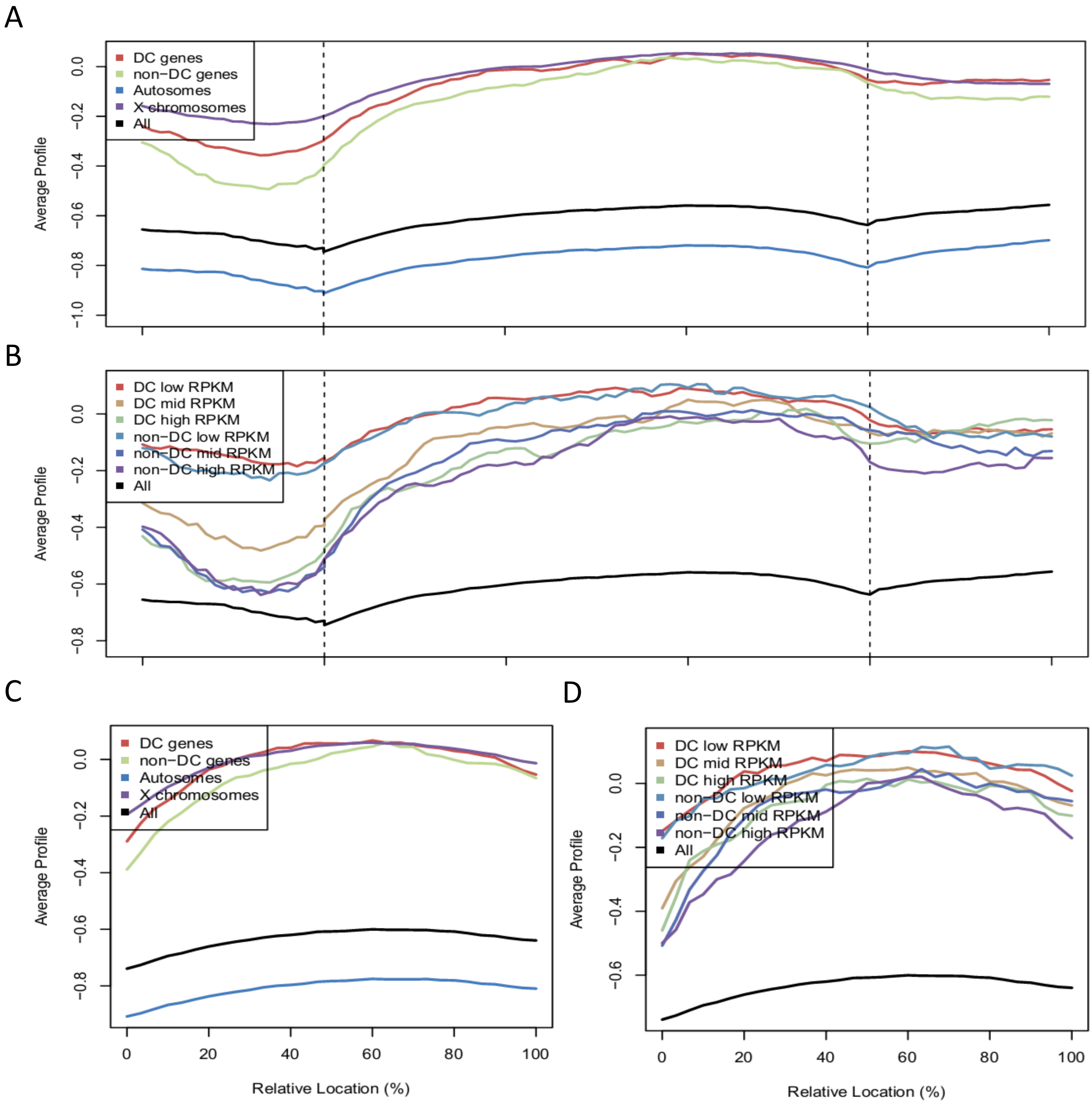

Figure 3.24. H3K27me3 EE gene group and transcription level metagene analysis. Shown are metagenes (A & B) or concatenated exon signal profiles (C & D) for dosage compensated, non-dosage compensated, active autosomal, or active X-linked genes (A & C) or low, medium, and high expression dosage compensated and non-dosage compensated gene groups (B & D). Results show similar levels at DC and non-DC genes and higher levels on active X-linked than active autosomal genes, in a manner that weakly correlates with transcriptional output.

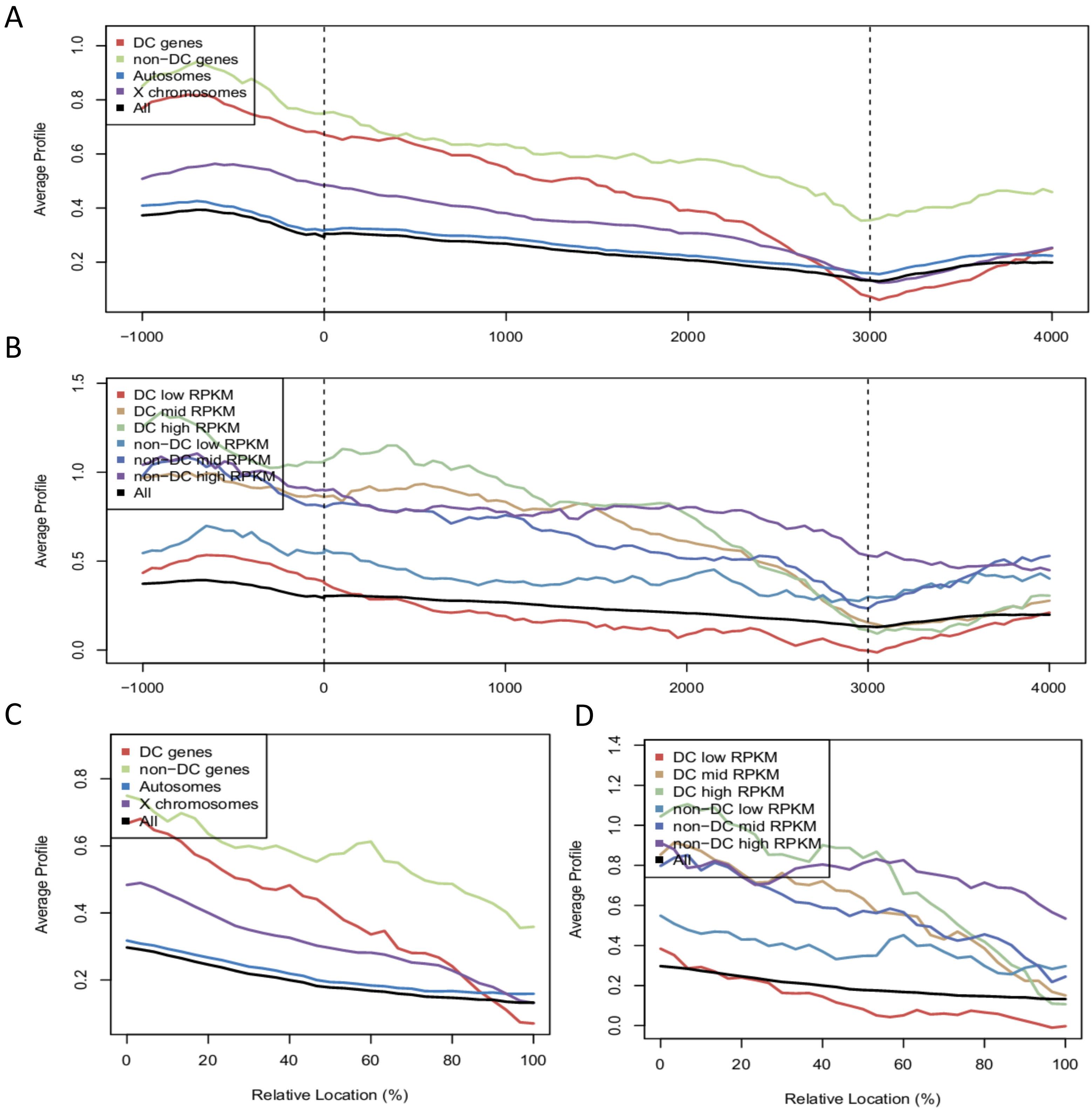

Figure 3.25. H3K4me1 EE gene group and transcription level metagene analysis. Shown are metagenes (A & B) or concatenated exon signal profiles (C & D) for dosage compensated, non-dosage compensated, active autosomal, or active X-linked genes (A & C) or low, medium, and high expression dosage compensated and non-dosage compensated gene groups (B & D). Results show higher levels on X than autosomes and lower levels at DC tss as compared to non-DC tss. Levels correlate well with transcription output.

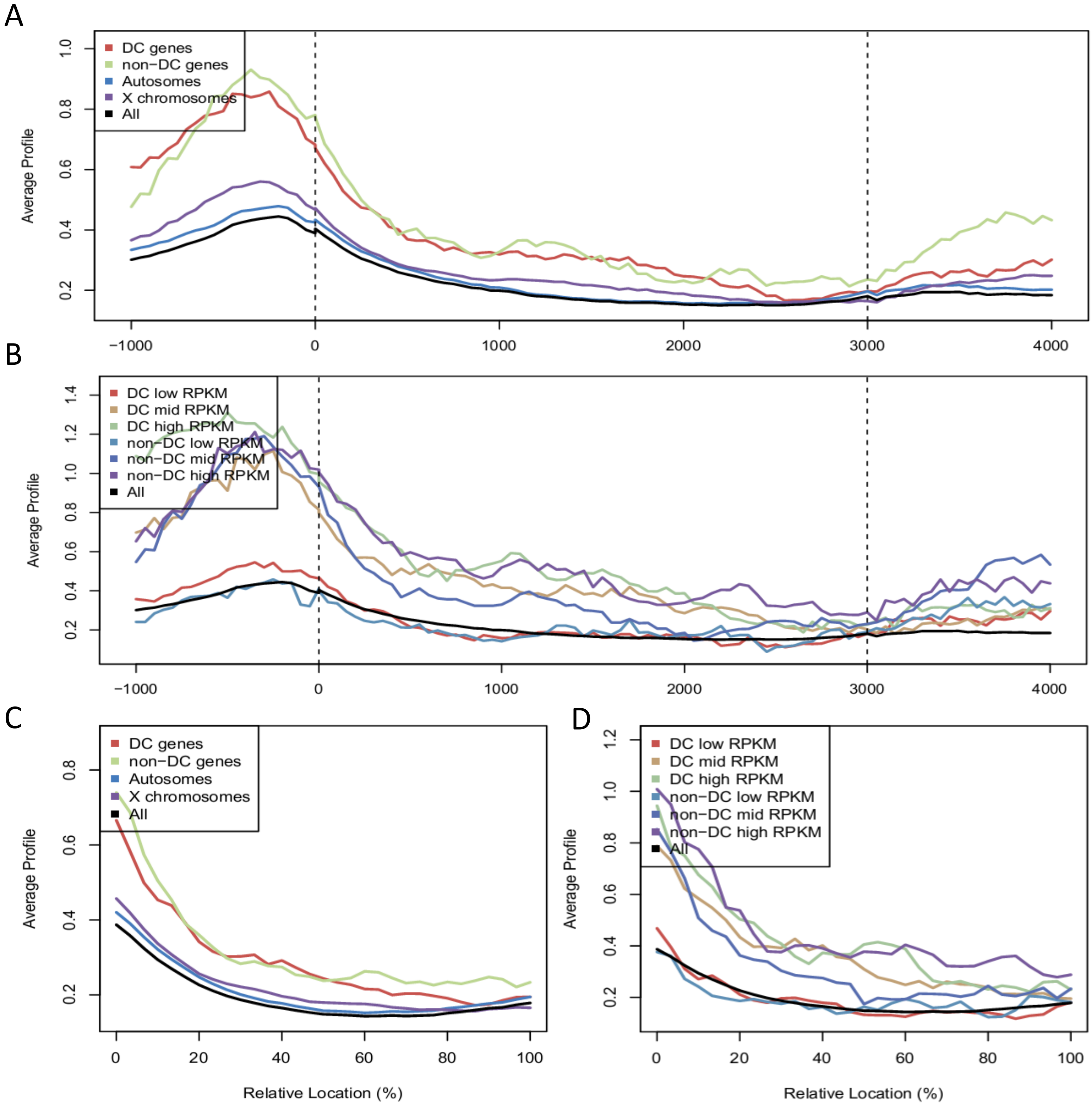

Figure 3.26. ASH-2, a COMPASS complex component, ME gene group and transcription level metagene analysis. Shown are metagenes (A & B) or concatenated exon signal profiles (C & D) for dosage compensated, non-dosage compensated, active autosomal, or active X-linked genes (A & C) or low, medium, and high expression dosage compensated and non-dosage compensated gene groups (B & D). Results show high levels at DC and non-DC upstream regions and a slight enrichment at X-linked as compared to autosomal upstream regions. Levels do not correlate well with transcription.

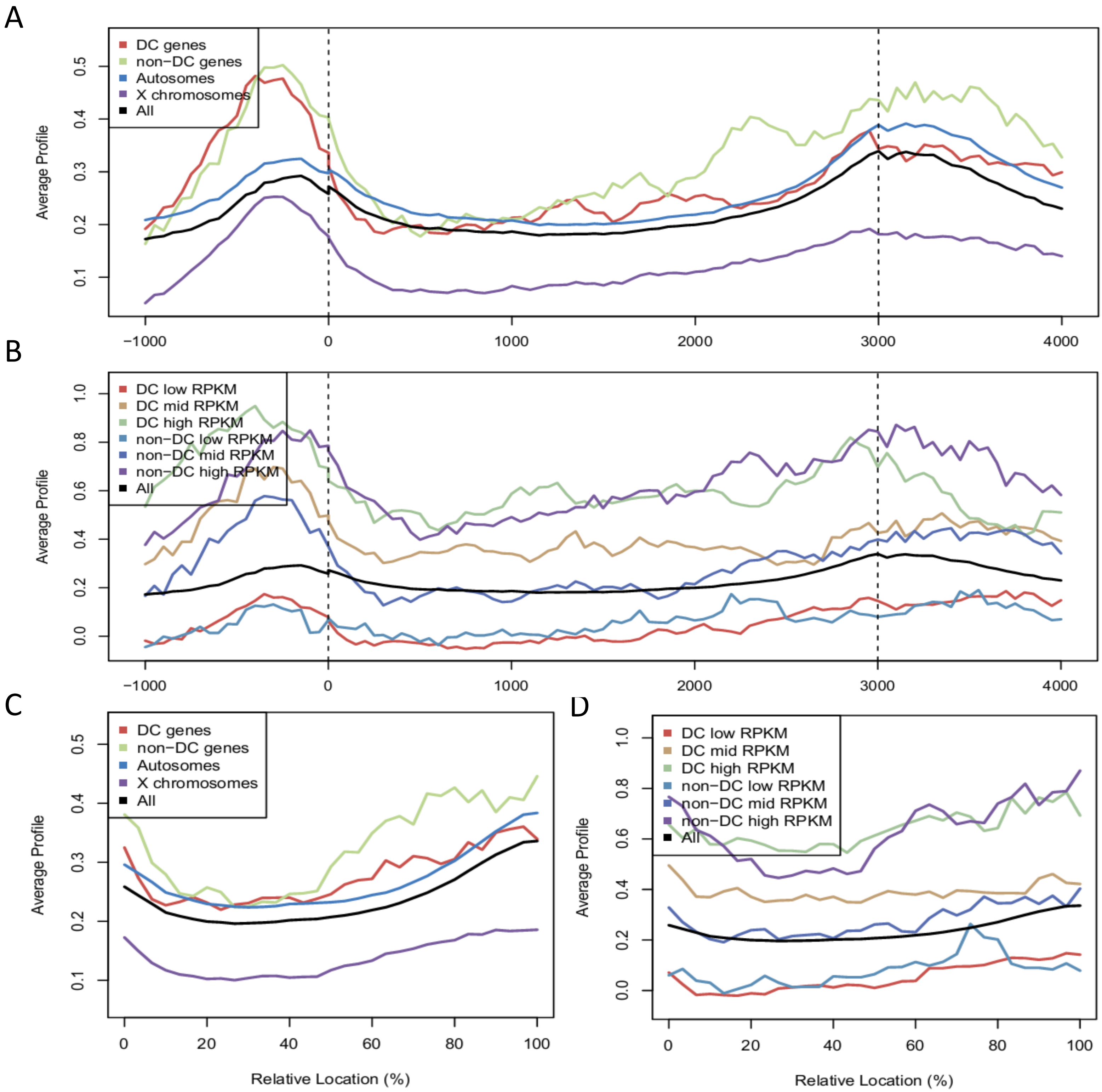

Figure 3.27. Bentley RNA Pol II ME gene group and transcription level metagene analysis. Shown are metagenes (A & B) or concatenated exon signal profiles (C & D) for dosage compensated, non-dosage compensated, active autosomal, or active X-linked genes (A & C) or low, medium, and high expression dosage compensated and non-dosage compensated gene groups (B & D). Results show this antibody (purported by Pferdehirt et al., 2011 to recognize unphosphorylated RNA Pol II) is low on active X genes and slightly enriched on DC and non-DC genic upstream regions. Levels correlate well with transcriptional activity.

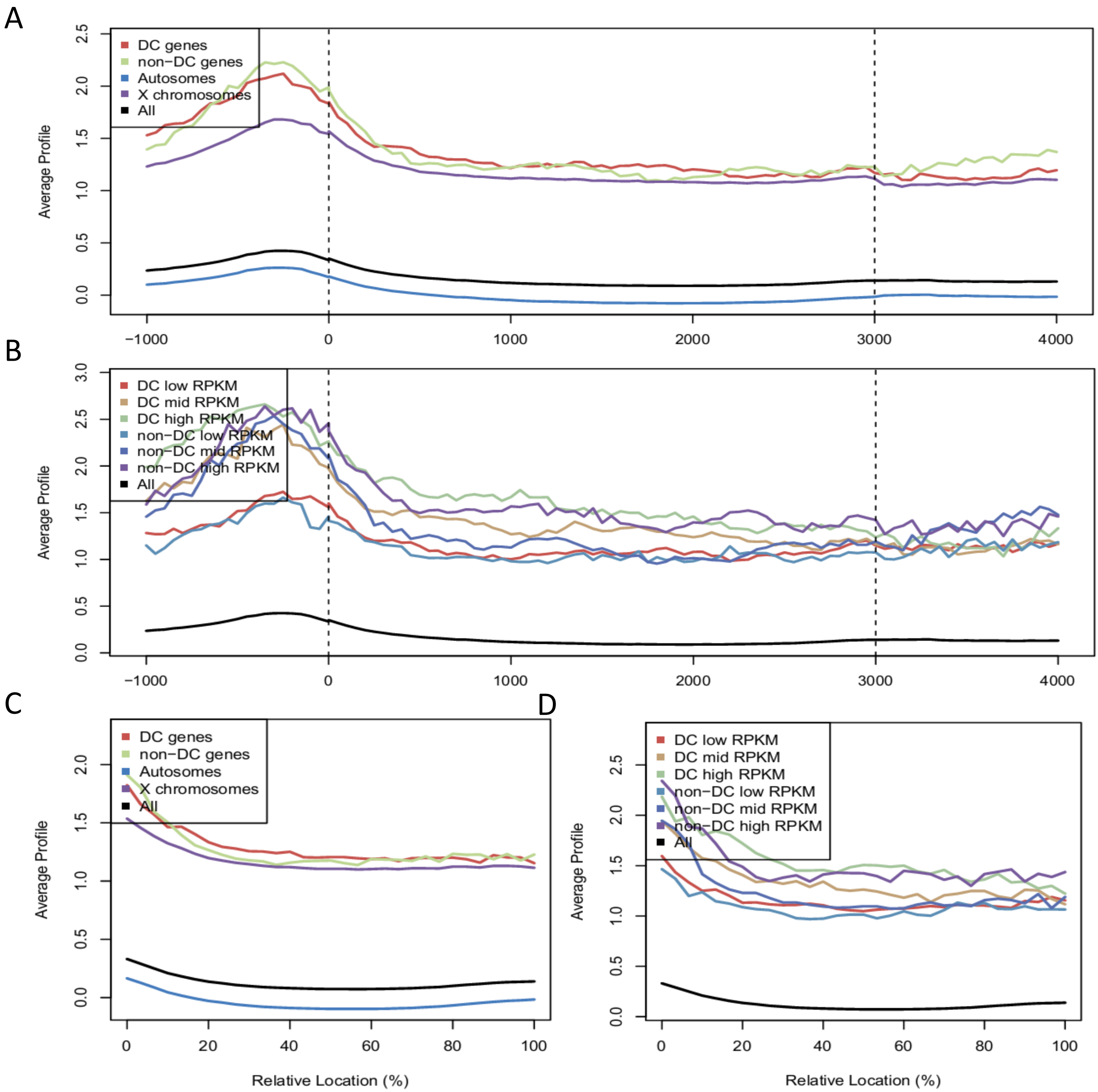

Figure 3.28. DPY-27, a DCC component, ME gene group and transcription level metagene analysis. Shown are metagenes (A & B) or concatenated exon signal profiles (C & D) for dosage compensated, non-dosage compensated, active autosomal, or active X-linked genes (A & C) or low, medium, and high expression dosage compensated and non-dosage compensated gene groups (B & D). Results show high levels on active X-linked, DC, and non-DC genes and levels roughly correlate with transcriptional output.

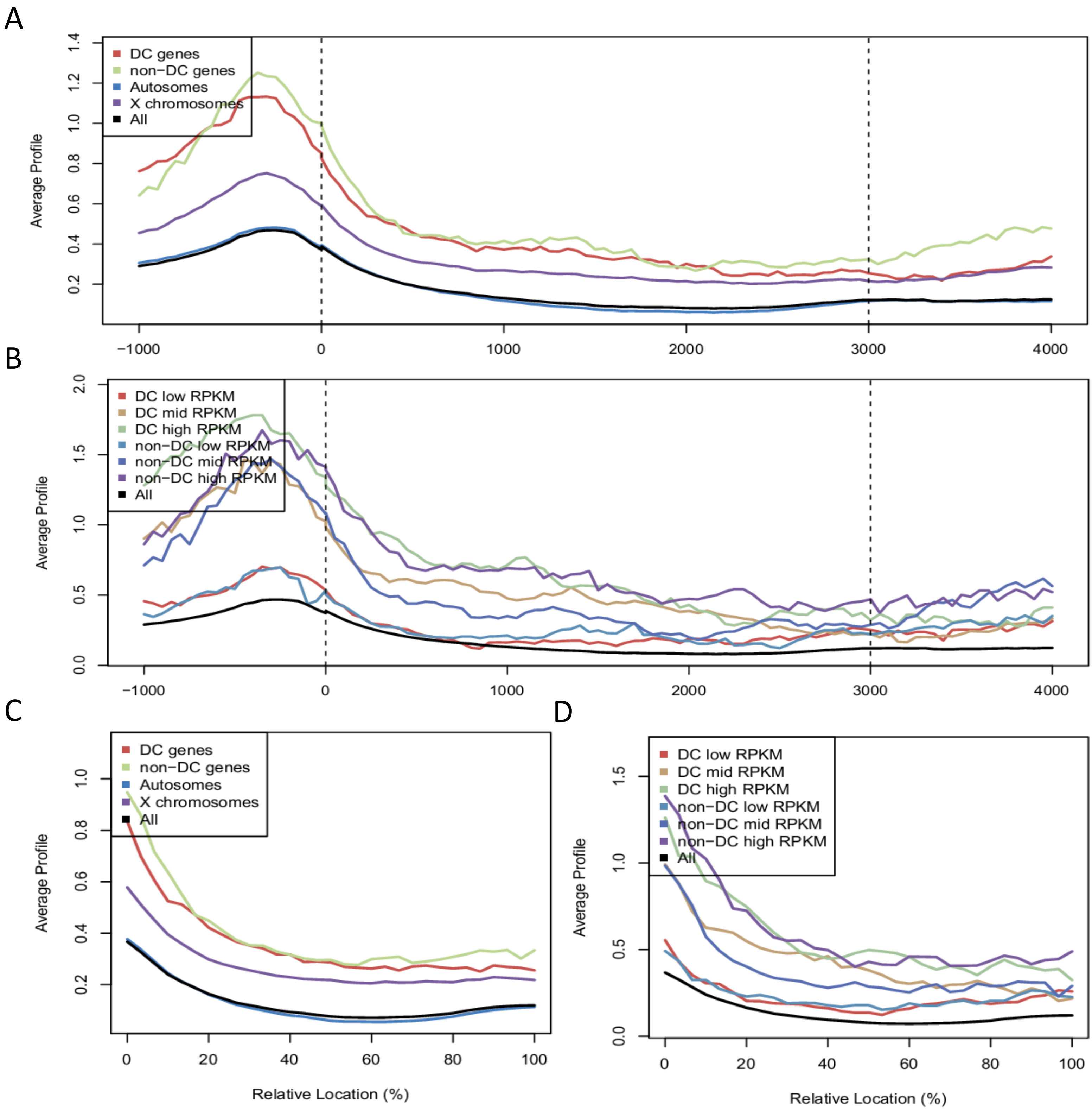

Figure 3.29. DPY-30 ME gene group and transcription level metagene analysis. Shown are metagenes (A & B) or concatenated exon signal profiles (C & D) for dosage compensated, non-dosage compensated, active autosomal, or active X-linked genes (A & C) or low, medium, and high expression dosage compensated and non-dosage compensated gene groups (B & D). Results show enrichment at DC, non-DC, and active X-linked genes that correlates with gene expression.

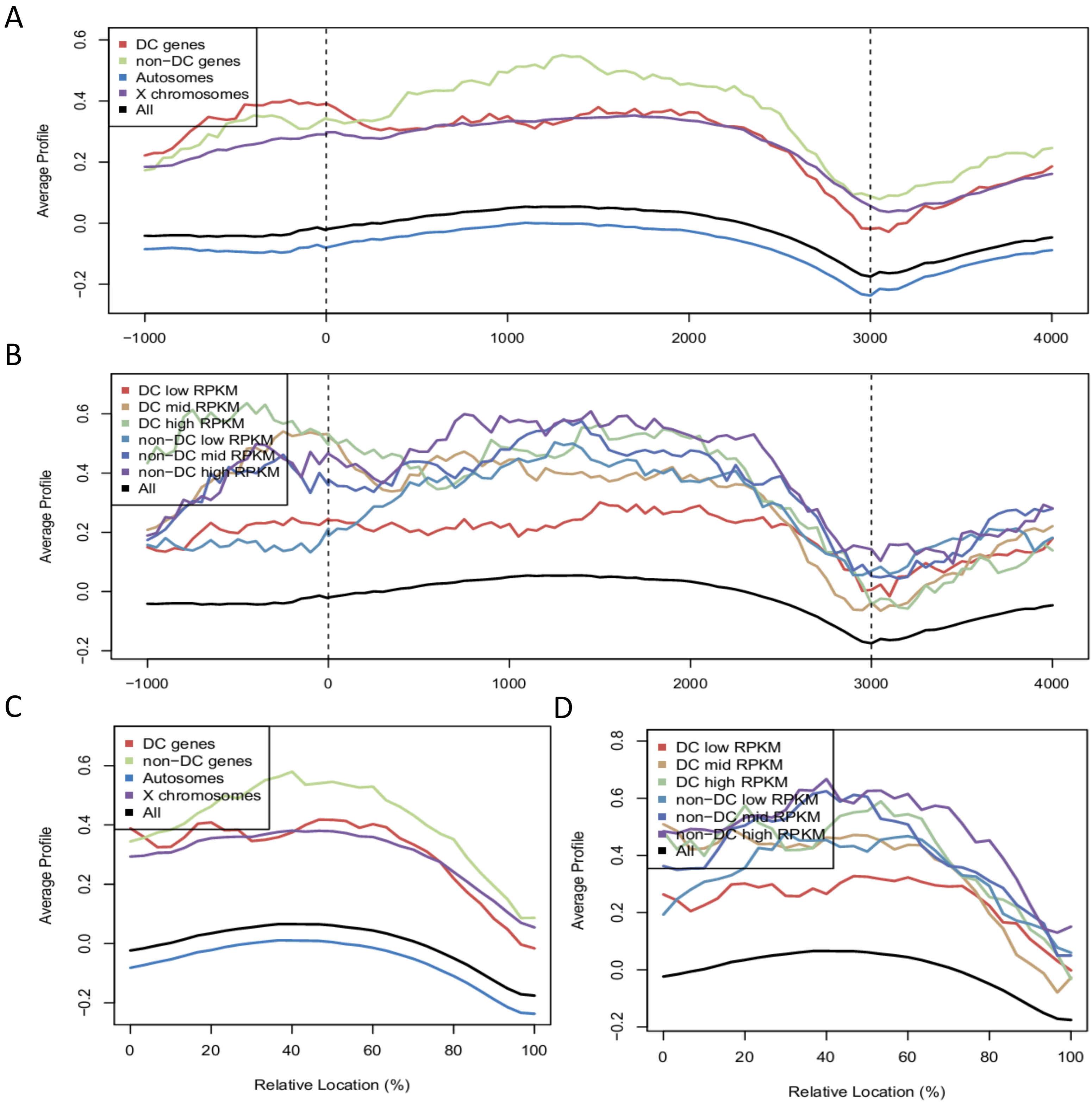

Figure 3.30. SMC-4, a condensin I and II component, ME gene group and transcription level metagene analysis. Shown are metagenes (A & B) or concatenated exon signal profiles (C & D) for dosage compensated, non-dosage compensated, active autosomal, or active X-linked genes (A & C) or low, medium, and high expression dosage compensated and non-dosage compensated gene groups (B & D). Results show high levels on active X and low levels on active autosomal genes that roughly correlate with transcription.

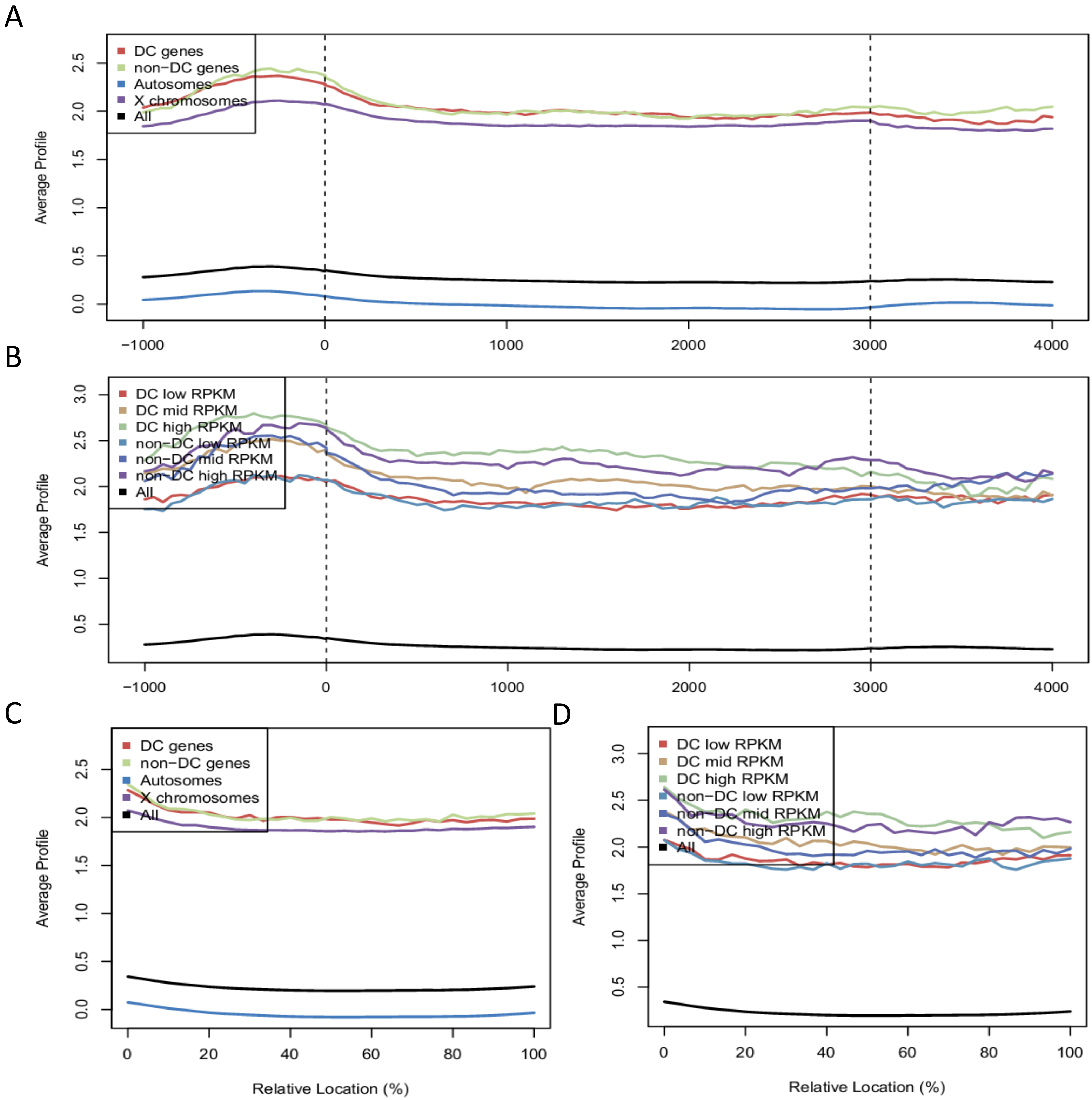

Figure 3.31. DPY-27, a DCC component, EE gene group and transcription level metagene analysis. Shown are metagenes (A & B) or concatenated exon signal profiles (C & D) for dosage compensated, non-dosage compensated, active autosomal, or active X-linked genes (A & C) or low, medium, and high expression dosage compensated and non-dosage compensated gene groups (B & D). Results show high levels on active X-linked, DC, and non-DC genes that roughly correlate with gene expression.

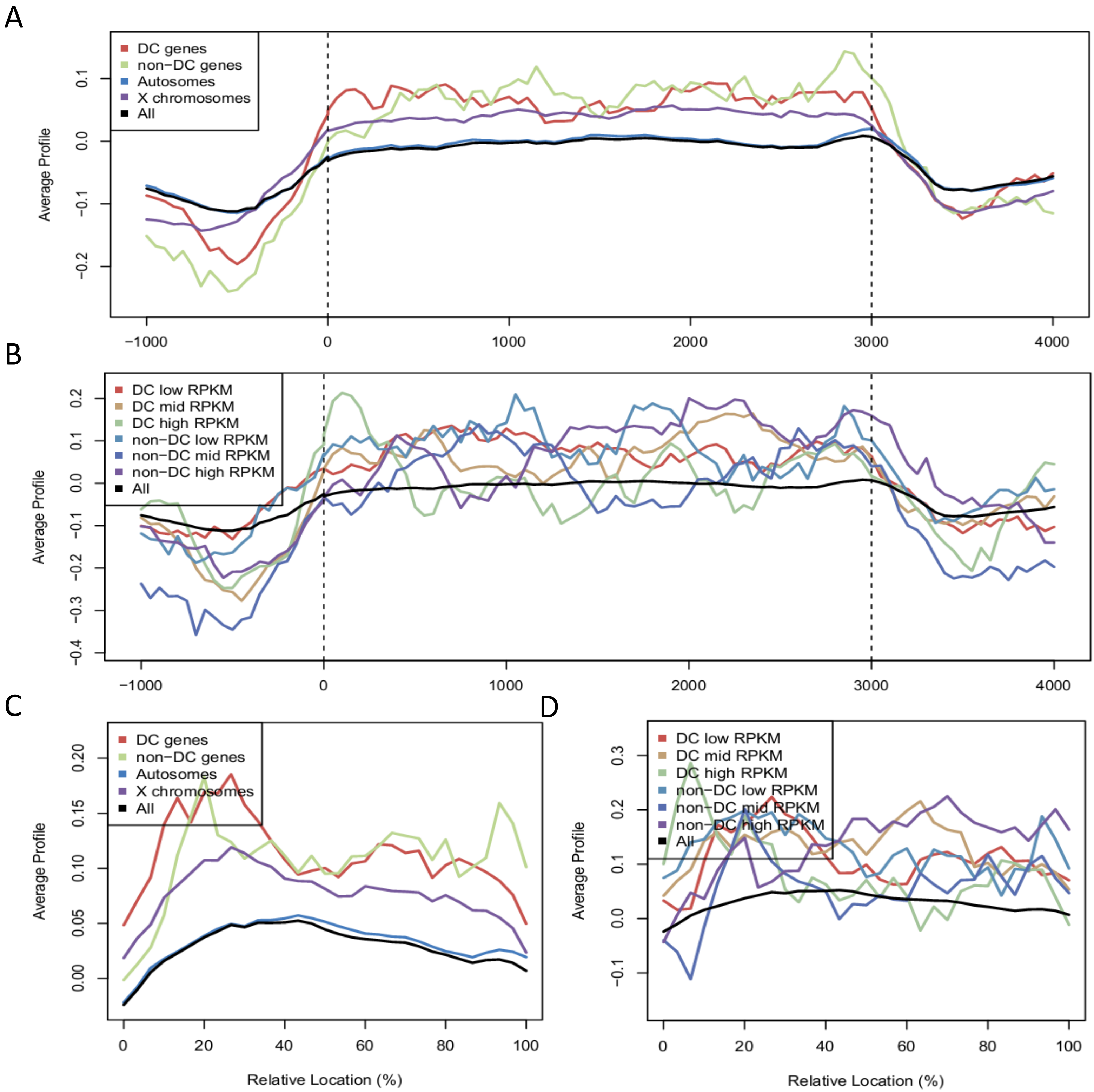

Figure 3.32. Histone H3 EE gene group and transcription level metagene analysis. Shown are metagenes (A & B) or concatenated exon signal profiles (C & D) for dosage compensated, non-dosage compensated, active autosomal, or active X-linked genes (A & C) or low, medium, and high expression dosage compensated and non-dosage compensated gene groups (B & D). Results show low levels at upstream regions and downstream regions, with levels slightly higher on active X, DC, and non-DC gene groups in a way that does not correlate with transcription level.

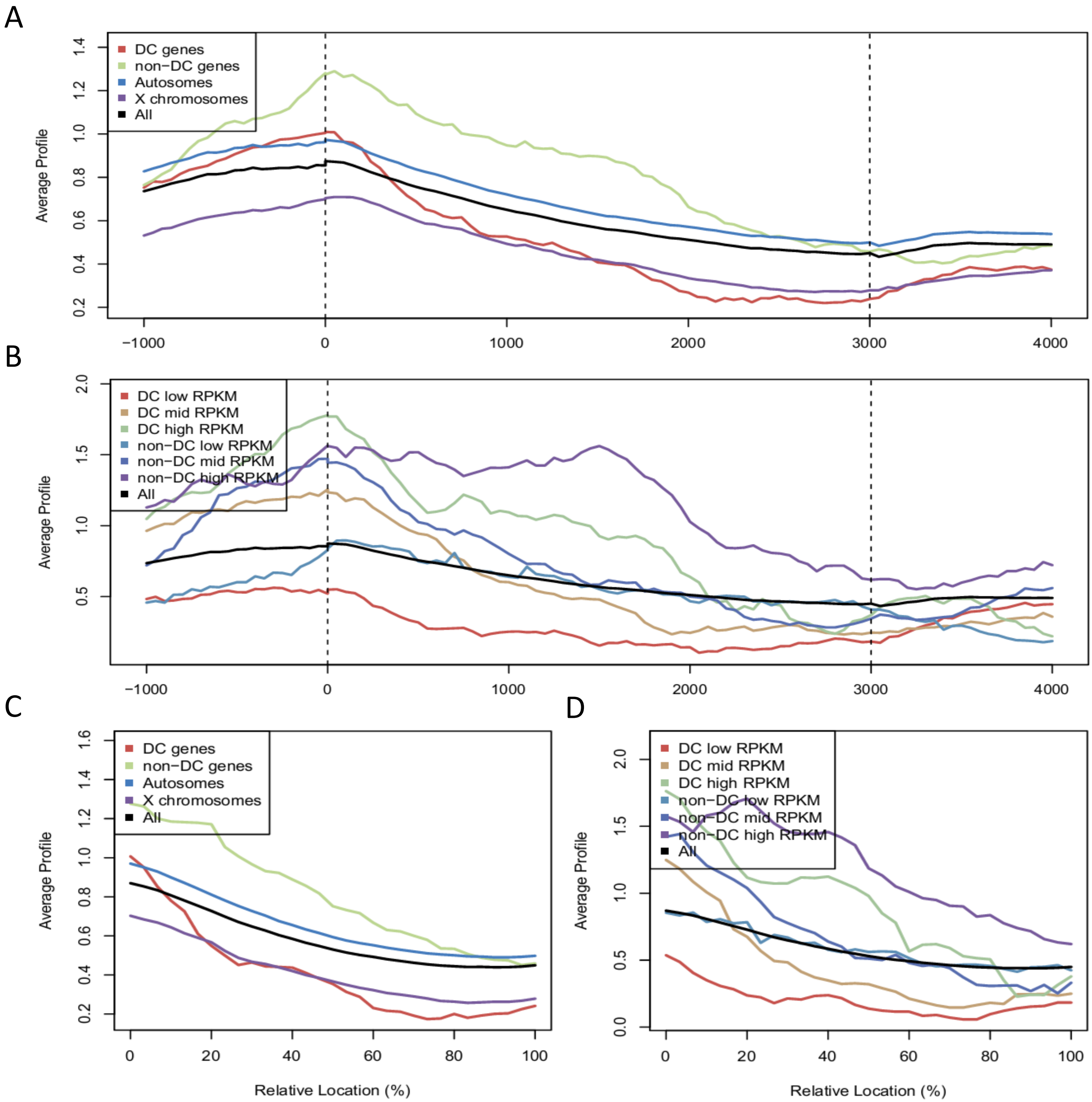

Figure 3.33. H3K4me3 EE gene group and transcription level metagene analysis. Shown are metagenes (A & B) or concatenated exon signal profiles (C & D) for dosage compensated, non-dosage compensated, active autosomal, or active X-linked genes (A & C) or low, medium, and high expression dosage compensated and non-dosage compensated gene groups (B & D). Results show higher levels at active autosomal and non-DC over active X-linked and DC genes in a way that roughly correlates with gene expression.

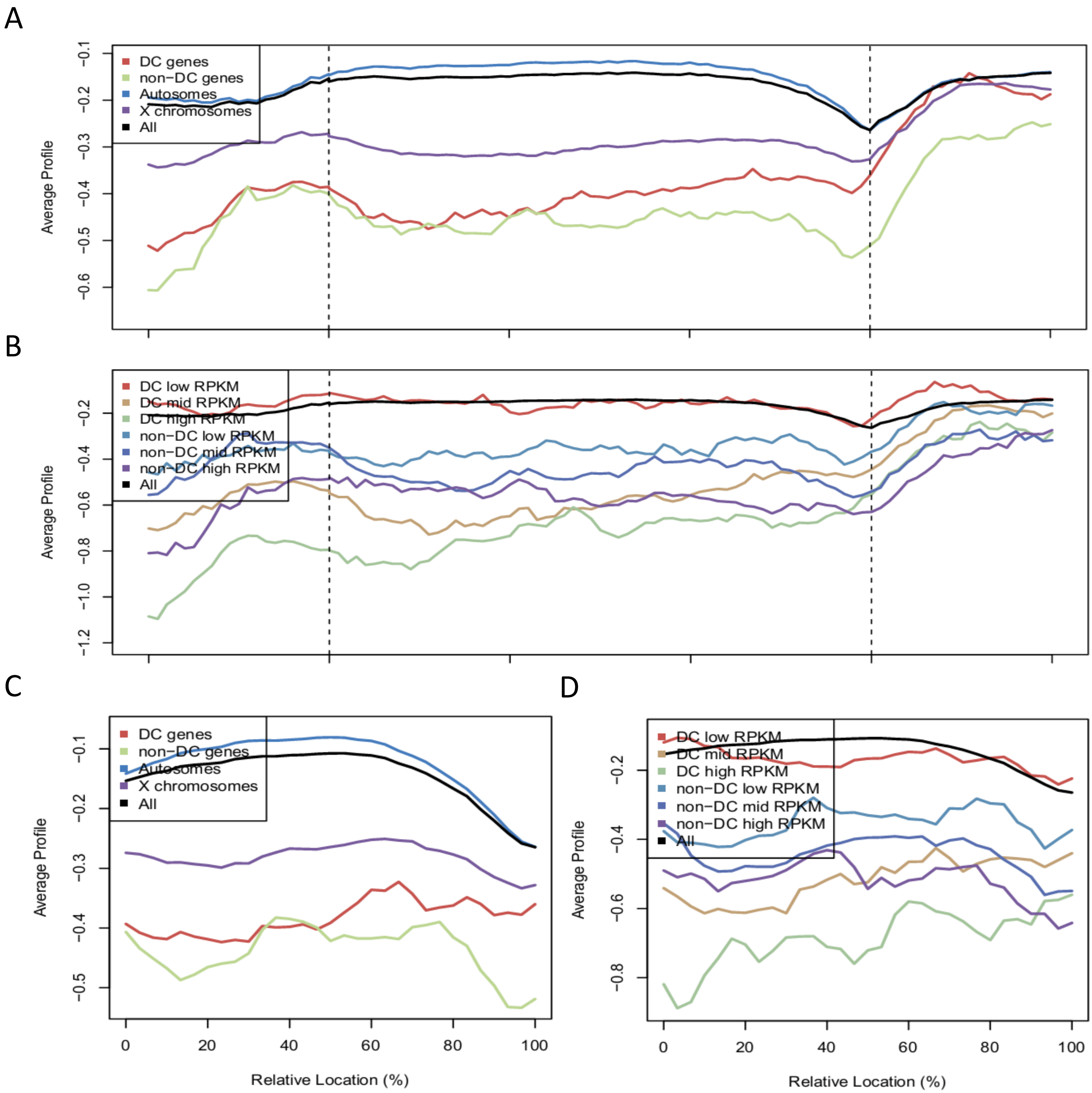

Figure 3.34. H3K9me1 EE gene group and transcription level metagene analysis. Shown are metagenes (A & B) or concatenated exon signal profiles (C & D) for dosage compensated, non-dosage compensated, active autosomal, or active X-linked genes (A & C) or low, medium, and high expression dosage compensated and non-dosage compensated gene groups (B & D). Results show lower levels on active X than active autosomal genes, but similar levels at DC and non-DC genes in a manner that correlates well with gene expression.

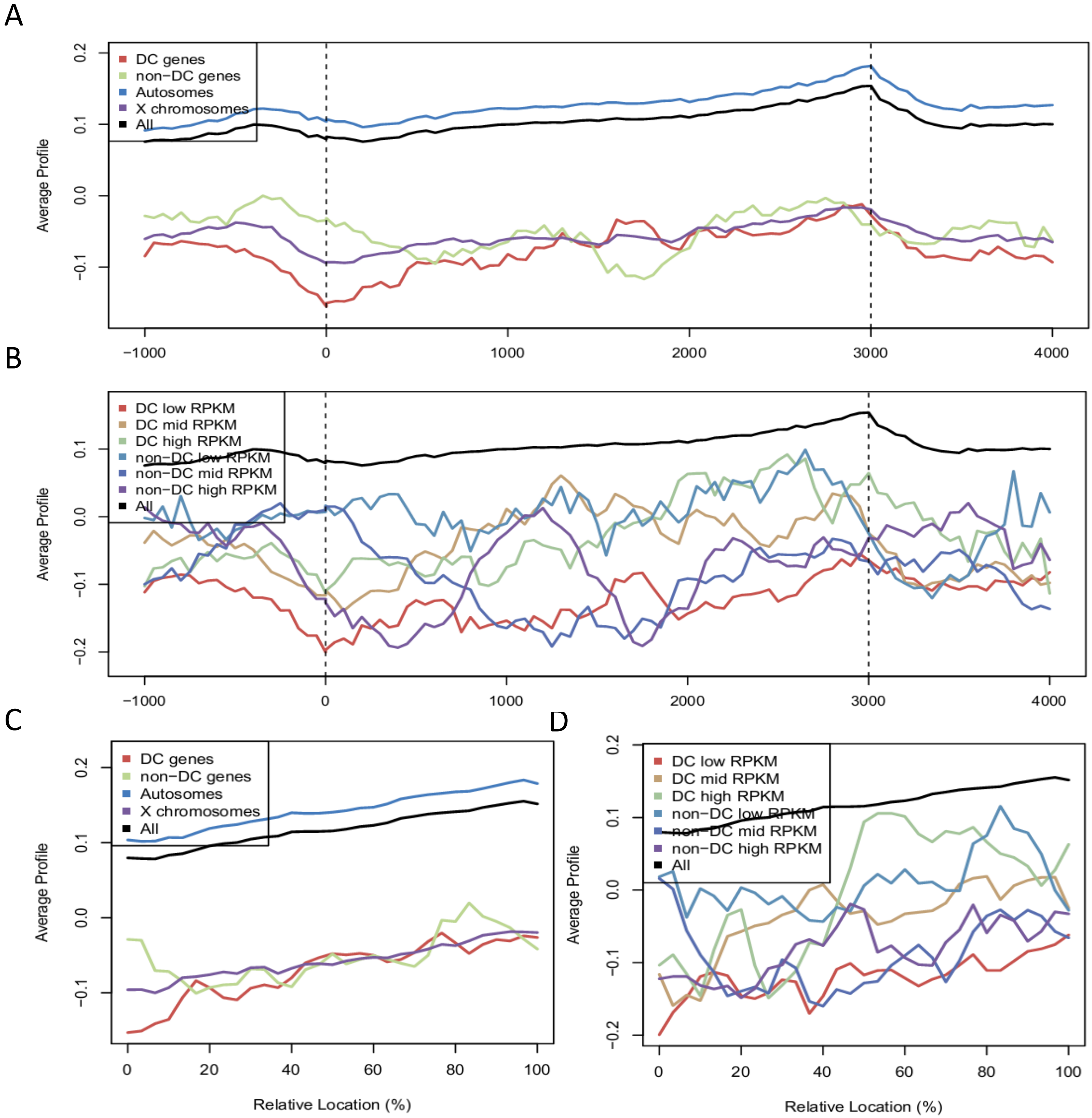

Figure 3.35. H3K9me2 EE gene group and transcription level metagene analysis. Shown are metagenes (A & B) or concatenated exon signal profiles (C & D) for dosage compensated, non-dosage compensated, active autosomal, or active X-linked genes (A & C) or low, medium, and high expression dosage compensated and non-dosage compensated gene groups (B & D). Results show low levels on active X, DC, and non-DC genes compared to active autosomal genes that do not correlate with gene expression.

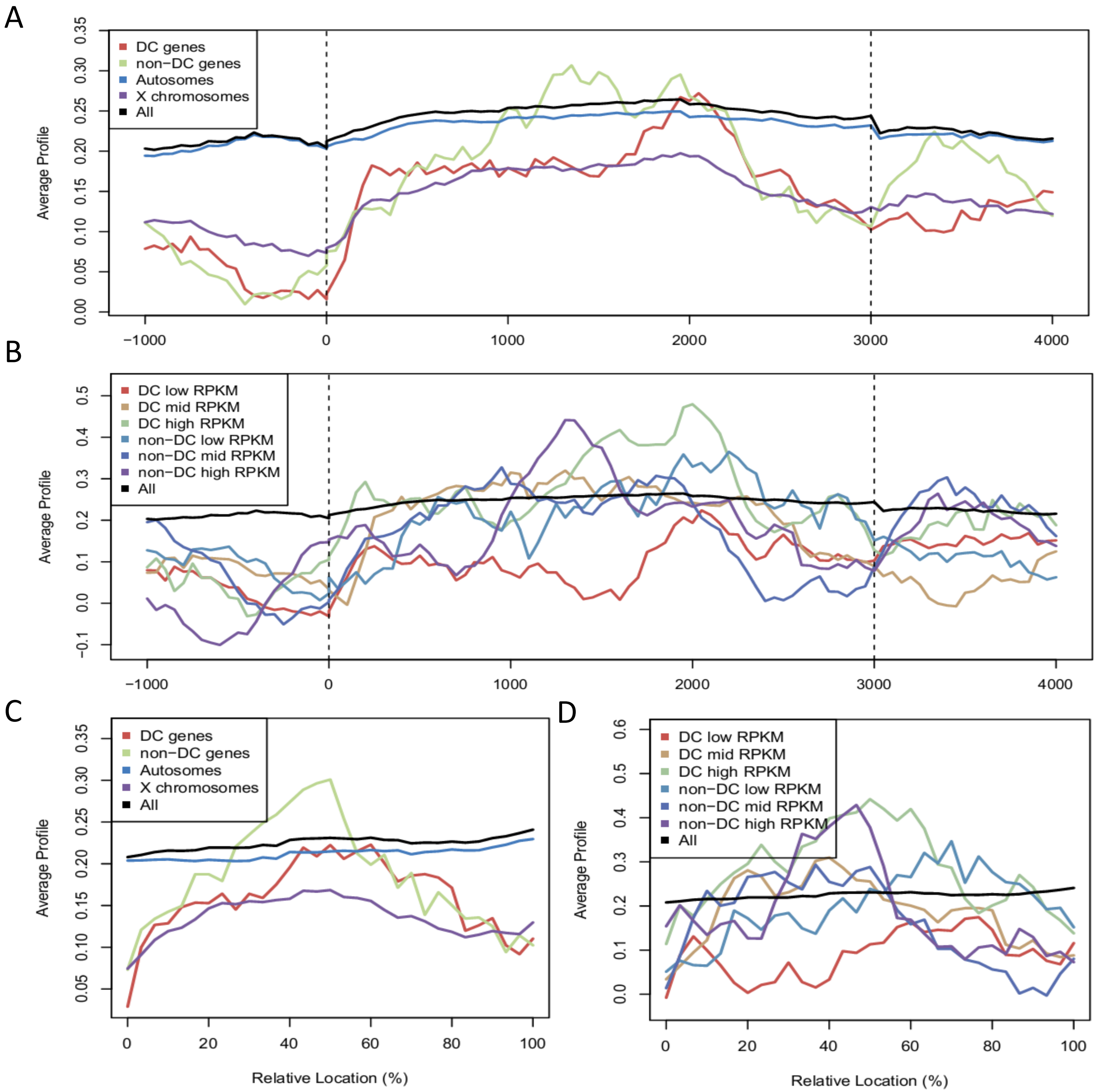

Figure 3.36. H3K9me3 EE gene group and transcription level metagene analysis. Shown are metagenes (A & B) or concatenated exon signal profiles (C & D) for dosage compensated, non-dosage compensated, active autosomal, or active X-linked genes (A & C) or low, medium, and high expression dosage compensated and non-dosage compensated gene groups (B & D). Results show lower levels at X-linked, DC, and non-DC genes compared to active autosomal genes in a manner not correlated with gene expression.

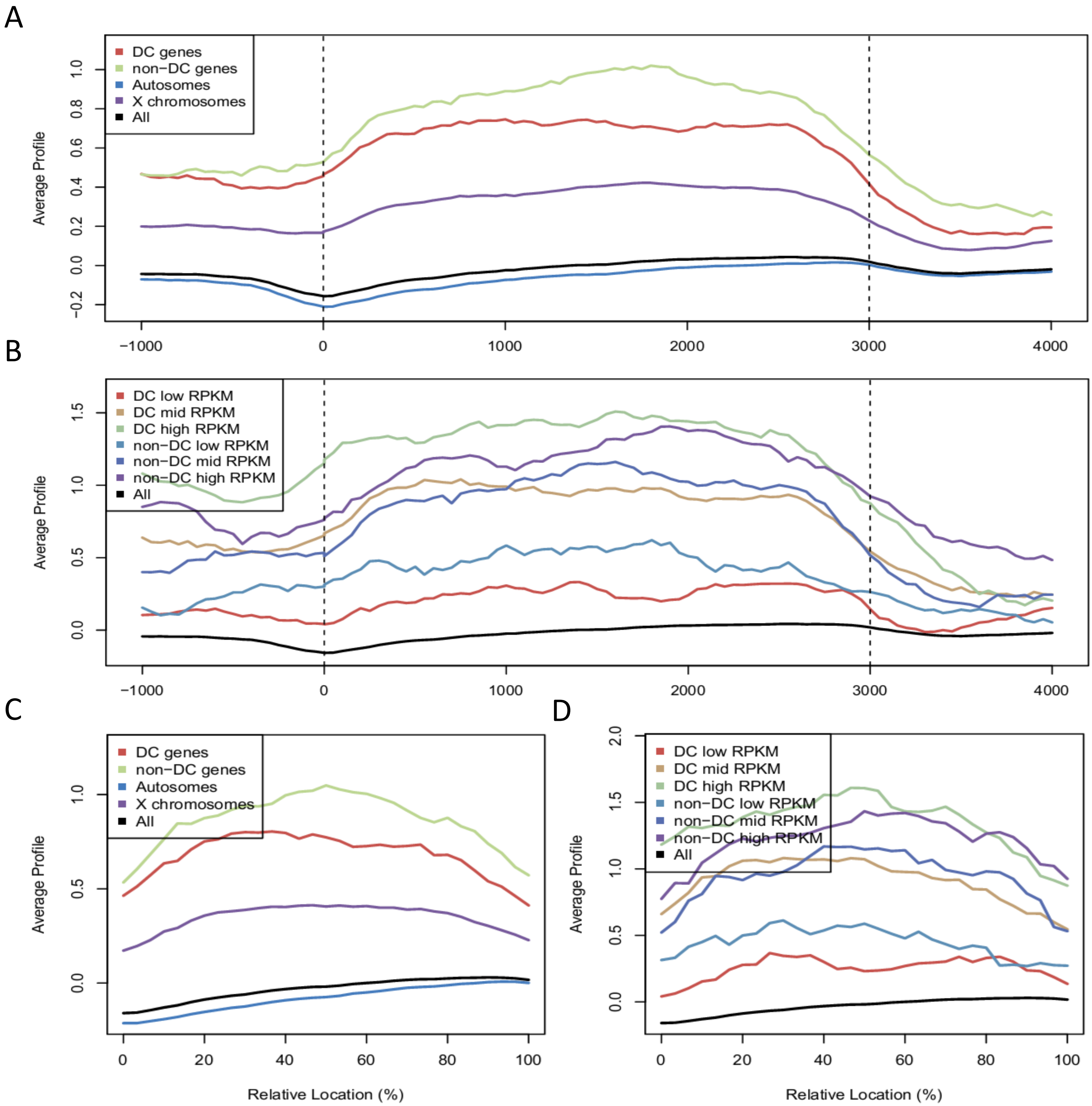

Figure 3.37. H3K27me1 EE gene group and transcription level metagene analysis. Shown are metagenes (A & B) or concatenated exon signal profiles (C & D) for dosage compensated, non-dosage compensated, active autosomal, or active X-linked genes (A & C) or low, medium, and high expression dosage compensated and non-dosage compensated gene groups (B & D). Results show higher levels at DC, non-DC, and active X-linked genes compared to autosomal genes in a manner consistent with gene expression levels.

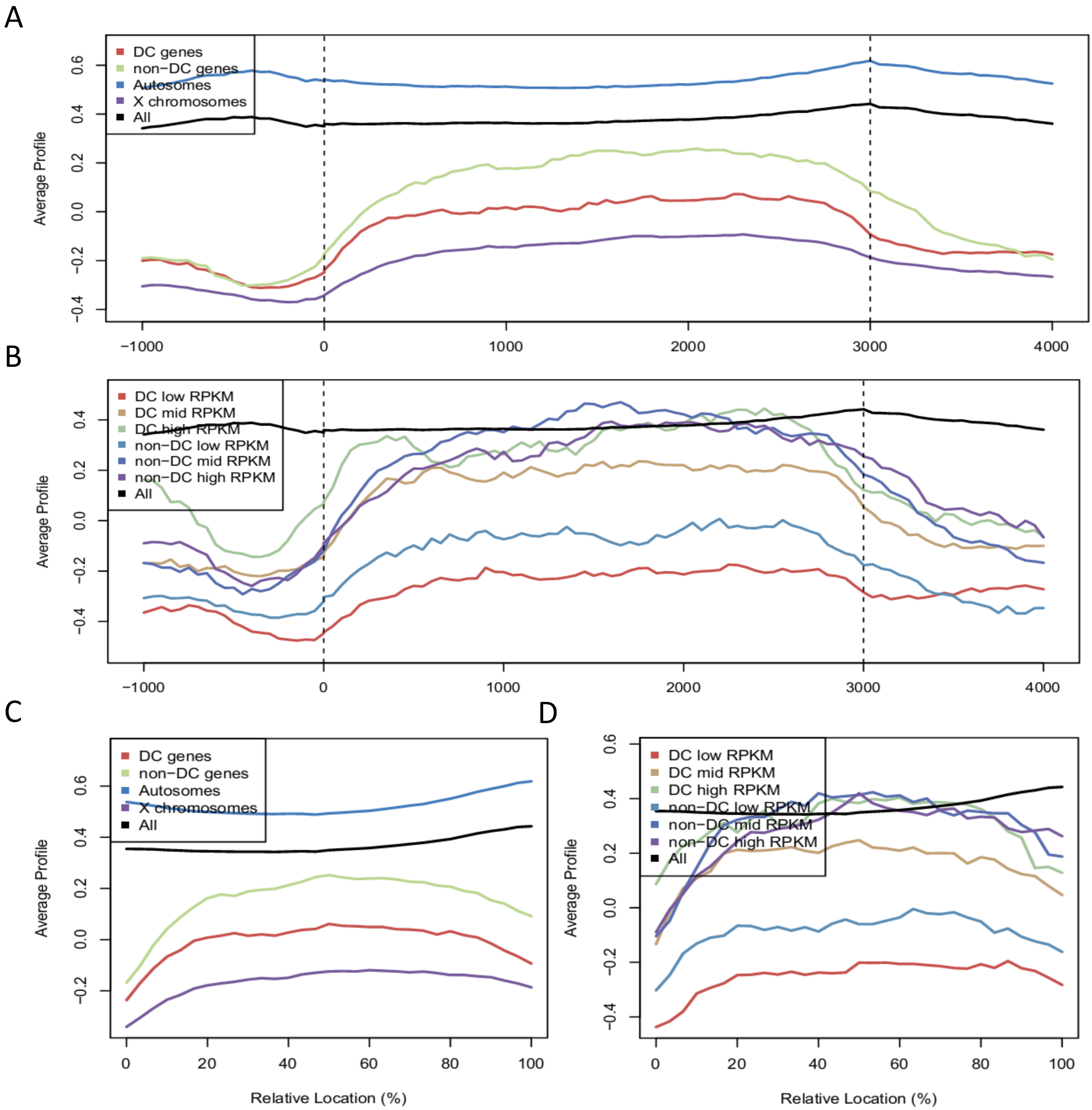

Figure 3.38. H3K36me1 EE gene group and transcription level metagene analysis. Shown are metagenes (A & B) or concatenated exon signal profiles (C & D) for dosage compensated, non-dosage compensated, active autosomal, or active X-linked genes (A & C) or low, medium, and high expression dosage compensated and non-dosage compensated gene groups (B & D). Results show lower levels at active X-linked, DC, and non-DC genes compared to autosomal genes in a manner consistent with gene expression.

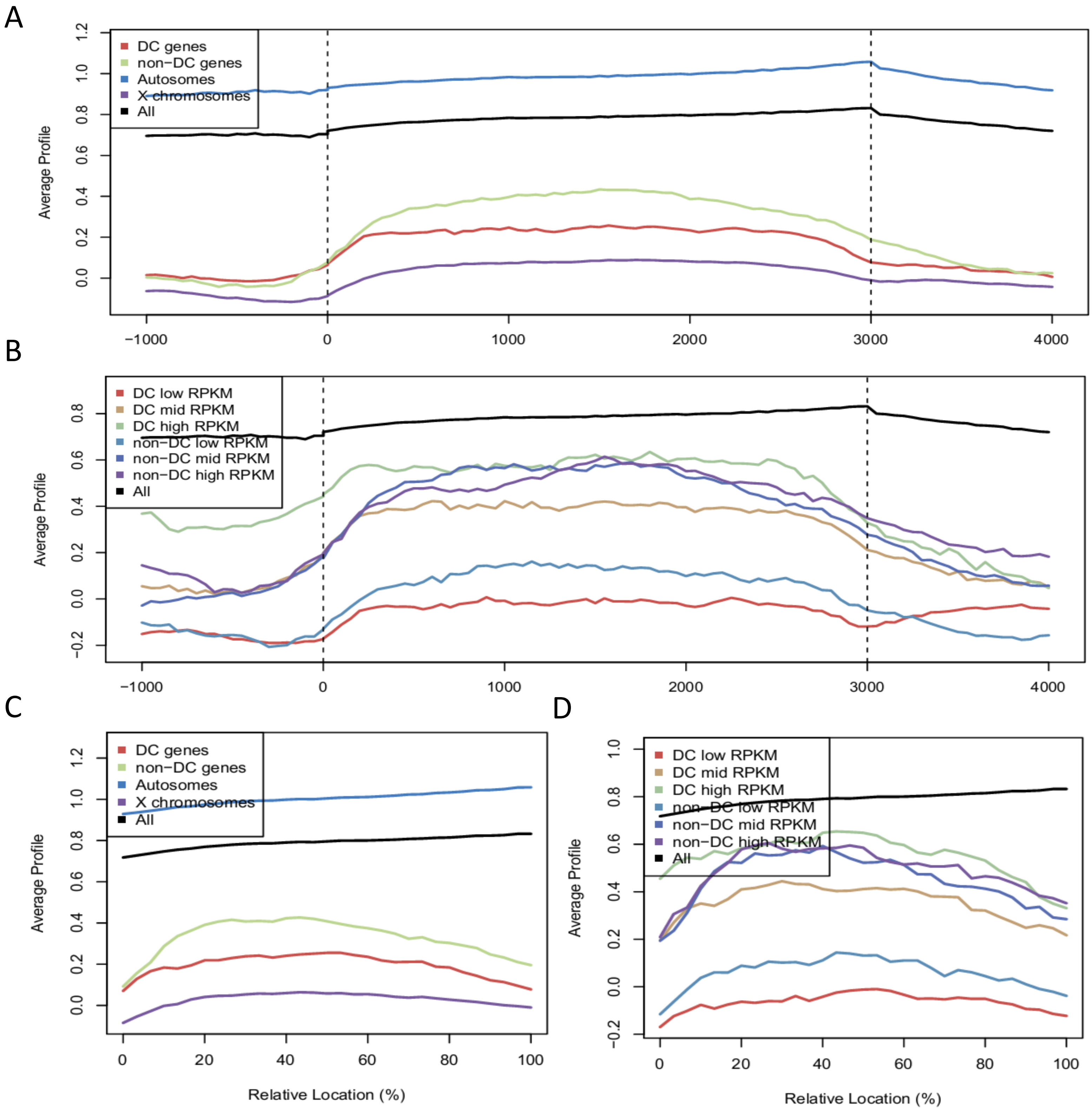

Figure 3.39. H3K36me2 EE gene group and transcription level metagene analysis. Shown are metagenes (A & B) or concatenated exon signal profiles (C & D) for dosage compensated, non-dosage compensated, active autosomal, or active X-linked genes (A & C) or low, medium, and high expression dosage compensated and non-dosage compensated gene groups (B & D). Results show lower levels at X-linked, DC, and non-DC genes in a manner consistent with gene expression.

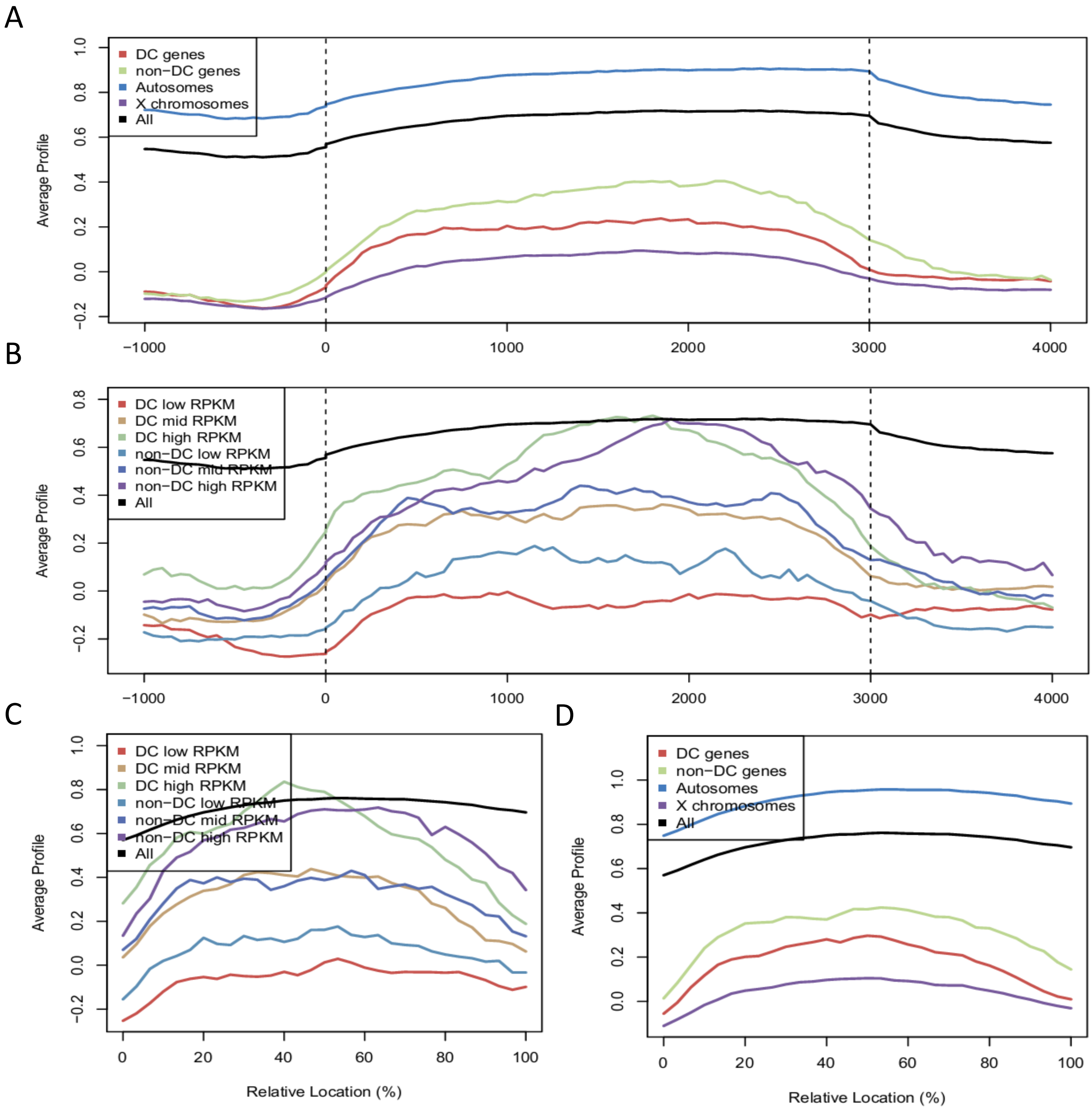

Figure 3.40. H3K36me3 EE ene group and transcription level metagene analysis. Shown are metagenes (A & B) or concatenated exon signal profiles (C & D) for dosage compensated, non-dosage compensated, active autosomal, or active X-linked genes (A & C) or low, medium, and high expression dosage compensated and non-dosage compensated gene groups (B & D). Results show lower levels at active X-linked, DC, and non-DC genes compared to autosomal genes in a manner consistent with gene expression.

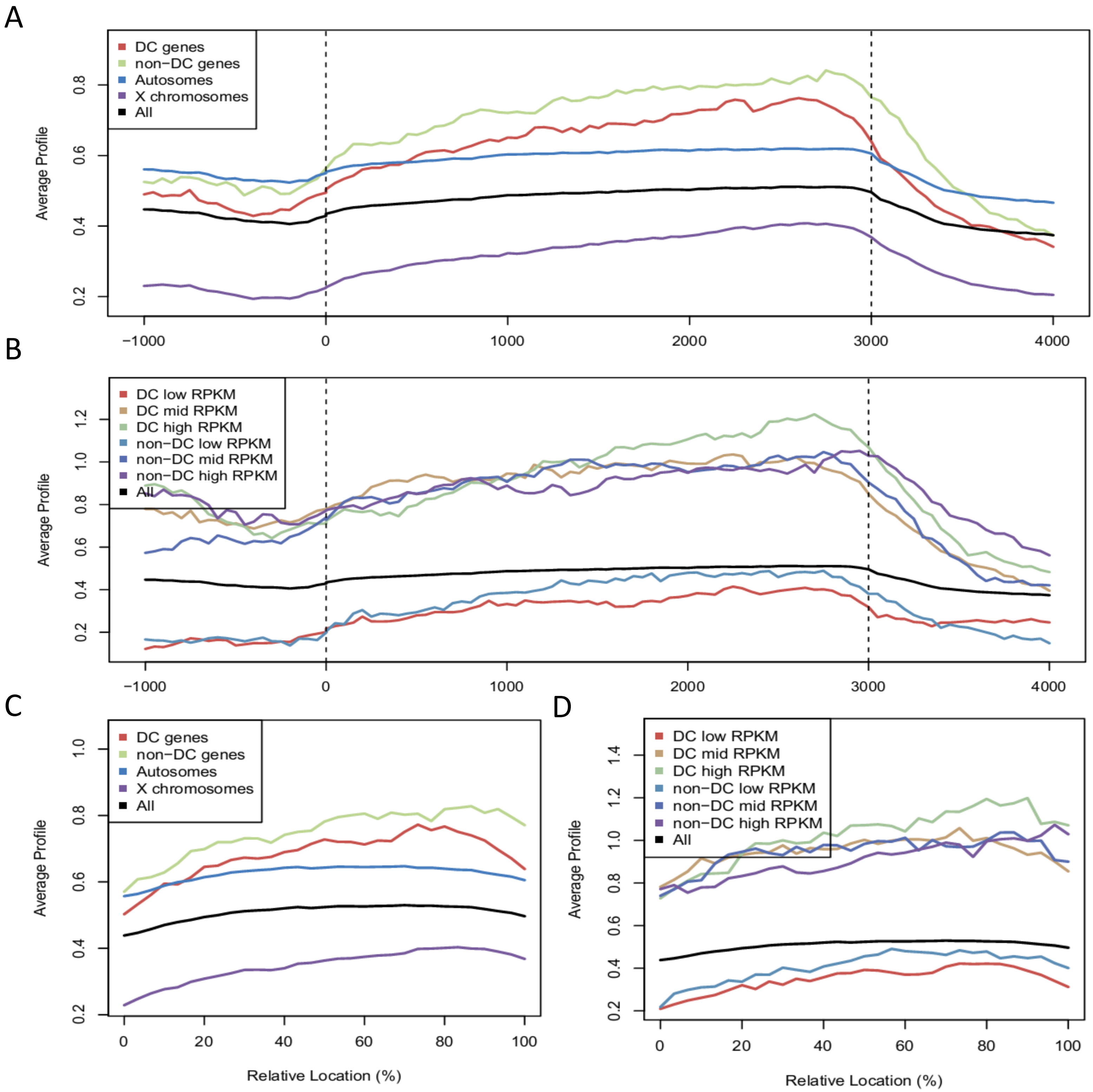

Figure 3.41. H3K79me1 EE gene group and transcription level metagene analysis. Shown are metagenes (A & B) or concatenated exon signal profiles (C & D) for dosage compensated, non-dosage compensated, active autosomal, or active X-linked genes (A & C) or low, medium, and high expression dosage compensated and non-dosage compensated gene groups (B & D). Results show similar levels at DC and non-DC genes and lower levels at active X-linked genes compared to autosomal genes in a manner that is roughly consistent with high and low gene expression levels.

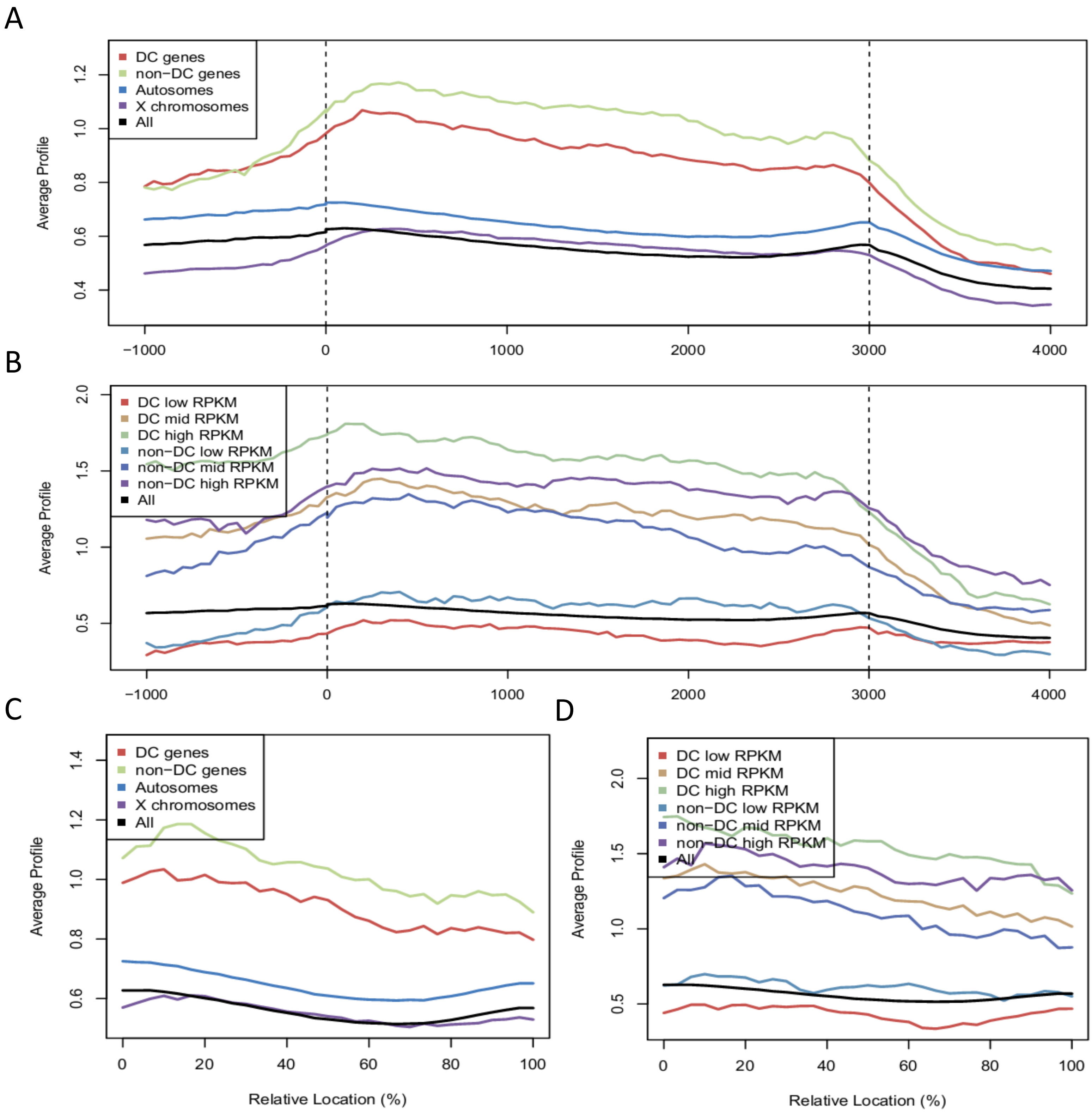

Figure 3.42. H3K79me2 EE gene group and transcription level metagene analysis. Shown are metagenes (A & B) or concatenated exon signal profiles (C & D) for dosage compensated, non-dosage compensated, active autosomal, or active X-linked genes (A & C) or low, medium, and high expression dosage compensated and non-dosage compensated gene groups (B & D). Results show similar levels at active X-linked and autosomal and higher levels at non-DC compared to DC genes in a manner consistent with gene expression.

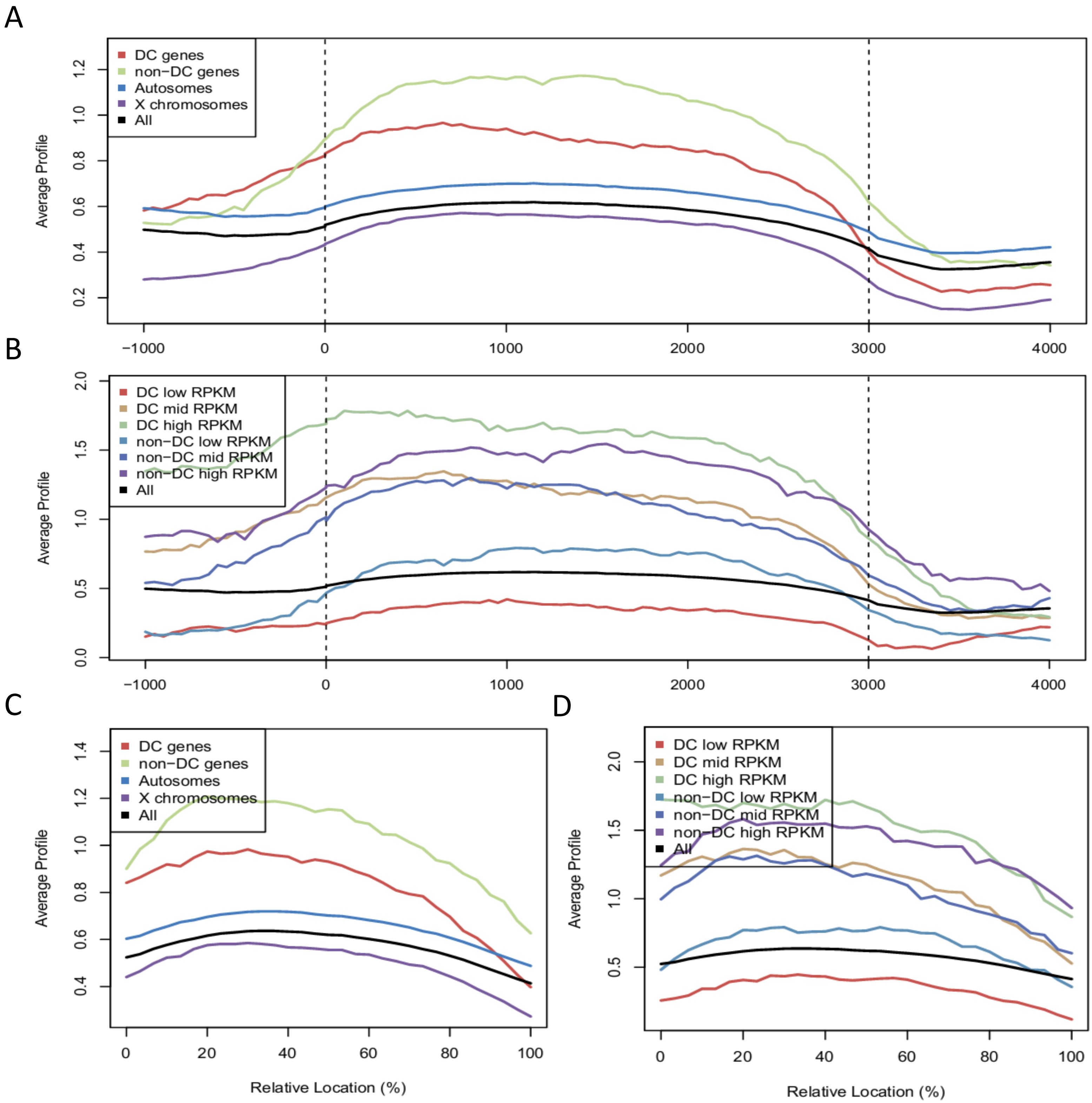

Figure 3.43. H3K79me3 EE gene group and transcription level metagene analysis. Shown are metagenes (A & B) or concatenated exon signal profiles (C & D) for dosage compensated, non-dosage compensated, active autosomal, or active X-linked genes (A & C) or low, medium, and high expression dosage compensated and non-dosage compensated gene groups (B & D). Results show similar levels at X-linked and autosomal genes, but lower levels at DC compared to non-DC genes in a manner consistent with gene expression.

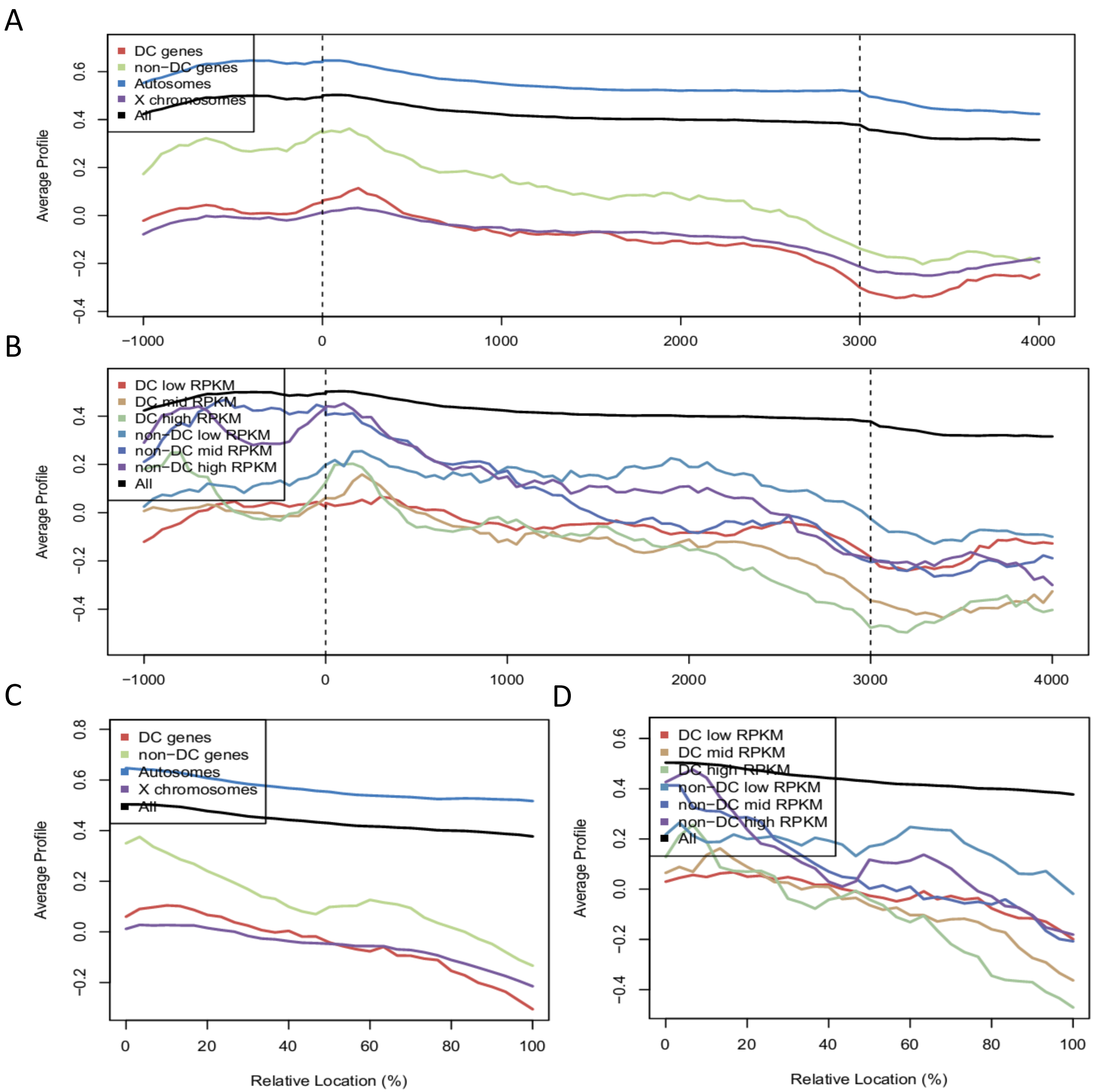

Figure 3.44. H4K8ac EE gene group and transcription level metagene analysis. Shown are metagenes (A & B) or concatenated exon signal profiles (C & D) for dosage compensated, non-dosage compensated, active autosomal, or active X-linked genes (A & C) or low, medium, and high expression dosage compensated and non-dosage compensated gene groups (B & D). Results show lower levels at DC and active X-linked compared to non-DC and autosomal genes in a manner somewhat consistent with gene expression.

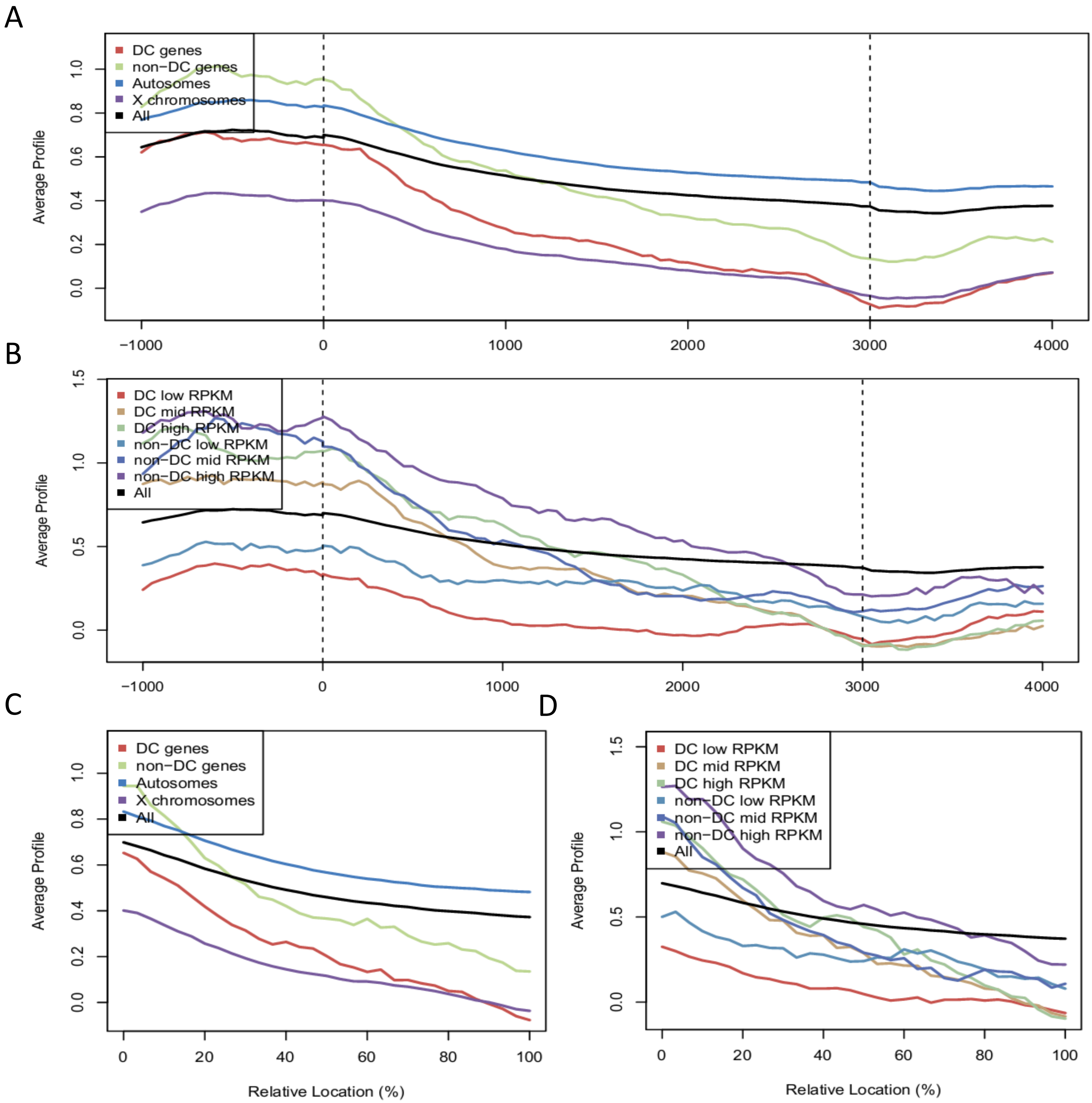

Figure 3.45. Tetra-acetyl histone H4 EE gene group and transcription level metagene analysis. Shown are metagenes (A & B) or concatenated exon signal profiles (C & D) for dosage compensated, non-dosage compensated, active autosomal, or active X-linked genes (A & C) or low, medium, and high expression dosage compensated and non-dosage compensated gene groups (B & D). Results show lower levels at DC and active-X-linked compared to non-DC and autosomal gens in a manner somewhat consistent with gene expression.

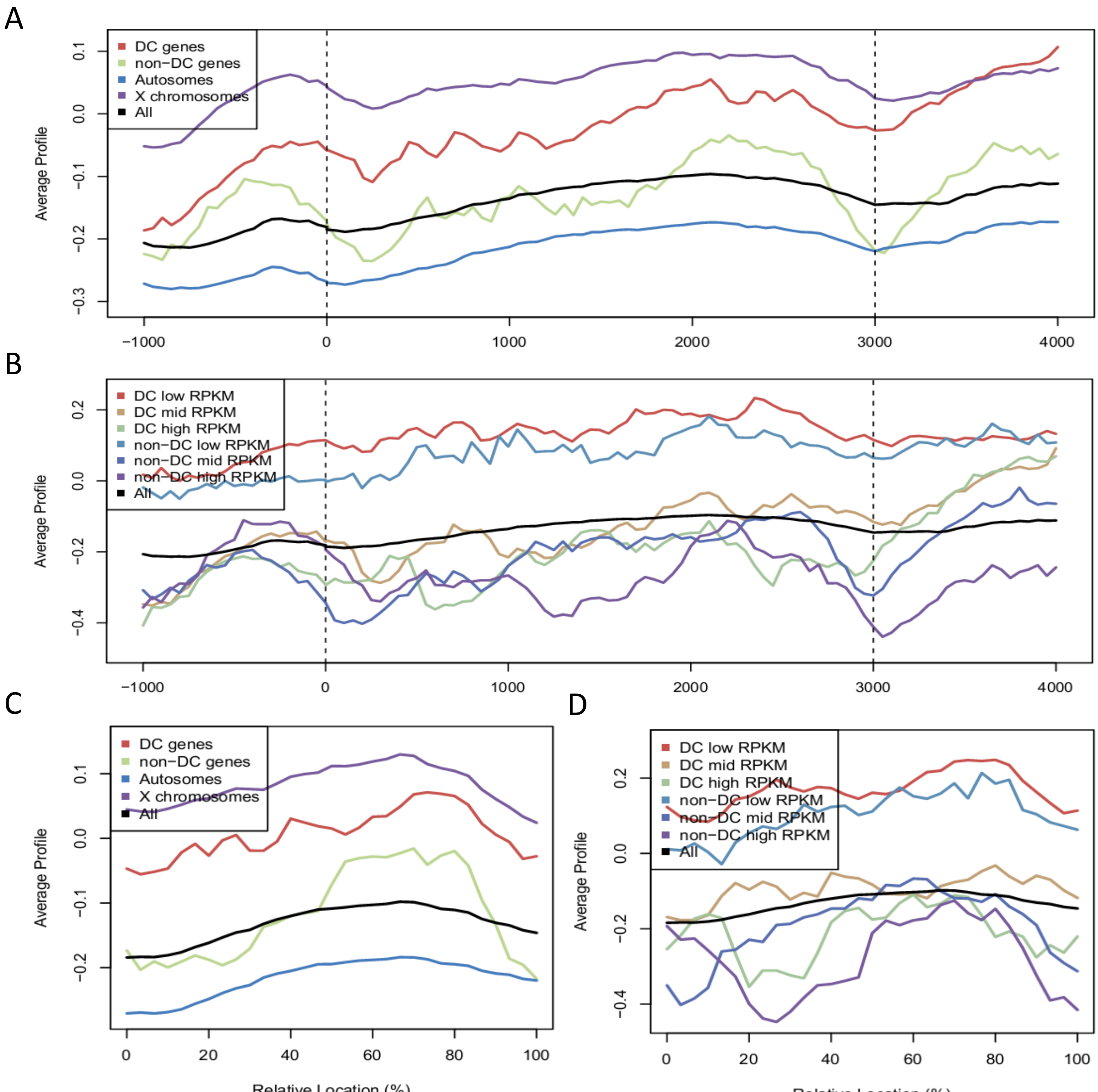

Figure 3.46. HCP-3, the *C. elegans* histone H3 variant CENP-A homolog, EE gene group and transcription level metagene analysis. Shown are metagenes (A & B) or concatenated exon signal profiles (C & D) for dosage compensated, non-dosage compensated, active autosomal, or active X-linked genes (A & C) or low, medium, and high expression dosage compensated and non-dosage compensated gene groups (B & D). Results show higher levels at DC and active X-linked as compared to non-DC and autosomal genes in a manner consistent with low and high gene expression levels.

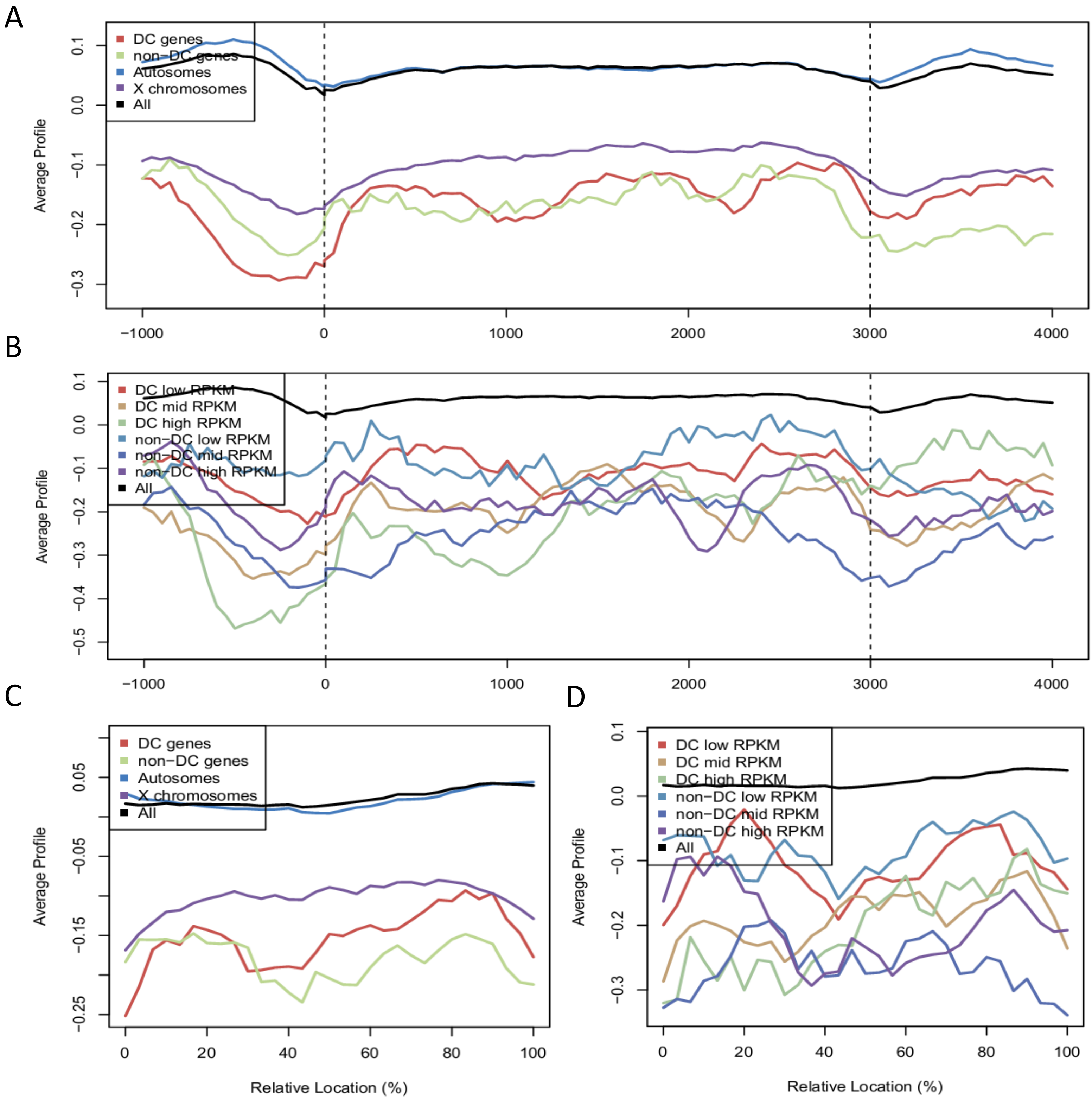

Figure 3.47. HPL-2, a *C. elegans* heterochromatin protein 1 (HP1) homolog, LE gene group and transcription level metagene analysis. Shown are metagenes (A & B) or concatenated exon signal profiles (C & D) for dosage compensated, non-dosage compensated, active autosomal, or active X-linked genes (A & C) or low, medium, and high expression dosage compensated and non-dosage compensated gene groups (B & D). Results show lower levels at DC, non-DC, and active X-linked genes compared to autosomal genes in a manner not consistent with gene expression.

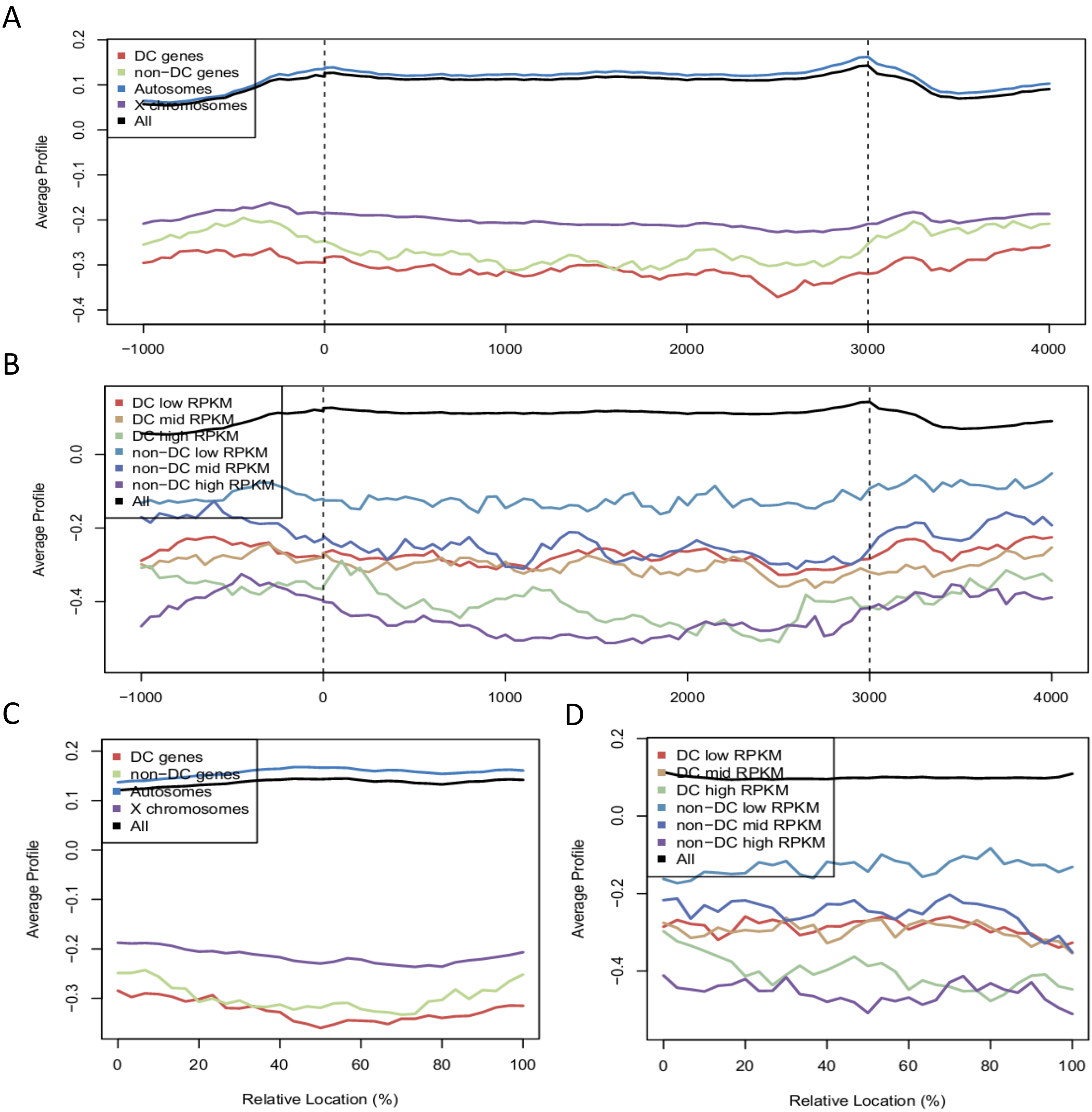

Figure 3.48. LEM-2, a nuclear lamin component, EE gene group and transcription level metagene analysis. Shown are metagenes (A & B) or concatenated exon signal profiles (C & D) for dosage compensated, non-dosage compensated, active autosomal, or active X-linked genes (A & C) or low, medium, and high expression dosage compensated and non-dosage compensated gene groups (B & D). Results show lower levels at DC, non-DC, and active X-linked genes compared to autosomal genes in a manner consistent with gene expression.

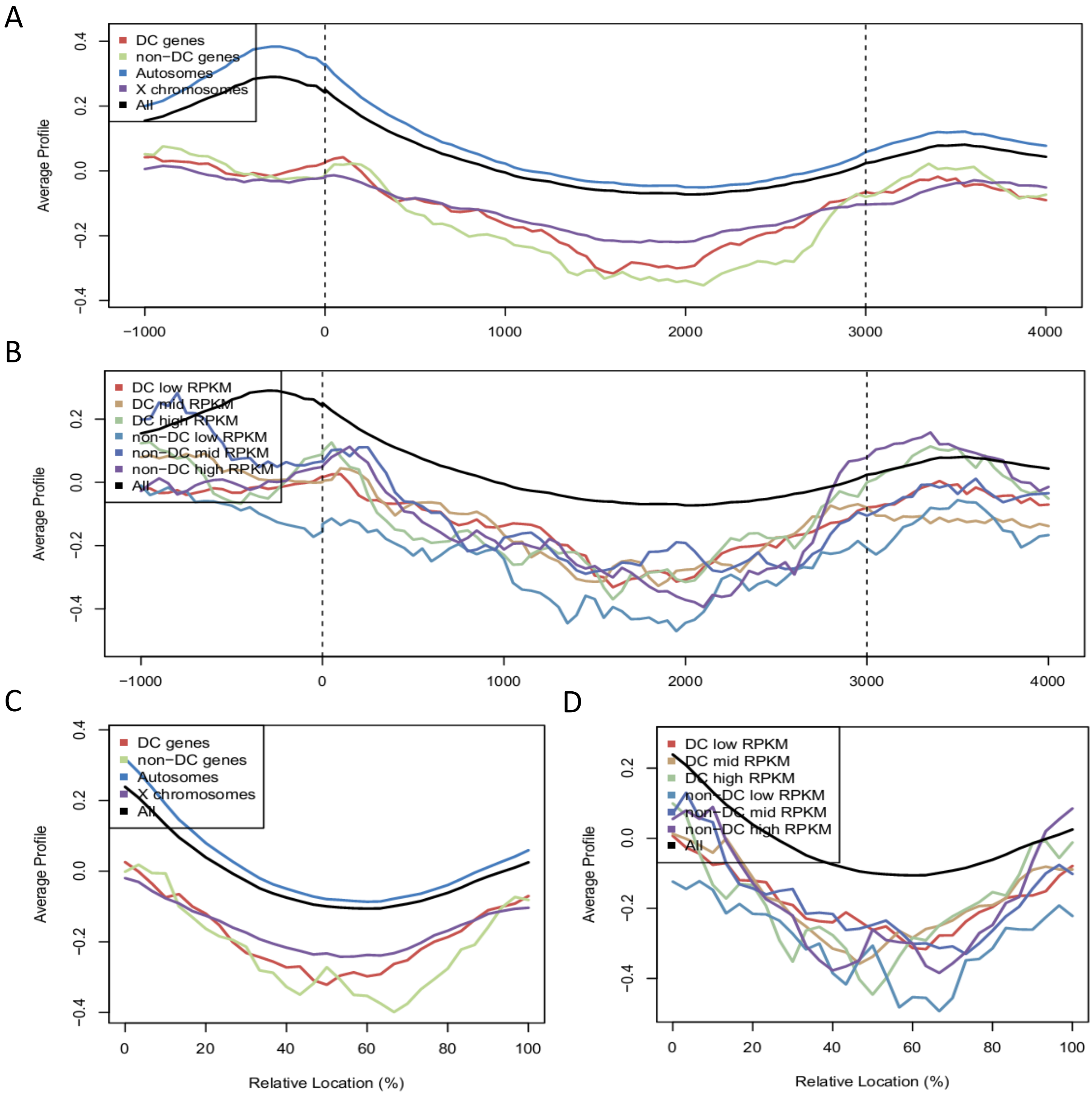

Figure 3.49. LIN-15B, a synMuv B gene, LE gene group and transcription level metagene analysis. Shown are metagenes (A & B) or concatenated exon signal profiles (C & D) for dosage compensated, non-dosage compensated, active autosomal, or active X-linked genes (A & C) or low, medium, and high expression dosage compensated and non-dosage compensated gene groups (B & D). Results show lower levels at DC, non-DC, and active X-linked genes compared to autosomal genes in a manner independent of gene expression.

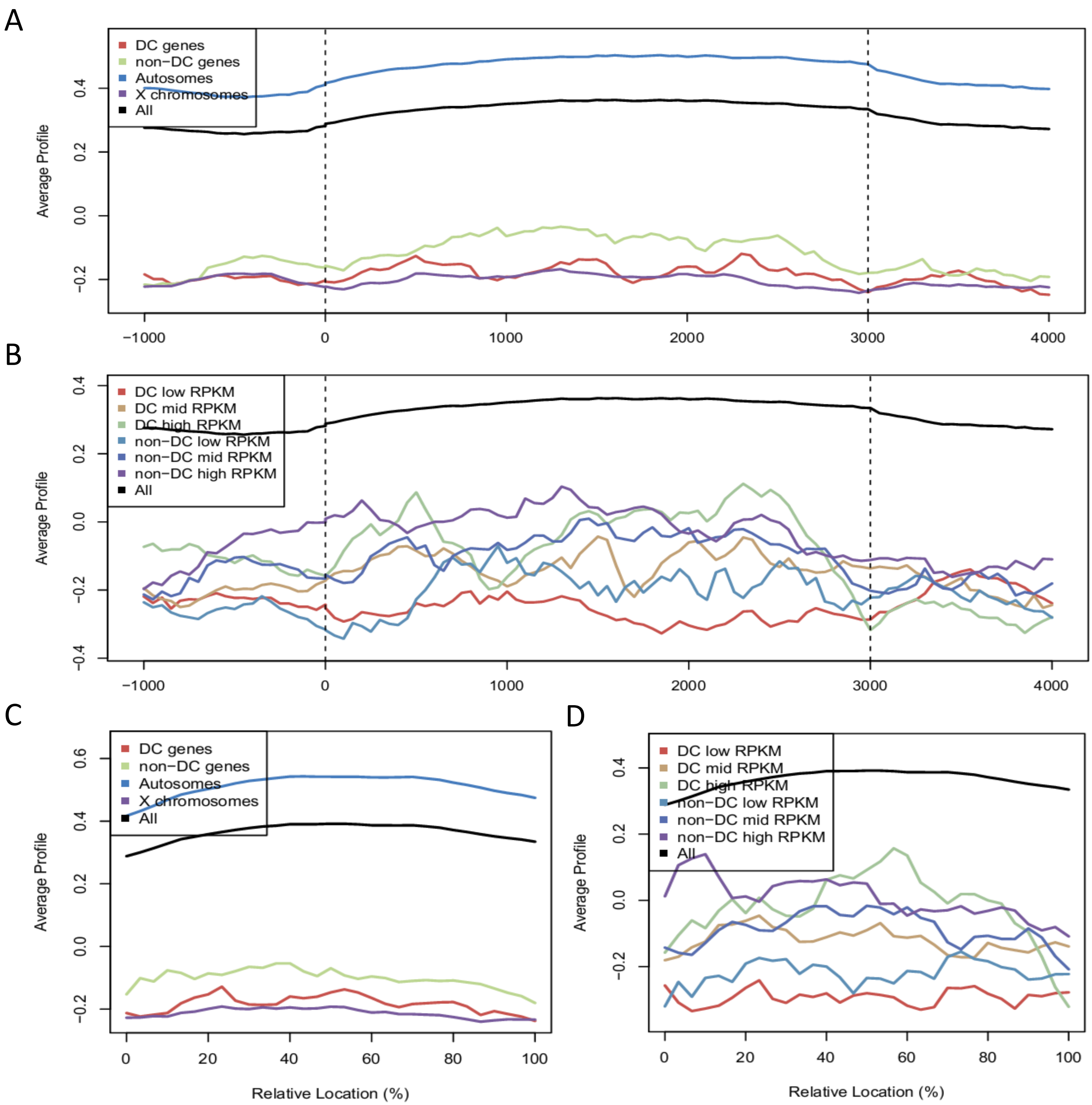

Figure 3.50. MES-4, an H3K36 methyltransferase, EE gene group and transcription level metagene analysis. Shown are metagenes (A & B) or concatenated exon signal profiles (C & D) for dosage compensated, non-dosage compensated, active autosomal, or active X-linked genes (A & C) or low, medium, and high expression dosage compensated and non-dosage compensated gene groups (B & D). Results show low levels at DC, non-DC, and active X-linked genes compared to autosomal genes in a manner not consistent with gene expression.

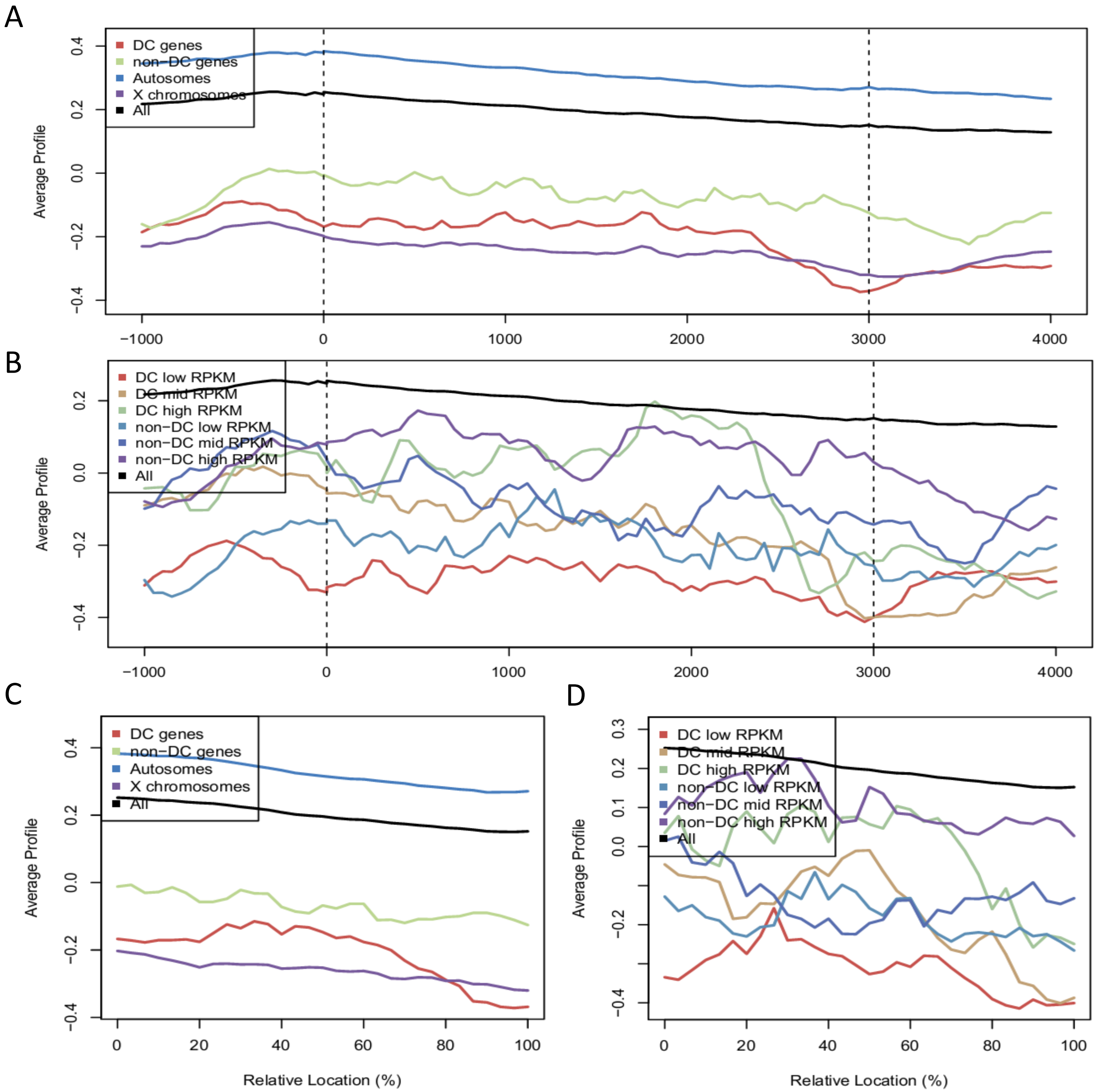

Figure 3.51. MRG-1, a component of both TIP60 and RPD3 complexes, EE gene group and transcription level metagene analysis. Shown are metagenes (A & B) or concatenated exon signal profiles (C & D) for dosage compensated, non-dosage compensated, active autosomal, or active X-linked genes (A & C) or low, medium, and high expression dosage compensated and non-dosage compensated gene groups (B & D). Results show lower levels at DC, non-DC, and active X-linked genes compared to autosomal genes in a manner roughly consistent with gene expression.

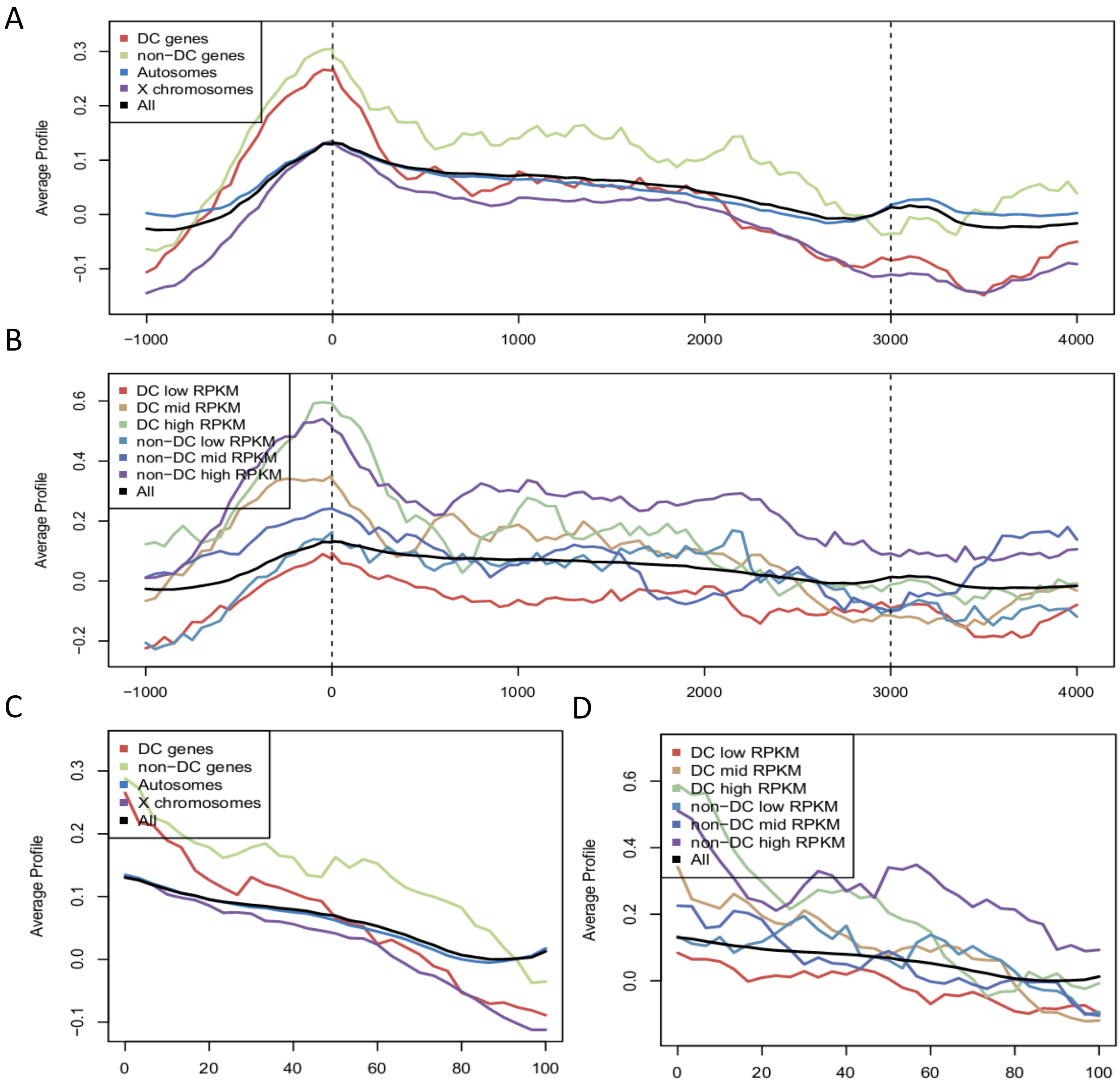

Figure 3.52. NPP-13, a nuclear pore component, ME gene group and transcription level metagene analysis. Shown are metagenes (A & B) or concatenated exon signal profiles (C & D) for dosage compensated, non-dosage compensated, active autosomal, or active X-linked genes (A & C) or low, medium, and high expression dosage compensated and non-dosage compensated gene groups (B & D). Results show upstream peaks and slightly higher levels at non-DC gene bodies and downstream regions compared to those of DC genes in a manner roughly consistent with gene expression.

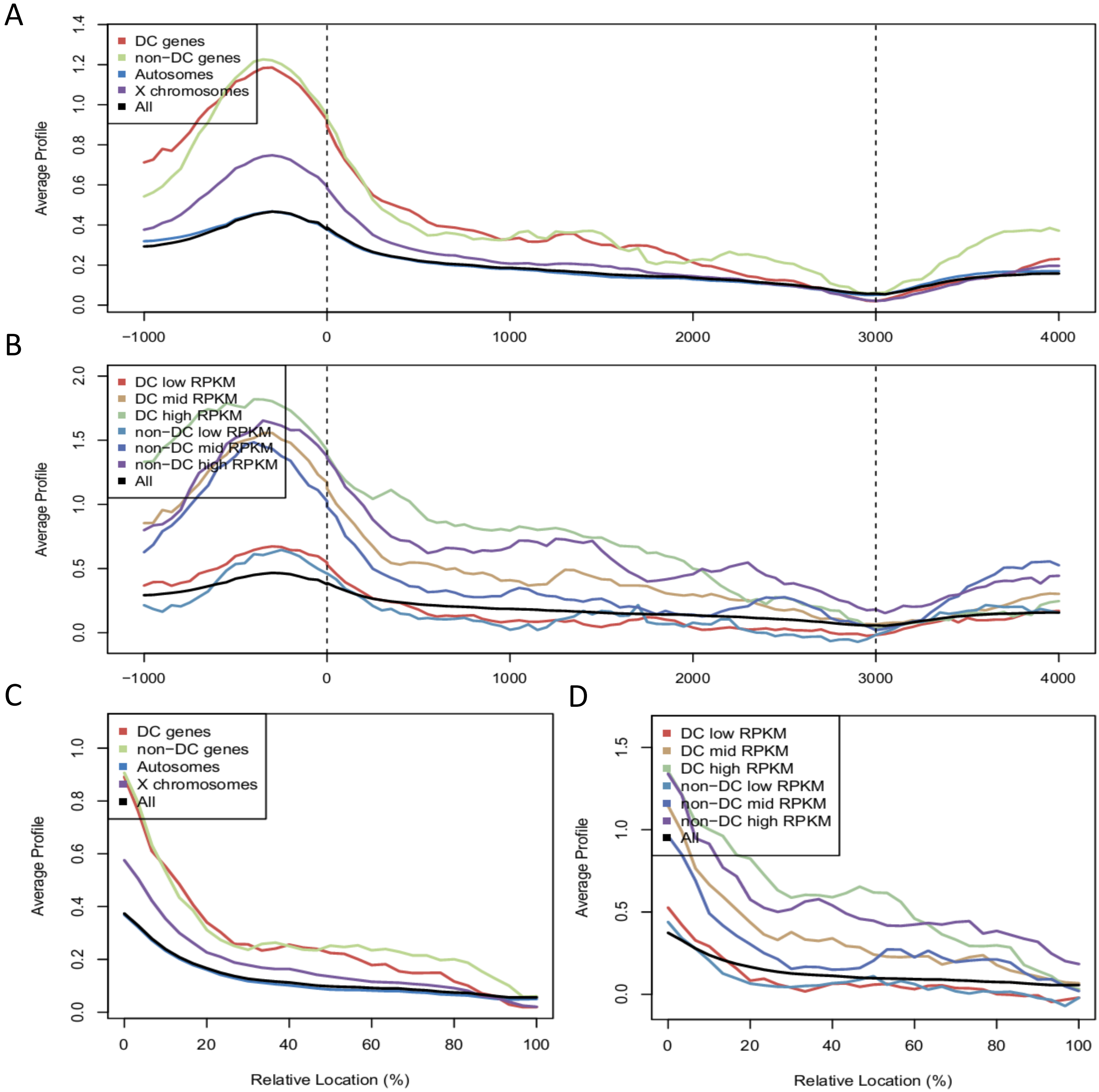

Figure 3.53. Y39G10AR.18, the *C. elegans* H3K79 methyltransferase Dot1p homolog, ME gene group and transcription level metagene analysis. Shown are metagenes (A & B) or concatenated exon signal profiles (C & D) for dosage compensated, non-dosage compensated, active autosomal, or active X-linked genes (A & C) or low, medium, and high expression dosage compensated and non-dosage compensated gene groups (B & D). Results show higher levels at active-X-linked upstream regions compared to autosomal counterparts and similar levels elsewhere in a manner consistent with gene expression.

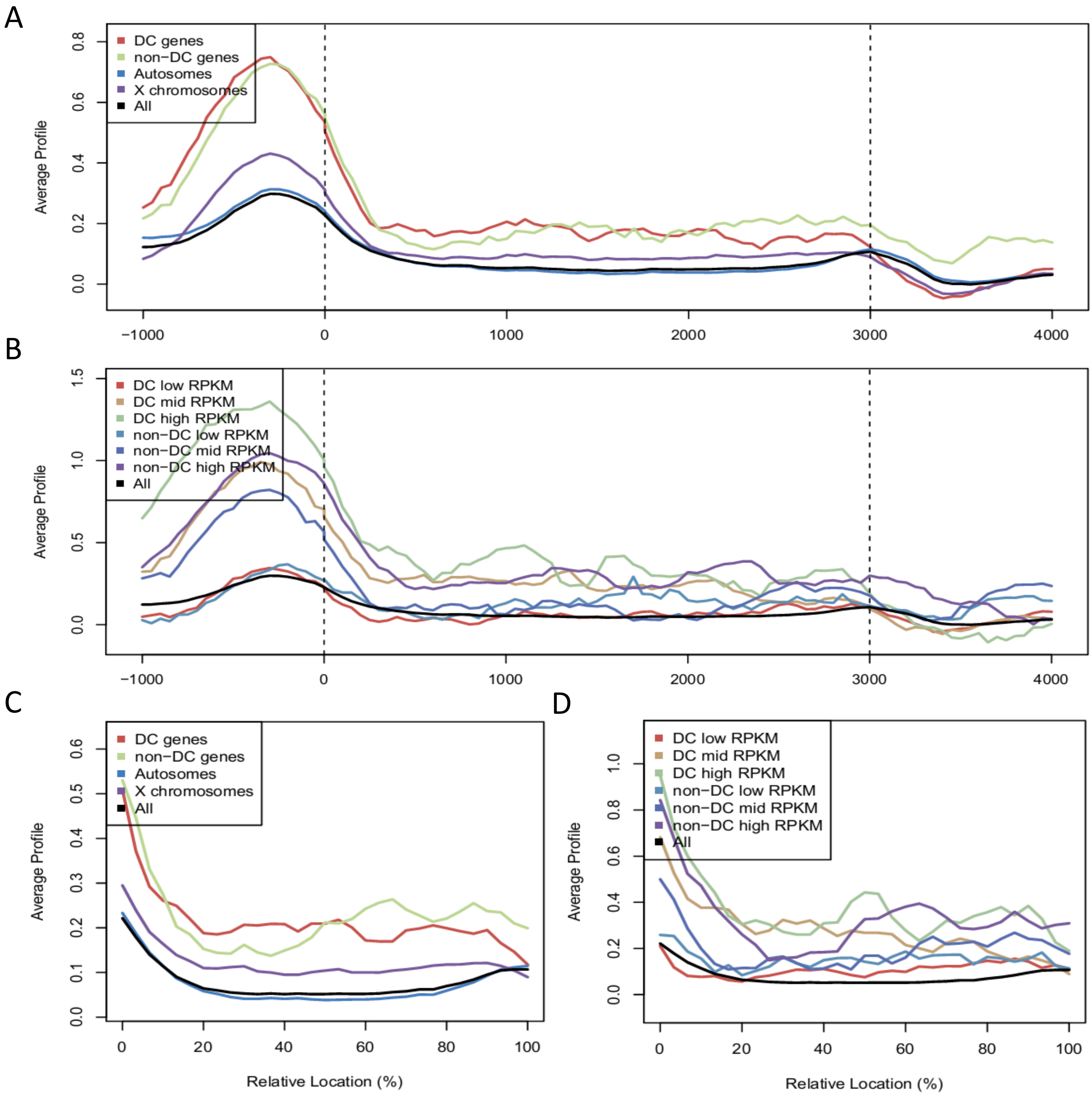

Figure 3.54. ZFP-1, a zinc finger-containing transcription factor, ME gene group and transcription level metagene analysis. Shown are metagenes (A & B) or concatenated exon signal profiles (C & D) for dosage compensated, non-dosage compensated, active autosomal, or active X-linked genes (A & C) or low, medium, and high expression dosage compensated and non-dosage compensated gene groups (B & D). Results show similar levels at DC and non-DC genes as well as active X-linked and autosomal genes in a manner not consistent with gene expression.

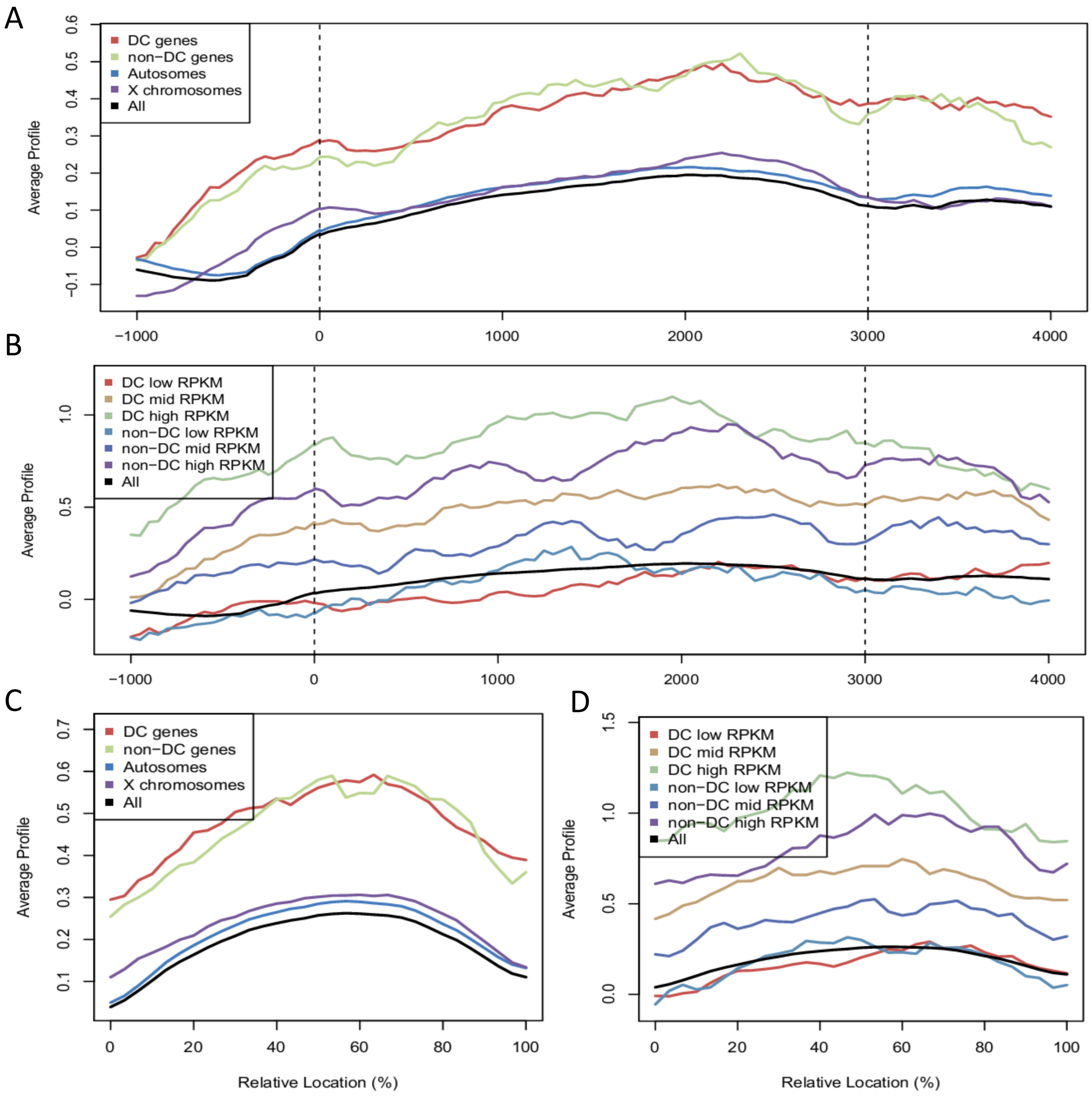

Figure 3.55. AMA-1, RNA polymerase II signal independent of the C-terminal domain, ME gene group and transcription level metagene analysis. Shown are metagenes (A & B) or concatenated exon signal profiles (C & D) for dosage compensated, non-dosage compensated, active autosomal, or active X-linked genes (A & C) or low, medium, and high expression dosage compensated and non-dosage compensated gene groups (B & D). Results show similar levels at DC and non-DC or active X-linked and autosomal genes in a manner consistent with gene expression.

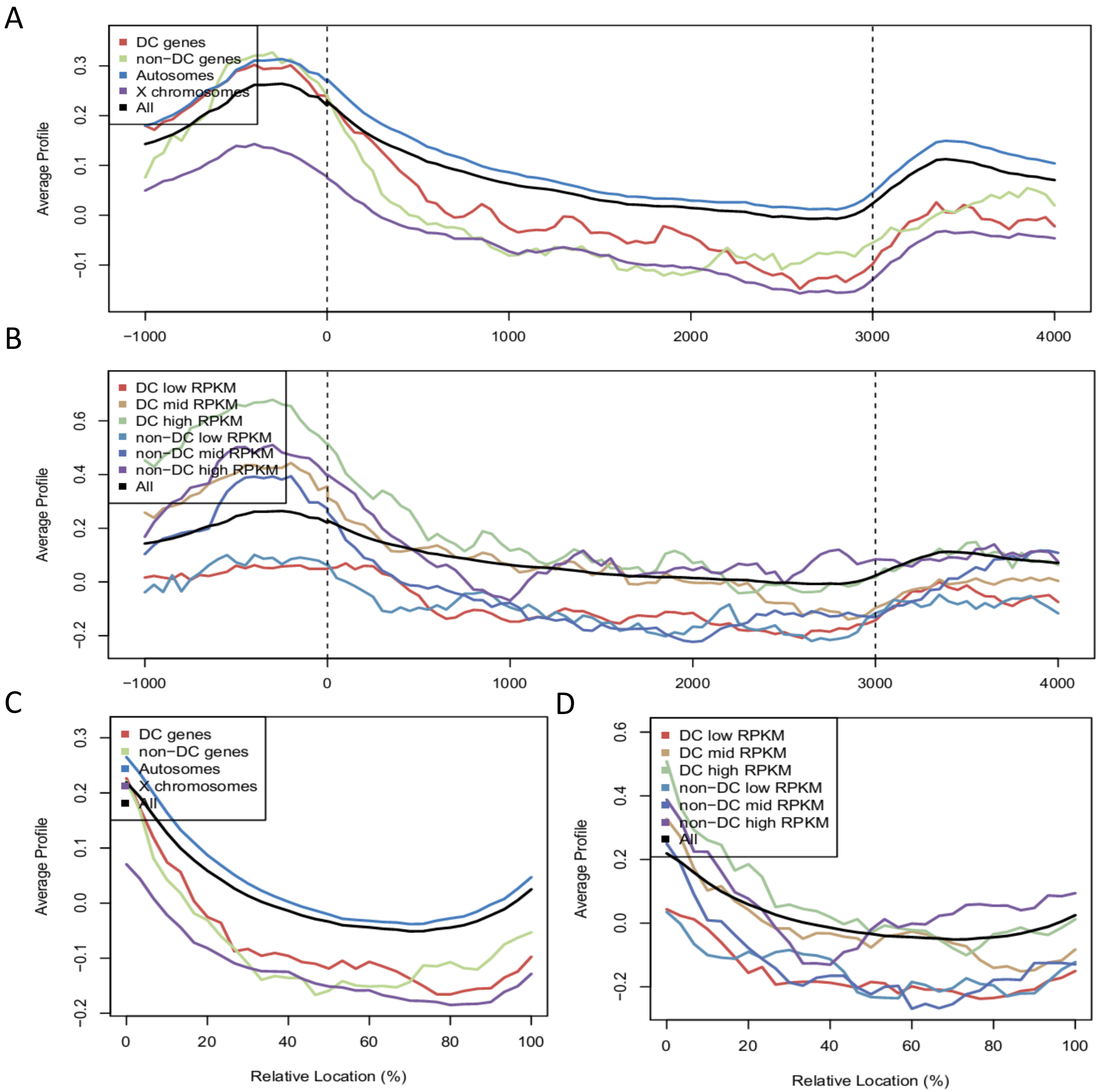

Figure 3.56. CBP-1, the conserved H3K27 and H3K56 acetyltransferase, ME gene group and transcription level metagene analysis. Shown are metagenes (A & B) or concatenated exon signal profiles (C & D) for dosage compensated, non-dosage compensated, active autosomal, or active X-linked genes (A & C) or low, medium, and high expression dosage compensated and non-dosage compensated gene groups (B & D). Results show similar levels at DC and non-DC genes and lower levels at active X-linked compared to autosomal genes in a manner roughly consistent with gene expression.

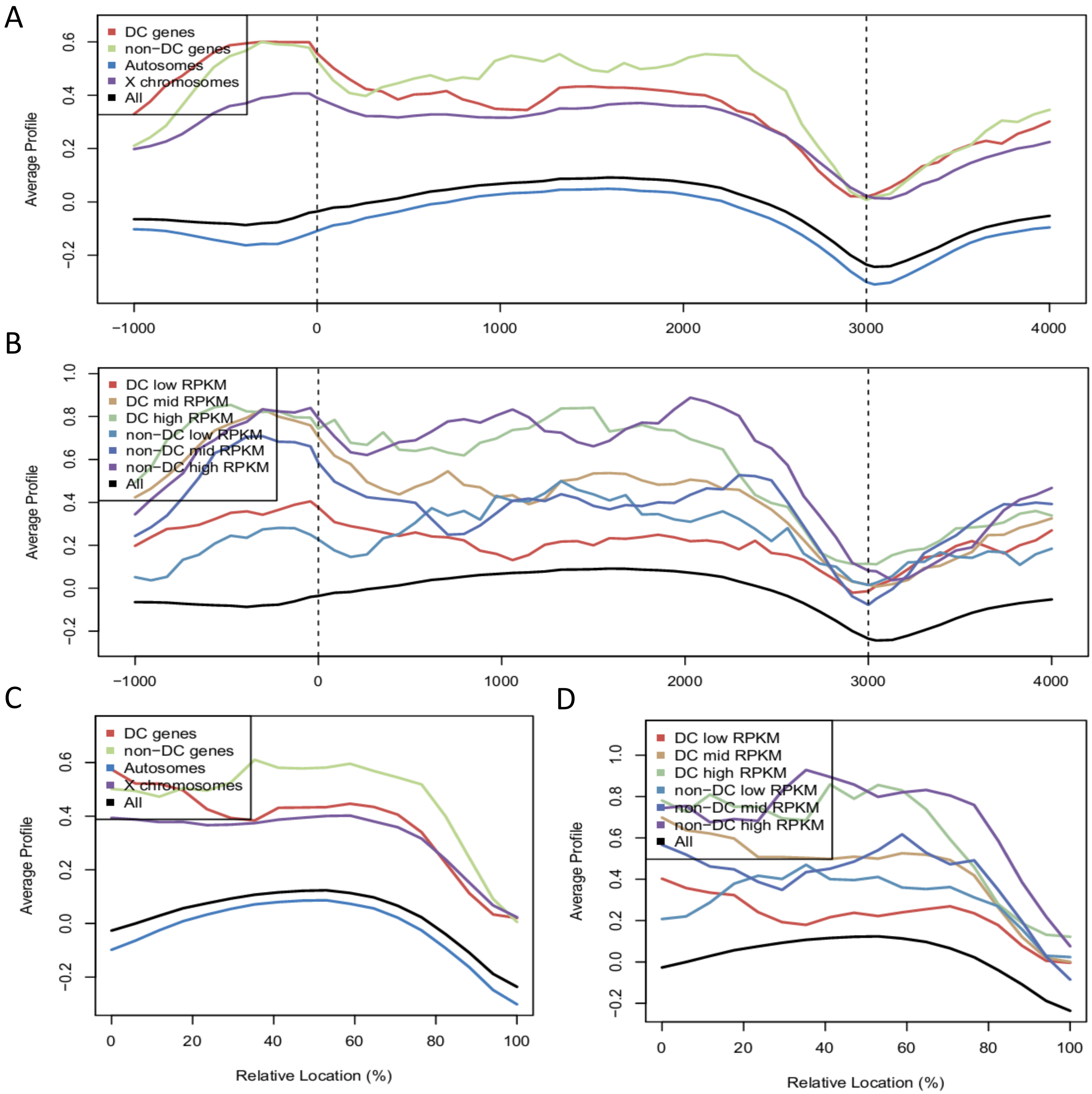

Figure 3.58. DPY-28, a DCC component, ME gene group and transcription level metagene analysis. Shown are metagenes (A & B) or concatenated exon signal profiles (C & D) for dosage compensated, non-dosage compensated, active autosomal, or active X-linked genes (A & C) or low, medium, and high expression dosage compensated and non-dosage compensated gene groups (B & D). Results show high levels at DC, non-DC, and active X-linked compared to autosomal genes in a manner roughly consistent with gene expression.

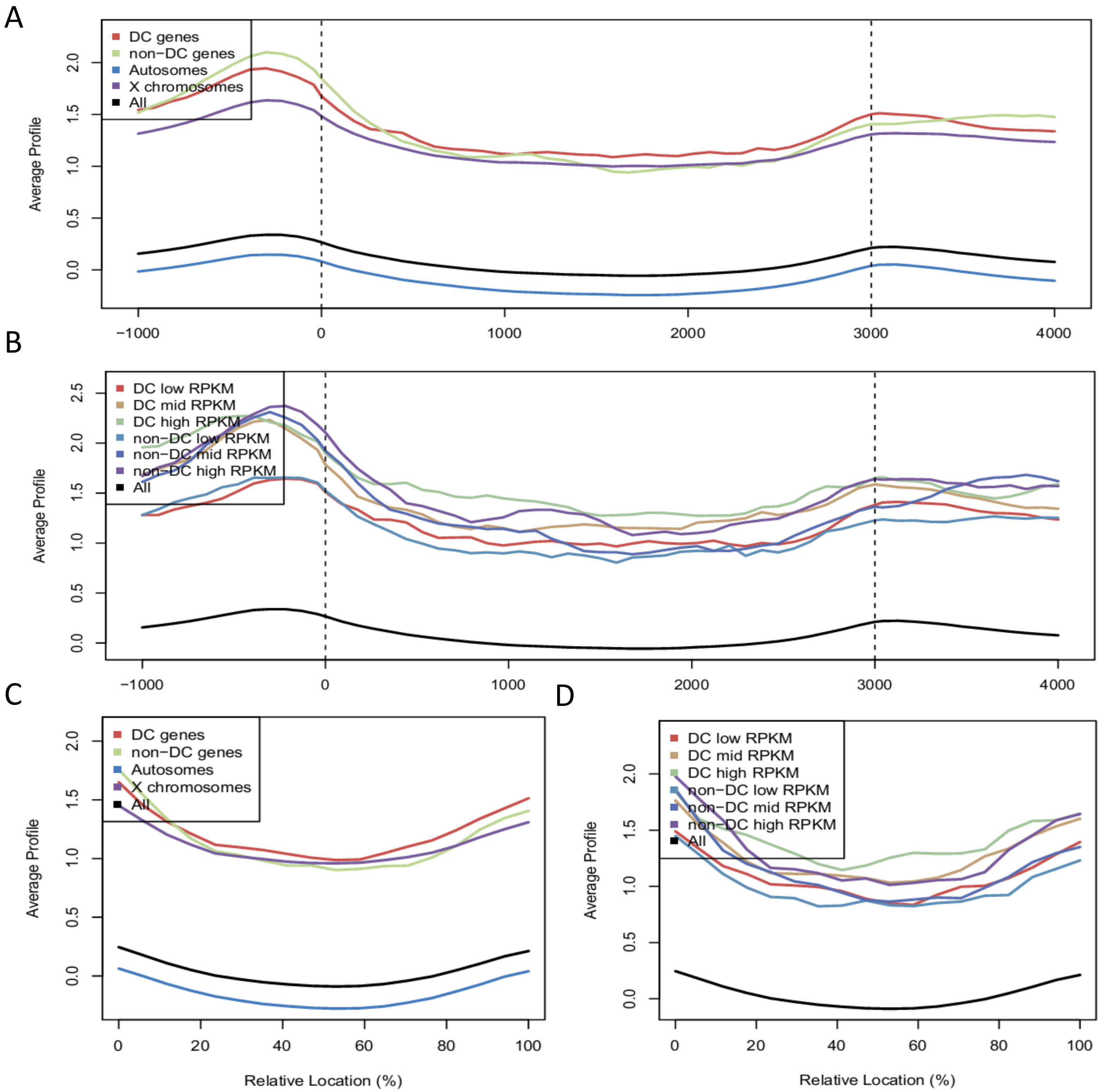

Figure 3.59. MIX-1, a DCC component, ME gene group and transcription level metagene analysis. Shown are metagenes (A & B) or concatenated exon signal profiles (C & D) for dosage compensated, non-dosage compensated, active autosomal, or active X-linked genes (A & C) or low, medium, and high expression dosage compensated and non-dosage compensated gene groups (B & D). Results show high levels at DC, non-DC, and active X-linked compared to autosomal genes in a manner only marginally consistent with gene expression.

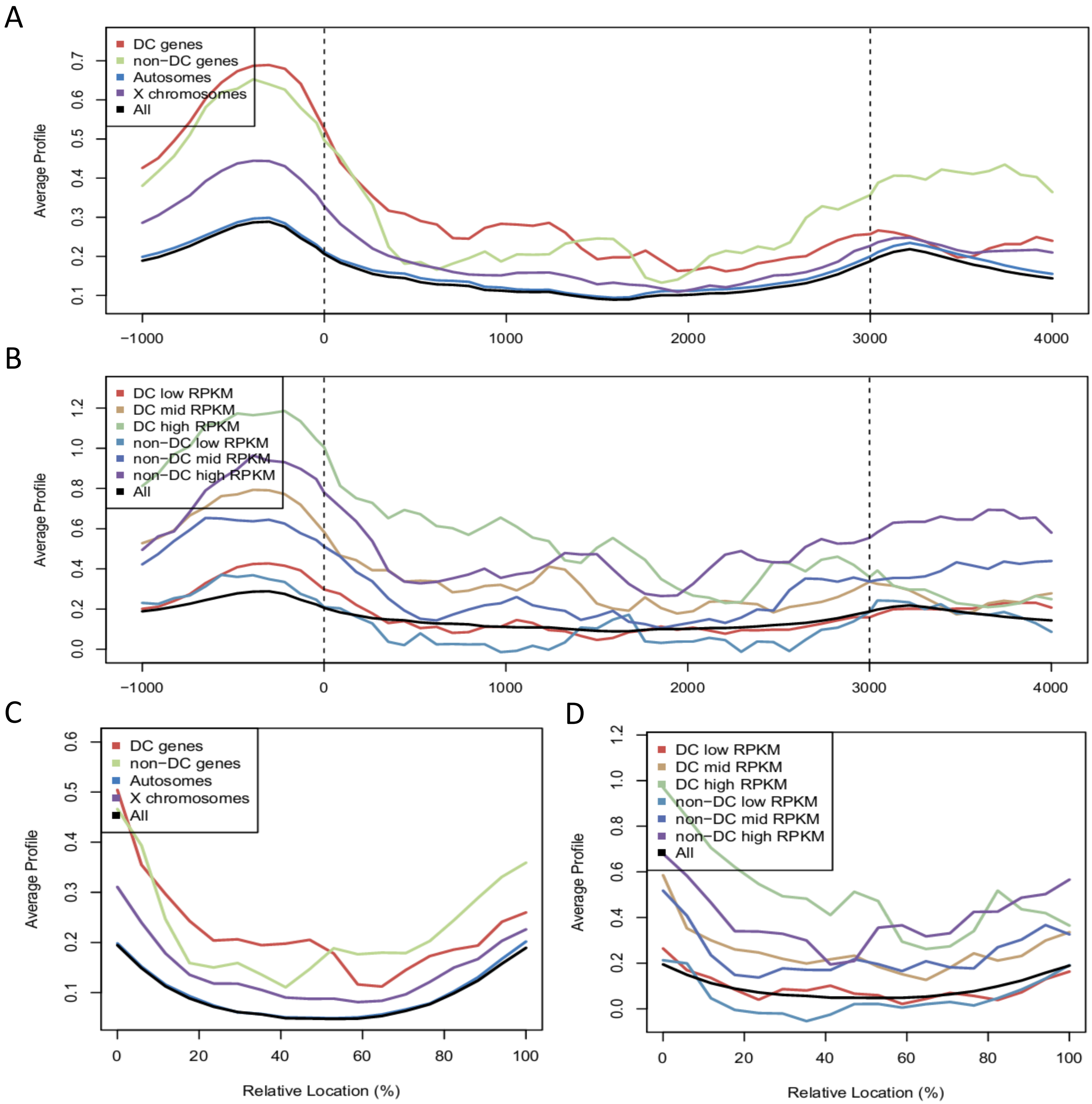

Figure 3.60. SDC-2, a DCC component, ME gene group and transcription level metagene analysis. Shown are metagenes x(A & B) or concatenated exon signal profiles (C & D) for dosage compensated, non-dosage compensated, active autosomal, or active X-linked genes (A & C) or low, medium, and high expression dosage compensated and non-dosage compensated gene groups (B & D). Results show high levels at DC, non-DC, and active X-linked compared to autosomal genes in a manner roughly consistent with gene expression.

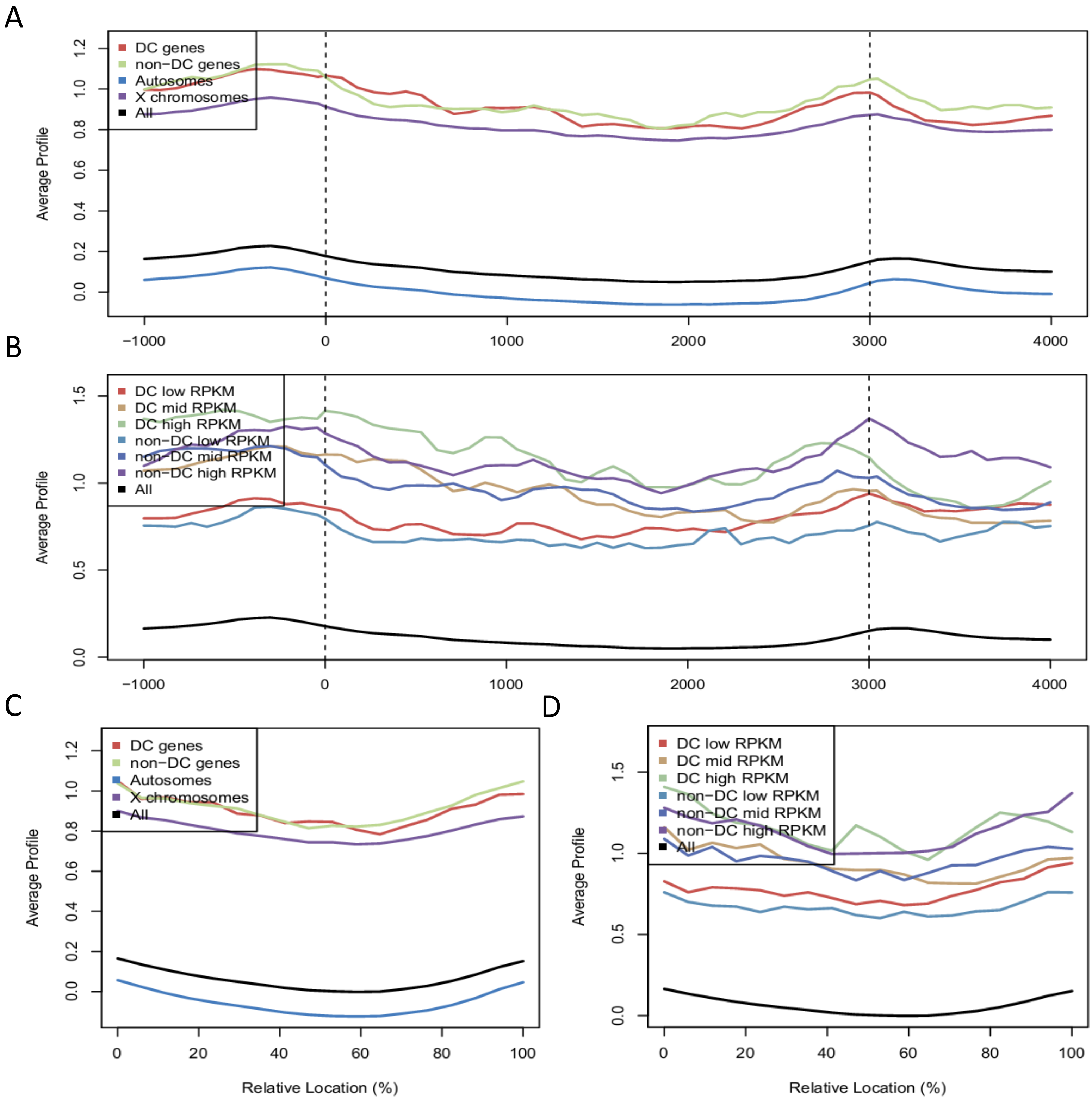

Figure 3.61. SDC-3, a DCC component, ME gene group and transcription level metagene analysis. Shown are metagenes (A & B) or concatenated exon signal profiles (C & D) for dosage compensated, non-dosage compensated, active autosomal, or active X-linked genes (A & C) or low, medium, and high expression dosage compensated and non-dosage compensated gene groups (B & D). Results show high levels at DC, non-DC, and active X-linked compared to autosomal genes in a manner roughly consistent with gene expression.

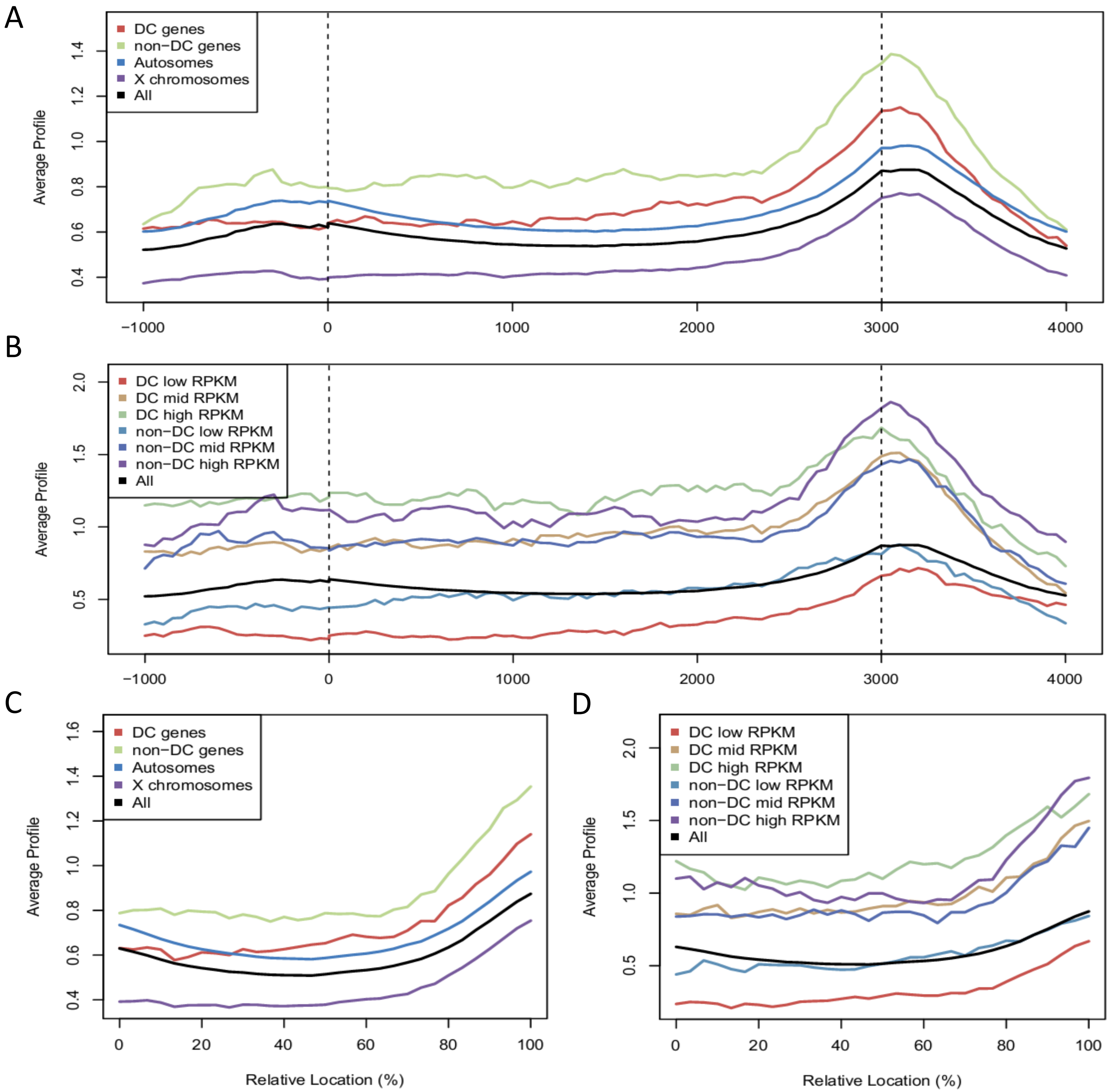

Figure 3.62. 8WG16, hypo-phosphorylated RNA polymerase II, EE gene group and transcription level metagene analysis. Shown are metagenes (A & B) or concatenated exon signal profiles (C & D) for dosage compensated, non-dosage compensated, active autosomal, or active X-linked genes (A & C) or low, medium, and high expression dosage compensated and non-dosage compensated gene groups (B & D). Results show somewhat lower levels at DC and active X-linked genes compared to non-DC and autosomal genes in a manner consistent with gene expression.

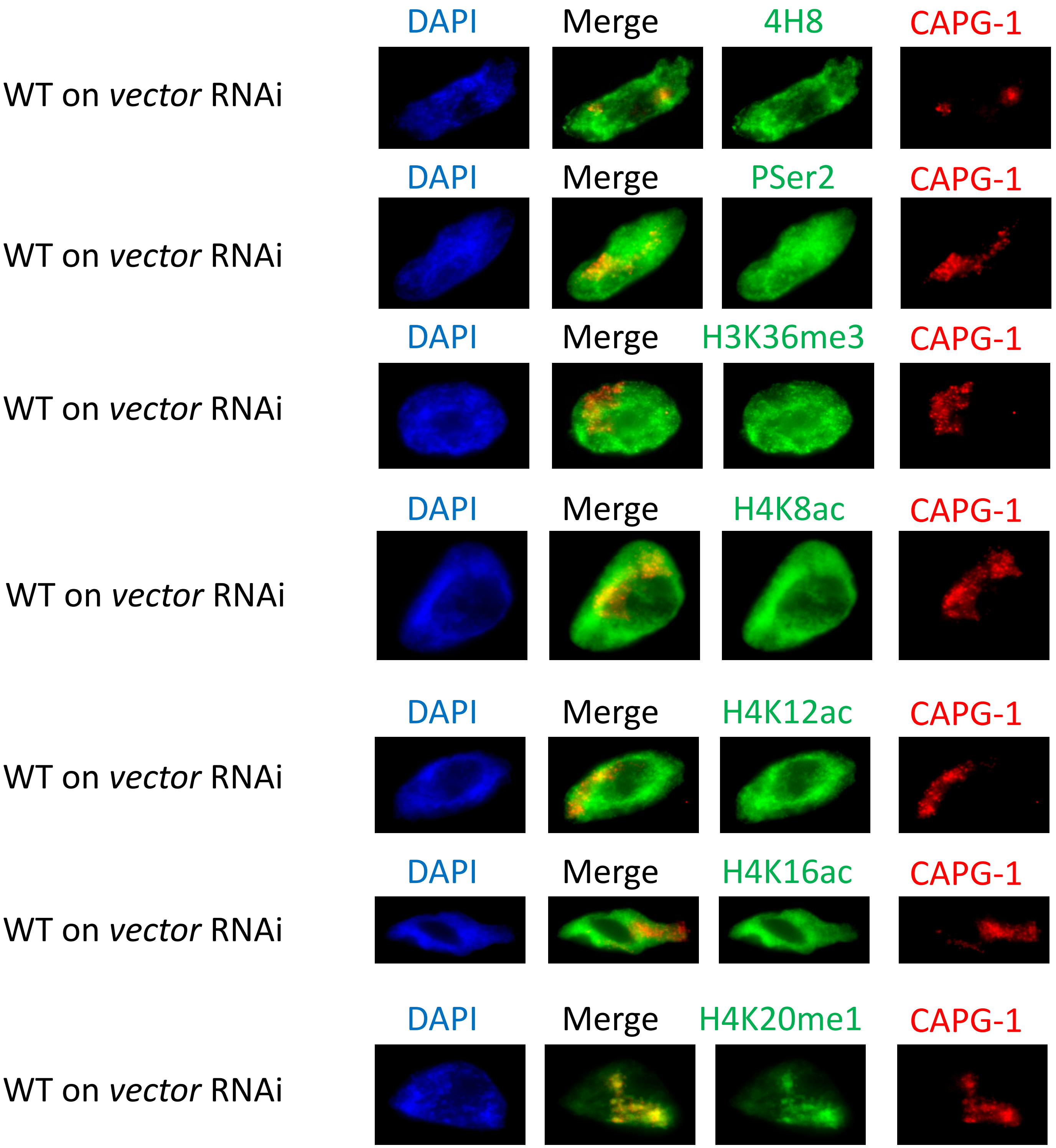

Figure 3.63. HAT effects on chromatin and RNA Pol II screen: *vector* RNAi controls. Shown are representative IF microscopy images from WT hermaphrodites treated with *vector* RNAi and stained with antibodies against RNA Pol II hypo-phosphorylation (4H8) or elongation (PSer2) or various histone modifications (as indicated) and antibodies to the DCC component CAPG-1. DAPI (DNA) is shown in blue. Results show low RNA Pol II hypo-phosphorylation, similar elongation, low or similar histone acetylation, and enriched H4K20me1 on X compared to autosomes.

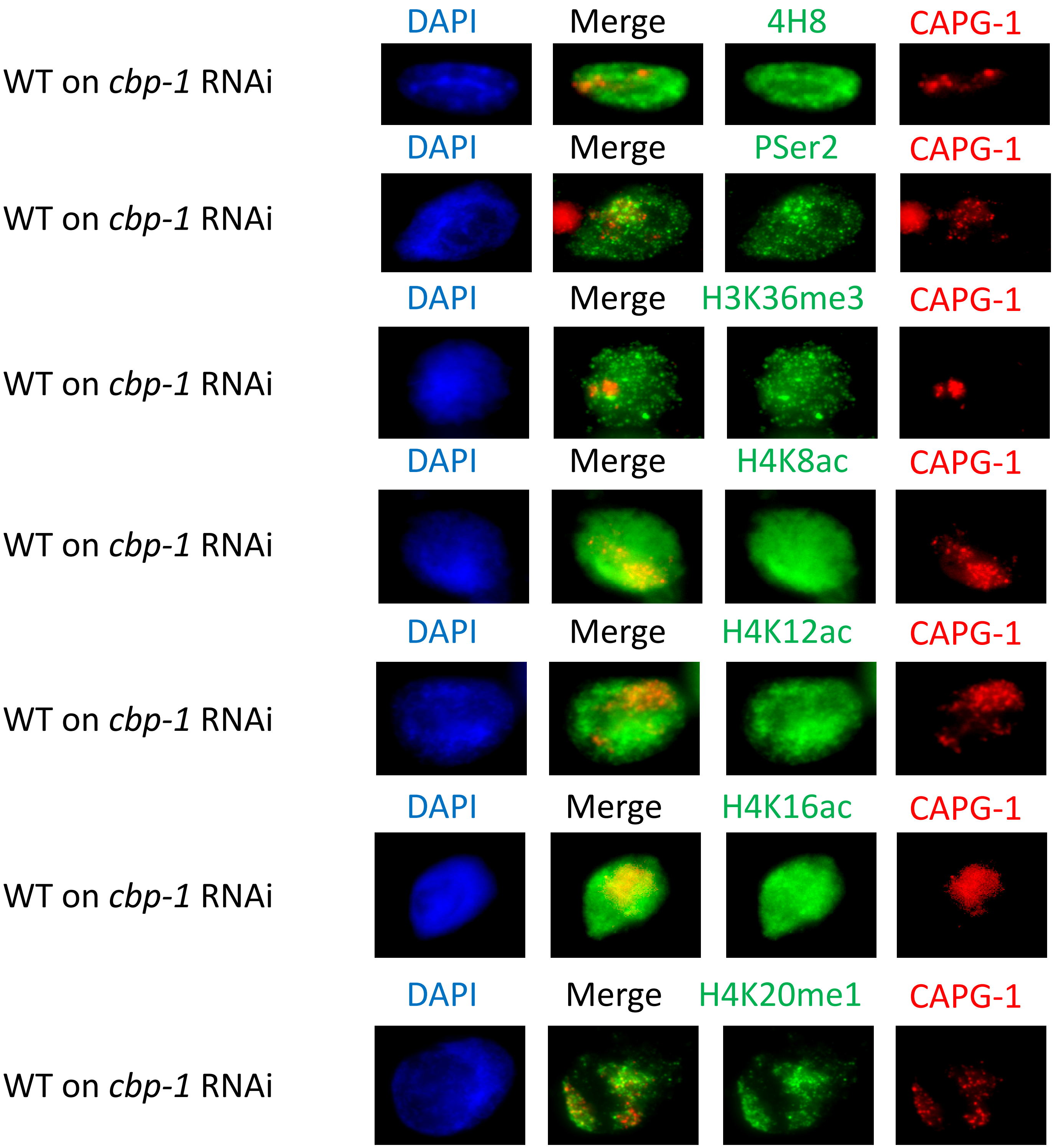

Figure 3.64. HAT effects on chromatin and RNA Pol II screen: *cbp-1* RNAi controls. Shown are representative IF microscopy images from WT hermaphrodites treated with *vector* RNAi and stained with antibodies against RNA Pol II hypo-phosphorylation (4H8) or elongation (PSer2) or various histone modifications (as indicated) and antibodies to the DCC component CAPG-1. DAPI (DNA) is shown in blue. Results show enriched PSer2 and minor H4K20me1 enrichment perturbation on the X chromosomes; all other markers appear similar to *vector* RNAi controls. Imaging assistance provided by Anna Cacciaglia.

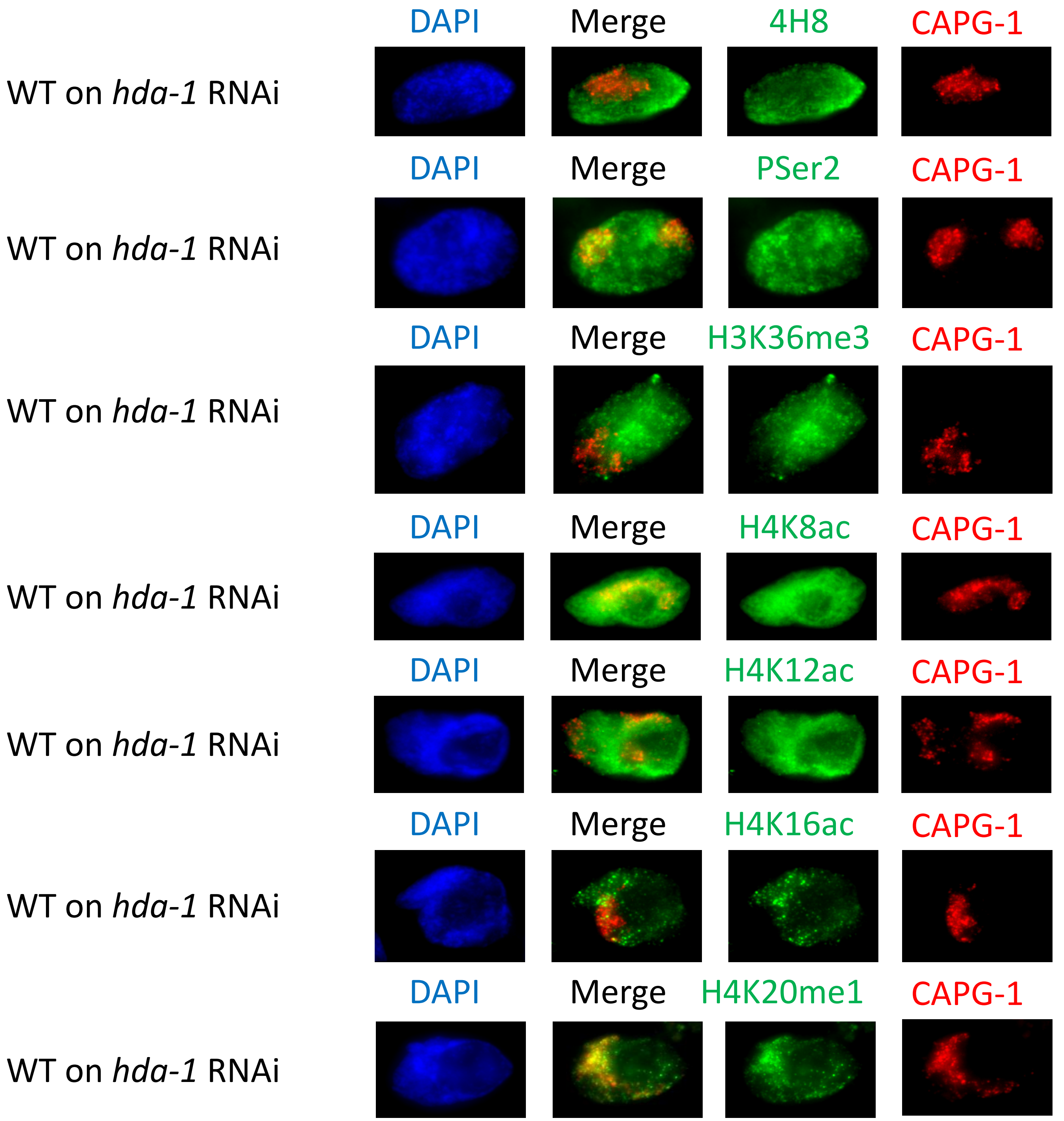

Figure 3.65. HAT effects on chromatin and RNA Pol II screen: *hda-1* RNAi controls. Shown are representative IF microscopy images from WT hermaphrodites treated with *vector* RNAi and stained with antibodies against RNA Pol II hypo-phosphorylation (4H8) or elongation (PSer2) or various histone modifications (as indicated) and antibodies to the DCC component CAPG-1. DAPI (DNA) is shown in blue. Results show RNA Pol II elongation enrichment on X, low levels of H4K16ac across the nucleus and similar levels of other staining compared to *vector* RNAi controls (Figure 3.63). Imaging assistance provided by Anna Cacciaglia.

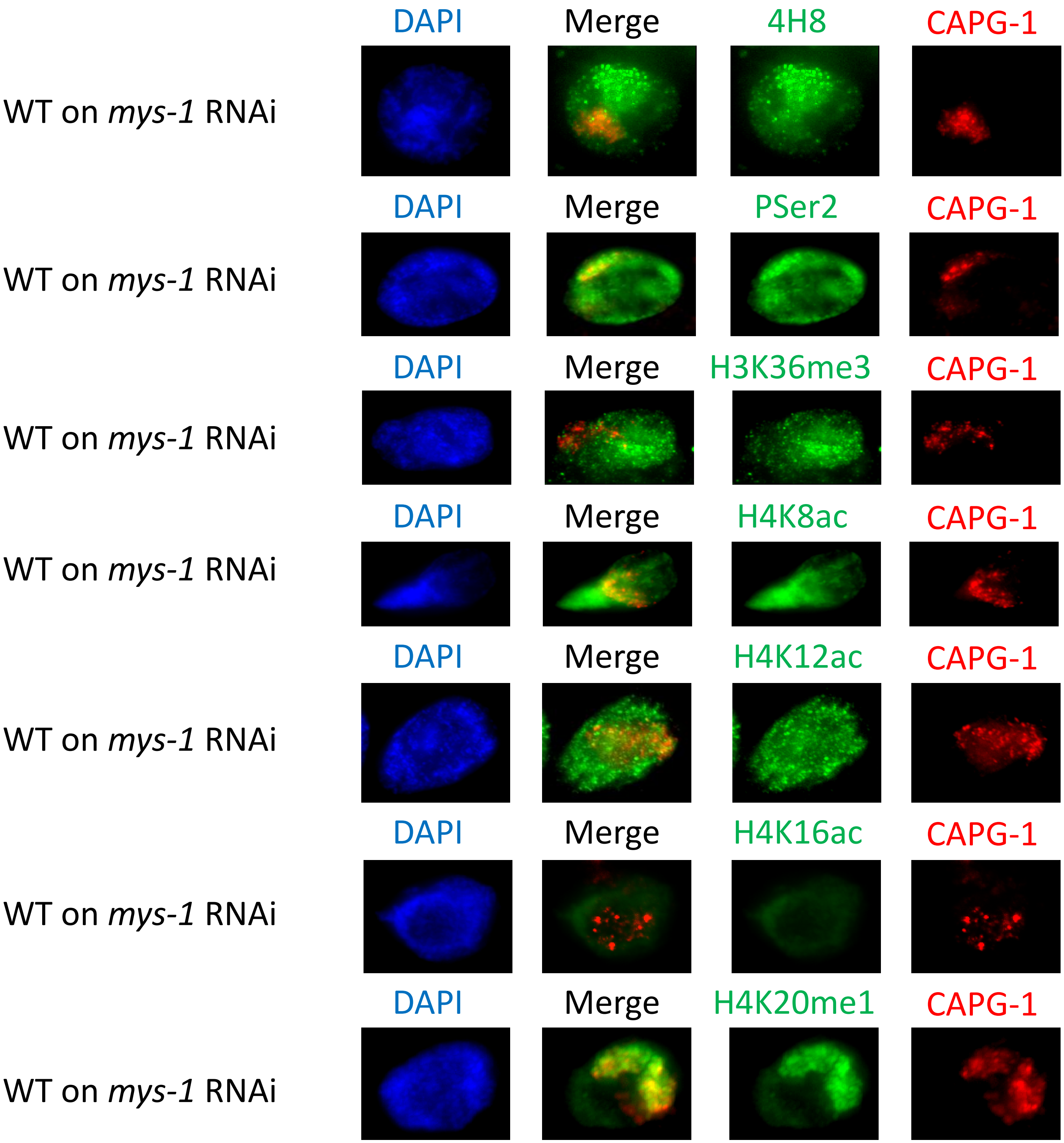

Figure 3.66. HAT effects on chromatin and RNA Pol II screen: *mys-1* RNAi controls. Shown are representative IF microscopy images from WT hermaphrodites treated with *vector* RNAi and stained with antibodies against RNA Pol II hypo-phosphorylation (4H8) or elongation (PSer2) or various histone modifications (as indicated) and antibodies to the DCC component CAPG-1. DAPI (DNA) is shown in blue. Results show enriched RNA Pol II elongation (PSer2) on X, reduced H4K12ac and H4K16ac across the nucleus, and similar staining of other markers as compared to *vector* RNAi controls (Figure 3.63).

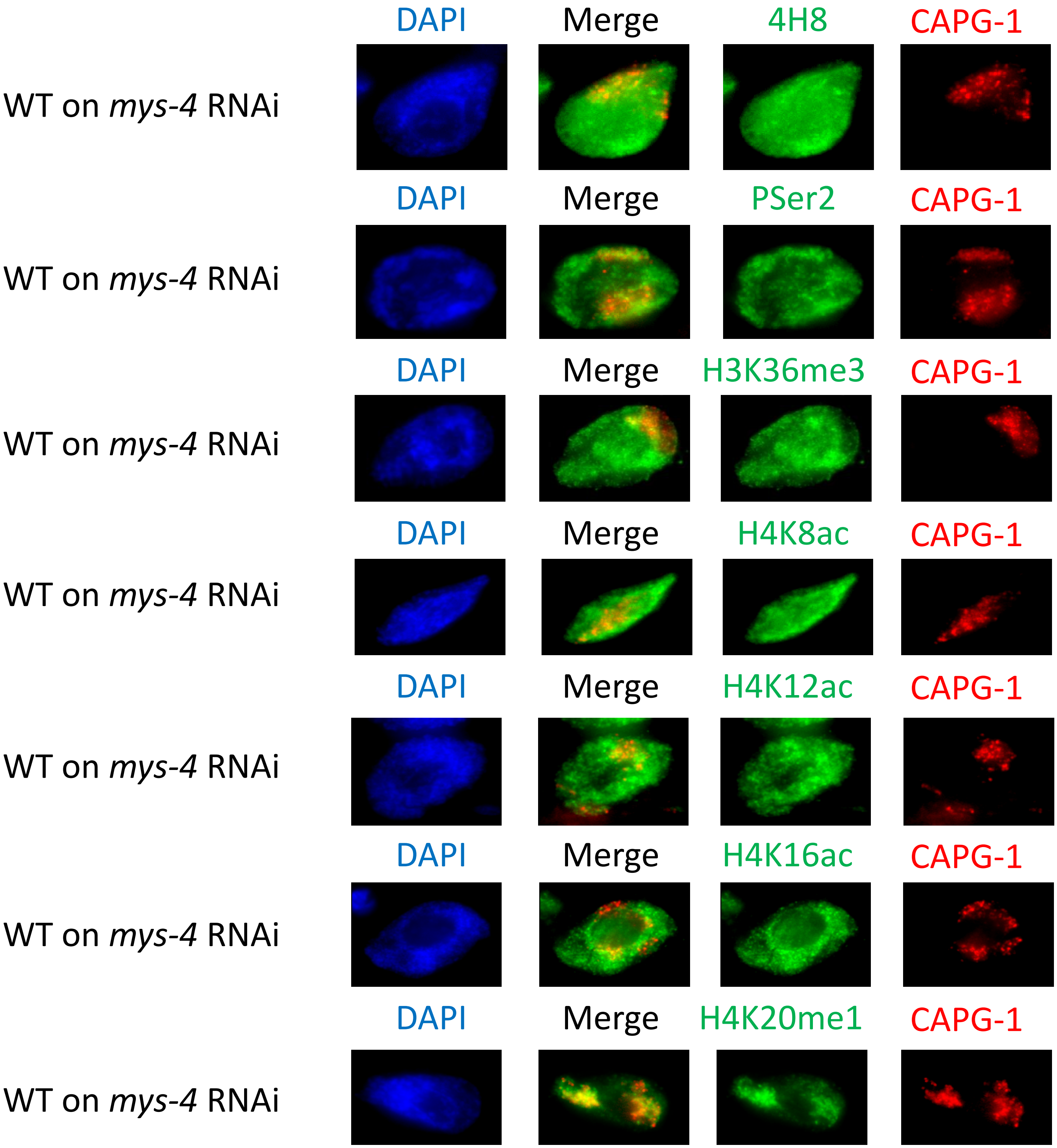

Figure 3.67. HAT effects on chromatin and RNA Pol II screen: *mys-4* RNAi controls. Shown are representative IF microscopy images from WT hermaphrodites treated with *vector* RNAi and stained with antibodies against RNA Pol II hypo-phosphorylation (4H8) or elongation (PSer2) or various histone modifications (as indicated) and antibodies to the DCC component CAPG-1. DAPI (DNA) is shown in blue. Results show reduced RNA Pol II elongation across the nucleus and loss of H4K16ac reduction on X, compared to *vector* RNAi controls (Figure 3.63). Imaging assistance provided by Anna Cacciaglia.

References

1. Al Nadaf S, Deakin JE, Gilbert C, Robinson TJ, Graves JA, et al. (2012) A cross-species comparison of escape from X inactivation in Eutheria: implications for evolution of X *chromosome inactivation. Chromosoma 121: 71-78.
2. Conrad T, Akhtar A (2012) Dosage compensation in Drosophila melanogaster: epigenetic fine-tuning of chromosome-wide transcription. Nat Rev Genet 13: 123-134.
3. Arthold S, Kurowski A, Wutz A (2011) Mechanistic insights into chromosome-wide silencing in X inactivation. Hum Genet 130: 295-305.
4. Escamilla-Del-Arenal M, da Rocha ST, Heard E (2011) Evolutionary diversity and developmental regulation of X-chromosome inactivation. Hum Genet 130: 307-327.
5. Okamoto I, Patrat C, Thepot D, Peynot N, Fauque P, et al. (2011) Eutherian mammals use diverse strategies to initiate X-chromosome inactivation during development. Nature 472: 370-374.
6. Meyer BJ (2010) Targeting X chromosomes for repression. Curr Opin Genet Dev 20: 179-189.
7. Csankovszki G, Petty EL, Collette KS (2009) The worm solution: a chromosome-full of condensin helps gene expression go down. Chromosome Res 17: 621-635.
8. Wells MB, Csankovszki G, Custer LM (2012) Finding a balance: how diverse dosage compensation strategies modify histone h4 to regulate transcription. Genet Res Int 2012: 795069.
9. Straub T, Becker PB (2011) Transcription modulation chromosome-wide: universal features and principles of dosage compensation in worms and flies. Curr Opin Genet Dev 21: 147-153.
10. Leeb M, Wutz A (2010) Mechanistic concepts in X inactivation underlying dosage compensation in mammals. Heredity 105: 64-70.
11. Baker BS, Gorman M, Marin I (1994) Dosage compensation in Drosophila. Annu Rev Genet 28: 491-521.
12. Prestel M, Feller C, Straub T, Mitlohner H, Becker PB (2010) The activation potential of MOF is constrained for dosage compensation. Mol Cell 38: 815-826.
13. Bashaw GJ, Baker BS (1996) Dosage compensation and chromatin structure in Drosophila. Curr Opin Genet Dev 6: 496-501.
14. Kotlikova IV, Demakova OV, Semeshin VF, Shloma VV, Boldyreva LV, et al. (2006) The Drosophila dosage compensation complex binds to polytene chromosomes independently of developmental changes in transcription. Genetics 172: 963-974.
15. Georgiev P, Chlamydas S, Akhtar A (2011) Drosophila dosage compensation: males are from Mars, females are from Venus. Fly (Austin) 5: 147-154.
16. Kelley RL, Solovyeva I, Lyman LM, Richman R, Solovyev V, et al. (1995) Expression of msl-2 causes assembly of dosage compensation regulators on the X chromosomes and female lethality in Drosophila. Cell 81: 867-877.
17. Morales V, Straub T, Neumann MF, Mengus G, Akhtar A, et al. (2004) Functional integration of the histone acetyltransferase MOF into the dosage compensation complex. EMBO J 23: 2258-2268.
18. Gorman M, Baker BS (1994) How flies make one equal two: dosage compensation in Drosophila. Trends Genet 10: 376-380.
19. Gorman M, Franke A, Baker BS (1995) Molecular characterization of the male-specific lethal-3 gene and investigations of the regulation of dosage compensation in Drosophila. Development 121: 463-475.

20. Franke A, Baker BS (1999) The rox1 and rox2 RNAs are essential components of the compensasome, which mediates dosage compensation in Drosophila. Mol Cell 4: 117-122.
21. Meller VH, Rattner BP (2002) The roX genes encode redundant male-specific lethal transcripts required for targeting of the MSL complex. EMBO J 21: 1084-1091.
22. Kind J, Vaquerizas JM, Gebhardt P, Gentzel M, Luscombe NM, et al. (2008) Genome-wide analysis reveals MOF as a key regulator of dosage compensation and gene expression in Drosophila. Cell 133: 813-828.
23. Smith ER, Pannuti A, Gu W, Steurnagel A, Cook RG, et al. (2000) The drosophila MSL complex acetylates histone H4 at lysine 16, a chromatin modification linked to dosage compensation. Mol Cell Biol 20: 312-318.
24. Smith ER, Allis CD, Lucchesi JC (2001) Linking global histone acetylation to the transcription enhancement of X-chromosomal genes in Drosophila males. J Biol Chem 276: 31483-31486.
25. Plath K, Fang J, Mlynarczyk-Evans SK, Cao R, Worringer KA, et al. (2003) Role of histone H3 lysine 27 methylation in X inactivation. Science 300: 131-135.
26. Shibata S, Yokota T, Wutz A (2008) Synergy of Eed and Tsix in the repression of Xist gene and X-chromosome inactivation. EMBO J 27: 1816-1826.
27. Maenner S, Blaud M, Fouillen L, Savoye A, Marchand V, et al. (2010) 2-D structure of the A region of Xist RNA and its implication for PRC2 association. PLoS Biol 8: e1000276.
28. Splinter E, de Wit E, Nora EP, Klous P, van de Werken HJ, et al. (2011) The inactive X chromosome adopts a unique three-dimensional conformation that is dependent on Xist RNA. Genes Dev 25: 1371-1383.
29. Csankovszki G, Collette K, Spahl K, Carey J, Snyder M, et al. (2009) Three distinct condensin complexes control C. elegans chromosome dynamics. Curr Biol 19: 9-19.
30. Tsai CJ, Mets DG, Albrecht MR, Nix P, Chan A, et al. (2008) Meiotic crossover number and distribution are regulated by a dosage compensation protein that resembles a condensin subunit. Genes Dev 22: 194-211.
31. Yonker SA, Meyer BJ (2003) Recruitment of C. elegans dosage compensation proteins for gene-specific versus chromosome-wide repression. Development 130: 6519-6532.
32. Lieb JD, Capowski EE, Meneely P, Meyer BJ (1996) DPY-26, a link between dosage compensation and meiotic chromosome segregation in the nematode. Science 274: 1732-1736.
33. Hsu DR, Meyer BJ (1994) The Dpy-30 Gene Encodes an Essential Component of the Caenorhabditis-Elegans Dosage Compensation Machinery. Genetics 137: 999-1018.
34. Chuang PT, Albertson DG, Meyer BJ (1994) DPY-27:a chromosome condensation protein homolog that regulates C. elegans dosage compensation through association with the X chromosome. Cell 79: 459-474.
35. DeLong L, Casson LP, Meyer BJ (1987) Assessment of X chromosome dosage compensation in Caenorhabditis elegans by phenotypic analysis of lin-14. Genetics 117: 657-670.
36. Meyer BJ, Casson LP (1986) Caenorhabditis elegans compensates for the difference in X chromosome dosage between the sexes by regulating transcript levels. Cell 47: 871-881.
37. Plenefisch JD, DeLong L, Meyer BJ (1989) Genes that implement the hermaphrodite mode of dosage compensation in Caenorhabditis elegans. Genetics 121: 57-76.
38. Csankovszki G (2009) Condensin function in dosage compensation. Epigenetics 4: 212-215.
39. Wells MB, Snyder MJ, Custer LM, Csankovszki G (2012) Caenorhabditis elegans dosage compensation regulates histone H4 chromatin state on X chromosomes. Mol Cell Biol 32: 1710-1719.

40. Pferdehirt RR, Kruesi WS, Meyer BJ (2011) An MLL/COMPASS subunit functions in the C. elegans dosage compensation complex to target X chromosomes for transcriptional regulation of gene expression. Genes Dev 25: 499-515.
41. Rawlings JS, Gatzka M, Thomas PG, Ihle JN (2011) Chromatin condensation via the condensin II complex is required for peripheral T-cell quiescence. EMBO J 30: 263-276.
42. Jans J, Gladden JM, Ralston EJ, Pickle CS, Michel AH, et al. (2009) A condensin-like dosage compensation complex acts at a distance to control expression throughout the genome. Genes Dev 23: 602-618.
43. Gosling KM, Goodnow CC, Verma NK, Fahrer AM (2008) Defective T-cell function leading to reduced antibody production in a kleisin-beta mutant mouse. Immunology 125: 208-217.
44. Gosling KM, Makaroff LE, Theodoratos A, Kim YH, Whittle B, et al. (2007) A mutation in a chromosome condensin II subunit, kleisin beta, specifically disrupts T cell development. Proc Natl Acad Sci U S A 104: 12445-12450.
45. Xu Y, Leung CG, Lee DC, Kennedy BK, Crispino JD (2006) MTB, the murine homolog of condensin II subunit CAP-G2, represses transcription and promotes erythroid cell differentiation. Leukemia 20: 1261-1269.
46. Bell O, Conrad T, Kind J, Wirbelauer C, Akhtar A, et al. (2008) Transcription-coupled methylation of histone H3 at lysine 36 regulates dosage compensation by enhancing recruitment of the MSL complex in Drosophila melanogaster. Mol Cell Biol 28: 3401-3409.
47. Sural TH, Peng S, Li B, Workman JL, Park PJ, et al. (2008) The MSL3 chromodomain directs a key targeting step for dosage compensation of the Drosophila melanogaster X chromosome. Nat Struct Mol Biol 15: 1318-1325.
48. Moore SA, Ferhatoglu Y, Jia Y, Al-Jiab RA, Scott MJ (2010) Structural and biochemical studies on the chromo-barrel domain of male specific lethal 3 (MSL3) reveal a binding preference for mono or dimethyl lysine 20 on histone H4. J Biol Chem.
49. Kim D, Blus BJ, Chandra V, Huang P, Rastinejad F, et al. (2010) Corecognition of DNA and a methylated histone tail by the MSL3 chromodomain. Nat Struct Mol Biol 17: 1027-1029.
50. Fauth T, Muller-Planitz F, Konig C, Straub T, Becker PB (2010) The DNA binding CXC domain of MSL2 is required for faithful targeting the Dosage Compensation Complex to the X chromosome. Nucleic Acids Res 38: 3209-3221.
51. Li F, Schiemann AH, Scott MJ (2008) Incorporation of the noncoding roX RNAs alters the chromatin-binding specificity of the Drosophila MSL1/MSL2 complex. Mol Cell Biol 28: 1252-1264.
52. Larschan E, Alekseyenko AA, Gortchakov AA, Peng S, Li B, et al. (2007) MSL complex is attracted to genes marked by H3K36 trimethylation using a sequence-independent mechanism. Mol Cell 28: 121-133.
53. Alekseyenko AA, Peng S, Larschan E, Gorchakov AA, Lee OK, et al. (2008) A sequence motif within chromatin entry sites directs MSL establishment on the Drosophila X chromosome. Cell 134: 599-609.
54. Kageyama Y, Mengus G, Gilfillan G, Kennedy HG, Stuckenholz C, et al. (2001) Association and spreading of the Drosophila dosage compensation complex from a discrete roX1 chromatin entry site. EMBO J 20: 2236-2245.
55. Prabhakaran M, Kelley RL (2010) A new strategy for isolating genes controlling dosage compensation in Drosophila using a simple epigenetic mosaic eye phenotype. BMC Biol 8: 80.

56. Jans J, Gladden JM, Ralston EJ, Pickle CS, Michel AsH, et al. (2009) A condensin-like dosage compensation complex acts at a distance to control expression throughout the genome. Genes & Development 23: 602-618.
57. Ercan S, Dick LL, Lieb JD (2009) The C. elegans dosage compensation complex propagates dynamically and independently of X chromosome sequence. Curr Biol 19: 1777-1787.
58. Petty E, Laughlin E, Csankovszki G (2011) Regulation of DCC localization by HTZ-1/H2A.Z and DPY-30 does not correlate with H3K4 methylation levels. PLoS ONE 6: e25973.
59. Petty EL, Collette KS, Cohen AJ, Snyder MJ, Csankovszki G (2009) Restricting dosage compensation complex binding to the X chromosomes by H2A.Z/HTZ-1. PLoS Genet 5: e1000699.
60. Gerstein MB, Lu ZJ, Van Nostrand EL, Cheng C, Arshinoff BI, et al. (2010) Integrative analysis of the Caenorhabditis elegans genome by the modENCODE project. Science 330: 1775-1787.
61. Liu T, Rechtsteiner A, Egelhofer TA, Vielle A, Latorre I, et al. (2011) Broad chromosomal domains of histone modification patterns in C. elegans. Genome Res 21: 227-236.
62. Grant CE, Bailey TL, Noble WS (2011) FIMO: scanning for occurrences of a given motif. Bioinformatics 27: 1017-1018.
63. Machanick P, Bailey TL (2011) MEME-ChIP: motif analysis of large DNA datasets. Bioinformatics 27: 1696-1697.
64. Bailey TL, Boden M, Buske FA, Frith M, Grant CE, et al. (2009) MEME SUITE: tools for motif discovery and searching. Nucleic Acids Res 37: W202-208.
65. Liu T, Ortiz JA, Taing L, Meyer CA, Lee B, et al. (2011) Cistrome: an integrative platform for transcriptional regulation studies. Genome Biol 12: R83.
66. Blauwkamp TA, Csankovszki G (2009) Two classes of dosage compensation complex binding elements along Caenorhabditis elegans X chromosomes. Mol Cell Biol 29: 2023-2031.
67. Hoffman BG, Robertson G, Zavaglia B, Beach M, Cullum R, et al. (2010) Locus co-occupancy, nucleosome positioning, and H3K4me1 regulate the functionality of FOXA2-, HNF4A-, and PDX1-bound loci in islets and liver. Genome Research 20: 1037-1051.
68. Bonn S, Zinzen RP, Girardot C, Gustafson EH, Perez-Gonzalez A, et al. (2012) Tissue-specific analysis of chromatin state identifies temporal signatures of enhancer activity during embryonic development. Nat Genet 44: 148-156.
69. Pferdehirt RR (2011) Targeting X Repression : Recruitment, Binding and Function of the C. elegans Dosage Compensation Complex. Berkeley, CA,. pp. 197 leaves.
70. Zinovyeva AY, Graham SM, Cloud VJ, Forrester WC (2006) The C. elegans histone deacetylase HDA-1 is required for cell migration and axon pathfinding. Dev Biol 289: 229-242.
71. Yuan H, Rossetto D, Mellert H, Dang W, Srinivasan M, et al. (2011) MYST protein acetyltransferase activity requires active site lysine autoacetylation. EMBO J.
72. Lu L, Li L, Lv X, Wu XS, Liu DP, et al. (2011) Modulations of hMOF autoacetylation by SIRT1 regulate hMOF recruitment and activities on the chromatin. Cell Res 21: 1182-1195.
73. Edmunds JW, Mahadevan LC, Clayton AL (2008) Dynamic histone H3 methylation during gene induction: HYPB/Setd2 mediates all H3K36 trimethylation. EMBO J 27: 406-420.
74. Liu XS, Meyer CA (2009) ChIP-Chip: algorithms for calling binding sites. Methods Mol Biol 556: 165-175.
75. Liu T, Rechtsteiner A, Egelhofer TA, Vielle A, Latorre I, et al. (2010) Broad chromosomal domains of histone modification patterns in C. elegans. Genome Res.
76. Chepelev I, Wei G, Wangsa D, Tang Q, Zhao K (2012) Characterization of genome-wide enhancer-promoter interactions reveals co-expression of interacting genes and modes of higher order chromatin organization. Cell Res.

77. Li G, Ruan X, Auerbach RK, Sandhu KS, Zheng M, et al. (2012) Extensive promoter-centered chromatin interactions provide a topological basis for transcription regulation. Cell 148: 84-98.
78. Moiseeva ED, Tchurikov NA (2011) Study of the effects of enhancer and insulator on the chromatin structure in Drosophila melanogaster. Dokl Biochem Biophys 437: 60-63.
79. Dean A (2011) In the loop: long range chromatin interactions and gene regulation. Brief Funct Genomics 10: 3-10.
80. Ong CT, Corces VG (2011) Enhancer function: new insights into the regulation of tissue-specific gene expression. Nat Rev Genet 12: 283-293.
81. Sapountzi V, Cote J (2011) MYST-family histone acetyltransferases: beyond chromatin. Cell Mol Life Sci 68: 1147-1156.
82. Fuda NJ, Ardehali MB, Lis JT (2009) Defining mechanisms that regulate RNA polymerase II transcription in vivo. Nature 461: 186-192.
83. Clarke AS, Samal E, Pillus L (2006) Distinct roles for the essential MYST family HAT Esa1p in transcriptional silencing. Mol Biol Cell 17: 1744-1757.
84. Akhtar A, Becker PB (2000) Activation of transcription through histone H4 acetylation by MOF, an acetyltransferase essential for dosage compensation in Drosophila. Mol Cell 5: 367-375.
85. Cai Y, Jin J, Swanson SK, Cole MD, Choi SH, et al. (2010) Subunit composition and substrate specificity of a MOF-containing histone acetyltransferase distinct from the male-specific lethal (MSL) complex. J Biol Chem 285: 4268-4272.
86. Raja SJ, Charapitsa I, Conrad T, Vaquerizas JM, Gebhardt P, et al. (2010) The nonspecific lethal complex is a transcriptional regulator in Drosophila. Mol Cell 38: 827-841.
87. Wilds CJ, Wawrzak Z, Krishnamurthy R, Eschenmoser A, Egli M (2002) Crystal structure of a B-form DNA duplex containing (L)-alpha-threofuranosyl (3'-->2') nucleosides: a four-carbon sugar is easily accommodated into the backbone of DNA. J Am Chem Soc 124: 13716-13721.
88. Drew HR, Wing RM, Takano T, Broka C, Tanaka S, et al. (1981) Structure of a B-DNA dodecamer: conformation and dynamics. Proc Natl Acad Sci U S A 78: 2179-2183.
89. Eichler EE, Archidiacono N, Rocchi M (1999) CAGGG repeats and the pericentromeric duplication of the hominoid genome. Genome Res 9: 1048-1058.
90. Eichler EE, Lu F, Shen Y, Antonacci R, Jurecic V, et al. (1996) Duplication of a gene-rich cluster between 16p11.1 and Xq28: a novel pericentromeric-directed mechanism for paralogous genome evolution. Hum Mol Genet 5: 899-912.
91. Weitzmann MN, Woodford KJ, Usdin K (1998) The mouse Ms6-hm hypervariable microsatellite forms a hairpin and two unusual tetraplexes. J Biol Chem 273: 30742-30749.
92. Eddy J, Maizels N (2008) Conserved elements with potential to form polymorphic G-quadruplex structures in the first intron of human genes. Nucleic Acids Res 36: 1321-1333.
93. Eddy J, Vallur AC, Varma S, Liu H, Reinhold WC, et al. (2011) G4 motifs correlate with promoter-proximal transcriptional pausing in human genes. Nucleic Acids Res 39: 4975-4983.
94. Eddy J, Maizels N (2006) Gene function correlates with potential for G4 DNA formation in the human genome. Nucleic Acids Res 34: 3887-3896.

CHAPTER 4

The *Caenorhabditis elegans* DCC Regulates RNA Polymerase II Activity at Multiple Points in the Transcription Cycle

Abstract

Dosage compensation equalizes X-linked gene expression between the sexes. In *Caenorhabditis elegans*, the dosage compensation complex (DCC) binds both X chromosomes in hermaphrodites and downregulates their gene expression by half, to equal X-linked product levels in males. Recent work has suggested that the DCC regulates levels of RNA polymerase II on the X chromosomes, but no further details of the mechanism of dosage compensation regulation of transcription are known. In this study, we demonstrate that DCC function acts on RNA Pol II at multiple points in the transcription cycle. Specifically, while the DCC does not restrict RNA Pol II loading onto X, we see DCC member-dependent restriction of initiation, the transition to elongation, and evidence for additional action on elongating RNA Pol II. Through a combination of live-imaging with FRAP (fluorescence recovery after photobleaching) microscopy; immunofluorescence and immunoFISH; and analysis of ChIP-chip, ChIP-seq, and RNA-seq datasets, we provide significant and substantial insights into the mechanism of transcriptional regulation on the X chromosomes by the DCC in *C. elegans*.

Introduction

Maintenance of proper gene expression levels is a complex and essential undertaking. One of two major determinants of gene expression levels is chromosome copy number. Aberrations in chromosome number are typically lethal [1-3], but those that are less severe still result in detrimental phenotypes for the organism. For example, Down syndrome in humans is due to the presence of three copies of chromosome 21 (trisomy 21) per nucleus and is characterized by substantial cognitive and developmental defects [1,4-10].

One important difference in chromosome number that must be accommodated in many organisms involves the X chromosome. A number of organisms utilize a chromosome-based method of sex determination, e.g. males have one X while females have two copies of X. X-linked gene expression between the sexes must be equalized at a proper level for viability of both sexes. This regulation of X is achieved by a process known as dosage compensation [11-25]. Dosage compensation is achieved by different mechanisms in various species [12,15,24-34] and has been most thoroughly studied in three systems.

In flies, the single male X chromosome is upregulated two-fold by the MSL complex [18,24,25,35-42]; the MSL complex subunit MOF hyperacetylates histone H4 lysine 16 leading to increased transcription [43-45]. H4K16ac is the only histone modification known to single-handedly change chromatin structure, making chromatin more open by disrupting formation of the 30nm fiber [46]. Multiple studies have demonstrated that H4K16 hyperacetylation, along with the activity of JIL-1 kinase (H3S10ph), on the male X in flies increases transcriptional output [47-50], and a major component of this enhancement is increased transcriptional elongation by RNA polymerase II [51].

In mammals, one X chromosome in female cells is transcriptionally silenced by the non-coding RNA *Xist* and the co-repressors that it recruits, including the Polycomb group proteins [52-55]. The inactivated X is the paternal X in mice and is chosen randomly in humans [56-60]. Certain genes escape X inactivation, and their biallelic expression is thought to be important for maintaining differences between the sexes [61-69]. The active X is occupied by RNA polymerase and a suite of active chromatin modifications, including histone H4 acetylation marks [15,70-80].

In contrast, the inactive X chromosome lacks RNA polymerase II and displays high levels of DNA methylation and repressive histone modifications, such as H3K27me3 [15,70-82]. *Xist* and the noncoding RNA *Tsix*, which is antisense to *Xist* and prevents *Xist* expression on the active X, reside in the *Xic* (X inactivation center) [83,84]. Recent work has demonstrated that the *Xic* and other regions of both X chromosomes contain blocks of co-regulated genes that associate in three-dimensional space (termed TADs), which possess, but do not require, similar histone modification profiles [83].

Finally, in worms such as *Caenorhabditis elegans*, both X chromosomes in hermaphrodite cells are downregulated by half through the action of the dosage compensation complex, or DCC [85-87]. The DCC is composed of two parts, a five-subunit condensin-like complex (Condensin I^{DC}), which includes: two enzymatic CAP (chromosome-associated polypeptide) proteins (MIX-1, DPY-27) and three regulatory SMC proteins (CAPG-1, DPY-26, and DPY-28) [88-93], and a recruitment complex composed of: SDC-1, SDC-2, and SDC-3 along with two additional proteins, DPY-21 and DPY-30 [94-103]. DCC occupancy on X is thought to be achieved in a two-step process: 1) the recruitment complex binds a set of highly attractive foci on X, denoted by the presence of a MEX motif, and binds the rest of the DCC [104]; 2) the DCC then spreads, dependent upon transcription to many promoters, genic, and downstream sites across the X chromosomes [105]. Overall DCC distribution and occupancy, but not recruitment site levels, depends on the particular transcriptional program at work in cells during different stages of development [105], which is not the case in *Drosophila* [37]. Condensin I^{DC} homology to condensin [106,107], the conserved meiotic and mitotic chromosome organization contributor, suggests that dosage compensation occurs in *C. elegans* through changes in X structure. Our prior work uncovered DCC-directed regulation of two histone H4 modifications, decreased H4K16ac and increased H4K20me1 [108,109], to maintain a repressive chromatin environment on the X chromosomes [110]. Previous work from our lab and others has identified the histone variant HTZ-1 (H2A.Z) as an important contributor to dosage compensation that is depleted on X [111-113]. Other work has also demonstrated regulation of overall RNA polymerase levels on X by the DCC [114], but no further details were uncovered.

A second major contributor to gene expression is transcriptional regulation. Transcription by RNA polymerase II occurs in a well-described cycle [115-118]. Activator proteins open promoter chromatin for general transcription factors to bind, which then recruit the Mediator complex and RNA polymerase II [115-118]. CDK-7 (TFIIH) phosphorylates RNA Pol II at the serine 5 residues of its C-terminal domain (CTD) [115-118]. RNA Pol II can now break free of the pre-initiation complex and traverse the promoter to the transcription start site, where it initiates transcription [115-118]. The early elongation that follows is unstable, or abortive, to a high degree, until the nascent transcript reaches 28 nucleotides in length [119-121]. The nascent transcript attracts and facilitates binding of the stalling and elongation factor DSIF to RNA Pol II [122], and DSIF then recruits the transcriptional repressor NELF complex to RNA Pol II [122]. RNA polymerase pausing has been demonstrated in many organisms, occurring around 50 to 100bp downstream of the transcription start site [116,123,124]. H4K16ac, H3S10ph (in some systems), and BRD proteins, along with DSIF and NELF, facilitate recruitment of the positive elongation factor P-TEFb [49,125-127]. CDK-9, a component of P-TEFb, phosphorylates the serine 2 residues of the RNA Pol II CTD and DSIF, releasing NELF and signaling the transition to productive elongation through the gene [127,128]. Soon after serine 2 phosphorylation begins, serine 5 phosphorylation is increasingly removed by particular CTD phosphatases. Serine 2 phosphorylation peaks in the 3’ end of the gene body [115,129]. During elongation, TFIIS functions to promote elongation by rescuing RNA Pol II from an arrested state, characterized by transient motion of the polymerase along DNA and misalignment of the nascent transcript to the RNA Pol II active site [130].

Transcriptional regulation is a conserved function of dosage compensation. In flies, dosage compensation increases RNA Pol II elongation for increased transcription on the male X [51]. In mammals, *Xist* and its cofactors cause RNA Pol II exclusion and the cessation of transcription at inactive X genes [81,82]. In worms, it is known that transcription plays a key role in the spreading of the DCC [105], and the DCC regulates levels of RNA Pol II on hermaphrodite X chromosomes [131]. Our study identifies the stages of X-linked transcription affected by DCC-mediated repression in worms.

Results

The goal of this work was to determine the steps of transcription regulated by DCC components. Figure 4.8 is a schematic diagram depicting the steps in transcription investigated. We began by examining a strain that expresses AMA-1, the large subunit of RNA polymerase II, tagged with GFP (OP34). AMA-1 signal was clearly visible and punctate across the nucleus with *vector* RNAi treatment, while *ama-1* RNAi abrogated the RNA Pol II GFP signal, as expected (Figure 4.1A). Consistent with prior work concerning RNA Pol II elongation [114], DCC localization was severely compromised after *ama-1* RNAi treatment (Figure 4.1A). *dpy-27* (Figure 4.1A) and several other DCC and chromatin modifier RNAi treatments (Figure 4.10A) did not change GFP fluorescence levels. Surprisingly, given that these worms reach adulthood, *sdc-2* RNAi treatment (Figure 4.10A) led to complete loss of AMA-1::GFP staining. A significant increase in AMA-1::GFP signal was seen with *sdc-3* or *dpy-21* RNAi such that exposure times were decreased by half to achieve the same level of maximum signal output. Interestingly, SDC-3, but not SDC-2, shows a unique enrichment over *ama-1* introns (Figure 4.11A), as opposed to the typical pattern of a peak of enrichment upstream of nearby genes (e.g. *kin-25*), and *ama-1* shows an upstream DCC binding peak (Figure 4.11B). Using live-imaging and FRAP microscopy, we observed AMA-1::GFP dynamics across the nucleus. Following photobleaching (marked by yellow ROI box), approximately half of all nuclei assayed (16/36) showed a region (marked by a red arrow) from which AMA-1::GFP does not redistribute to the rest of the nucleus (Figure 4.1B), while the remainder do show complete redistribution of AMA-1::GFP across the nucleus. This implies greatly reduced RNA Pol II dynamics on the X chromosomes. Metagene analysis of ChIP-chip data acquired using an antibody raised against a part of RNA Pol II outside of the CTD (AMA-1 CTD-independent) shows similar occupancy at DC and non-DC or active X and A (Figure 4.10C), further indicating that DCC function does not restrict RNA Pol II loading at DC genes. These data suggest that dosage compensation does not restrict RNA Pol II loading on X and suggest that DPY-21, SDC-2, and SDC-3 may play a direct role in AMA-1 regulation.

To gain further insight, we sought to manually quantify bulk RNA Pol II at promoters and over genes at high-resolution. First, we validated our manual quantification method for ChIP-seq data using a DPY-27::GFP mixed embryo dataset. Consistent with our previously published DPY-27 ChIP-chip metagene analysis [110], DPY-27::GFP occupancy is higher on X than autosomes and slightly higher at non-dosage compensated gene upstream regions than dosage compensated gene upstream regions (Figure 4.2A; Student's t-test, $p<0.05$). We then applied this method to the AMA-1::GFP late embryo ChIP-seq dataset. Results showed a significantly higher bulk RNA Pol II between 1kb, but not 500bp, upstream of autosomal compared to X-linked genes (Figure 4.2B; Student's t-test, $p<0.05$). These data indicate that RNA Pol II loading differences on X is minor, even at high resolution, and no difference between dosage compensated and non-dosage compensated genes was observed.

We next turned our attention to the 8WG16 antibody, which recognizes hypo-phosphorylated RNA Pol II (all RNA Pol II except for CTD repeats marked by serine 2 phosphorylation), used for ChIP-chip analysis by other groups [131]. A genome browser view of DCC recruitment elements shows a strong increase in 8WG16 ChIP-chip [131] signal height, and spreading - even in the absence of immediately proximal transcription, with loss of dosage compensation function by *sdc-2* RNAi (Figure 4.2C). When expanding this view to look at all *rex* sites, *dox* sites, or all DPY-27 ChIP-seq binding peaks using SitePro analysis, all categories showed increased 8WG16, and *dox* sites showed the greatest increase in signal (Figure 4.2D). These data strongly argue that dosage compensation limits RNA Pol II initiation on the X chromosomes.

To look for effects of dosage compensation on transcript production, we analyzed WT early or late embryo and L3 RNA-seq datasets generated by the modENCODE consortium. In late embryos, transcript production severely drops just downstream of the transcript start site at DC, but not non-DC, active X, or active autosomal genes (Figure 4.3A) or concatenated exons (Figure 4.3C), and similar differences are seen in the L3 dataset (Figure 4.13). This drop is not seen in the early-biased embryo dataset (Figures 4.12A, C), consistent with a smaller proportion of dosage compensated tissue and reduced levels of transcription overall. The early elongation disruption at dosage compensated genes was also seen across DC and non-DC gene groupings by RPKM value in the late-biased embryo (Figures 4.3B, D) and larval stage 3 (Figures 4.13B, D) samples, but not an early-biased embryo (Figures 4.12B, D) dataset. These data suggest that dosage compensation also restricts early Pol II elongation specifically at dosage compensated genes.

To further explore this conclusion, we used antibodies against RNA Pol II CTD serine 5 phosphorylation (PSer5) as a marker of initiated RNA Pol II. Using IF microscopy, we validated the specificity of this antibody (Figure 4.14) by RNAi treatment against RNA Pol II and CTD kinases. We then found that PSer5 staining was punctate and found across the nucleus in WT animals (Figures, 4.4A, B). To our surprise, loss of function in one DCC component, DPY-21, resulted in undetectable PSer5 signal across the nucleus (Figure 4.4A). Because *dpy-21(e428)* mutants are alive, and we observe elongating RNA Pol II signal (Figure 4.16B; discussed below), we interpret these data to suggest that DPY-21 regulates PSer5 accessibility, possibly also governing the transition from initiated to elongating RNA Pol II genome-wide. Thus, DPY-21 is unique among DCC proteins in its seeming control over a slower transition for RNA Pol II to an elongation state, and this activity is enriched on the X chromosomes in hermaphrodites by the DCC as a whole.

Previous work [132] identified three histone modifications (H3K4me2, H3K79me2, and H3K79me3) that are tightly correlated with gene expression. We used these marks as a means to interrogate RNA Pol II elongation. Metagene analysis indicates that each mark is 1.5-2.5-fold enriched at non-DC over DC genes (Figure 4.15). We expanded this analysis of RNA Pol II elongation to include DCC and chromatin regulator effects on PSer2 levels. First, we showed that the PSer2 antibody is specific (Figures 4.14B, C). We found that PSer2 levels are similar across the nucleus in WT animals (Figure 4.16). Using fluorescence intensity quantification, results show increased PSer2 staining on X with loss/knockdown of DCC and SIR-2.1, but not SET-1 or SET-4 (Figure 4.16). As demonstrated in Figure 4.9, these PSer2 differences on X in DCC mutants are consistent with a change in the X:A signal intensity of about two-fold. In sum, these data suggest that RNA Pol II elongation is restricted on X by DCC function.

To further investigate the connection between the DCC and RNA Pol II elongation, we examined regulators of RNA Pol II for effects on DCC localization and dosage compensation-mediated repression (Figure 4.5). In previous work [110], we demonstrated that the DCC maintains a repressive chromatin environment on X through reduction of H4K16ac and enrichment of H4K20me1. RNAi of the RNA Pol II stalling and elongation factor DSIF component *spt-4* showed a loss of H4K16ac reduction (Figure 4.5A) and a loss of H4K20me1 enrichment (Figure 4.5B) on X, while DCC loading on X was normal. In contrast, knockdown of both components of DSIF (DSIF RNAi: *spt-4 spt-5* RNAi) caused both a similar disruption in histone H4 chromatin state and DCC mislocalization away from X (Figures 4.5A, B). In line with previous work suggesting that DCC function depends on transcriptional elongation, knockdown of the kinase responsible for RNA Pol II serine 2 phosphorylation, *cdk-9*, also led to a disruption of X chromatin state and a milder DCC mislocalization phenotype (Figures 4.5A, B). Knockdown of CTD phosphatases (*rtr-1* and *ssup-72*) and TFIIS (*T24H10.1*) caused a modest reduction in H4K20me1 on X, but these effects could not be uncoupled from a reduction in transcriptional elongation (data not shown). *cdk-9* RNAi also showed a substantial effect on Condensin I localization during mitotic metaphase and anaphase in developing embryos (Figure 4.5C). These data highlight the strong connections between transcriptional elongation and dosage compensation, and suggest the potential for dosage compensation regulation of RNA Pol II elongation independent of earlier steps in transcription.

To investigate the contribution of RNA Pol II regulators to dosage compensation function, we employed a modified *xol-1* suppression assay [133]. Specifically, in a strain in which male progeny die due to inappropriate dosage compensation [*him-8(e1489)*; *xol-1(y9) sex-1(y263)*], treatment with RNAi against factors that are important for DCC function can rescue male viability. *vector* RNAi rescues only ~1%, while *dpy-27* (DCC) RNAi rescued ~49% of the expected number of males (Figure 4.6A). In all, *dpy-21* (DCC), *cdk-7*, *cdk-9*, and *spt-4* RNAi caused significant male rescue (~7%, ~5%, ~16%, and ~21%, respectively; Figure 4.6A). Other RNA Pol II regulators, such as: a Mediator subunit, CTD phosphatases, TFIIS, and TLK-1, did not show substantial rescue of male viability, compared to control RNAi. *spt-5*, the second DSIF component, and sequential DSIF RNAi led to very low viability (<5%), precluding these analyses.

We validated the gender identity of rescue animals by immunoFISH (Figure 4.6B). While hermaphrodite *him-8; xol-1 sex-1* animals showed two DCC-coated X chromosome regions in interphase intestinal nuclei, only one was observed in males (Figure 4.6B). Further, anaphase II sperm images confirm the presence of only one X chromosome that is also coated by the DCC. These results indicate that DPY-21, DSIF, and P-TEFb genetically interact with the DCC and contribute to dosage compensation function.

Discussion

Our results demonstrate regulation by dosage compensation at multiple points in the transcription cycle, summarized in Figure 4.7. The DCC does not appear to limit RNA Pol II recruitment to X (Figure 4.1), but DCC function limits RNA Pol II initiation (Figures 4.2C-E), summarized in Figure 4.7A, and early genic elongation (Figures 4.3 and 4.13). PSer5 across the genome is stabilized by DPY-21 function (Figure 4.4), perhaps restricting the transition to productive elongation, summarized in Figure 4.7B. Marks of elongation are enriched at non-dosage compensated genes about 2-fold over dosage compensated genes (Figure 4.15), and PSer2 is limited by DCC function on X (Figure 4.16). The DSIF component SPT-4 is required for DCC-mediated chromatin regulation, while SPT-5 is required for proper DCC localization restriction to X (Figure 4.5). Finally, *cdk-7*, *cdk-9*, and *spt-4* are genetically important for DCC function (Figure 4.6). Relative strength of DCC connections to stages of the transcription cycle, strongest at the initiation and early elongation stages, are shown in Figure 4.7C.

This study builds upon the results of our previous work, which highlighted the particular importance of DPY-21 in regulation of H4K20me1 and H4K16ac on X [110]. We now show that DPY-21 increases PSer5 perdurance across the nucleus. In total, we have shown that DPY-21 is required to maintain a repressive chromatin state on the X chromosomes [110] and delay the transition from Ser5 phosphorylation to Ser2 phosphorylation (this work). H4K16ac is known to be important for the transition to productive elongation by RNA Pol II, through P-TEFb recruitment [49]. These data, along with previous work showing that DPY-21 is only loosely associated with the rest of the DCC [103] and also localizes to autosomes ([103] and MW, unpublished results), *dpy-21* loss does not disrupt localization of the rest of the DCC [103], and genetic assays suggesting that DPY-21 fine-tunes expression in response to changes in gene dose [101], indicate that DPY-21 is working downstream and/or in parallel to the action of Condensin I^{DC} to affect chromatin and transcription for dosage compensation as well as genome-wide gene regulation.

Interestingly, our data support the hypothesis that worm dosage compensation involves a combination of effects from different pieces of the DCC. Our analyses show that SDC-2, SDC-3, and DPY-21, and not other DCC subunits, may regulate AMA-1 levels directly (Figures 4.1A, 4.10A). Second, we observed changes in the RNA Pol II transition to elongation dependent solely on DPY-21 (Figure 4.4). This work has uncovered details of the true degree of complexity involved in the mechanism of transcriptional regulation by *C. elegans* dosage compensation.

Our data confirm that worm dosage compensation, like the fly and mammalian methods, involves regulation of gene expression at the transcriptional level. In each system, the mechanism of dosage compensation is uniquely positioned to affect the desired changes: RNA Pol II elongation in flies [51] to upregulate expression, RNA Pol II recruitment in mammals [81] to turn off transcription, and RNA Pol II initiation and elongation in worms (current study) to downregulate transcription. This suggests that while each strategy developed in response to changes in selective pressures on X, transcription is a process uniquely amenable to influences from dosage compensation in order to achieve a suitable gene expression balance between the sexes and within individuals.

Methods

Strains

JH1288 *cdk-7(ax224)* I

MT14911 *set-4(n4600)* II

OP34 *unc-119(ed3)* III; wgIs34

TY2386 wild type (WT) (N2)

TY3936 *dpy-21(e428)* V

TY4161 *sdc-1(y415)* X

TY4341 *dpy-26(n199) unc-30(e191)* IV/nT1 [qIs51] (III;IV)

TY4381 *dpy-28(s939)* III/qC1 III

TY1936 *dpy-30(y228)* V/nT1 [*unc-?* (*n754*) *let-?*] (IV; V)

TY1140 *sdc-2 (y46)* X

TY0420 *dpy-27(y57)* III

VC199 *sir-2.1(ok434)* IV

Nematode strains used in this work were provided by the Caenorhabditis Genetics Center, which is funded by the NIH National Center for Research Resources.

RNAi Treatment

RNAi treatment was performed as described previously [110].

Public Datasets

Downloaded from http://www.modencode.org or (http://www.ncbi.nlm.nih.gov/geo/).

Format: Dataset ID (GSE denotes NCBI GEO), Description (Stage), Array (if applicable)

3432, AMA-1 ME, 080922

334, DPY-26 ME, 7685

3435, DPY-27 EE, 080922

578, DPY-27 ME, 7685

644, DPY-28 ME, 080922

GSE25834, DPY-30 ME, 8134

GSE25834, MIX-1 ME, 8134

645, SDC-2 ME, 080922

553 & 575, SDC-3 ME, 7685

2767, CBP-1 ME, 080922

3438, HPL-2 LE, 080922

3439, LIN-15B LE, 080922

911, MES-4 EE, 080922

897, MRG-1 EE, 080922

2738, NPP-13 ME, 080922

2969, ZFP-1 ME, 080922

3206, H3 EE, 080922

2726, H3K4me1 EE, 080922

GSE22741, H3K4me2 EE, 080922

GSE22721, H3K4me3 EE, 080922

2646, H3K9me1 EE, 080922

2444, H3K9me2 EE, 080922

982, H3K9me3 EE, 080922

2727, H3K27ac EE, 080922

3179, H3K27me1 EE, 080922

3171, H3K27me3 EE, 080922

2604, H3K36me1 EE, 080922

909, H3K36me2 EE, 080922

973, H3K36me3 EE, 080922

2410, H3K79me1 EE, 080922

2442, H3K79me2 EE, 080922

2443, H3K79me3 EE, 080922

3181, H4K8ac EE, 080922

3182, H4K16ac EE, 080922

2765, H4K20me1 EE, 080922

2766, H4tetraAc EE, 080922

GSE25834, RNA Pol II (8WG16 on vector or *sdc-2* RNAi), 8134

3977, WT EE RNA-seq

3978, WT LE RNA-seq

43, HTZ-1 ME, direct wiggle file download

2436, AMA-1::GFP LE ChIP-seq

2416, DPY-27 ME ChIP-seq

Notes: 1) Many experiments have dyeswaps, which are not always properly annotated on modencode.org. 2) Number of replicates varies from one to four. 3) Inconsistent or poor quality replicates were discarded.

Cistrome analysis

Cistrome [134] can be accessed at: http://cistrome.org/ap/root.

Definition of DC and non-DC genes

Using the microarray datasets from [104] loaded into Cistrome, statistically significant changes in gene expression were determined by comparing WT to: A) *dpy-27(y57)*, B) *sdc-2(y93)*, or C) *her-1(hv1y101); xol-1(y9) sdc-2(y74) unc-9(e101)* samples using MAT with default settings and "calculate differential expression" using default settings, except a Benjamini-Hochberg FDR Type II error control at a maximum p-value of 0.05 and a minimum fold-change of 1.5. Qualifications for dosage compensated and non-dosage compensated gene status were the same as in [104]. Dosage compensated genes will change expression in (A) and (B), but not (C) as compared to WT, and non-dosage compensated genes will change expression in (C), but not (A) or (B) as compared to WT.

Wiggle file creation and metagene profiles

All .wig files were created with respect to the ce6 genome build. For ChIP-chip datasets, raw pair, ndf, and pos files were downloaded from modencode.org or NCBI Accession #GSE25834. These files were uploaded and used as input for MA2C normalization in Cistrome using default settings. This results in creation of a .wig file, which was used for metagene profiling. For RNA-seq metagenes, the generated wiggle file detailed above was used for metagene profiling. Wiggle files and gene lists [MW dosage compensated, MW non-dosage compensated, active X (late embryo), active A (late embryo), low RPKM (1-49.5) MW DC or non-DC, mid RPKM (50-149) MW DC or non-DC, and high RPKM (150 to max) MW DC or non-DC] were used as input for metagene profiling ("CEAS: Enrichment on chromosome and annotation" function) using the appropriate profiling resolution (either 50bp or 86bp, depending on the array design).

BED file creation

BED files representing rex sites, dox sites, waystations, these three site types combined, all DPY-27 ChIP-seq peaks, no DPY-27 peak control sites from [135], active enhancer (bimodal H3K4me1) *rex* and *dox* sites, poised enhancer (monomodal H3K4me1) *rex* and *dox* sites, off (no H4K16ac signal) enhancer *rex* and *dox* sites, or HTZ-1 peaks on X) were generated by hand in Microsoft Excel 2007 or download as modencode.org peak call files.

Cross-correlation plots

Wiggle files were used as input to generate cross-correlation tables in Cistrome relating any two datasets ("Multiple wiggle files correlation" or "Multiple wiggle files correlation in given regions" function) either at 20kb resolution or within specified bed files.

SitePro analysis

Wiggle files and bed files explained above were used as input for SitePro (feature-centric) analysis using a span of 1000bp and the appropriate profiling resolution (either 50bp or 86bp, depending on the array design).

Browser Screenshots

The applicable WIG (wiggle) public dataset tracks were loaded into the Integrated Genome Viewer (IGV; Broad Institute). Screenshots were taken of regions of interest using the "print screen" and "paste" functions in Windows 7 and Microsoft PowerPoint 2007. *rex* and *dox* sites were labeled as referenced in [104].

ImmunoFISH and Immunofluorescence Microscopy

FISH, immunostaining, and imaging were conducted as described previously [110].

Live-Imaging and FRAP Microscopy

Live imaging was completed using an Olympus/Andor Spinning Disk Confocal Microscope setup and iQ software with technical assistance from Gregg Sobocinski.

ChIP-seq Data Quantification

WIG (wiggle) file value columns were summed over: 1) all genes in the specified gene lists (dosage compensated, non-dosage compensated, active autosomes, or active X chromosome); 2) a region 500bp upstream of each gene in each list from (1); or 3) a region 1kb upstream of each gene in each list from (1). Then, totals for each group were divided by the total kilobases included in each entry to normalize for gene and list length. Asterisk indicates a difference significant at $p<0.05$ by Student's T-test (run in Microsoft Excel 2007).

Male Rescue Assay

Male rescue assay was performed as described previously [110].

Acknowledgements

I would like to Gregg Sobocinski and Dr. Josh Bembenek for assistance with live imaging and FRAP microscopy. I would also like to thank Ken Cadigan, Ray Chan, Yali Dou, Anuj Kumar, Kentaro Nabeshima, Andrzej Wierzbicki, and the other members of the Csankovszki Lab for helpful project discussions.

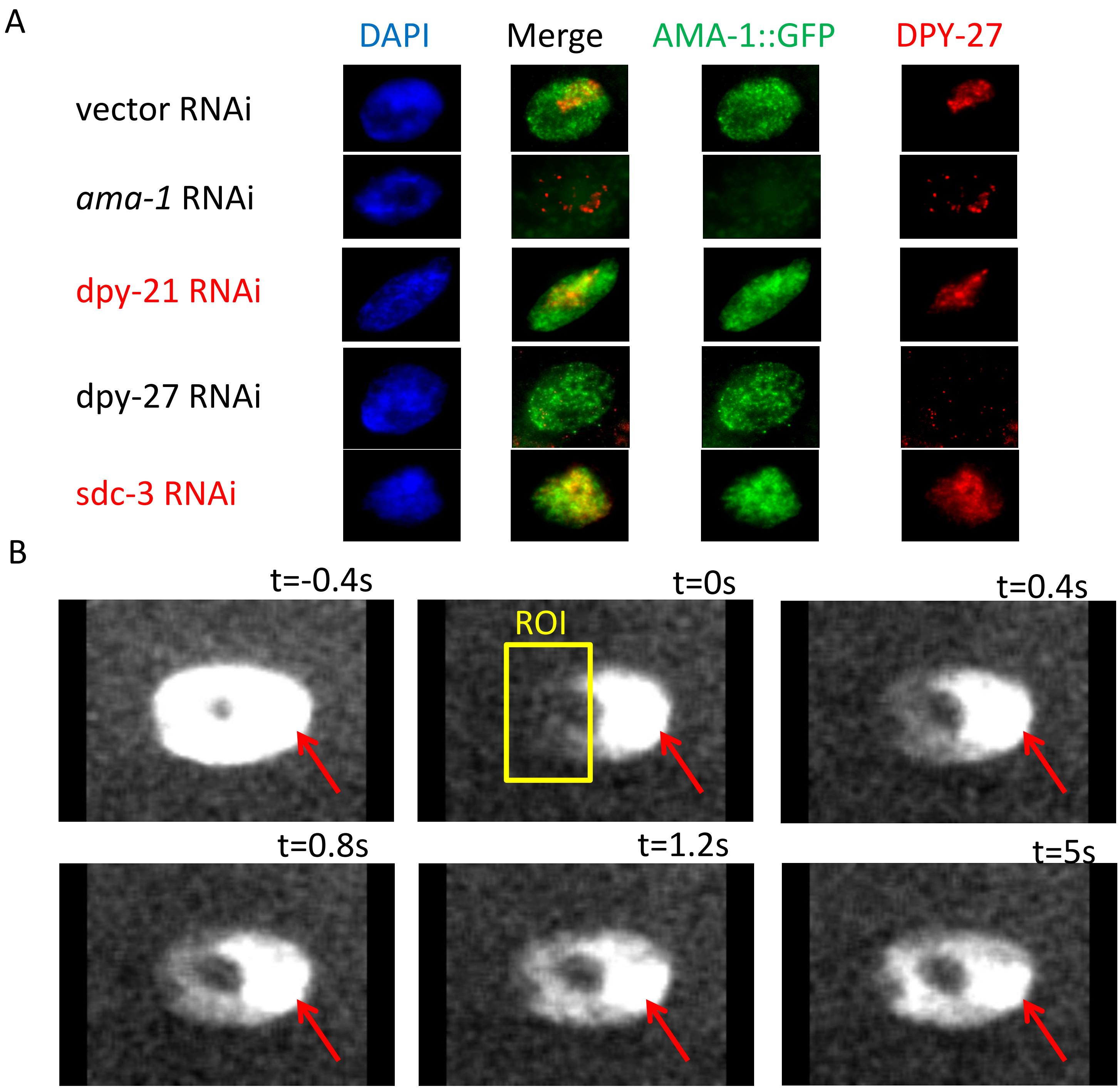

Figure 4.1. AMA-1 dynamics and regulation by DCC components. Shown are IF microscopy images from OP34 (AMA-1::GFP) worms after various RNAi treatments (A) or still images from live imaging with FRAP microscopy of OP34 (AMA-1::GFP) worms (B). DAPI (DNA) is shown in blue. A) Results show that AMA-1::GFP signal is specific to *ama-1*. Additionally, *dpy-21* and *sdc-3*, but not *dpy-27*, RNAi led to increased AMA-1::GFP signal sufficient to reduce the required exposure time by half to achieve similar signal. B) In approximately half of all nuclei photobleached (16/36), a region of chromatin with AMA-1::GFP signal equivalent to t=-0.4s persists. These data suggest that dosage compensation does not restrict RNA Pol II loading onto the X chromosomes, but does restrict one or more downstream steps in transcription.

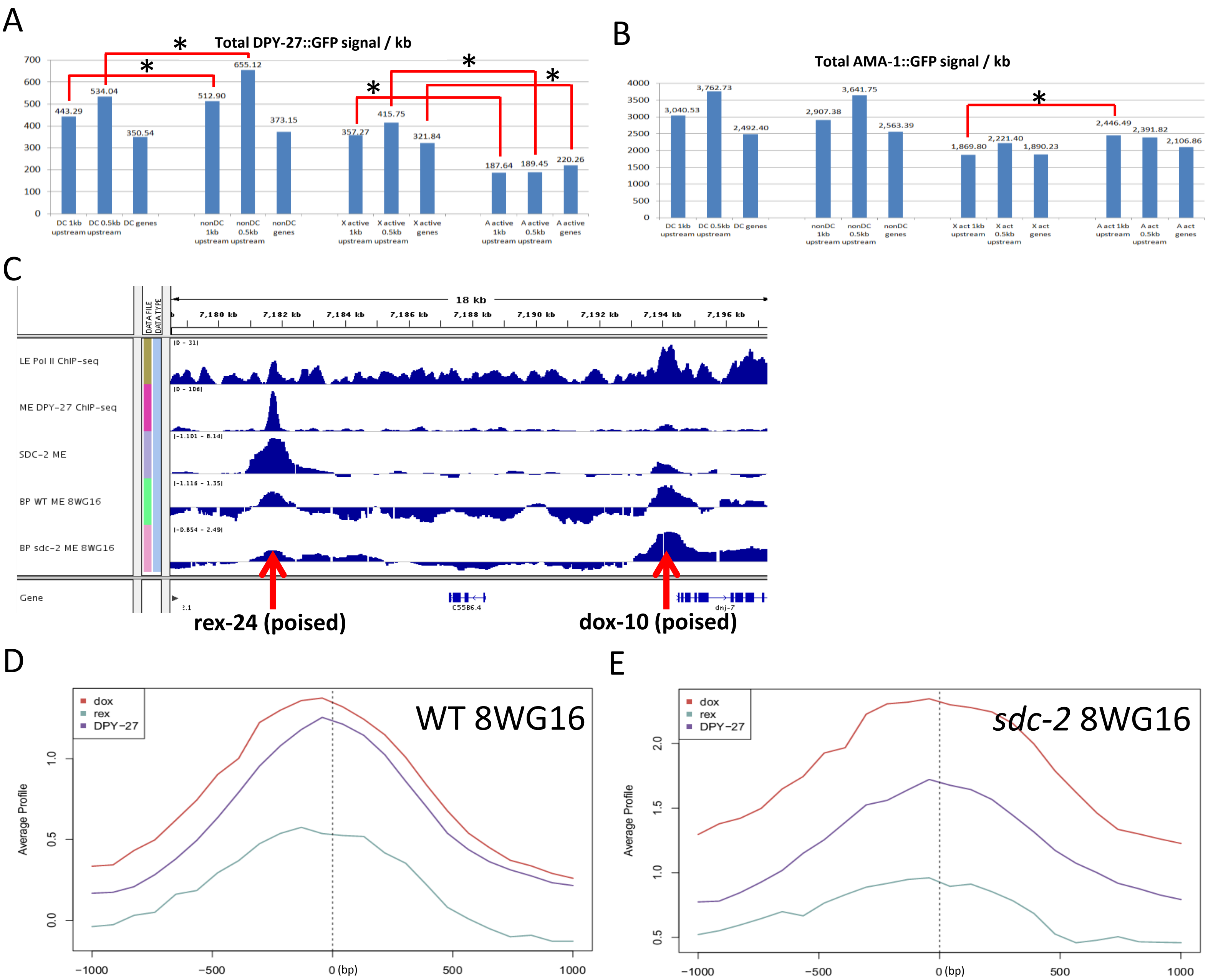

Figure 4.2. RNA Pol II loading differs slightly on X versus autosomes, but initiation varies greatly with loss of dosage compensation. Shown are: (A) DPY-27 mixed-embryo or (B) AMA-1::GFP late embryo ChIP-seq reads per kilobase for dosage compensated, non-dosage compensated, X, autosomes, 500bp upstream of each gene, or 1kb upstream of each gene; (C) a browser screenshot demonstrating RNA Pol II 8WG16 (CTD is hypo-phosphorylated) signal change with loss of dosage compensation; (D) SitePro analysis comparison of RNA Pol II 8WG16 ChIP-chip signal at *rex*, *dox*, or all DPY-27 ChIP-seq peaks in WT or *sdc-2* RNAi-treated samples. Results confirm DCC enrichment on X by ChIP-seq and show a significant difference in RNA Pol II ChIP-seq occupancy between 500bp and 1kb upstream of X-linked compared to autosomal genes. Also, 8WG16 signal becomes enriched and spreads, even in the absence of nearby transcription, especially at *dox* sites, with loss of dosage compensation.

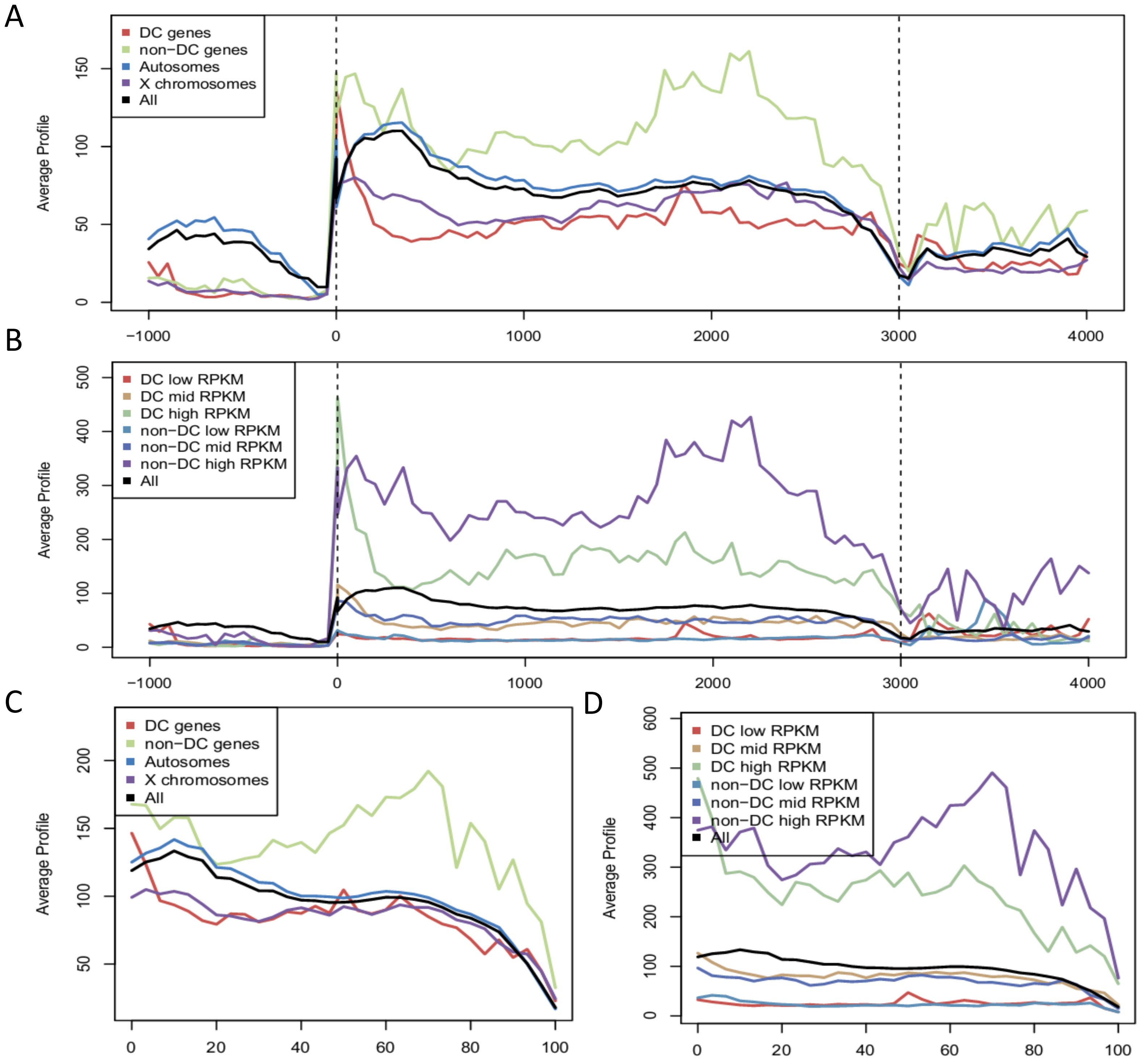

Figure 4.3. A defect in early elongation at dosage compensated genes during transcription. Shown are metagene profiles (A & B) or concatenated exon profiles (C & D) comparing dosage compensated, non-dosage compensated, active X, and active autosome (A & C) or low, medium, and highly transcribed dosage compensated or non-dosage compensated (B & D) gene RNA-seq transcript levels from WT late-biased embryo stage datasets. Results show a major deficiency in transcript levels just downstream of the transcript start site at dosage compensated, but not non-dosage compensated, genes that is independent of the levels of transcript produced. This suggests that early elongation control is important to the mechanism of dosage compensation.

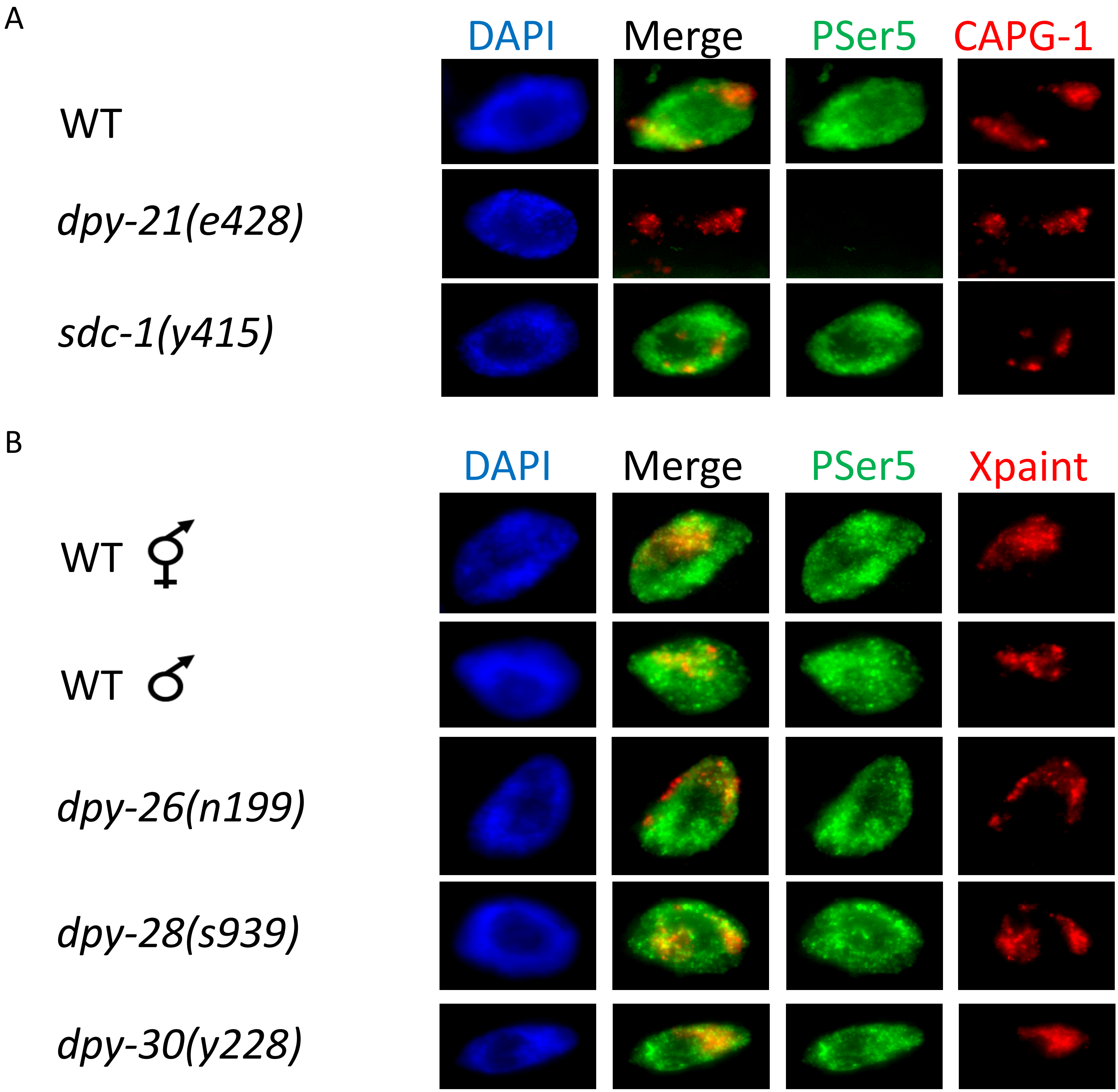

Figure 4.4. Regulation of RNA Pol II CTD PSer5 perdurance by DPY-21. Shown are: (A) IF microscopy or (B) immunoFISH images from WT or dosage compensation mutant worms stained with antibodies against RNA Pol II CTD serine 5 phosphorylation. DAPI (DNA) is shown in blue. Results show that DPY-21, and not other DCC components, is responsible for perdurance of PSer5 signal across the nucleus, suggesting that DPY-21 participates in RNA Pol II elongation control.

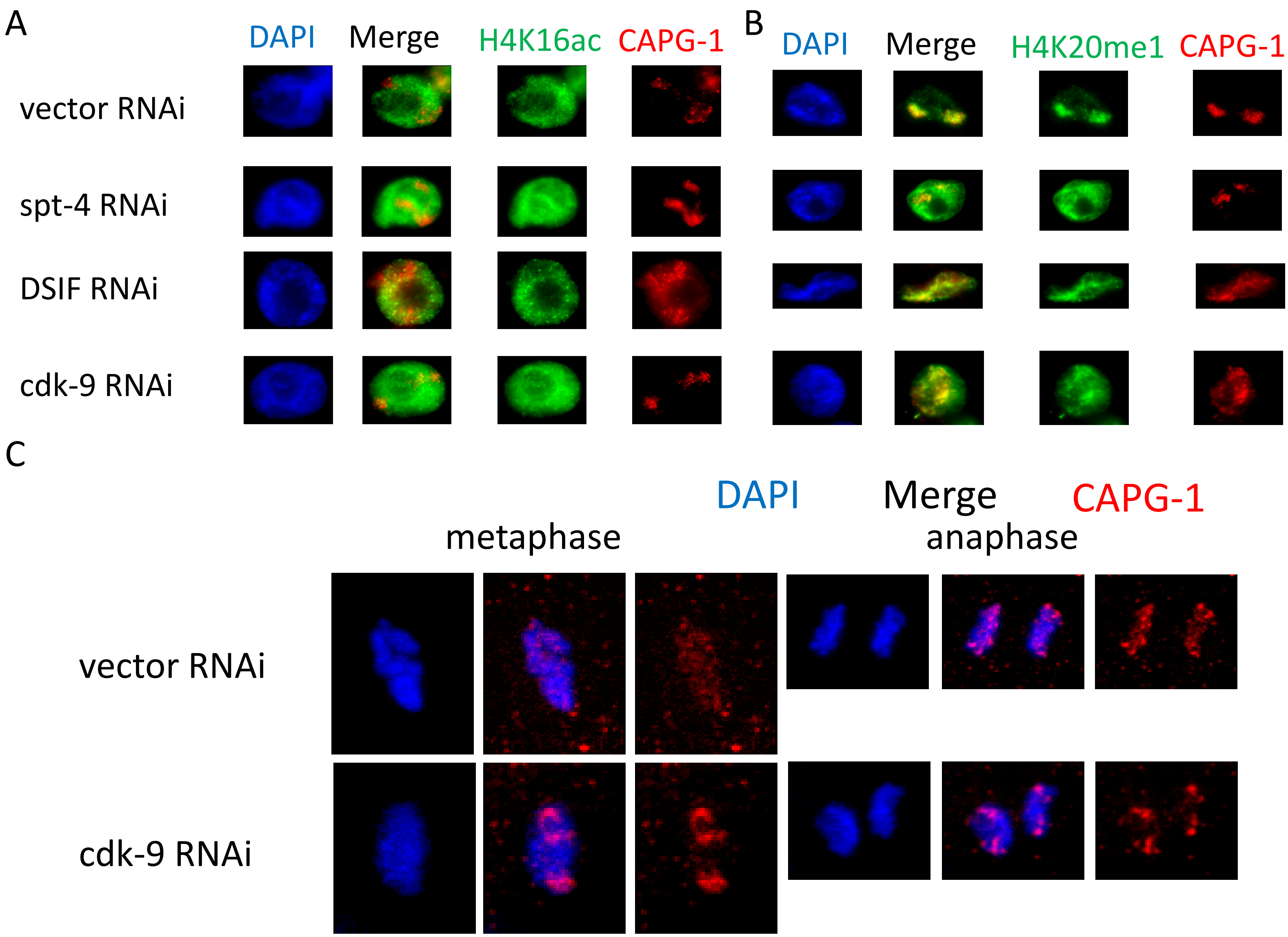

Figure 4.5. RNA Pol II elongation regulators affect DCC localization and function. Shown are IF images from WT hermaphrodites treated with *vector*, DSIF component (*spt-4* or both *spt-4* and *spt-5*), or P-TEFb (*cdk-9*) RNAi stained with antibodies against CAPG-1 and (A) H4K16ac or (B) H4K20me1. Part (C) shows CAPG-1 localization in metaphase or anaphase mitotic nuclei from ~20-cell embryos. Results show substantial spreading of the DCC from X to autosomes with DSIF, not just *spt-4*, RNAi (A & B); H4K16ac is less reduced on X after any of these RNAi treatments, and H4K20me1 enrichment on X is either completely (*spt-4* or DSIF) or partially (*cdk-9*) lost. After *cdk-9* RNAi, CAPG-1/Condensin I is mislocalized during metaphase and anaphase in mitotic embryonic nuclei. These data suggest that DCC-mediated repression and CAPG-1 localization in mitosis are compromised under RNA Pol II elongation regulator RNAi conditions.

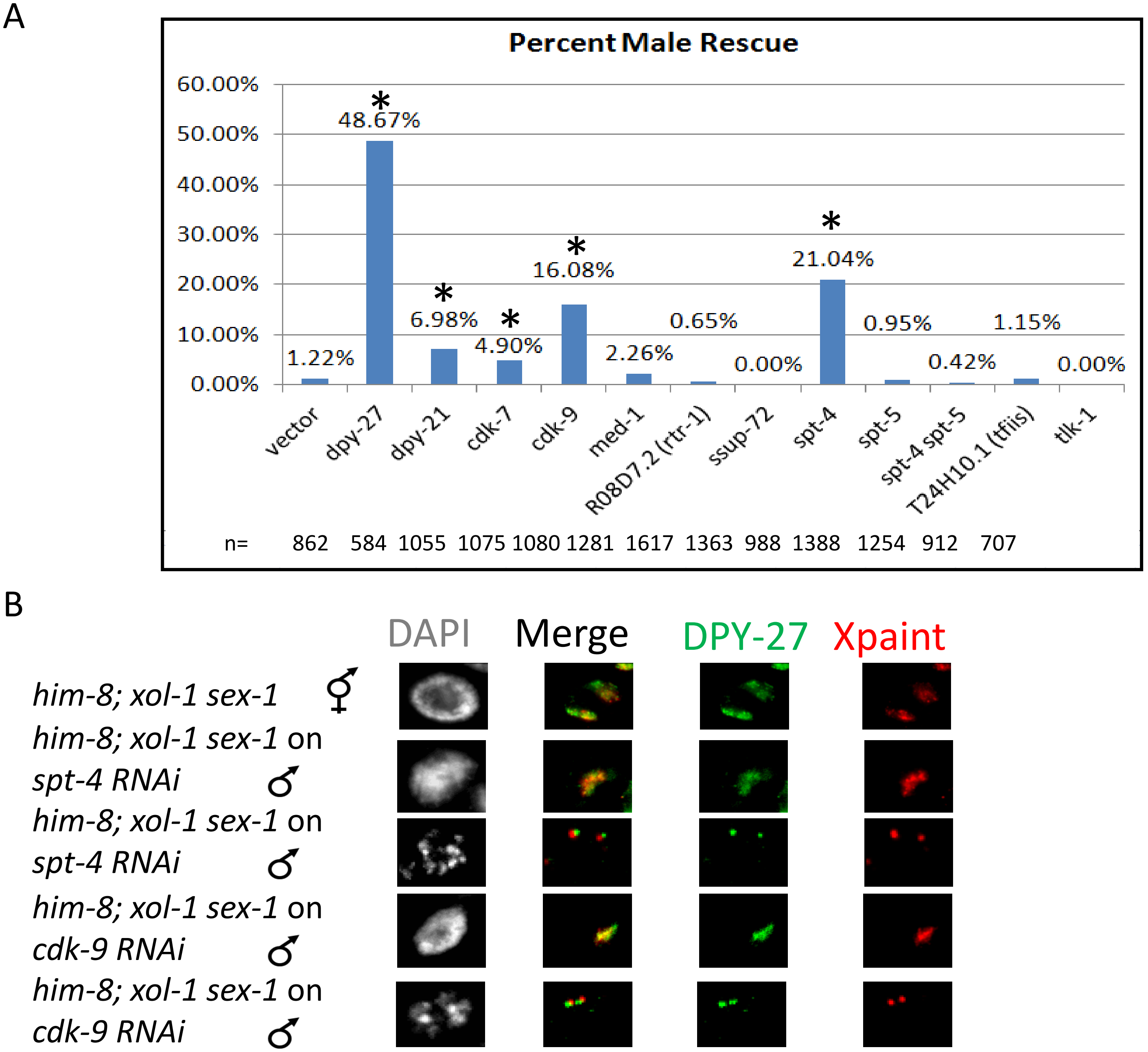

Figure 4.6. RNA Pol II elongation regulators are functionally important for dosage compensation. Shown is a graph of *him-8(e1489); xol-1(y9) sex-1(y263)* male rescue assay results (A) and representative immunoFISH images (Xpaint, anti-DPY-27) male and hermaphrodite *him-8; xol-1 sex-1* animals. DAPI (DNA) is shown in grey. Results indicate that DPY-27 (known), DPY-21 (known), CDK-7, CDK-9, and SPT-4 are each important for DCC function. Substantial (around 5% or more) rescue is indicated by an asterisk. (B) Confirmation of maleness in RNAi-rescued male worms. Results show that hermaphrodite somatic nuclei possess two X chromosome regions stained by DCC, while males had only one (lines 1, 2, and 4). Further, imaging of mitotic anaphase II sperm from males confirms the presence of only one DCC-coated X chromosome.

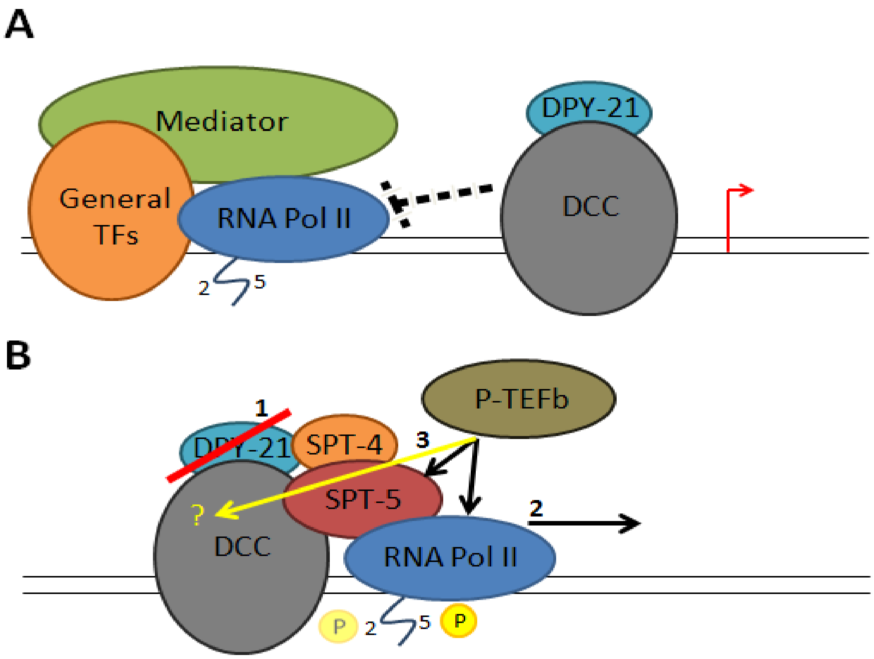

C

	DCC effects
1) Pol II Recruitment	-
2) Initiation (PSer5)	+
3) Promoter Clearance / Early Elongation	+++
4) DSIF regulation of Elongation	++
5) Productive Elongation (PSer2)	+
6) CTD Serine 5 phosphatases	+
7) TFIIS-rescued transcription arrest	-
8) Bulk Pol II occupancy	++

Figure 4.7. Model and summary of DCC-mediated effects on X-linked transcription. A) Schematic diagram. The DCC restricts RNA Pol II initiation, but largely not loading, onto the X chromosomes. B) Schematic diagram. Our data suggest that DPY-21 restricts the transition from initiated to productively elongating RNA Pol II across the genome. Also, P-TEFb (CDK-9) is critical for proper CAPG-1 localization in mitosis, suggesting that it may regulate DCC activity both directly and indirectly. C) Chart of the strength of DCC-mediated effects on transcription (this paper; data not shown) at various stages. Promoter clearance / early elongation, DSIF-mediated regulation, and AMA-1::GFP occupancy showed the greatest DCC-mediated restrictions or connections to DCC localization.

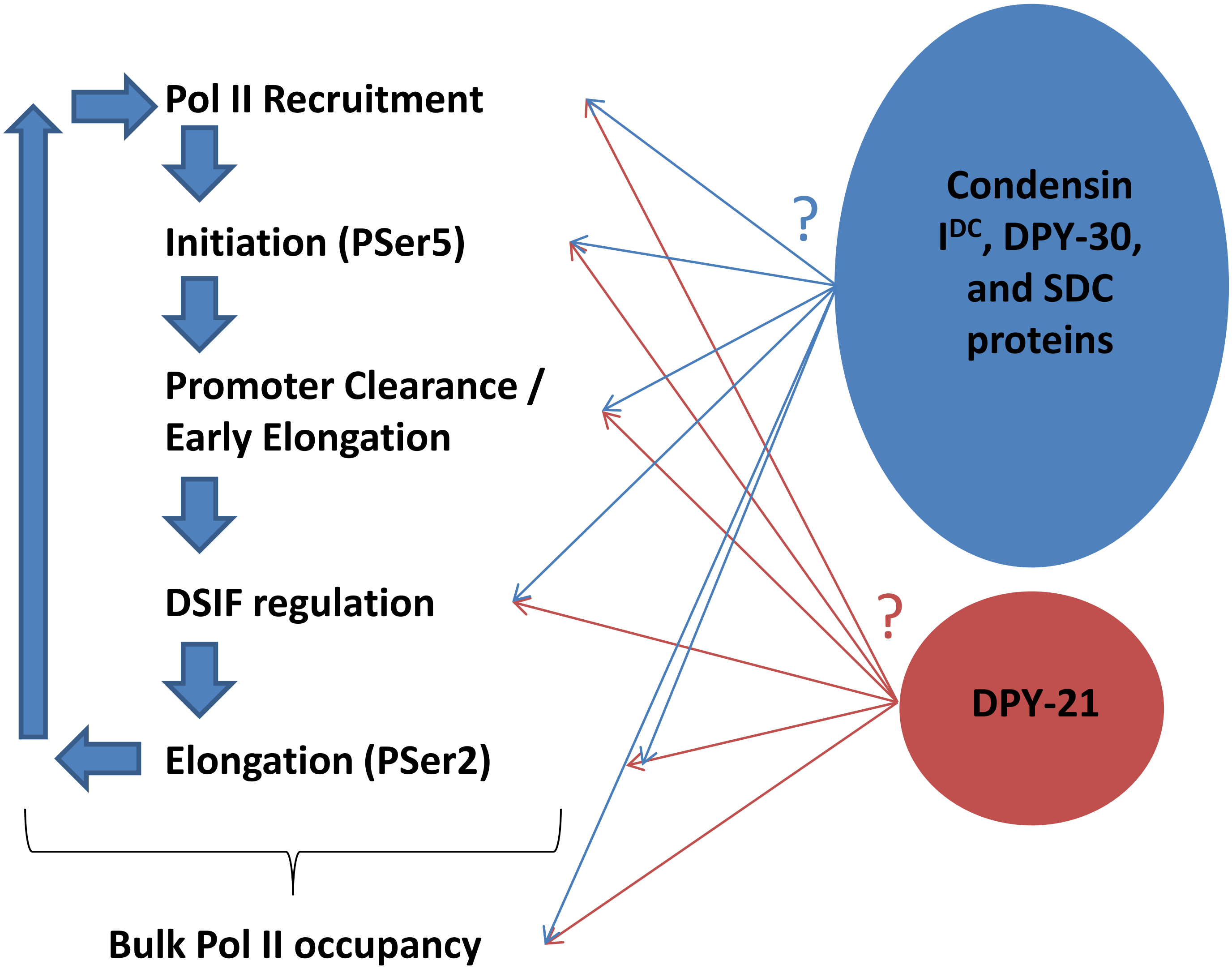

Figure 4.8. Possible stages at which the DCC could act to limit transcription. A schematic diagram highlighting points in the RNA Pol II transcription cycle assayed in this study for connections to dosage compensation. We hypothesize that DPY-21 may play an overlapping or fully distinct role from the rest of the complex.

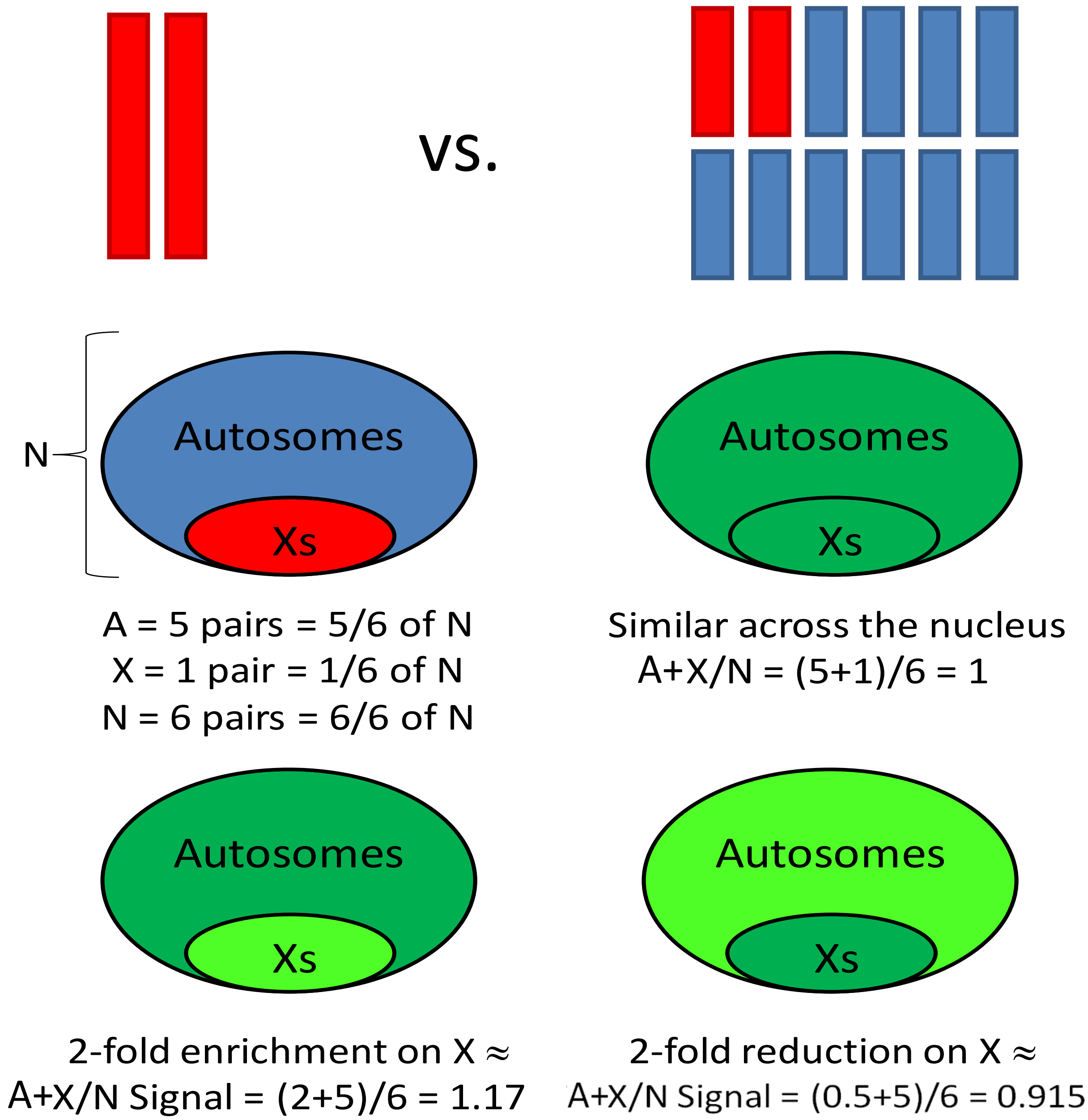

Figure 4.9. Explanation of expected conversions logic from X:nucleus to X:A for fluorescence intensity quantification (FIQ). Results of FIQ comparisons represent a net effect – potentially a combination of changes on X and A. So, we have to look for a whole nucleus-centered ratio that is consistent with changes in X:A of two-fold, not a direct change in raw X values (which we cannot directly compare across nuclei anyhow). Thus, a change from 6/6 to 7/6 signals per nucleus is a close comparison, and a two-fold change between X and A is consistent with a change in the FIQ percentage of +17% or -8.5%. A general formula to calculate the expected X:nucleus FIQ value given a net fold-change, c, in signal on X vs. autosomes is: new FIQ = 2[(5+1) + 0.5c]/(2*6).

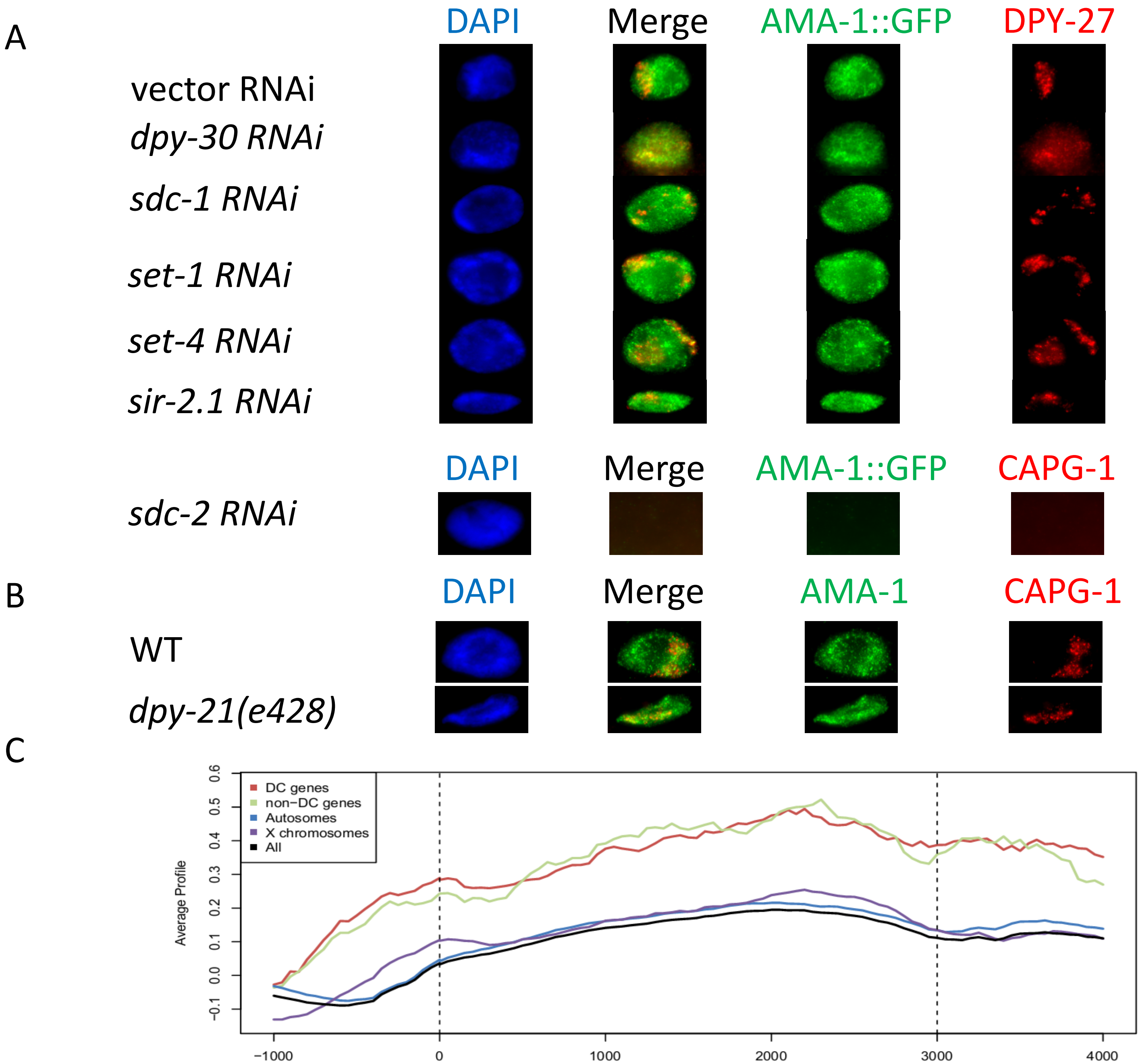

Figure 4.10. Most additional DCC or chromatin regulator RNAi treatments yielded no difference in AMA-1::GFP signal. Shown are IF microscopy images from OP34 (AMA-1::GFP) worms after various RNAi treatments costained with either DPY-27 (A), WT worms stained with AMA-1 (CTD-independent) and CAPG-1 antibodies, (B) or metagene analysis of AMA-1 (CTD-independent antibody) comparing dosage compensated, non-dosage compensated, active autosome, and active X-linked gene signal levels (C). DAPI (DNA; A & B) is shown in blue. A) Results show no effect on AMA-1::GFP levels from any of these RNAi treatments. B) Surprisingly, in addition to loss of CAPG-1 signal, *sdc-2* RNAi led to complete loss of AMA-1::GFP. It is possible that these embryos have arrested. C) CTD-independent AMA-1 levels are similar at dosage compensated and non-dosage compensated genes as well as between X and autosomes.

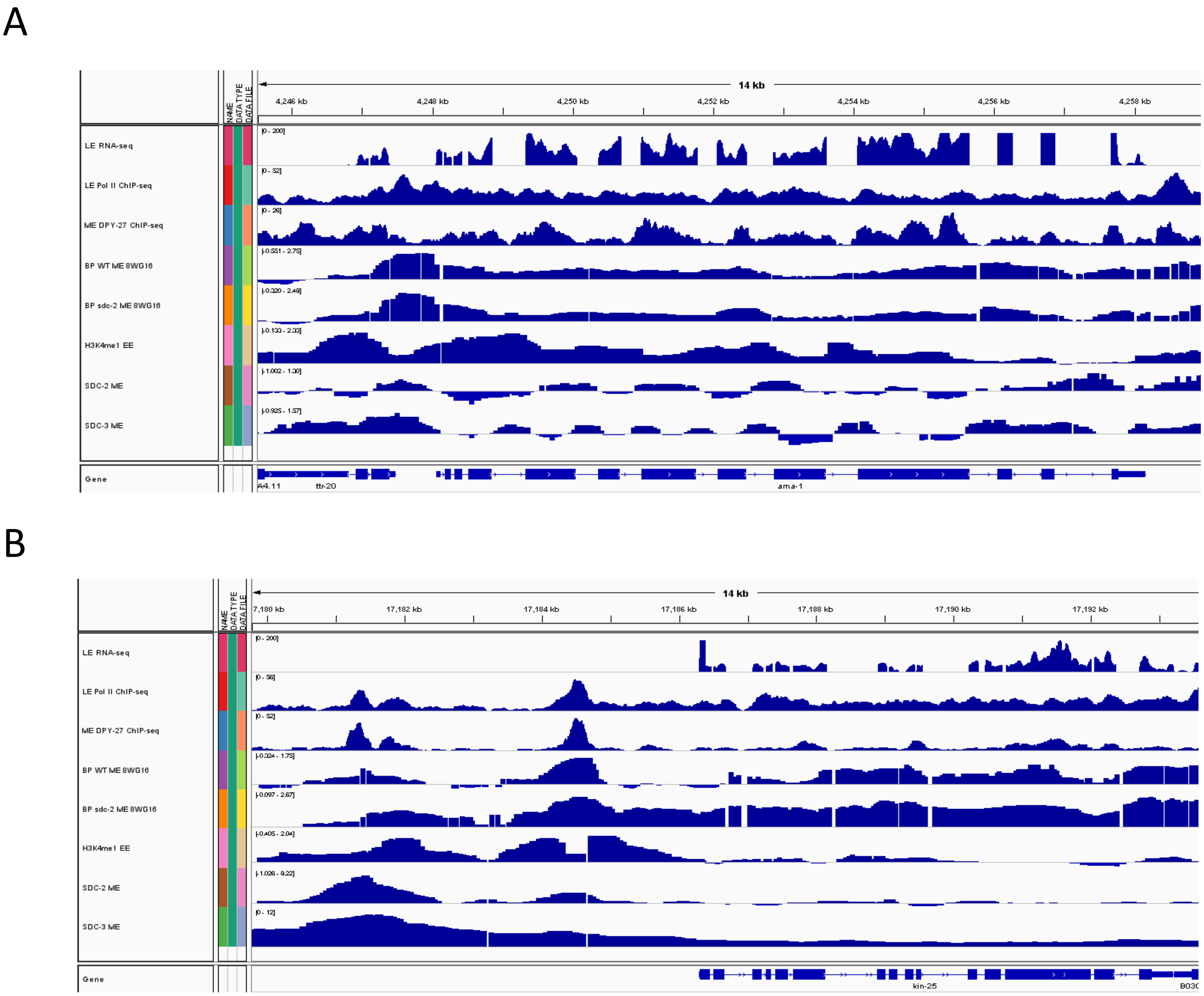

Figure 4.11. Unique localization of SDC-3 at AMA-1 suggests a direct repressive role. Shown are browser screenshots of the genomic regions surrounding either *ama-1* (A) or *kin-25* (B). Results suggest that SDC-3 binding is enriched over *ama-1* introns, as opposed to the more typical upstream enrichment seen at other DCC binding sites (such as the *kin-25* promoter).

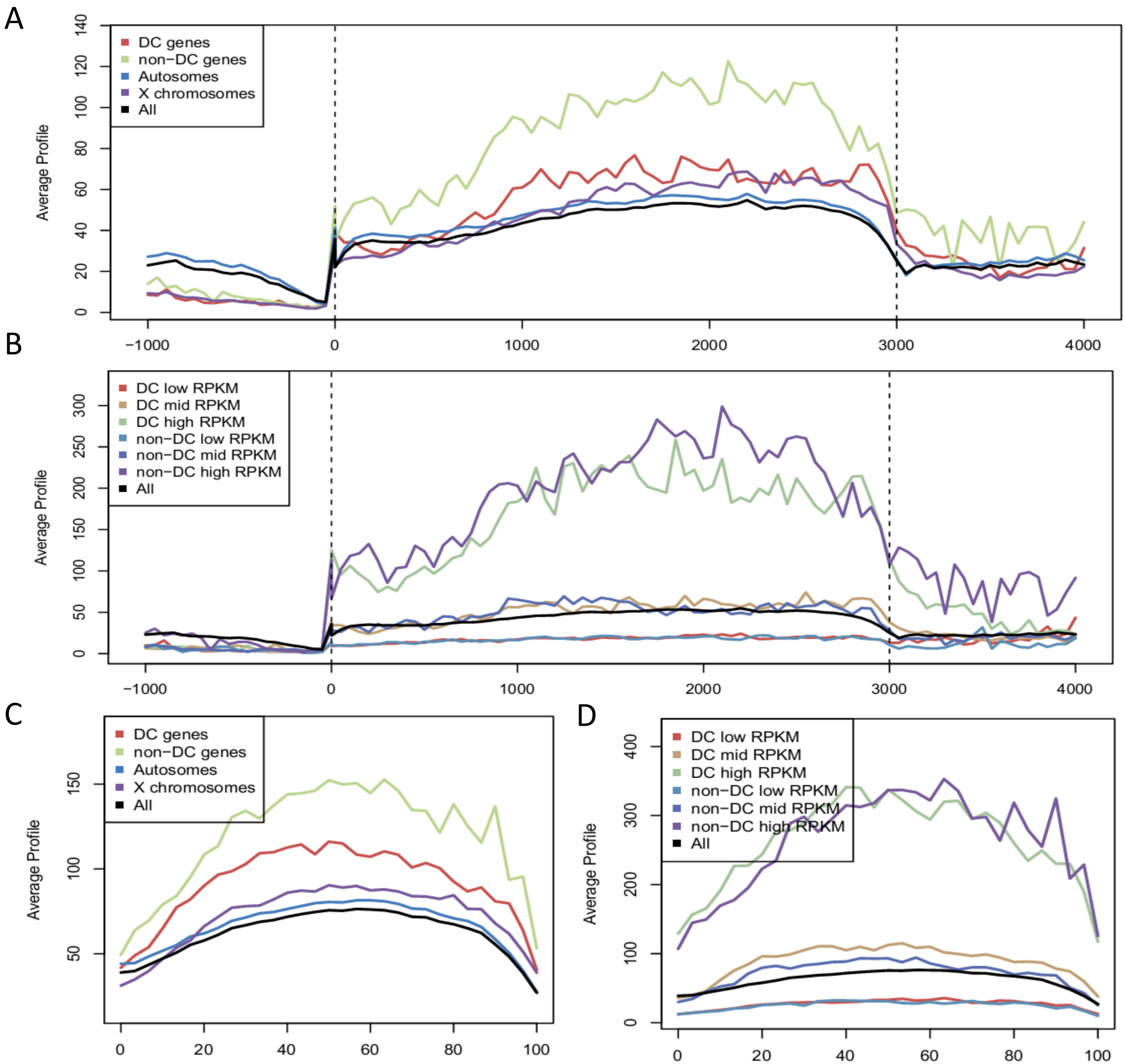

Figure 4.12. No early elongation defect is seen at dosage compensated genes prior to dosage compensation onset. Shown are metagene profiles (A & B) or concatenated exon profiles (C & D) comparing dosage compensated, non-dosage compensated, active X, and active autosome (A & C) or low, medium, and highly transcribed dosage compensated or non-dosage compensated (B & D) gene RNA-seq transcript levels from WT early-biased embryo stage datasets. Results show similar transcript production profiles at dosage compensated and non-dosage compensated genes, as well as X-linked and autosomal genes in early-biased embryonic samples. These data support the view that the early elongation defect at dosage compensated genes seen in late-biased samples is, in fact, dosage compensation-dependent.

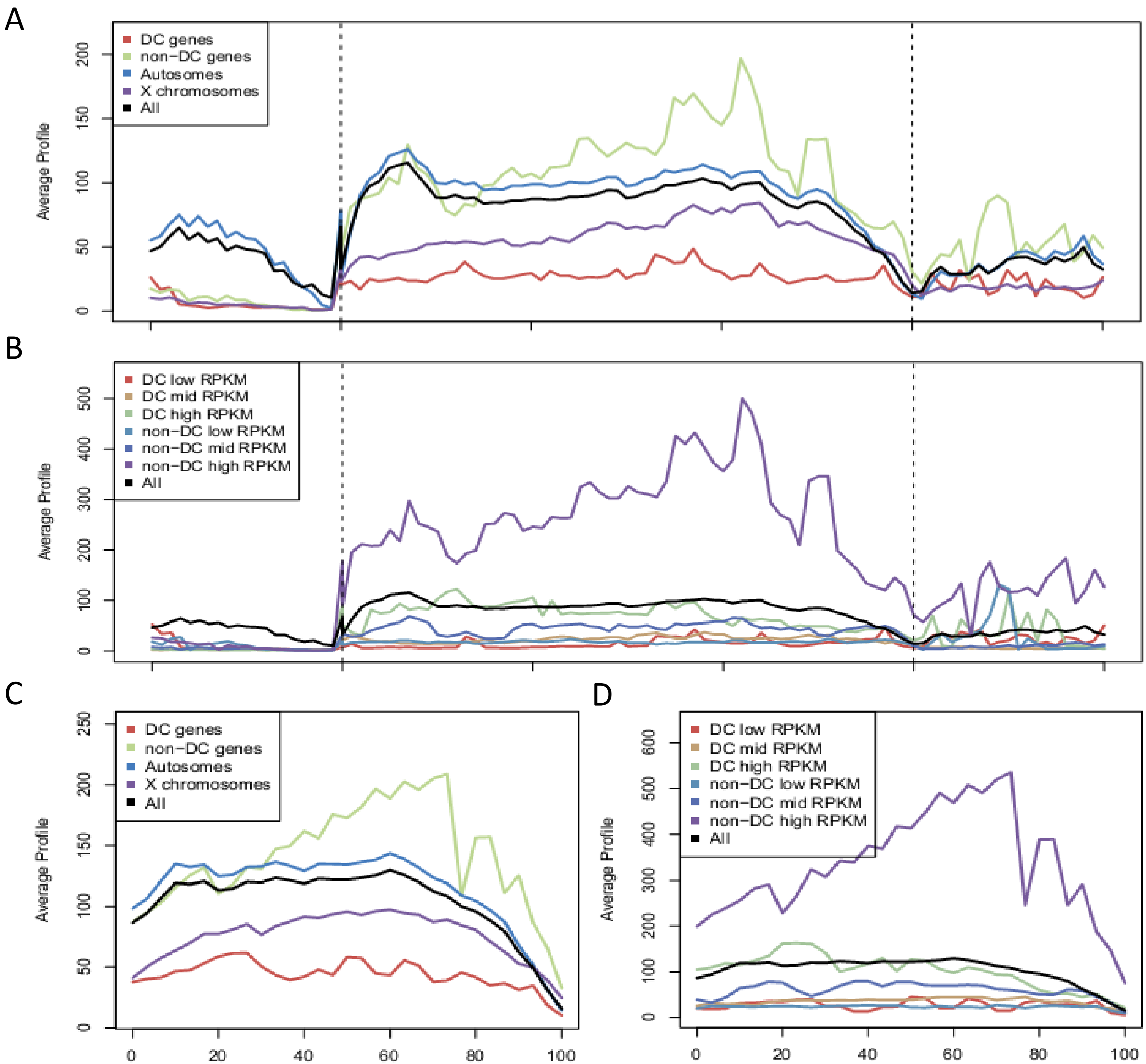

Figure 4.13. The early elongation defect is still seen at dosage compensated genes at the L3 stage. Shown are metagene profiles (A & B) or concatenated exon profiles (C & D) comparing dosage compensated, non-dosage compensated, active X, and active autosome (A & C) or low, medium, and highly transcribed dosage compensated or non-dosage compensated (B & D) gene RNA-seq transcript levels from WT early-biased embryo stage datasets. Results show decreased transcript production profiles at dosage compensated compared to non-dosage compensated genes, as well as X-linked and autosomal genes in larval stage 3 (L3) samples. These data suggest that dosage compensation-mediated repression of early elongation remains steady, or perhaps intensifies, later in worm development (much later than DCC binding and enrichment on the X chromosomes).

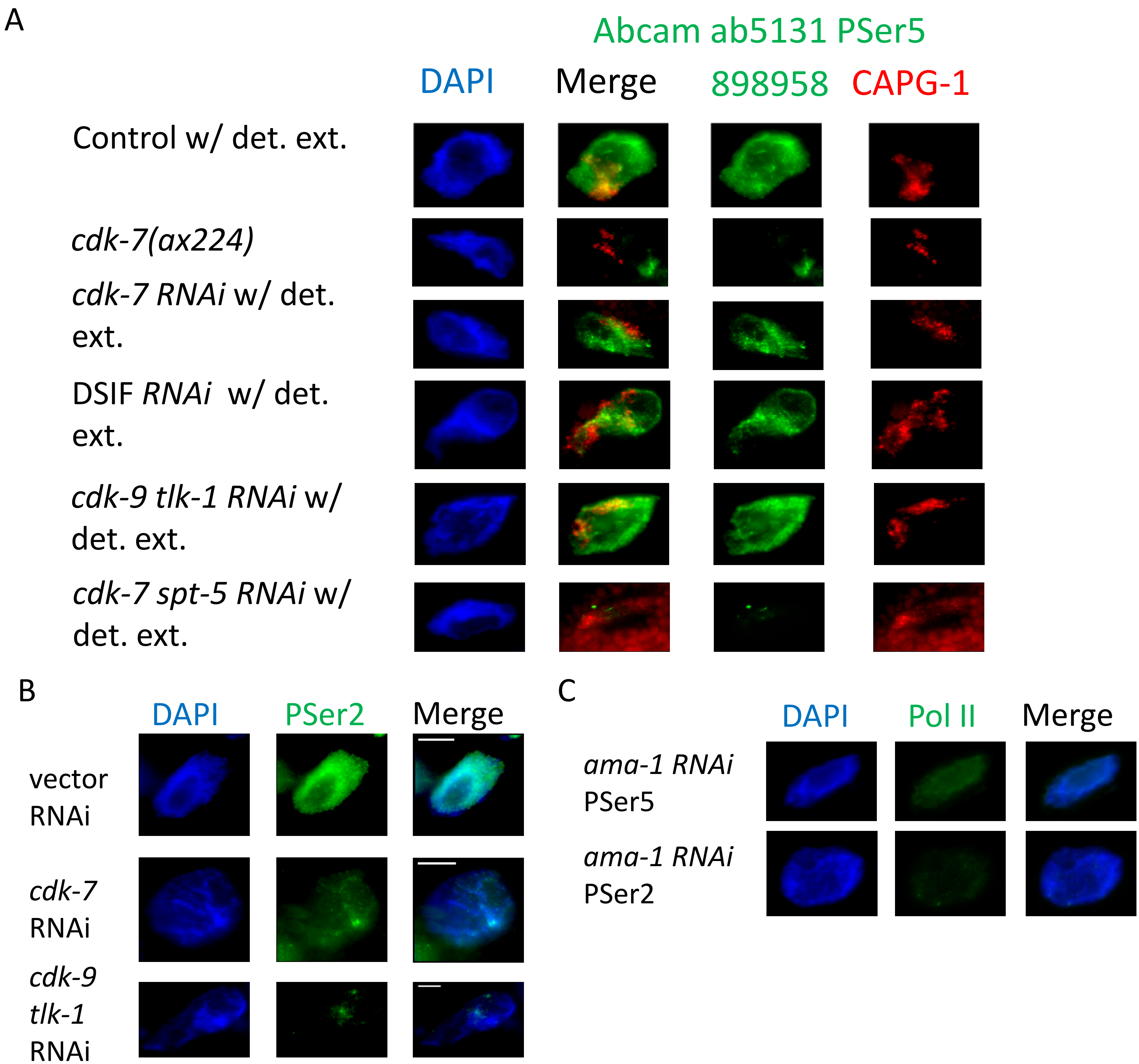

Figure 4.14. RNA Pol II antibody validation. Shown are IF images from WT or *cdk-7(TS)* worms after various RNAi treatments stained with either: (A & C) CAPG-1 and PSer-5, (B & C) PSer2, or antibodies. DAPI (DNA) is shown in blue. Results show that CDK-7 and DSIF, surprisingly, contribute to PSer5 staining (A). PSer2 antibody does not cross-react with PSer5 (B). The PSer5 and PSer2 antibodies are both specific for the RNA Pol II subunit AMA-1 (C).

A

B

C

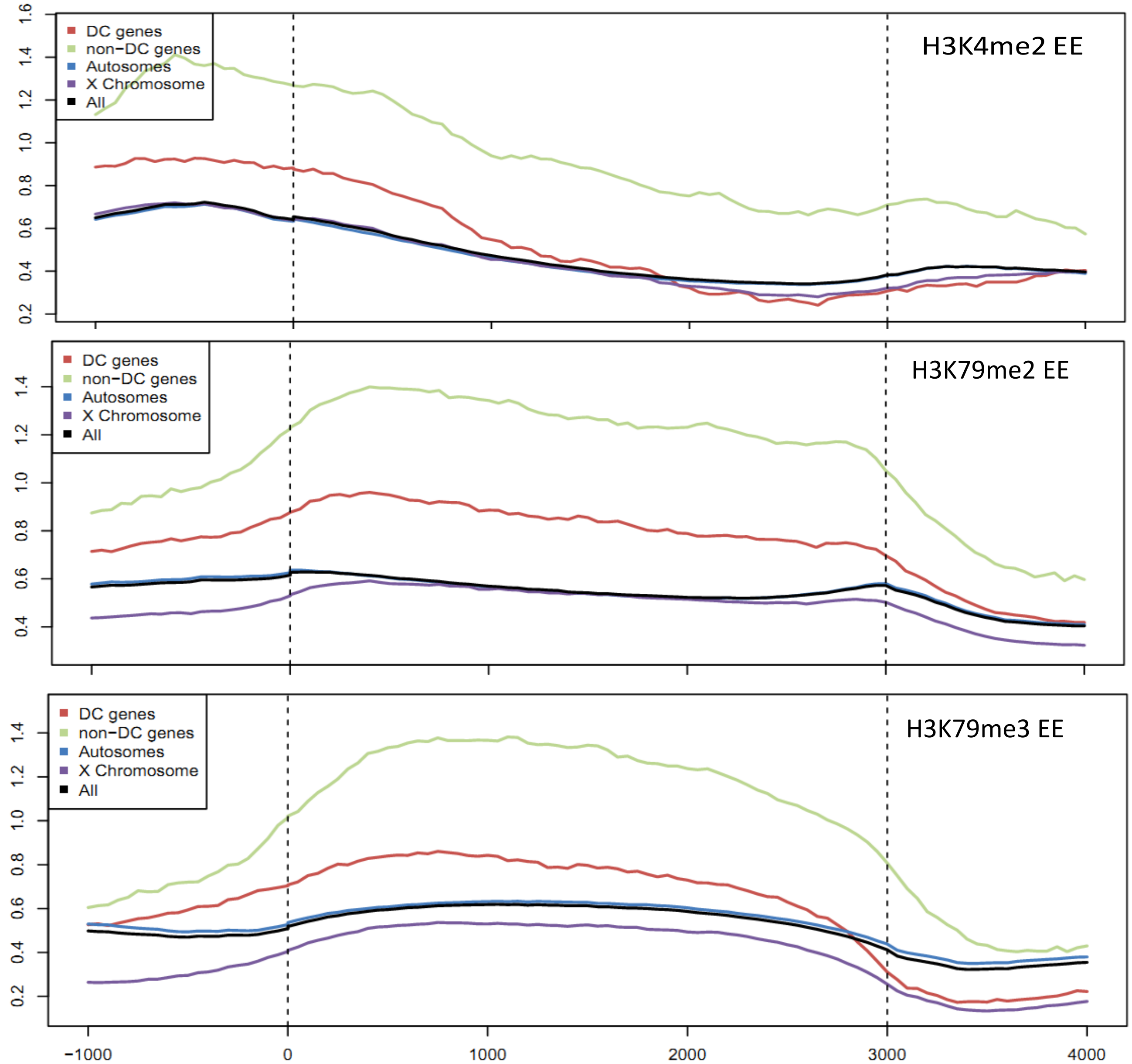

Figure 4.15. Histone marks associated with RNA Pol II elongation at dosage compensated and non-dosage compensated genes. Shown are metagene profiles for three histone modifications tightly correlated with RNA Pol II elongation [H3K4me2 (A), H3K79me2 (B), and H3K79me3 (C)]. Results show 1.5-2.5-fold higher levels of each over non-dosage compensated, as compared to dosage compensated, gene bodies.

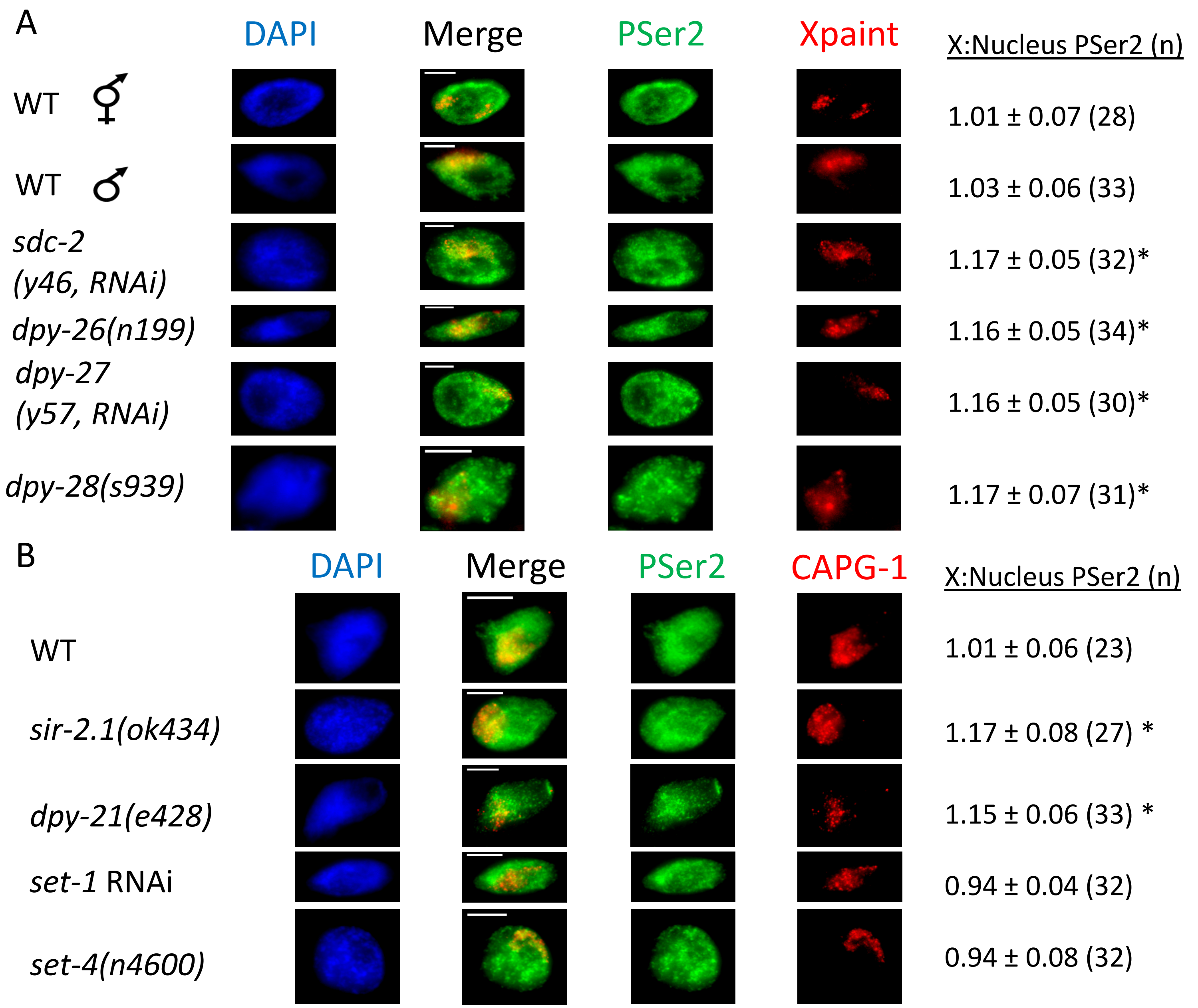

Figure 4.16. Restriction of RNA Pol II CTD PSer2 levels on X by DCC function. Shown are (A) immunoFISH or (B) immunofluorescence microscopy images from WT or loss of DCC function strains and RNAi treatments stained with antibodies against RNA Pol II CTD PSer2 (elongation). DAPI (DNA) is shown in blue. Scale bars are 5 microns in length. Fluorescence intensity quantification values (average PSer2 on X / average nuclear PSer2) with standard deviations and sample size (in parentheses) are shown to the right of each image panel. Statistically significant differences compared to WT are denoted by an asterisk. Results show that dosage compensation and *sir-2.1* mutants, but not *set-1* or *set-4* mutants, show increased PSer2 on X relative to the entire nucleus average.

References

1. Epstein CJ (1990) The consequences of chromosome imbalance. Am J Med Genet Suppl 7: 31-37.
2. Cupisti S, Conn CM, Fragouli E, Whalley K, Mills JA, et al. (2003) Sequential FISH analysis of oocytes and polar bodies reveals aneuploidy mechanisms. Prenat Diagn 23: 663-668.
3. Terry J H (1986) Chromosome abnormalities in human reproductive wastage. Trends in Genetics 2: 105-110.
4. Granic A, Padmanabhan J, Norden M, Potter H (2010) Alzheimer Abeta peptide induces chromosome mis-segregation and aneuploidy, including trisomy 21: requirement for tau and APP. Mol Biol Cell 21: 511-520.
5. Nakajima W, Ishida A, Takahashi M, Sato Y, Ito T, et al. (2007) Aseptic meningitis associated with cephalosporins in an infant with trisomy 21. J Child Neurol 22: 780-782.
6. M. Guijarro CV, B. Paule, J. Gonzalez-Macias, J. A. Riancho, (2008) Bone mass in young adults with Down syndrome. Journal of Intellectual Disability Research 52: 182-189.
7. Wallerstein R, Yu MT, Neu RL, Benn P, Lee Bowen C, et al. (2000) Common trisomy mosaicism diagnosed in amniocytes involving chromosomes 13, 18, 20 and 21: karyotype-phenotype correlations. Prenat Diagn 20: 103-122.
8. Flanagan T, Enns JT, Murphy MM, Russo N, Abbeduto L, et al. (2007) Differences in visual orienting between persons with Down or fragile X syndrome. Brain Cogn 65: 128-134.
9. Korenberg JR, Chen XN, Schipper R, Sun Z, Gonsky R, et al. (1994) Down syndrome phenotypes: the consequences of chromosomal imbalance. Proc Natl Acad Sci U S A 91: 4997-5001.
10. Epstein CJ, Berger CN, Carlson EJ, Chan PH, Huang TT (1990) Models for Down syndrome: chromosome 21-specific genes in mice. Prog Clin Biol Res 360: 215-232.
11. Bopp D (2010) About females and males: continuity and discontinuity in flies. J Genet 89: 315-323.
12. Cheng MK, Disteche CM (2006) A balancing act between the X chromosome and the autosomes. J Biol 5: 2.
13. Prestel M, Feller C, Becker PB (2010) Dosage compensation and the global re-balancing of aneuploid genomes. Genome Biol 11: 216.
14. Straub T, Dahlsveen IK, Becker PB (2005) Dosage compensation in flies: mechanism, models, mystery. FEBS Lett 579: 3258-3263.
15. Heard E, Disteche CM (2006) Dosage compensation in mammals: fine-tuning the expression of the X chromosome. Genes Dev 20: 1848-1867.
16. Straub T, Becker PB (2007) Dosage compensation: the beginning and end of generalization. Nat Rev Genet 8: 47-57.
17. Gelbart ME, Kuroda MI (2009) Drosophila dosage compensation: a complex voyage to the X chromosome. Development 136: 1399-1410.
18. Georgiev P, Chlamydas S, Akhtar A (2011) Drosophila dosage compensation: males are from Mars, females are from Venus. Fly (Austin) 5: 147-154.
19. Kharchenko PV, Xi R, Park PJ (2011) Evidence for dosage compensation between the X chromosome and autosomes in mammals. Nat Genet 43: 1167-1169; author reply 1171-1162.
20. Wells MB, Csankovszki G, Custer LM (2012) Finding a balance: how diverse dosage compensation strategies modify histone h4 to regulate transcription. Genet Res Int 2012: 795069.
21. Graves JA, Disteche CM, Toder R (1998) Gene dosage in the evolution and function of mammalian sex chromosomes. Cytogenet Cell Genet 80: 94-103.

22. Lyon MF (1999) Imprinting and X-chromosome inactivation. Results Probl Cell Differ 25: 73-90.
23. Gilfillan GD, Dahlsveen IK, Becker PB (2004) Lifting a chromosome: dosage compensation in Drosophila melanogaster. FEBS Lett 567: 8-14.
24. Gorman M, Baker BS (1994) How flies make one equal two: dosage compensation in Drosophila. Trends Genet 10: 376-380.
25. Baker BS, Gorman M, Marin I (1994) Dosage compensation in Drosophila. Annu Rev Genet 28: 491-521.
26. Ercan S, Lieb JD (2009) C. elegans dosage compensation: a window into mechanisms of domain-scale gene regulation. Chromosome Res 17: 215-227.
27. Deng X, Disteche CM (2007) Decoding dosage compensation. Genome Biol 8: 204.
28. Graves JA, Disteche CM (2007) Does gene dosage really matter? J Biol 6: 1.
29. Wells MB, Csankovszki G, Custer LM (2012) Finding a Balance: How Diverse Dosage Compensation Strategies Modify Histone H4 to Regulate Transcription. Genetics Research International 2012: 1-12.
30. Mendjan S, Akhtar A (2007) The right dose for every sex. Chromosoma 116: 95-106.
31. Cline TW, Meyer BJ (1996) Vive la difference: males vs females in flies vs worms. Annu Rev Genet 30: 637-702.
32. Bisoni L, Batlle-Morera L, Bird AP, Suzuki M, McQueen HA (2005) Female-specific hyperacetylation of histone H4 in the chicken Z chromosome. Chromosome Res 13: 205-214.
33. Grimaud C, Becker PB (2010) Form and function of dosage-compensated chromosomes--a chicken-and-egg relationship. Bioessays 32: 709-717.
34. Deakin JE, Hore TA, Koina E, Marshall Graves JA (2008) The status of dosage compensation in the multiple X chromosomes of the platypus. PLoS Genet 4: e1000140.
35. Prestel M, Feller C, Straub T, Mitlohner H, Becker PB (2010) The activation potential of MOF is constrained for dosage compensation. Mol Cell 38: 815-826.
36. Bashaw GJ, Baker BS (1996) Dosage compensation and chromatin structure in Drosophila. Curr Opin Genet Dev 6: 496-501.
37. Kotlikova IV, Demakova OV, Semeshin VF, Shloma VV, Boldyreva LV, et al. (2006) The Drosophila dosage compensation complex binds to polytene chromosomes independently of developmental changes in transcription. Genetics 172: 963-974.
38. Kelley RL, Solovyeva I, Lyman LM, Richman R, Solovyev V, et al. (1995) Expression of msl-2 causes assembly of dosage compensation regulators on the X chromosomes and female lethality in Drosophila. Cell 81: 867-877.
39. Morales V, Straub T, Neumann MF, Mengus G, Akhtar A, et al. (2004) Functional integration of the histone acetyltransferase MOF into the dosage compensation complex. EMBO J 23: 2258-2268.
40. Gorman M, Franke A, Baker BS (1995) Molecular characterization of the male-specific lethal-3 gene and investigations of the regulation of dosage compensation in Drosophila. Development 121: 463-475.
41. Franke A, Baker BS (1999) The rox1 and rox2 RNAs are essential components of the compensasome, which mediates dosage compensation in Drosophila. Mol Cell 4: 117-122.
42. Meller VH, Rattner BP (2002) The roX genes encode redundant male-specific lethal transcripts required for targeting of the MSL complex. EMBO J 21: 1084-1091.

43. Kind J, Vaquerizas JM, Gebhardt P, Gentzel M, Luscombe NM, et al. (2008) Genome-wide analysis reveals MOF as a key regulator of dosage compensation and gene expression in Drosophila. Cell 133: 813-828.
44. Smith ER, Pannuti A, Gu W, Steurnagel A, Cook RG, et al. (2000) The drosophila MSL complex acetylates histone H4 at lysine 16, a chromatin modification linked to dosage compensation. Mol Cell Biol 20: 312-318.
45. Smith ER, Allis CD, Lucchesi JC (2001) Linking global histone acetylation to the transcription enhancement of X-chromosomal genes in Drosophila males. J Biol Chem 276: 31483-31486.
46. Shogren-Knaak M, Ishii H, Sun JM, Pazin MJ, Davie JR, et al. (2006) Histone H4-K16 acetylation controls chromatin structure and protein interactions. Science 311: 844-847.
47. Lerach S, Zhang W, Deng H, Bao X, Girton J, et al. (2005) JIL-1 kinase, a member of the male-specific lethal (MSL) complex, is necessary for proper dosage compensation of eye pigmentation in Drosophila. Genesis 43: 213-215.
48. Jin Y, Wang Y, Johansen J, Johansen KM (2000) JIL-1, a chromosomal kinase implicated in regulation of chromatin structure, associates with the male specific lethal (MSL) dosage compensation complex. J Cell Biol 149: 1005-1010.
49. Zippo A, Serafini R, Rocchigiani M, Pennacchini S, Krepelova A, et al. (2009) Histone crosstalk between H3S10ph and H4K16ac generates a histone code that mediates transcription elongation. Cell 138: 1122-1136.
50. Ivaldi MS, Karam CS, Corces VG (2007) Phosphorylation of histone H3 at Ser10 facilitates RNA polymerase II release from promoter-proximal pausing in Drosophila. Genes Dev 21: 2818-2831.
51. Larschan E, Bishop EP, Kharchenko PV, Core LJ, Lis JT, et al. (2011) X chromosome dosage compensation via enhanced transcriptional elongation in Drosophila. Nature 471: 115-118.
52. Plath K, Fang J, Mlynarczyk-Evans SK, Cao R, Worringer KA, et al. (2003) Role of histone H3 lysine 27 methylation in X inactivation. Science 300: 131-135.
53. Shibata S, Yokota T, Wutz A (2008) Synergy of Eed and Tsix in the repression of Xist gene and X-chromosome inactivation. EMBO J 27: 1816-1826.
54. Maenner S, Blaud M, Fouillen L, Savoye A, Marchand V, et al. (2010) 2-D structure of the A region of Xist RNA and its implication for PRC2 association. PLoS Biol 8: e1000276.
55. Splinter E, de Wit E, Nora EP, Klous P, van de Werken HJ, et al. (2011) The inactive X chromosome adopts a unique three-dimensional conformation that is dependent on Xist RNA. Genes Dev 25: 1371-1383.
56. Chadwick LH, Willard HF (2005) Genetic and parent-of-origin influences on X chromosome choice in Xce heterozygous mice. Mamm Genome 16: 691-699.
57. Lee JT (2002) Homozygous Tsix mutant mice reveal a sex-ratio distortion and revert to random X-inactivation. Nat Genet 32: 195-200.
58. Migeon BR, Chowdhury AK, Dunston JA, McIntosh I (2001) Identification of TSIX, encoding an RNA antisense to human XIST, reveals differences from its murine counterpart: implications for X inactivation. Am J Hum Genet 69: 951-960.
59. Cheng MK, Disteche CM (2004) Silence of the fathers: early X inactivation. Bioessays 26: 821-824.
60. Morey C, Arnaud D, Avner P, Clerc P (2001) Tsix-mediated repression of Xist accumulation is not sufficient for normal random X inactivation. Hum Mol Genet 10: 1403-1411.

61. Goldman MA, Reeves PS, Wirth CM, Zupko WJ, Wong MA, et al. (1998) Comparative methylation analysis of murine transgenes that undergo or escape X-chromosome inactivation. Chromosome Res 6: 397-404.
62. Tsuchiya KD, Greally JM, Yi Y, Noel KP, Truong JP, et al. (2004) Comparative sequence and x-inactivation analyses of a domain of escape in human xp11.2 and the conserved segment in mouse. Genome Res 14: 1275-1284.
63. Al Nadaf S, Deakin JE, Gilbert C, Robinson TJ, Graves JA, et al. (2012) A cross-species comparison of escape from X inactivation in Eutheria: implications for evolution of X chromosome inactivation. Chromosoma 121: 71-78.
64. Disteche CM, Filippova GN, Tsuchiya KD (2002) Escape from X inactivation. Cytogenet Genome Res 99: 36-43.
65. Disteche CM (1995) Escape from X inactivation in human and mouse. Trends Genet 11: 17-22.
66. Berletch JB, Yang F, Disteche CM (2010) Escape from X inactivation in mice and humans. Genome Biol 11: 213.
67. Lingenfelter PA, Adler DA, Poslinski D, Thomas S, Elliott RW, et al. (1998) Escape from X inactivation of Smcx is preceded by silencing during mouse development. Nat Genet 18: 212-213.
68. Berletch JB, Yang F, Xu J, Carrel L, Disteche CM (2011) Genes that escape from X inactivation. Hum Genet 130: 237-245.
69. Yang F, Babak T, Shendure J, Disteche CM (2010) Global survey of escape from X inactivation by RNA-sequencing in mouse. Genome Res 20: 614-622.
70. Chadwick BP, Willard HF (2003) Barring gene expression after XIST: maintaining facultative heterochromatin on the inactive X. Semin Cell Dev Biol 14: 359-367.
71. Filippova GN, Cheng MK, Moore JM, Truong JP, Hu YJ, et al. (2005) Boundaries between chromosomal domains of X inactivation and escape bind CTCF and lack CpG methylation during early development. Dev Cell 8: 31-42.
72. Kohlmaier A, Savarese F, Lachner M, Martens J, Jenuwein T, et al. (2004) A chromosomal memory triggered by Xist regulates histone methylation in X inactivation. PLoS Biol 2: E171.
73. Ohhata T, Hoki Y, Sasaki H, Sado T (2008) Crucial role of antisense transcription across the Xist promoter in Tsix-mediated Xist chromatin modification. Development 135: 227-235.
74. Goto Y, Gomez M, Brockdorff N, Feil R (2002) Differential patterns of histone methylation and acetylation distinguish active and repressed alleles at X-linked genes. Cytogenet Genome Res 99: 66-74.
75. Okamoto I, Otte AP, Allis CD, Reinberg D, Heard E (2004) Epigenetic dynamics of imprinted X inactivation during early mouse development. Science 303: 644-649.
76. Csankovszki G, Nagy A, Jaenisch R (2001) Synergism of Xist RNA, DNA methylation, and histone hypoacetylation in maintaining X chromosome inactivation. J Cell Biol 153: 773-784.
77. Navarro P, Pichard S, Ciaudo C, Avner P, Rougeulle C (2005) Tsix transcription across the Xist gene alters chromatin conformation without affecting Xist transcription: implications for X-chromosome inactivation. Genes Dev 19: 1474-1484.
78. Shibata S, Lee JT (2004) Tsix transcription- versus RNA-based mechanisms in Xist repression and epigenetic choice. Curr Biol 14: 1747-1754.
79. Yildirim E, Sadreyev RI, Pinter SF, Lee JT (2011) X-chromosome hyperactivation in mammals via nonlinear relationships between chromatin states and transcription. Nat Struct Mol Biol 19: 56-61.

80. Marks H, Chow JC, Denissov S, Francoijs KJ, Brockdorff N, et al. (2009) High-resolution analysis of epigenetic changes associated with X inactivation. Genome Res 19: 1361-1373.
81. Chaumeil J, Le Baccon P, Wutz A, Heard E (2006) A novel role for Xist RNA in the formation of a repressive nuclear compartment into which genes are recruited when silenced. Genes Dev 20: 2223-2237.
82. Kucera KS, Reddy TE, Pauli F, Gertz J, Logan JE, et al. (2011) Allele-specific distribution of RNA polymerase II on female X chromosomes. Hum Mol Genet 20: 3964-3973.
83. Nora EP, Lajoie BR, Schulz EG, Giorgetti L, Okamoto I, et al. (2012) Spatial partitioning of the regulatory landscape of the X-inactivation centre. Nature 485: 381-385.
84. Lee JT, Davidow LS, Warshawsky D (1999) Tsix, a gene antisense to Xist at the X-inactivation centre. Nat Genet 21: 400-404.
85. Meyer BJ (2010) Targeting X chromosomes for repression. Curr Opin Genet Dev 20: 179-189.
86. Meyer BJ, McDonel P, Csankovszki G, Ralston E (2004) Sex and X-chromosome-wide repression in Caenorhabditis elegans. Cold Spring Harb Symp Quant Biol 69: 71-79.
87. Csankovszki G, Petty EL, Collette KS (2009) The worm solution: a chromosome-full of condensin helps gene expression go down. Chromosome Res 17: 621-635.
88. Lieb JD, Albrecht MR, Chuang PT, Meyer BJ (1998) MIX-1: an essential component of the C. elegans mitotic machinery executes X chromosome dosage compensation. Cell 92: 265-277.
89. Chuang PT, Albertson DG, Meyer BJ (1994) DPY-27:a chromosome condensation protein homolog that regulates C. elegans dosage compensation through association with the X chromosome. Cell 79: 459-474.
90. Lieb JD, Capowski EE, Meneely P, Meyer BJ (1996) DPY-26, a link between dosage compensation and meiotic chromosome segregation in the nematode. Science 274: 1732-1736.
91. Meyer BJ, Casson LP (1986) Caenorhabditis elegans compensates for the difference in X chromosome dosage between the sexes by regulating transcript levels. Cell 47: 871-881.
92. Plenefisch JD, DeLong L, Meyer BJ (1989) Genes that implement the hermaphrodite mode of dosage compensation in Caenorhabditis elegans. Genetics 121: 57-76.
93. Csankovszki G, Collette K, Spahl K, Carey J, Snyder M, et al. (2009) Three distinct condensin complexes control C. elegans chromosome dynamics. Curr Biol 19: 9-19.
94. Villeneuve AM, Meyer BJ (1987) sdc-1: a link between sex determination and dosage compensation in C. elegans. Cell 48: 25-37.
95. Villeneuve AM, Meyer BJ (1990) The role of sdc-1 in the sex determination and dosage compensation decisions in Caenorhabditis elegans. Genetics 124: 91-114.
96. Nusbaum C, Meyer BJ (1989) The Caenorhabditis elegans gene sdc-2 controls sex determination and dosage compensation in XX animals. Genetics 122: 579-593.
97. Delong L, Plenefisch JD, Klein RD, Meyer BJ (1993) Feedback-Control of Sex Determination by Dosage Compensation Revealed through Caenorhabditis-Elegans Sdc-3 Mutations. Genetics 133: 875-896.
98. Klein RD, Meyer BJ (1993) Independent domains of the Sdc-3 protein control sex determination and dosage compensation in C. elegans. Cell 72: 349-364.
99. Hsu DR, Meyer BJ (1994) The Dpy-30 Gene Encodes an Essential Component of the Caenorhabditis-Elegans Dosage Compensation Machinery. Genetics 137: 999-1018.
100. Hsu DR, Chuang PT, Meyer BJ (1995) Dpy-30, a Nuclear-Protein Essential Early in Embryogenesis for Caenorhabditis-Elegans Dosage Compensation. Development 121: 3323-3334.

101. Meneely PM, Wood WB (1984) An autosomal gene that affects X chromosome expression and sex determination in Caenorhabditis elegans. Genetics 106: 29-44.
102. Meneely PM, Wood WB (1987) Genetic analysis of X-chromosome dosage compensation in Caenorhabditis elegans. Genetics 117: 25-41.
103. Yonker SA, Meyer BJ (2003) Recruitment of C. elegans dosage compensation proteins for gene-specific versus chromosome-wide repression. Development 130: 6519-6532.
104. Jans J, Gladden JM, Ralston EJ, Pickle CS, Michel AH, et al. (2009) A condensin-like dosage compensation complex acts at a distance to control expression throughout the genome. Genes Dev 23: 602-618.
105. Ercan S, Giresi PG, Whittle CM, Zhang X, Green RD, et al. (2007) X chromosome repression by localization of the C. elegans dosage compensation machinery to sites of transcription initiation. Nat Genet 39: 403-408.
106. Hirano T, Kobayashi R, Hirano M (1997) Condensins, chromosome condensation protein complexes containing XCAP-C, XCAP-E and a Xenopus homolog of the Drosophila Barren protein. Cell 89: 511-521.
107. Kimura K, Hirano T (1997) ATP-dependent positive supercoiling of DNA by 13S condensin: a biochemical implication for chromosome condensation. Cell 90: 625-634.
108. Liu T, Rechtsteiner A, Egelhofer TA, Vielle A, Latorre I, et al. (2011) Broad chromosomal domains of histone modification patterns in C. elegans. Genome Res 21: 227-236.
109. Gerstein MB, Lu ZJ, Van Nostrand EL, Cheng C, Arshinoff BI, et al. (2010) Integrative analysis of the Caenorhabditis elegans genome by the modENCODE project. Science 330: 1775-1787.
110. Wells MB, Snyder MJ, Custer LM, Csankovszki G (2012) Caenorhabditis elegans dosage compensation regulates histone H4 chromatin state on X chromosomes. Mol Cell Biol 32: 1710-1719.
111. Whittle CM, McClinic KN, Ercan S, Zhang X, Green RD, et al. (2008) The genomic distribution and function of histone variant HTZ-1 during C. elegans embryogenesis. PLoS Genet 4: e1000187.
112. Petty E, Laughlin E, Csankovszki G (2011) Regulation of DCC Localization by HTZ-1/H2A.Z and DPY-30 Does not Correlate with H3K4 Methylation Levels. PLoS ONE 6: e25973.
113. Petty EL, Collette KS, Cohen AJ, Snyder MJ, Csankovszki G (2009) Restricting dosage compensation complex binding to the X chromosomes by H2A.Z/HTZ-1. PLoS Genet 5: e1000699.
114. Ercan S, Dick LL, Lieb JD (2009) The C. elegans dosage compensation complex propagates dynamically and independently of X chromosome sequence. Curr Biol 19: 1777-1787.
115. Svejstrup JQ (2004) The RNA polymerase II transcription cycle: cycling through chromatin. Biochim Biophys Acta 1677: 64-73.
116. Nechaev S, Adelman K (2010) Pol II waiting in the starting gates: Regulating the transition from transcription initiation into productive elongation. Biochim Biophys Acta.
117. Buratowski S (2009) Progression through the RNA polymerase II CTD cycle. Mol Cell 36: 541-546.
118. Conaway RC, Conaway JW (1994) Transcription : mechanisms and regulation. New York: Raven Press. xix, 570 p. p.
119. Sims RJ, 3rd, Belotserkovskaya R, Reinberg D (2004) Elongation by RNA polymerase II: the short and long of it. Genes Dev 18: 2437-2468.
120. Gnatt AL, Cramer P, Fu J, Bushnell DA, Kornberg RD (2001) Structural basis of transcription: an RNA polymerase II elongation complex at 3.3 A resolution. Science 292: 1876-1882.

121. Liu X, Bushnell DA, Silva DA, Huang X, Kornberg RD (2011) Initiation complex structure and promoter proofreading. Science 333: 633-637.
122. Missra A, Gilmour DS (2010) Interactions between DSIF (DRB sensitivity inducing factor), NELF (negative elongation factor), and the Drosophila RNA polymerase II transcription elongation complex. Proc Natl Acad Sci U S A 107: 11301-11306.
123. Fujita T, Schlegel W (2010) Promoter-proximal pausing of RNA polymerase II: an opportunity to regulate gene transcription. J Recept Signal Transduct Res 30: 31-42.
124. Gilmour DS (2009) Promoter proximal pausing on genes in metazoans. Chromosoma 118: 1-10.
125. Ai N, Hu X, Ding F, Yu B, Wang H, et al. (2011) Signal-induced Brd4 release from chromatin is essential for its role transition from chromatin targeting to transcriptional regulation. Nucleic Acids Res 39: 9592-9604.
126. Hanyu-Nakamura K, Sonobe-Nojima H, Tanigawa A, Lasko P, Nakamura A (2008) Drosophila Pgc protein inhibits P-TEFb recruitment to chromatin in primordial germ cells. Nature 451: 730-733.
127. Fujita T, Piuz I, Schlegel W (2009) The transcription elongation factors NELF, DSIF and P-TEFb control constitutive transcription in a gene-specific manner. FEBS Lett 583: 2893-2898.
128. Yamada T, Yamaguchi Y, Inukai N, Okamoto S, Mura T, et al. (2006) P-TEFb-mediated phosphorylation of hSpt5 C-terminal repeats is critical for processive transcription elongation. Mol Cell 21: 227-237.
129. Reyes-Reyes M, Hampsey M (2007) Role for the Ssu72 C-terminal domain phosphatase in RNA polymerase II transcription elongation. Mol Cell Biol 27: 926-936.
130. Fish RN, Kane CM (2002) Promoting elongation with transcript cleavage stimulatory factors. Biochim Biophys Acta 1577: 287-307.
131. Pferdehirt RR, Kruesi WS, Meyer BJ (2011) An MLL/COMPASS subunit functions in the C. elegans dosage compensation complex to target X chromosomes for transcriptional regulation of gene expression. Genes Dev 25: 499-515.
132. Cheng C, Yan KK, Yip KY, Rozowsky J, Alexander R, et al. (2011) A statistical framework for modeling gene expression using chromatin features and application to modENCODE datasets. Genome Biol 12: R15.
133. Miller LM, Plenefisch JD, Casson LP, Meyer BJ (1988) xol-1: a gene that controls the male modes of both sex determination and X chromosome dosage compensation in C. elegans. Cell 55: 167-183.
134. Liu T, Ortiz JA, Taing L, Meyer CA, Lee B, et al. (2011) Cistrome: an integrative platform for transcriptional regulation studies. Genome Biol 12: R83.
135. Blauwkamp TA, Csankovszki G (2009) Two classes of dosage compensation complex binding elements along Caenorhabditis elegans X chromosomes. Mol Cell Biol 29: 2023-2031.

CHAPTER 5

Conclusions and Further Directions

Conclusions

Complex genetic programs designed to achieve proper gene dosage are essential to the viability, development, and fitness of all organisms. Two levels of effects integral to proper gene dosage are: chromosome copy number and transcriptional regulation. Differences in chromosome copy number are typically lethal to the organism [1], and the rare aneuploidies that are not lethal result in substantial handicaps toward evolutionary fitness in that individual [1,2]. One exception, a difference in X chromosome copy number, must be tolerated across many organisms. This difference is the underpinnings of a chromosome-based method of sex determination, which is utilized by many species [3-5]. Dosage compensation is thought to have evolved in response to the development of this difference in order to equalize X-linked gene expression between the sexes [6-8].

Dosage compensation involves different mechanisms across different species [9-21]. In mammals, one X chromosome in females is inactivated [22]; in flies, the single male X chromosome is transcriptionally upregulated two-fold [23,24]. In the worm *Caenorhabditis elegans*, dosage compensation is achieved by two-fold downregulation of X-linked expression by the dosage compensation complex [25,26]. The DCC contains a condensin-like complex, similar to the meiotic and mitotic chromosome condensation machinery regulator, suggesting that worm dosage compensation occurs through changes in X chromosome structure [27]. To date, the only further detail concerning the molecular mechanism of worm dosage compensation known is that the DCC regulates RNA Pol II occupancy [27].

The primary aim of my thesis work was to uncover further mechanistic details of worm dosage compensation action. In undertaking this work, we sought to improve general understanding of worm dosage compensation and condensin function in gene regulation in general. In other systems, condensin is known to be important for gene expression regulation during immune cell differentiation [28,29] and localization of the histone deacetylase Sir2 [30], but mechanistic details in these instances are also lacking.

My initial experiments centered around an immunofluorescence-based screen of histone modifications, looking for differences in staining on the X chromosomes that might be indicative of changes in chromatin structure. Several modifications showed X-specific differences (see Chapter 2 and Appendix A); we chose to focus on H4K16ac and H4K20me1, due to their conserved roles in other dosage compensation paradigms and transcription [31]. Through this work, we sought to understand DCC-directed changes in X chromosome structure that might be indicative of changes in gene expression.

This work uncovered gender-specific and DCC-specific regulation of both modifications in worms. DCC action shifts the balance of H4 chromatin to a more repressive state, leading to a reduction in H4K16ac and an enrichment of H4K20me1 preserved on X. I identified the enzymes which act at these histone tail residues in *C. elegans*, the hierarchical nature of regulation of these marks on X, and functional significance for the H4K20 methyltransferases SET-1 and SET-4 in dosage compensation [32]. Our study of chromatin modifications associated with dosage compensation has led to a new understanding of two structural changes to X chromatin that promote a state repressive to transcription, forming the basis for a molecular mechanism of dosage compensation in *C. elegans*.

Following this study, I was interested in examining recently-released high-resolution datasets from the modENCODE consortium [33] for additional differences in histone modification and protein occupancy on X and at dosage compensated versus non-dosage compensated gene groups. I began by improving upon the lists of known dosage compensated (DC) and non-dosage compensated (non-DC) genes using up-to-date statistical methods. This led to a list of genes that did not include questionable candidates such as non-coding transcripts and decommissioned genes. With the help of a Bioinformatician on campus, we also identified a set of expressed genes from RNA-seq data at multiple developmental stages. With these improved boundaries, I set out to construct a compendium of histone modification and protein occupancy profiles and cross-correlations associated with X to autosome and DC to non-DC gene lists.

This work not only highlights the ease and functionality of using Cistrome [34], an online toolset for high-resolution dataset analysis, but it also led to several important discoveries relating to *C. elegans* dosage compensation. First, genome browser analysis identified an enhancer-like chromatin state surrounding known DCC recruitment and binding elements. Cistrome analysis allowed us both to confirm that this pattern was maintained across all *rex* sites, *dox* sites, and waystations, and to identify over 300 novel candidate enhancer-like DCC binding elements on X. Next, H4K16ac and H3K27ac peaks often overlapped with DCC peaks and showed a positive correlation value in Cistrome analysis. This led me to investigate the role of histone acetyltransferases in DCC localization. RNAi against CBP-1, MYS-1, and MYS-4, known H4K16 and H3K27 acetyltransferases ([35,36], MW unpublished results), led to measurable DCC mislocalization by immunoFISH analysis. Knockdown of any two of these HAT proteins led to increased DCC mislocalization. Analysis of HAT mutant strains revealed similar results, but more severe consequences, for DCC localization and X chromosome structure. In all, these results suggest that HAT proteins play a critical role in DCC localization through dual mechanisms, regulation of X chromatin structure and regulation of transcriptional elongation. My results from this work highlight the value of public dataset mining, reaffirm previous work examining the role of histone acetylation in transcription, and add to the importance of chromatin state for dosage compensation function.

From here, I sought to uncover and understand regulation of RNA polymerase II itself and transcription by dosage compensation function. My studies of RNA polymerase state on X and DCC function's influence on transcription uncovered action on gene expression at multiple points in the transcription cycle. First, using Cistrome analysis, immunofluorescence (IF), and FRAP microscopy, we demonstrated that RNA Pol II loading is likely not restricted by the DCC. Next, I found using Cistrome analysis and IF analysis with antibodies against initiated RNA Pol II (anti-PSer5, 8WG16, and 4H8) that the DCC is limiting RNA Pol II initiation, and further, that DPY-21 in particular gates the transition from initiated to productively elongating RNA Pol II. Cistrome analysis of RNA-seq data demonstrates a clear and substantial defect in early genic elongation at dosage compensated genes, within both exons and introns, which could represent a major contribution to DCC regulation of gene expression. Further, the DCC limits staining on X from antibodies against productively elongating RNA Pol II (anti-PSer2), and the molecular switch from transcriptional initiation to elongation, DSIF, is crucial for proper DCC localization to X. Multiple factors, including RNA Pol II CTD kinases and the DSIF component SPT-4, are genetically important for DCC function. This project has uncovered substantial mechanistic details explaining the intricate relationship between DCC function and transcriptional regulation that leads to the overall gene regulation goals of dosage compensation. This work also contributes novel details to our understanding of condensin regulation of interphase gene expression, perhaps shedding light on results from other systems [27,37].

In total, my thesis work forms a foundation of molecular details linking dosage compensation, chromatin state, and transcription that represent a great advancement in our knowledge of the *C. elegans* dosage compensation mechanism. My work has used a variety of genome-wide high- and low-resolution methods to explore DCC function at multiple levels, forming, in part, a comprehensive picture of chromatin, protein occupancy, and transcription on X. I have also uncovered genetic roles for many chromatin and transcription regulators in DCC function, again highlighting the connections between the DCC and global regulators.

Proposed Further Directions

I will now lay out seven research aims that would greatly extend the conclusions from my thesis work and their importance to the fields of dosage compensation and condensin function. Aim I involves exploring the possibility of direct DCC regulation of H4K20 methyltransferases, clarifying the details of chromatin regulation by dosage compensation uncovered in Chapter 2. Aim II involves additional RNA-seq analysis to reveal the direct contributions of DCC function to transcript production. Aim III involves a strategy for further investigation of DPY-21 function, in part, as a follow-up to the specific contribution of DPY-21 to limiting RNA Pol II elongation uncovered in Chapter 4. Aim IV suggests a path to deeper understanding of the balance between X and autosome gene expression through autosome downregulation, not X upregulation, prior to dosage compensation onset. Aim V suggests real-time investigation of RNA Pol II dynamics on X in live worm nuclei. Aim VI seeks to understand the contribution of histone acetyltransferase proteins and acetylation to expression and DCC localization in greater detail using high-resolution ChIP-chip or ChIP-seq. Finally, Aim VII offers several methods for addressing DCC-mediated suppression of RNA Pol II elongation within gene bodies through regulation of the RNA Pol II CTD kinase B0285.1 (the *C. elegans* CDK12 homolog).

Aim I: Investigate H4K20 HMT Proteins for Localization Reliance and Interaction with DCC Components. In Chapter 2, I showed that SET-1 and SET-4 (conserved H4K20 mono- and di-/tri-methyltransferases, respectively) and DCC function were all critical for H4K20me1 enrichment on the X chromosomes. Other work from our lab suggests that the onset of H4K20me1 enrichment on X does not coincide with DCC enrichment on X in young embryos (Laura Custer, unpublished results). To further explore the relationship between these SET proteins and the DCC, a LAP tagging strategy [38], should be employed on the SET proteins. This would allow for both IF localization of SET-1 and SET-4 with GFP antibodies and purification of each SET to look for physical interactions with DCC member proteins. Additionally, SET protein localization could be assayed in DC mutants to further explore the influence of dosage compensation on SET protein localization.

Aim II: Explore the Role of DCC Member Proteins, Chromatin Modifiers, and Transcription Regulators in Transcript Production on X vs. Autosomes or at Dosage Compensated vs. non-Dosage Compensated Genes. Cistrome analysis of available RNA-seq data suggests that a major contributor to transcriptional regulation by the DCC is restriction of early genic RNA Pol II elongation. By conducting RNA-seq analysis in dosage compensation, chromatin modifier, or transcription regulator mutant or knockdown backgrounds at multiple developmental stages would accomplish several goals: 1) allow for a more precise determination of dosage compensated and non-dosage compensated genes, 2) uncover the contributions of all genes tested to dosage compensation effects on transcription, 3) serve as a resource for other groups interested in chromatin influences on transcription, or in the regulation of particular genes or gene groups.

Aim III: Toward the Determination of DPY-21 Function. Employing a LAP tagging strategy [38] on DPY-21, perhaps twice, at either the N- or C-terminus, would allow for further investigation and clarification of DPY-21 function. Antibodies against DPY-21 have yielded limited and inconsistent results with regards to DPY-21 localization and interaction partners (see Appendix A). Further analysis of DPY-21 will shed light onto the role of this loosely-associated DCC member and its global regulatory function.

Aim IV: Autosome Downregulation as a Mechanism of Gene Expression Balance Between X and Autosomes Within An Individual. It is not necessary that X upregulation be employed to balance X and autosome expression within an individual; another intriguing possibility is that autosome expression is downregulated in order to achieve this goal. Preliminary evidence from our *xol-1* suppression assay suggests that LEM-2 may be a part of this mechanism: addition of *lem-2* RNAi is able to suppress male rescue seen by DCC component or *htz-1* knockdown. Further investigation of DCC/LEM-2 physical interactions by IP-Western blot analysis and chromatin conformation capture (5C) or DPY-27 ChIA-PET analysis in WT versus *lem-2* knockdown conditions would go a long way to understanding the influence of LEM-2 on chromosome dosage effects and the interplay between LEM-2 and dosage compensation.

AIM V: Investigation of RNA Polymerase II Dynamics on X in Live Worms over Time. Preliminary work using a strain expressing AMA-1::GFP and FRAP analysis suggests that RNA Pol II remains on X-linked loci much longer than autosomal loci (See Chapter 4). Construction of a DCC::RFP expressing strain and crossing of this strain with the AMA-1::GFP strain would allow for greater exploration of the relationship between dosage compensation and RNA Pol II dynamics. Possible experimental tracks include: 1) RNAi treatments on the combined strain to assay the contributions of the DCC, chromatin modifiers, and transcription regulators to RNA Pol

II and DCC occupancy; 2) exploration of DCC spreading reliance on RNA Pol II elongation through elongation factor RNAi; and 3) single molecule particle tracking to explore differences in transcription rate on X and autosomes.

AIM VI: Expression and DCC Mislocalization by HAT Knockdown Assayed at High Resolution Genome-wide. Results detailed in Chapter 3 suggest that HAT proteins and acetylation are important for proper DCC localization through promoting RNA Pol II elongation (Figures 3.5, 3.6, 3.63-3.67). I propose ChIP-chip or ChIP-seq of DPY-27 following HAT knockdown in order to learn where the DCC now binds. In particular, does the DCC now bind autosomal enhancer-like elements? Valuable extension of this analysis could involve transcript level comparisons in vector, HAT RNAi, and HAT/DCC double RNAi conditions by RNA-seq. In sum, these studies could lead to a better understanding of whether suppression of expression affects X and autosomes differently, and whether DCC redistribution in HAT RNAi is intended to rebalance genome-wide expression.

AIM VI: Does DCC-Mediated Restriction of X-Linked Transcription Involve Exclusion of CDK-12? Recent work [39,40] has described CDK12 (in partnership with cyclin K) function as a major RNA Pol II CTD serine 2 kinase acting through gene bodies. My analysis of serine 2 phosphorylation (Fig. 4.16), RNA-seq data (Figs. 4.3, 4.12, and 4.13), and histone modifications associated with RNA Pol II elongation (see Chapter 3) is consistent with the hypothesis that dosage compensation acts, in part, to limit the elongation activity of RNA Pol II on X. Several lines of experiments could help to clarify whether DCC-mediated elongation control in gene bodies through regulation of CDK12 or its activity occurs on the dosage compensated X chromosomes. First, the *C. elegans* Cdk12 homolog (B0285.1) could be tested in the modified *xol-1* suppression assay for male rescue. Second, it would be important to check B0285.1 RNAi-treated worms for the expected drop in PSer2 levels, as well as changes in DCC, H4K16ac, and H4K20me1 staining. Finally, using antibodies or tagging strategies (such as LAP tagging [38]) to visualize B0285.1 localization and test whether B0285.1 localization changes in response to DCC loss would further support a more direct effect of the DCC on RNA Pol II genic elongation.

References

1. Epstein CJ (1990) The consequences of chromosome imbalance. Am J Med Genet Suppl 7: 31-37.
2. Epstein CJ, Berger CN, Carlson EJ, Chan PH, Huang TT (1990) Models for Down syndrome: chromosome 21-specific genes in mice. Prog Clin Biol Res 360: 215-232.
3. Carmi I, Meyer BJ (1999) The primary sex determination signal of Caenorhabditis elegans. Genetics 152: 999-1015.
4. Clepet C, Schafer AJ, Sinclair AH, Palmer MS, Lovell-Badge R, et al. (1993) The human SRY transcript. Hum Mol Genet 2: 2007-2012.
5. Salz HK, Erickson JW (2010) Sex determination in Drosophila: The view from the top. Fly (Austin) 4: 60-70.
6. Livernois AM, Graves JA, Waters PD (2012) The origin and evolution of vertebrate sex chromosomes and dosage compensation. Heredity (Edinb) 108: 50-58.
7. Deng X, Hiatt JB, Nguyen DK, Ercan S, Sturgill D, et al. (2011) Evidence for compensatory upregulation of expressed X-linked genes in mammals, Caenorhabditis elegans and Drosophila melanogaster. Nat Genet 43: 1179-1185.
8. Vicoso B, Bachtrog D (2009) Progress and prospects toward our understanding of the evolution of dosage compensation. Chromosome Res 17: 585-602.
9. Cheng MK, Disteche CM (2006) A balancing act between the X chromosome and the autosomes. J Biol 5: 2.
10. Ercan S, Lieb JD (2009) C. elegans dosage compensation: a window into mechanisms of domain-scale gene regulation. Chromosome Res 17: 215-227.
11. Deng X, Disteche CM (2007) Decoding dosage compensation. Genome Biol 8: 204.
12. Graves JA, Disteche CM (2007) Does gene dosage really matter? J Biol 6: 1.
13. Heard E, Disteche CM (2006) Dosage compensation in mammals: fine-tuning the expression of the X chromosome. Genes Dev 20: 1848-1867.
14. Wells MB, Csankovszki G, Custer LM (2012) Finding a Balance: How Diverse Dosage Compensation Strategies Modify Histone H4 to Regulate Transcription. Genetics Research International 2012: 1-12.
15. Mendjan S, Akhtar A (2007) The right dose for every sex. Chromosoma 116: 95-106.
16. Cline TW, Meyer BJ (1996) Vive la difference: males vs females in flies vs worms. Annu Rev Genet 30: 637-702.
17. Bisoni L, Batlle-Morera L, Bird AP, Suzuki M, McQueen HA (2005) Female-specific hyperacetylation of histone H4 in the chicken Z chromosome. Chromosome Res 13: 205-214.
18. Grimaud C, Becker PB (2010) Form and function of dosage-compensated chromosomes--a chicken-and-egg relationship. Bioessays 32: 709-717.
19. Deakin JE, Hore TA, Koina E, Marshall Graves JA (2008) The status of dosage compensation in the multiple X chromosomes of the platypus. PLoS Genet 4: e1000140.
20. Gorman M, Baker BS (1994) How flies make one equal two: dosage compensation in Drosophila. Trends Genet 10: 376-380.
21. Baker BS, Gorman M, Marin I (1994) Dosage compensation in Drosophila. Annu Rev Genet 28: 491-521.
22. Lyon MF (1963) Lyonisation of the X Chromosome. Lancet 2: 1120-1121.
23. Gorman M, Kuroda MI, Baker BS (1993) Regulation of the sex-specific binding of the maleless dosage compensation protein to the male X chromosome in Drosophila. Cell 72: 39-49.
24. Conrad T, Akhtar A (2012) Dosage compensation in Drosophila melanogaster: epigenetic fine-tuning of chromosome-wide transcription. Nat Rev Genet 13: 123-134.

25. Meyer BJ (2010) Targeting X chromosomes for repression. Curr Opin Genet Dev 20: 179-189.
26. Csankovszki G, Petty EL, Collette KS (2009) The worm solution: a chromosome-full of condensin helps gene expression go down. Chromosome Res 17: 621-635.
27. Csankovszki G (2009) Condensin function in dosage compensation. Epigenetics 4: 212-215.
28. Rawlings JS, Gatzka M, Thomas PG, Ihle JN (2011) Chromatin condensation via the condensin II complex is required for peripheral T-cell quiescence. EMBO J 30: 263-276.
29. Gosling KM, Makaroff LE, Theodoratos A, Kim YH, Whittle B, et al. (2007) A mutation in a chromosome condensin II subunit, kleisin beta, specifically disrupts T cell development. Proc Natl Acad Sci U S A 104: 12445-12450.
30. Machin F, Paschos K, Jarmuz A, Torres-Rosell J, Pade C, et al. (2004) Condensin regulates rDNA silencing by modulating nucleolar Sir2p. Curr Biol 14: 125-130.
31. Wells MB, Csankovszki G, Custer LM (2012) Finding a balance: how diverse dosage compensation strategies modify histone h4 to regulate transcription. Genet Res Int 2012: 795069.
32. Wells MB, Snyder MJ, Custer LM, Csankovszki G (2012) Caenorhabditis elegans dosage compensation regulates histone H4 chromatin state on X chromosomes. Mol Cell Biol 32: 1710-1719.
33. Gerstein MB, Lu ZJ, Van Nostrand EL, Cheng C, Arshinoff BI, et al. (2010) Integrative analysis of the Caenorhabditis elegans genome by the modENCODE project. Science 330: 1775-1787.
34. Liu T, Ortiz JA, Taing L, Meyer CA, Lee B, et al. (2011) Cistrome: an integrative platform for transcriptional regulation studies. Genome Biol 12: R83.
35. Tie F, Banerjee R, Stratton CA, Prasad-Sinha J, Stepanik V, et al. (2009) CBP-mediated acetylation of histone H3 lysine 27 antagonizes Drosophila Polycomb silencing. Development 136: 3131-3141.
36. Thomas T, Dixon MP, Kueh AJ, Voss AK (2008) Mof (MYST1 or KAT8) is essential for progression of embryonic development past the blastocyst stage and required for normal chromatin architecture. Mol Cell Biol 28: 5093-5105.
37. Dej KJ, Ahn C, Orr-Weaver TL (2004) Mutations in the Drosophila condensin subunit dCAP-G: defining the role of condensin for chromosome condensation in mitosis and gene expression in interphase. Genetics 168: 895-906.
38. Cheeseman IM, Desai A (2005) A combined approach for the localization and tandem affinity purification of protein complexes from metazoans. Sci STKE 2005: pl1.
39. Kohoutek J, Blazek D (2012) Cyclin K goes with Cdk12 and Cdk13. Cell Division 7: 12.
40. Bartkowiak B, Liu P, Phatnani HP, Fuda NJ, Cooper JJ, et al. (2010) CDK12 is a transcription elongation-associated CTD kinase, the metazoan ortholog of yeast Ctk1. Genes Dev 24: 2303-2316.